PhytoKeys 226: 1–16 (2023)
doi: 10.3897/phytokeys.226.96351
https://phytokeys.pensoft.net

RESEARCH ARTICLE

A peer-reviewed open-access journal
PhytoKeys
Launched to accelerate biodiversity research

Primulina jiulianshanensis, a new species of Gesneriaceae from Jiangxi Province, China

Guo-Liang Xu[1*], Li-Fen Liang[2*], Di-Ya Chen[3,4], Zhi-Fang Jing[1], Xiao-Hai Zuo[1], Zheng-Yu Zuo[5], Fang Wen[3,6]

1 *Jiulianshan National Nature Reserve Administrative Bureau, Longnan, CN-341700, China* **2** *Jiangxi Environmental Engineering Vocational College, Ganzhou, CN-341000, China* **3** *Guangxi Key Laboratory of Plant Conservation and Restoration Ecology in Karst Terrain, Guangxi Institute of Botany, Guangxi Zhuang Autonomous Region and Chinese Academy of Sciences, CN-541006, Guilin, China* **4** *College of Tourism and Landscape Architecture, Guilin University of Technology, Guilin, CN-541006, China* **5** *Germplasm Bank of Wild Species, Kunming Institute of Botany, Chinese Academy of Sciences, Kunming, CN-650201, China* **6** *National Gesneriaceae Germplasm Resources Bank of GXIB, Gesneriad Committee of China Wild Plant Conservation Association, Gesneriad Conservation Center of China (GCCC), Guangxi Institute of Botany, Guilin Botanical Garden, Guangxi Zhuang Autonomous Region and Chinese Academy of Sciences, CN-541006, Guilin, China*

Corresponding authors: Fang Wen (wenfang760608@139.com); Zheng-Yu Zuo (zuozhengyu@mail.kib.ac.cn)

Academic editor: Alan Paton | Received 15 October 2022 | Accepted 2 April 2023 | Published 9 May 2023

Citation: Xu G-L, Liang L-F, Chen D-Y, Jing Z-F, Zuo X-H, Zuo Z-Y, Wen F (2023) *Primulina jiulianshanensis*, a new species of Gesneriaceae from Jiangxi Province, China. PhytoKeys 226: 1–16. https://doi.org/10.3897/phytokeys.226.96351

Abstract

Primulina jiulianshanensis F.Wen & G.L.Xu, a new species of Gesneriaceae from Jiulianshan National Nature Reserve of Jiangxi Province, China, is described and illustrated here. Molecular evidence showed it was sister to *P. wenii* Jian Li & L.J.Yan, while the morphological observation found clear differences between them, petiole, both sides of leaf blades, adaxial surface of the calyx lobes, corolla inside toward the bottom, bract margins covered glandular-pubescent hairs in *P. jiulianshanensis* (*vs.* no glandular-pubescent hairs in *P. wenii*); lateral bracts 4–9 × ca. 2 mm, the central one 2–5 × 1–1.5 mm, adaxially glabrous but sparsely pubescent at apex (*vs.* lateral bracts 14–16 × 2.5–3.0 mm, the central one 10–12 × 1.3–1.6 mm, all adaxially pubescent); calyx lobes 8–11 × ca. 2 mm, each side with several brown serrate teeth at apex (*vs.* 14–15 × ca. 2.5 mm, margin entire); filaments and staminodes sparsely yellow glandular-puberulent (*vs.* white, glabrous).

Keywords

Flora of Jiangxi, Jiulianshan National Nature Reserve, new taxon, *Primulina wenii*, taxonomy

* The authors contributed equally to this work.

Introduction

The genus *Primulina* Hance (Hance 1883) in Gesneriaceae is mainly distributed in the mountainous areas of southern and southwestern China to northern Vietnam, especially in Karst landforms (Wei 2018; Xu et al. 2020b). Since it was redefined (Wang et al. 2011; Weber et al. 2011), many new species have been discovered and published. For example, ten new taxa of *Primulina* from China were reported in 2020 (Du et al. 2021). As of December 2022, about 240 species (including infraspecies, the same below) have been confirmed throughout the world, of which 224 species are distributed in China. So far, this genus is the largest genus of Gesneriaceae in China (POWO 2022).

Jiangxi Province is located in the mid-subtropical region of East China; the species number of *Primulina* is not very rich. After consulting references, checking herbarium specimens, and excluding the species that have been mistakenly identified, only 13 species of *Primulina* have been confirmed in Jiangxi Province (Peng et al. 2021). Three of them were discovered and published after 2011, which are *P. lepingensis* Z.L.Ning & M.Kang (Ning et al. 2014), *P. suichuanensis* X.L.Yu & J.J.Zhou (Zhou et al. 2016) and *P. inflata* Li H.Yang & M.Z.Xu (Xu et al. 2020a).

In April 2021, an interesting population of *Primulina* was found on a cliff of Danxia landform under the evergreen broad-leaved forest in Jiulianshan National Nature Reserve, Longnan City, Jiangxi Province. Morphologically, this species is similar to *P. wenii* Jian Li & L.J.Yan (Li et al. 2017) in some characteristics. For example, leaf blades are oblong or broadly rounded, corolla purple, and so on.

We collected the plants at the flowering and fruiting stage in the type locality to make specimens, and at the same time carried out botanical fine anatomical photography to observe carefully. We saw that the indumentum characters of petiole, leaf, bract, calyx, corolla tube, filaments, staminodes of this unknown species were obviously different from *P. wenii*, and the differences of two species' calyx lobes and bracts characters can help us easily distinguish them. In order to understand the phylogenetic placements of this unknown species in *Primulina*, ITS and *trnL-F* sequences of this species were amplified and included for phylogenetic analysis to examine the relationships of the putative new species.

Materials and methods

Morphological observation

All available specimens of *Primulina* were used and compared (i. e. those stored in the following herbaria ANU, HITBC, IBK, IBSC, KUN, PE), as was the material of *Primulina* from recent fieldwork by the authors' team in South and Southwest China. All the morphological characters, such as leaves, inflorescences, flowers and capsules, were observed and measured in the field. The description, measurements, shape, color

and other details given in this description are based on living plants and specimens. We examined distinguished morphological characters of the presumed new species and the compared one, *P. wenii*, under a dissecting microscope. We described this presumed new species using the terminology of Wang et al. (1990, 1998).

Sampling and DNA sequencing

We randomly selected one plant from the population to collect its leaves for a DNA experiment. Fresh leaf materials were preserved in silica gel for quick drying. Total genomic DNA was extracted from dried leaves using modified cetyltrimethylammonium bromide (CTAB) protocol (Doyle and Doyle 1987). ITS and *trnL-F* were amplified and sequenced following the methods of Möller et al. (2009) and Smissen et al. (2004), respectively. Besides, we downloaded the ITS and *trnL-F* sequences from GenBank for 188 *Primulina* species and two *Petrocodon* species. Species and GenBank accession numbers employed in this study are listed in Table 1.

Phylogenetic analysis

We assembled and aligned the newly obtained sequences and those from GenBank using MAFFT v.7.017 (Katoh et al. 2002) and subsequently corrected and combined the ITS and *trnL-F* sequences in Geneious 9.1.4 (Kearse et al. 2012). We used the Maximum likelihood (ML) and Bayesian inference (BI) analyses to do the phylogenetic analysis of the ITS and *trnL-F* matrixes, and the combined ITS + *trnL-F* sequences data-set. The two best supported tree topologies from maximum likelihood (ML) analyses of ITS and *trnL-F* were visually compared for topological incongruence. A conflict in tree topologies of each tree was considered significant when incongruent topologies both received bootstrap values ≥ 80% (Fu et al. 2022). The ML analyses were conducted using IQ-TREE 1.6.12 (Nguyen et al. 2015) with the GTR+R6 model and 1000 ultrafast bootstrap replicates. For BI analysis, we employed MrBayes v.3.2.6 (Ronquist et al. 2012) to obtain a maximum clade credibility (MCC) tree. Bayesian inference was performed using one million generations, four runs, four chains, a temperature of 0.001, 25% trees discarded as burn-in, and trees sampled every 1,000 generations (1,000 trees sampled in total) with GTR+I+G model.

Results

Phylogenetic analysis

The ITS matrix had a length of 782 characters, with 449 (57.4%) variable characters and 355 (45.4%) parsimony-informative. In comparison, the *trnL-F* matrix had a length of 836 characters, with 198 (23.6%) variable characters and 93 (11.1%) were parsimony-informative. The comparison of trees for ITS and *trnL-F* revealed no

Table 1. Species names and GenBank accession numbers of ITS and *trnL-F* DNA sequences used in this study.

Species name	Voucher number	ITS	*trnL-F*
Petrocodon ainsliifolius	CWH88	KF202291	KF202298
Petrocodon hancei	CIPeng22903	KY796057	KY796059
Primulina alutacea	YD07	KY394847	KY393441
Primulina argentea	YMBC	KY394848	KY393442
Primulina baishouensis	GXLG05	KY394849	KY393443
Primulina balansae	BALAN	MK747141	MK746274
Primulina beiliuensis	GXBLBC	KY394850	KY393444
Primulina beiliuensis var. *fimbribracteata*	SGQJ04	KY394851	KY393445
Primulina bicolor	SLHLCB	KY394852	KY393446
Primulina bipinnatifida	GXLG04	KY394853	KY393447
Primulina bobaiensis	BBGL01	KY394854	KY393448
Primulina bogneriana	WF7	MK747166	MK746225
Primulina brachytricha	DWDMCZ	KF498048	KY393450
Primulina brachytricha var. *magnibracteata*	KFC4193	MK369979	MK369994
Primulina brunnea	BRUN	MK747142	MK746275
Primulina bullata	GXJX06	KF498071	KY393451
Primulina cangwuensis	GXLG04	KY394853	KY393447
Primulina cardaminifolia	GXLB	MK747131	MK746255
Primulina carinata	NTBC	KY394858	KY393452
Primulina cataractarum	N1	MW900263	MW960358
Primulina chizhouensis	JXFY01	KY394860	KY393454
Primulina colaniae	WF8	MK747167	MK746224
Primulina confertiflora	GDYS05	MK747101	MK746253
Primulina cordata	HYH010	KC190200	KC190207
Primulina cordifolia	GXRA02	KY394863	KY393457
Primulina cordistigma	GDYCXZ	MK747118	MK746251
Primulina crassirhizoma	CJGL01	KY394864	KY393458
Primulina crassituba	HNSP	MK747147	MK746230
Primulina curvituba	GXHJ01	MK747137	MK746242
Primulina danxiaensis	P22865	JX506886	JX506778
Primulina debaoensis	DBGL01	KY394868	KY393462
Primulina depressa	DXS02	KY394869	KY393463
Primulina diffusa	PJGL01	KY394871	KY393465
Primulina dongguanica	DGBC	KY394872	KY393466
Primulina drakei	YNCP01	KY394873	KY393467
Primulina dryas	HKDMS	KY394875	KY393469
Primulina duanensis	DABC	KY394877	KY393471
Primulina eburnea	P22908	JX506891	JX506783
Primulina effusa	KFC4167	MK369976	MK369991
Primulina fengkaiensis	KFC4130	MK369975	MK369990
Primulina fengshanensis	KFC4195	MK369970	MK369985
Primulina fimbrisepala	P22863	JX506894	JX506786
Primulina fimbrisepala var. *mollis*	GXIB	JX506895	JX506787
Primulina flavimaculata	KFC3988	MK369974	MK369989
Primulina floribunda	DHGL01	KY394886	KY393480
Primulina fordii	LJM1207202	MG727881	MG727878
Primulina fordii var. *dolichotricha*	DHS01	MK747125	MK746247
Primulina gemella	GEME	MK747146	MK746254
Primulina glabrescens	GZLBSM	MK747132	MK746278

Species name	Voucher number	ITS	*trnL-F*
Primulina glandaceistriata	GXLCHW	MK747114	MK746256
Primulina glandulosa	GXPLCG	KY394887	KY393481
Primulina gongchengensis	GCGL01	KY394889	KY393483
Primulina grandibracteata	YNHK	MK747121	MK746266
Primulina guigangensis	GXGGBC	KY394892	KY393486
Primulina guihaiensis	GXLG036	KY394893	KY393487
Primulina guizhongensis	GXGZBC	KY394894	KY393488
Primulina halongensis	HLW01	KY394895	KY393489
Primulina hedyotidea	XWB	JX506905	JX506797
Primulina heterochroa	GXMES01	KY394898	KY393492
Primulina heterotricha	HNBT01	KY394899	KY393493
Primulina hezhouensis	HZXH	MK747143	MK746258
Primulina hiepii	WF2	MK747144	MK746223
Primulina hochiensis	GXIB	JX506903	JX506795
Primulina huaijiensis	GDHJ02	KF498127	KY393495
Primulina huangii	WF12	MK747138	MK746231
Primulina hunanensis	Xu11697	KU220602	KU220608
Primulina jiangyongensis	HNJY01	KY394902	KY393496
Primulina jingxiensis	LZXHGL01	KY394903	KY393497
Primulina jiuwanshanica	JWS	MK747116	MK746260
Primulina juliae	LJM1210011	MG727889	MG727873
Primulina langshanica	LSCZ	KY394907	KY393501
Primulina latinervis	XIN1	KY394908	KY393502
Primulina laxiflora	P22927	JX506910	JX506802
Primulina lechangensis	GDLC12	KY394910	KY393504
Primulina leeii	LSGL01	KY394911	KY393505
Primulina leiophylla	GXJX07	KY394912	KY393506
Primulina lepingensis	JXLP01	KY394913	KY394913
Primulina leprosa	GXMS055	KY394914	KY393508
Primulina lianpingensis	CHLT016	MH343910	MH344542
Primulina liboensis	GXJX08	KY394917	KY393511
Primulina liguliformis	GXIB	JX506912	JX506804
Primulina lijiangensis	GLS01	KY394919	KY393513
Primulina linearicalyx	KFC4141	MH032854	MH032841
Primulina linearifolia	GXNN01	KY394921	KY393515
Primulina lingchuanensis	LCXHGL01	KY394922	KY393516
Primulina linglingensis	LLBC	KY394923	KY393517
Primulina linglingensis var. *fragrans*	XHLLBC2	MK746285	MK746285
Primulina liujiangensis	LJGL01	KY394924	KY393518
Primulina lobulata	GDQX04	KF498054	KY393519
Primulina longgangensis	P22948	JX506916	JX506808
Primulina longicalyx	GXGL01	KY394927	KY393521
Primulina longii	XWB	JX506917	JX506809
Primulina longzhouensis	P22963	JX506918	JX506810
Primulina lunglinensis	GZXY04	KY394930	KY393524
Primulina lunglinensis var. *amblyosepala*	LCDE	MK747105	MK746281
Primulina lungzhouensis	GXJX10	KY394931	KY393525
Primulina luochengensis	LCWCGL01	KY394932	KY393526
Primulina lutea	1844	JX506921	JX506813
Primulina lutescens	PBLS01	MK747135	MK746263
Primulina lutvittata	KFC4149	MK369978	MK369993

Species name	Voucher number	ITS	*trnL-F*
Primulina luzhaiensis	HYH019	KC190197	KC190204
Primulina mabaensis	SZY02	KY394937	KY393531
Primulina macrodonta	GXIB	JX506923	JX506815
Primulina maculata	Xu11916	KU220604	KU220609
Primulina maguanensis	YNMG	MK747127	MK746267
Primulina malipoensis	YNMLP01	MK747123	MK746240
Primulina medica	GXPLCM	KY394940	KY393534
Primulina melanofilamenta	GXXA	MK747158	MK746277
Primulina minor	WXXH1	MK747160	MK746290
Primulina minutimaculata	GXLZ10	KY394941	KY393535
Primulina moi	SGWY03	KF498115	KY393536
Primulina mollifolia	GXESWC	KY394943	KY393537
Primulina multifida	DLXHGL01	KY394946	KY393540
Primulina nandanensis	GXJX02	KY393541	KY393541
Primulina napoensis	GXIB	JX506930	JX506821
Primulina ningmingensis	NMGL01	KY394949	KY393543
Primulina obtusidentata	GZJK01	KF498096	KY393544
Primulina ophiopogoides	GXFS01	KF498062	KY393545
Primulina orthandra	ZRBC2	MK747128	MK746286
Primulina parvifolia	GGSL01	KY394952	KY393546
Primulina pengii	W0397	KU220603	KU220610
Primulina petrocosmeoides	SHDBC	KY394953	KY393547
Primulina pinnatifida	MS02	KY394954	KY393548
Primulina polycephala	GDLZ06	KY394955	KY393549
Primulina porphyrea	DNGL01	KU173793	KU173799
Primulina pseudoeburnea	KY394958	KY394958	KY393552
Primulina pseudoglandulosa	GXYS06	KF498138	KY393482
Primulina pseudoheterotricha	XWB	JX506933	JX506824
Primulina pseudolinearifolia	JXY	MK747140	MK746280
Primulina pseudomollifolia	JMMXH1	MK747134	MK746244
Primulina pseudoroseoalba	JFHGL01	KY394959	KY393553
Primulina pteropoda	HNCJ01	KY394960	KY393554
Primulina pungentisepala	JEGL01	KY394962	KY393556
Primulina purpurea	ZHGL01	KY394964	KY393558
Primulina qingyuanensis	GDQX01	KY394965	KY394965
Primulina renifolia	GXDA02	KY394966	KY393560
Primulina repanda	GXBM03	KY394968	KY393562
Primulina ronganensis	GXRA01	KF498135	KY393564
Primulina rongshuiensis	GXRS01	KF498088	KY393565
Primulina roseoalba	LDGL01	KY394972	KY393566
Primulina rosulata	GXPL05	KU528874	KU528884
Primulina rotundifolia	OO3	KY394975	KY393569
Primulina rubribracteata	JH01R	KU173791	KU173797
Primulina sclerophylla	GXDA01	KY394979	KY393573
Primulina secundiflora	GZQZ	MK747119	MK746279
Primulina shouchengensis	GXYF02	KY394980	KY393574
Primulina sichuanensis	SCBC	MK747162	MK746264
Primulina dryas	HKDMS	KY394875	KY393469
Primulina sinovietnamica	Peng21956	MK369973	MK369988

Species name	Voucher number	ITS	*trnL-F*
Primulina spinulosa	GXFS02	KF498063	KY393576
Primulina subrhomboidea	GXYS02	KY395018	KY393577
Primulina subulata	GDYA01	KY395020	KY393579
Primulina subulata var. *guilinensis*	GXHYXH	KY394967	KY393561
Primulina subulatisepala	CQAYH01	MK747122	MK746246
Primulina suichuanensis	GDLC07	KY395021	KY393580
Primulina swinglei	GXRX01	KY395022	KY393581
Primulina tabacum	LZ01	KY395023	KY393582
Primulina tenuifolia	GXBM01	KY395024	KY393583
Primulina tenuituba	GZGY01	KY395025	KY393584
Primulina tiandengensis	GXTD03	KY395027	KY393586
Primulina tribracteata	GXFS04	KY395028	KY393587
Primulina tribracteata var. *zhuana*	1877	JX506952	JX506843
Primulina tsoongii	ZSGL01	KY395029	KY393588
Primulina varicolor	GXNP01	KF498086	KY393589
Primulina verecunda	LBJX01	KY395031	KY393590
Primulina versicolor	GDYD01	MK747155	MK746252
Primulina vestita	QZXT	MK747156	MK746282
Primulina villosissima	QXY01	KY395032	KY393591
Primulina wenii	WENI	MK747148	MK746284
Primulina wentsaii	GXLZ047	KY395033	KY393592
Primulina wuae	WSBC	MK747159	MK746265
Primulina xinningensis	GGGL01	KY394891	KY393485
Primulina xiziae	ZJHZ01	KY395038	KY393597
Primulina yangchunensis	GDYC01	KY395039	KY393598
Primulina yangshanensis	GDNX01	KY395040	KY393599
Primulina yangshuoensis	GXYS07	KY395042	KY393601
Primulina yingdeensis	YD03	KU528876	KU528886
Primulina yungfuensis	GXIB	JX506957	JX506848
Primulina zhoui	WF18	MK747104	MK746222
Primulina jiulianshanensis	WF217	OP243287	OP243283

significant incongruence topology and both indicated that *Primulina jiuyishanensis* is closely related to *P. wenii* (Suppl. materials 1, 2). Because the combined dataset resulted in a better-resolved tree with higher support values, we use the combined dataset to do the further molecular studies. The combined data-set was 1628 characters, with 653 (40.1%) variable characters and 452 (27.8%) parsimony-informative, including the indels in all matrixes. The undescribed species and *P. wenii* were sister groups [Bayesian posterior probabilities (BIPP) = 1.00, ML ultrafast bootstrap support values (UFBoot) = 100%], and we found 10 and 1 different sites in the ITS (totally 615 bp) and the *trnL-F* (totally 750 bp) sequences between them, respectively (Table 2). belonging to a strongly supported clade (BIPP = 0.99, UFBoot = 98%) included *Primulina crassituba* (W.T.Wang) Mich.Möller & A.Weber, *P. effusa* F.Wen & B.Pan and *P. lobulata* (W.T.Wang) Mich.Möller & A.Weber (Wang 1982, 1989; Weber et al. 2011; Pan et al. 2017) (Fig. 1).

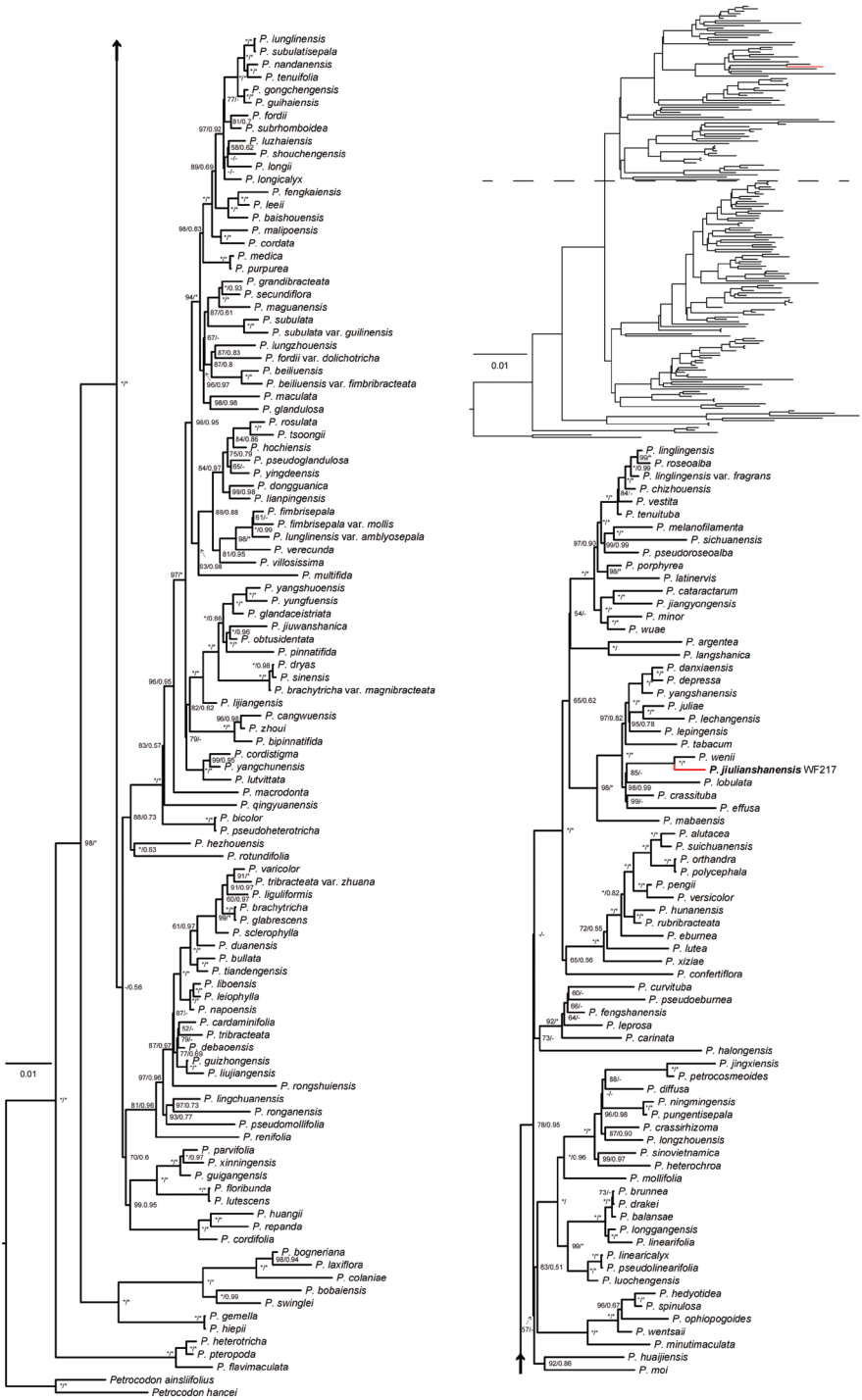

Figure 1. Phylogenetic tree of *Primulina* generated from maximum likelihood (ML) of combined *trn*L-F and ITS data-set. Numbers of each branch are support values in the order of UFBoot/BIPP. Stars indicate UFBoot = 100% or BIPP = 1.0. The dash (–) indicates a node with UFBoot or < 50% or BIPP < 0.5.

Table 2. Sequence differences of ITS and *trnL-F* regions between *Primulina jiulianshanensis* and *P. wenii*.

Species & marker	Sequences
P. jiulianshanensis ITS	1-CCCGAGAACATGTTTAAAACACGCTTGCGT-30
P. wenii ITS	1-CCCGAGAACATGTTTAAGACACGCTTGCGT-30
P. jiulianshanensis ITS	141-CGAGCGCCTCTCCGTCCTGGCTAAGTTCGC-170
P. wenii ITS	141-CGAGCGCCTCTCCGTACCGGTGAAGTTCGC-170
P. jiulianshanensis ITS	396-CGTTTTTTCCACGCTCAAAAGGTGTC–GGGGACGA-430
P. wenii ITS	396-CGTCTTTTCCACGCTCCAAAGGTGTCGGGGGAAGA-430
P. jiulianshanensis trnL-F	501-GTTCAAAAGTCCTTTATCTT-520
P. wenii trnL-F	501-GTTCAAAATTCCTTTATCTT-520

Taxonomic treatment

***Primulina jiulianshanensis* F.Wen & G.L.Xu, sp.nov.**
urn:lsid:ipni.org:names:77318694-1
Figs 2, 3

Diagnosis. This new species differs from *P. wenii* by the combination of the following characteristics: petiole, both sides of leaf blades, adaxial surface of the calyx lobes, corolla inside toward the bottom, bract margins glandular-pubescent (*vs.* what abovementioned eglandular-pubescent in *P. wenii*); lateral bracts 4–9 × ca. 2 mm, the central one 2–5 × 1–1.5 mm, adaxially glabrous but sparsely pubescent at apex (*vs.* lateral bracts 14–16 × 2.5–3.0 mm, the central one 10–12 × 1.3–1.6 mm, all adaxially pubescent); calyx lobes 8–11 × ca. 2 mm, each side with several brown serrate teeth at apex (*vs.* 14–15 × ca. 2.5 mm and entire); filaments and staminodes sparsely glandular-puberulent (*vs.* glabrous). Detailed morphological comparisons with *P. wenii* are provided in Table 3.

Holotype. China, Jiangxi Province: Ganzhou City, Longnan County, Jiulianshan National Nature Reserve, growing in shady and moist cliffs in the forest, 24°34'8.9"N, 114°25'49.7"E, altitude ca. 440 m, April 20, 2021, *Guo-Liang Xu, JLSXGL-20210420* (Holotype IBK!; Isotype: KUN!)

Description. Herbs perennial, acaulescent, rhizome terete, 1–4 cm long, 0.8–1.5 cm in diam., leaves all basal, 4–8, petiole 10–40 × 4–13 mm, densely villous and very sparsely glandular-pubescent. Leaf blade oblong-elliptic or broadly elliptic, 4–13 × 4–8 cm, thickly chartaceous, more and less fleshly, adaxially pale green to dark green, densely white to light red villous and very sparsely glandular-pubescent, abaxially pale green, densely white villous and pubescent, and very sparsely glandular-pubescent, base apparently asymmetric but cuneate, margin irregularly obtuse-serrate, apex slightly obtuse, lateral veins 4–6 on each side, adaxially inconspicuously sunken, abaxially prominently raised. Inflorescence dichotomous cymes 2–4, axillary, 1–3-branched, 3–9-flowered or more; peduncle and pedicle green, erectly white or light red pubescent; peduncle 5–10 cm long, 2–3 mm in diam.; pedicle 5–15 mm long, 1–2 mm in diam. Bracts 3, lanceolate or spatulate, a pair on either side in same size, opposite, 4–9 mm long, ca. 2 mm wide, the middle one smaller, 2–5 mm long, 1–1.5 mm

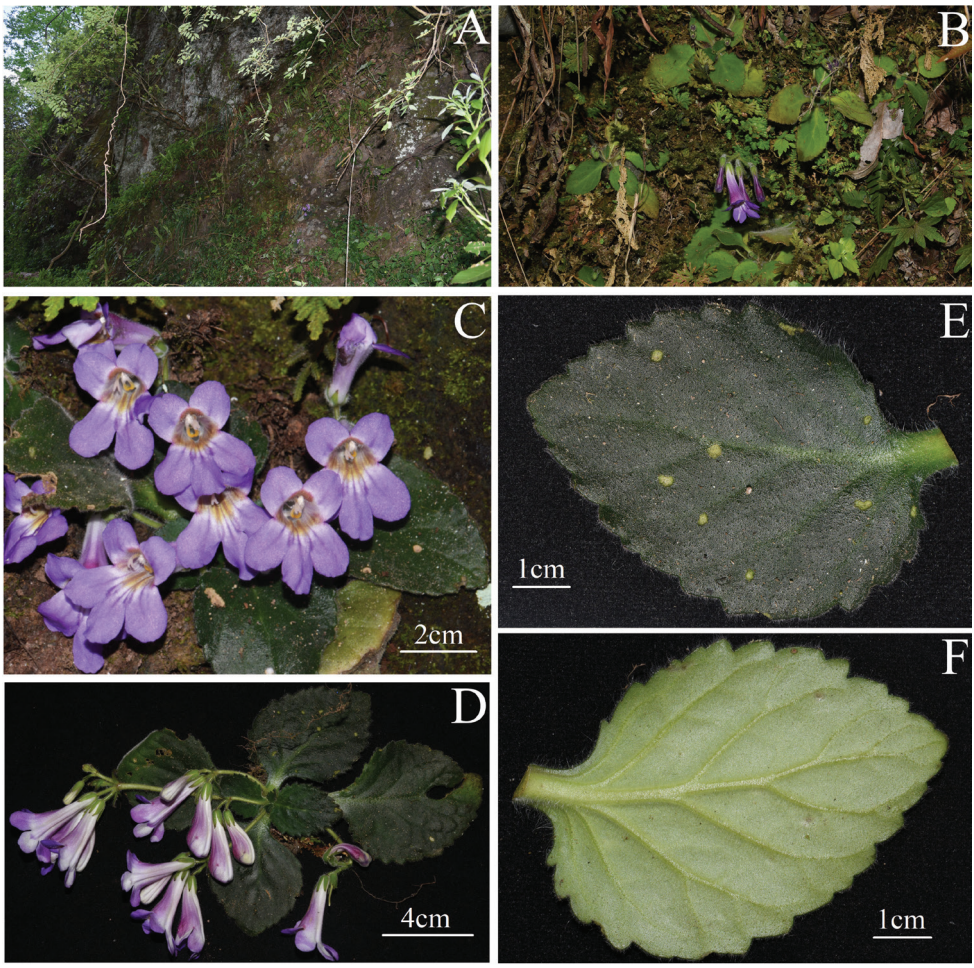

Figure 2. *Primulina jiulianshanensis* sp. nov. **A** habitat **B** population **C** plant in blooming **D** habit **E** adaxial surface of mature leaf blades and petiole **F** abaxial surface of mature leaf blade and petiole.

wide, all three abaxially white or reddish pubescent, adaxially glabrous but sparsely pubescent at apex, margin entire, ciliate and very sparsely glandular-puberulent, apex acute; bracteoles 3, shape and indumentum same as bracts, 2–5 mm long, 1–1.5 mm wide. Calyx 5-parted, lobes lanceolate, 8–11 mm long, ca. 2 mm wide, nearly equal, abaxially densely white or light red villous, adaxially sparsely white puberulent and glandular-puberulent, margin entire but each side of calyx lobes with 1–3 purplish brown crenate at the apex. Corolla pinkish purple to bluish purple, 3.6–4.0 cm long; corolla tube funnelform, 2.6–3 cm long, mouth 1.3–1.6 cm in diam., base ca. 5 mm in diam., outside densely glandular-pubescent, inside from the middle to the base sparsely glandular-puberulent, and the upper part of the corolla tube glabrous; corolla tube abdomen with two obviously longitudinal ridges, the upper part (close to the mouth) of the longitudinal ridge dark bluish purple, and the lower part (close to the bottom)

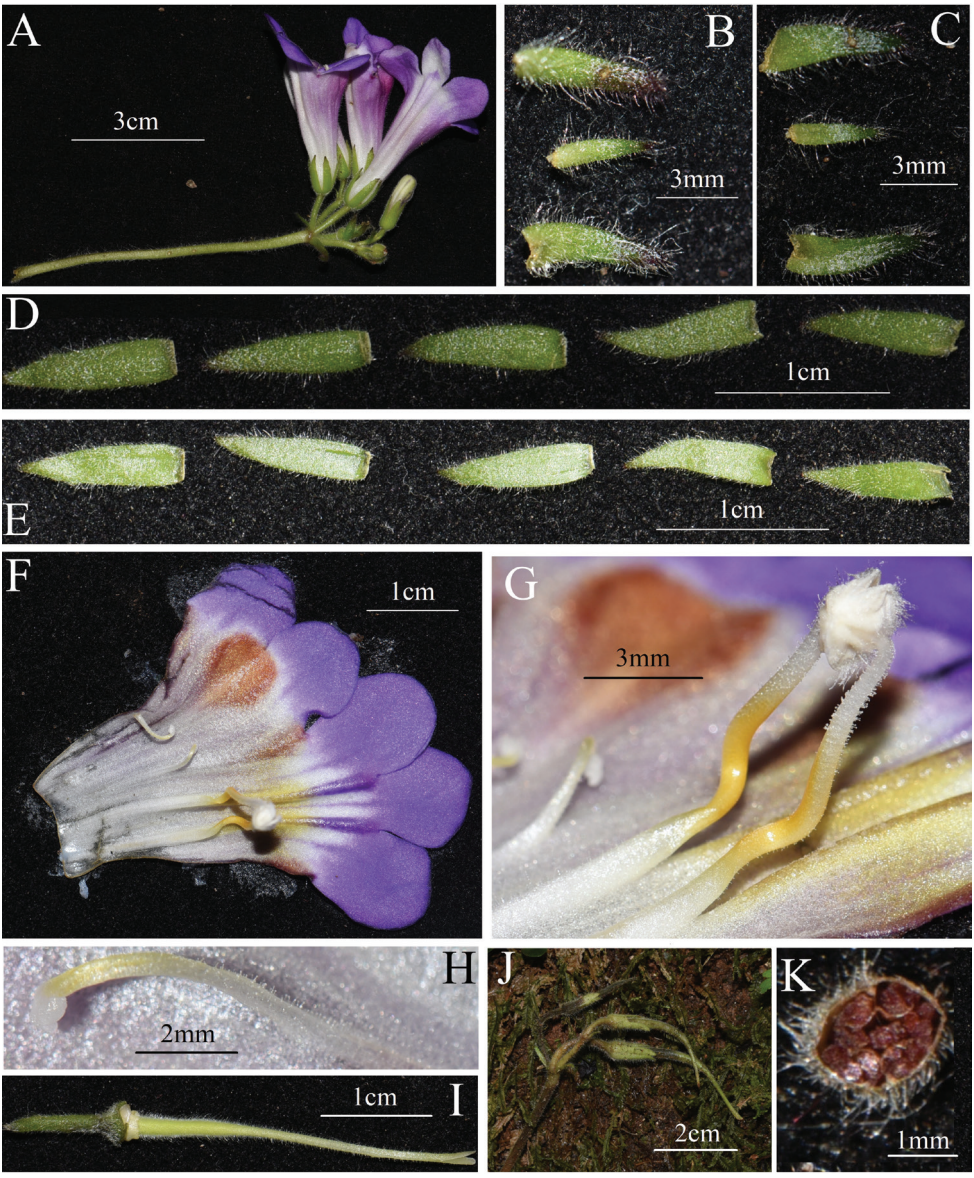

Figure 3. *Primulina jiulianshanensis* sp. nov. **A** cyme **B** adaxial surfaces of bracts **C** abaxial surfaces of bracts **D** adaxial surfaces of calyx lobes **E** abaxial surfaces of calyx lobes **F** opened corolla **G** stamens and anthers **H** one of lateral staminodes **I** pistil **J** immature capsules **K** transverse section of capsule.

changing into yellowish brown; a dark reddish-brown lump on the upper throat of the corolla tube inside and between upper lip lobes, ovate to spatulate, extending to the middle of the corolla tube, the lump densely glandular-puberulent; a narrow triangular thickened dark reddish-brown stripe extending to the middle of the corolla tube inside at each side of corolla tube and at the junction of the abaxial and adaxial lip;

limb distinctly 2-lipped, adaxial lip 2-parted to the middle, lobes broadly ovate to semicircular, apex round, 6–8 mm long, 6–9 mm wide at the bottom; abaxial lip 3-parted to near the base, lobes elliptical to oblong, 8–12 mm long, 7–9 mm wide at the bottom. Stamens 2, adnate to 1.8 cm above the base of corolla tube; filaments linear, yellow from middle to base but white upper half, 8–11 mm long, geniculate near the base, glandular-puberulent; anthers reniform, slightly constricted at the middle, densely villous and fewer glandular-puberulent; staminodes 3, yellowish, lateral ones ca. 6 mm long, adnate to 14 mm above the base of corolla tube, straight, linear, very sparsely glandular-puberulent, apex capitate, the central one ca. 1 mm long, adnate to 5–6 mm above the base of corolla tube, glabrous. Disc annular, ca. 1 mm high, margin undulate, glabrous, white. Pistil pale green, 2.8–3.2 cm long; style linear, 1.9–2.3 cm long, ca. 1 mm in diam., upper part densely glandular-puberulent, lower part densely glandular-puberulent and eglandular-puberulent, ovary oblong, ca. 10 mm long, ca. 2 mm in diam., densely villous and glandular-pubescent, parietal placenta. Stigma acute triangle to narrowly obtrapeziform, 2-lobed, ca. 3 mm long. Capsule linear, 2–4 cm long, parietal placenta, densely villous and glandular-pubescent.

Phenology. Flowering from April to May, fruiting from June to September.

Etymology. The specific epithet '*jiulianshanensis*' is derived from the type locality, Jiulianshan National Natural Reserve, Jiangxi Province, China.

Vernacular name. 九连山报春苣苔 (Chinese name); Jǐu Lían Shān Bào Chūn Jù Tái (Chinese pronunciation).

Distribution and habitat. We found three small subpopulations in Jiulianshan National Nature Reserve in Jiangxi Province, which are distributed in the shady and wet place on the cliffs under the evergreen broad-leaved forest in the reserve. And the new species is mainly acccompanied by *Begonia palmata* D.Don, *Utricularia striatula* J.Smith, *Selaginella moellendorffii* Hieron., *S. involvens* (Sw.) Spring, etc.

Conservation status. At present, only three small subpopulations with total ca. 300 mature individuals of the new species are known in the type locality, Jiulianshan National Natural Reserve, Jiangxi Province, China. The three subpopulations are stable because they are in the reserve. The known AOO and EOO of the new species are about 0.2 km^2 and 25 m^2, respectively. Thus, if considering its fewer individuals of three subpopulations, it should be temporarily assessed as Near Threated (NT), following the IUCN Red List Categories and Criteria (IUCN Standards and petitions committee 2022).

Notes. The mainly morphological differences are showed in diagnosis and Table 3. In addition, the insides of the corolla tube are also somewhat different. For example, at the junction of the abaxial and adaxial lip, there are two narrow triangular thickened dark reddish-brown stripes inside the corolla tube in *Primulina jiulianshanensis*, but there are only two bluish purple spots at the same places in *P. wenii*; at corolla tube abdomen of *P. jiulianshanensis*, the upper parts of the longitudinal ridges are dark bluish purple, and the lower parts are yellowish brown, but the longitudinal ridges inside corolla tube of *P. wenii* are all dark bluish purple; the lump on the upper throat inside corolla tube of *P. jiulianshanensis* is dark reddish-brown, but *P. wenii* is dark bluish brown(Li et al. 2017).

Table 3. Comparisons between the characters of *Primulina jiulianshanensis* and *P. wenii*.

Characters	*Primulina jiulianshanensis*	*P. wenii*
Petiole indumentum	densely villous and very sparsely glandular pubescent	densely villous
Leaf blades indumentum	adaxially densely white to light red villous and very sparsely glandular pubescent, abaxially densely white villous and pubescent, and very sparsely glandular -pubescent	adaxially densely pubescent and villous, abaxially densely appressed pubescent
Bract	lateral ones 4–9 × ca. 2 mm, the middle one 2–5 × 1–1.5 mm, all abaxially white or reddish pubescent, adaxially glabrous but sparsely pubescent at apex, margin ciliate and very sparsely glandular-puberulent	lateral ones 14–16 × 2.5–3.0 mm, the central one 10–12 × 1.3–1.6 mm; outside white pubescent and villous, adaxially white pubescent, margin entire and ciliate
Calyx lobes	adaxially sparsely white puberulent and glandular puberulent, margin entire but each side of calyx lobes with 1–3 brown crenate teeth at apex; lobes 8–11 × ca. 2 mm	adaxially sparsely shortly pubescent to nearly glabrous, margin entire, lobes 14–15 × ca. 2.5 mm
Filament	yellow from middle to base but white upper half, glandular-puberulent	white, glabrous
Staminodes	yellowish, lateral ones very sparsely glandular-puberulent	white, glabrous

The type locality of *Primulina wenii* is Rixi Township, Fuzhou, Fujian Province, while the type locality of *P. jiulianshanensis* is Jiulian Mountain, Jiangxi Province. Their type localities are separated by the Wuyi Mountains, and the two places are more than 500 kilometers apart. *P. wenii* has a narrow distribution range and is only recorded in Rixi Township, Fuzhou, Fujian Province (Li et al. 2017). This area is coastal and the climate zone of this region belongs to the typical subtropical marine monsoon climate. *P. wenii* grows in the limestone evergreen broad-leaved forest area with stable morphology. *P. jiulianshanensis*, grows on the rocks under the evergreen broad-leaved forest in Jiulianshan Nature Reserve, which is a typical Danxia landform. The soil forming rock are mainly sandstone and conglomerate in Jiulianshan Nature Reserve, which has a subtropical monsoon humid climate. The morphology of the *P. jiulianshanensis* in three subpopulations is also relatively stable. Therefore, considering the differences in molecular, morphological, and habitats between *P. jiulianshanensis* and *P. wenii*, they should be classified as two different species.

Except for a few species, such as *Primulina fimbrisepala* (Hand.-Mazz.) Yin Z.Wang, *P. eburnea* (Hance)Yin Z.Wang, *P. tenuituba* (W.T.Wang) Yin Z.Wang, *P. juliae* (Hance) Mich.Möller & A.Weber, most of the species of *Primulina* are narrowly distributed and endemic. Among the known species worldwide, more than 170 species are endemic to Karst areas in southern to southwestern China and to northern Vietnam (Wei 2018; Xu et al. 2020b). However, the diversity of *Primulina* in the Danxia landform has not been well understood so far (Yu et al. 2019). For example, the new species, *P. suichuanensis*, was found in the Danxia landform in Jiangxi Province (Zhou et al. 2016). It should be noted that a new provincial record for *Primulina wenii* from Jiangxi Province was discovered in Jiulianshan Nature Reserve (Liao et al. 2020). However, we carefully examined the voucher specimen (No. PVHJX-05557, stored in GNNU), and we noted that the voucher was collected from the same subpopulation of *P. jiulianshanensis* from the same site in Jiulianshan Nature Reserve. Further, we found there are many incon-

sistencies between the morphological description from the article (Liao et al. 2020) and the corresponding voucher specimens. Thus, this species' new provincial record of *P. wenii* in Jiangxi province is a mistaken identification. Lastly, none of the close relatives of *Primulina* are morphologically similar to this new species found in Jiangxi (Fig. 1). Thus, the new taxon is not easily confused with the others in this province.

Acknowledgements

We want to thank Stephen Maciejewski, the Gesneriad Society, and Michael LoFurno, Associate Professor, Temple University, Philadelphia, USA, for their editorial assistance. This study was financially supported by the Basic Research Fund of Guangxi Academy of Sciences (CQZ-C-1901), the Key Sci. & Tech. Research and Development Project of Guangxi (Guike AD20159091 & ZY21195050), the capacity-building project of SBR of CAS (KFJ-BRP-017-68), Basal Research Fund of GXIB (Guizhifa010) and the Fund of Technology Innovation Alliance of Flower Industry (2020hhlm005).

References

Doyle JJ, Doyle JL (1987) A rapid DNA isolation procedure for small quantities of fresh leaf tissue. Phytochemical Bulletin 19: 11–15.

Du C, Liu J, Ye W, Liao S, Ge BJ, Liu B, Ma JS (2021) Annual report of new taxa and new names for Chinese plants in 2020. Shengwu Duoyangxing 29(8): 1011–1020. https://doi.org/10.17520/biods.2021122

Fu LF, Wen F, Maurin O, Rodda M, Gardner EM, Xin ZB, Wei YG, Monro AK (2022) A revised delimitation of the species-rich genus *Pilea* (Urticaceae) supports the resurrection of *Achudemia* and a new infrageneric classification. Taxon 71(4): 796–813. https://doi.org/10.1002/tax.12711

Hance HF (1883) New Chinese Cyrtandreae. Journal of Botany. British and Foreign 21: 165–170.

IUCN Standards and petitions committee (2022) Guidelines for Using the IUCN Red List Categories and Criteria. Version 15. Prepared by the Standards and petitions committee. https://www.iucnredlist.org/resources/redlistguidelines [Accessed on 4 Mar. 2022]

Katoh K, Misawa K, Kuma K, Miyata T (2002) MAFFT: A novel method for rapid multiple sequence alignment based on fast Fourier transform. Nucleic Acids Research 30(14): 3059–3066. https://doi.org/10.1093/nar/gkf436

Kearse M, Moir R, Wilson A, Stones-Havas S, Cheung M, Sturrock S, Buxton S, Cooper A, Markowitz S, Duran C, Thierer T, Ashton B, Meintjes P, Drummond A (2012) Geneious Basic: An integrated and extendable desktop software platform for the organization and analysis of sequence data. Bioinformatics 28(12): 1647–1649. https://doi.org/10.1093/bioinformatics/bts199

Li J, Chen X, Li S, Yan LJ (2017) *Primulina wenii* (Gesneriaceae), a new species from China. Bangladesh Journal of Plant Taxonomy 24(2): 173–182. https://doi.org/10.3329/bjpt.v24i2.35113

Liao HH, Li L, Wei Y, Liang YL (2020) *Primulina wenii* (Gesneriaceae), a new record species from Jiangxi Province. South China Forestry Science 48(3): 45–46, 71. https://doi.org/10.16259/j.cnki.36-1342/s.2020.03.009

Möller M, Pfosser M, Jang CG, Mayer V, Clark A, Hollingsworth ML, Barfuss MHJ, Wang YZ, Kiehn M, Weber A (2009) A preliminary phylogeny of the 'Didymocarpoid Gesneriaceae' based on three molecular data sets: Incongruence with available tribal classifications. American Journal of Botany 96(5): 989–1010. https://doi.org/10.3732/ajb.0800291

Nguyen LT, Schmidt HA, Haeseler A, Minh BQ (2015) IQ-TREE: A fast and effective stochastic algorithm for estimating maximum-likelihood phylogenies. Molecular Biology and Evolution 32(1): 268–274. https://doi.org/10.1093/molbev/msu300

Ning ZL, Wang J, Tao JJ, Kang M (2014) *Primulina lepingensis* (Gesneriaceae), a new species from Jiangxi, China. Annales Botanici Fennici 51(5): 322–325. https://doi.org/10.5735/085.051.0508

Pan B, Zou LL, Zhang RL, Kang M, Wen F (2017) *Primulina effusa* F.Wen & B.Pan, a new species of Gesneriaceae from limestone areas of South China. Guangxi Zhi Wu 37(10): 1250–1256. https://doi.org/10.11931/guihaia.gxzw201706006

Peng YS, Tang ZB, Xie YF (2021) Inventory of species diversity of Jiangxi vascular plants. China Forestry Publishing House, Beijing, 434 pp.

POWO (2022) Plants of the World Online. Royal Botanic Gardens, Kew. [Accessed 31 October 2022] http://www.plantsoftheworldonline.org/

Ronquist F, Teslenko M, van der Mark P, Ayres DL, Darling A, Höhna S, Larget B, Liu L, Suchard MA, Huelsenbeck JP (2012) Mrbayes 3.2: Efficient Bayesian phylogenetic inference and model choice across a large model space. Systematic Biology 61(3): 539–542. https://doi.org/10.1093/sysbio/sys029

Smissen RD, Breitwieser I, Ward JM (2004) Phylogenetic implications of trans-specific chloroplast DNA sequence polymorphism in New Zealand Gnaphalieae (Asteraceae). Plant Systematics and Evolution 249(1–2): 37–53. https://doi.org/10.1007/s00606-004-0209-0

Wang WT (1982) Notulae de Gesneriaceis Sinensibus (IV). Bulletin of Botanical Research 2(4): 37–64.

Wang WT (1989) Tres Species Novae *Chiritae* (Gesneriaceae) e Hunan. Bulletin of Botanical Research 9(4): 21–28.

Wang WT, Pan KY, Li ZY (1990) Gesneriaceae. In: Wang WT (Ed.) Flora Republicae Popularis Sinicae, Vol. 69. Science Press, Beijing, 331–418.

Wang WT, Pan KY, Li ZY, Weitzman AL, Skog LE (1998) Gesneriaceae. In: Wu ZY, Raven PH (Eds) Flora of China Vol. 18. Science Press, Beijing, and Missouri Botanical Garden Press, St. Louis.

Wang YZ, Mao RB, Liu Y, Li JM, Dong Y, Li ZY, Smith JF (2011) Phylogenetic reconstruction of *Chirita* and allies (Gesneriaceae) with taxonomic treatments. Journal of Systematics and Evolution 49(1): 50–64. https://doi.org/10.1111/j.1759-6831.2010.00113.x

Weber A, Middleton DJ, Forrest A, Kiew R, Lim CL, Rafidah AR, Sontag S, Triboun P, Wei YG, Yao TL, Möller M (2011) Molecular systematics and remodeling of *Chirita* and associated genera (Gesneriaceae). Taxon 60(3): 767–790. https://doi.org/10.1002/tax.603012

Wei YG (2018) The Distribution and Conservation Status of Native Plants in Guangxi, China. China Forestry Publishing House, Beijing, 876 pp.

Xu MZ, Kong HH, Kang M, Yang LH (2020a) A new species of *Primulina* (Gesneriaceae) from Danxia landform in Jiangxi, China. Taiwania 65(2): 163–166. https://doi.org/10.6165/tai.2020.65.163

Xu MZ, Yang LH, Kong HH, Wen F, Kang M (2020b) Congruent spatial patterns of species richness and phylogenetic diversity in karst flora: Case study of *Primulina* (Gesneriaceae). Journal of Systematics and Evolution 59(2): 251–261. https://doi.org/10.1111/jse.12558

Yu XY, Li JM, Ren MX (2019) Adaptive differentiation of Gesneriaceae on karst and Danxia landforms in Southern China. Guangxi Sciences 26(1): 132–140. https://doi.org/10.13656/j.cnki.gxkx.20190321.003

Zhou DS, Zhou JJ, Li M, Yu XL (2016) *Primulina suichuanensis* sp. nov. (Gesneriaceae) from Danxia landform in Jiangxi, China. Nordic Journal of Botany 34(2): 148–151. https://doi.org/10.1111/njb.00956

Supplementary material 1

The tree of the trnL-F plastid marker for *Primulina* species

Author: Zheng-Yu Zuo

Data type: (phylogenetic, genomic, tree)

Explanation note: The *trnL-F* plastid marker and the ITS nuclear marker separately and discuss any incongruences between the two markers, particularly with respect to the position of the new species.

Link: https://doi.org/10.3897/phytokeys.226.96351.suppl1

Supplementary material 2

The tree of the ITS nuclear marker for *Primulina* species

Author: Zheng-Yu Zuo

Data type: (phylogenetic, genomic, tree)

Explanation note: The *trnL-F* plastid marker and the ITS nuclear marker separately and discuss any incongruences between the two markers, particularly with respect to the position of the new species.

Link: https://doi.org/10.3897/phytokeys.226.96351.suppl2

PhytoKeys 226: 17–32 (2023)
doi: 10.3897/phytokeys.226.101221
https://phytokeys.pensoft.net

RESEARCH ARTICLE

A peer-reviewed open-access journal
PhytoKeys
Launched to accelerate biodiversity research

The identity of *Sasa oblongula* C.H.Hu (Poaceae, Bambusoideae, Arundinarieae): evidence from morphology and molecular data

Xing Li[1,2,3], Jing-Bo Ni[1,2], Nian-He Xia[1,2]

1 *Key Laboratory of Plant Resources Conservation and Sustainable Utilization & Guangdong Provincial Key Laboratory of Applied Botany, South China Botanical Garden, Chinese Academy of Sciences, CN-510650, Guangzhou, China* **2** *South China National Botanical Garden, CN-510650, Guangzhou, China* **3** *University of Chinese Academy of Sciences, CN-100049, Beijing, China*

Corresponding author: Nian-He Xia (nhxia@scbg.ac.cn)

Academic editor: E. Ruiz-Sanchez | Received 31 January 2023 | Accepted 20 March 2023 | Published 9 May 2023

Citation: Li X, Ni J-B, Xia N-H (2023) The identity of *Sasa oblongula* C.H.Hu (Poaceae, Bambusoideae, Arundinarieae): evidence from morphology and molecular data. PhytoKeys 226: 17–32. https://doi.org/10.3897/phytokeys.226.101221

Abstract

Sasa oblongula was described in 1987 based on a cultivated plant at the bamboo garden of Sun Yat-sen University. This species has two or three branches at the upper nodes, which differ from the rest of *Sasa* species that have a single branch per node. During the field trip to Baishi Town, Yunfu City, Guangdong Province in July 2021, one bamboo species with oblong foliage leaves was collected and matches the isotype. Then, our question was to test the identity of *S. oblongula* concerning other *Sasa* species based on morphology and molecular data. To do that, we sequenced the whole chloroplast genome of *S. oblongula* and did a phylogenetic analysis. Our morphological results indicate that the new collection is *S. oblongula*. The phylogenetic tree showed that *S. oblongula* is close to *Pseudosasa*, instead of *Sasa* species. Therefore, we transferred it to the genus *Pseudosasa*, and a revised description of *P. oblongula* is provided here.

Keywords

bamboo, China, phylogeny, *Pseudosasa*, taxonomy

Introduction

Sasa oblongula C.H.Hu (1987) was described based on two collections, i.e., *Y. L. Yang & C. H. Hu 198001* (Type) and *T. H. Wen & G. Y. Sheng 79413*, from the bamboo garden of Sun Yat-sen University, Guangdong Province. According to its protologue,

it was transplanted from somewhere in Guangdong with lack of a detailed address and could be distinguished by having small-medium-sized and oblong foliage leaves. It was well recognized and accepted as a distinctive species in the floras (Hu 1996; Wang and Stapleton 2006; Yi et al. 2008; Xia and Lin 2009; Vorontsova et al. 2016; Shi et al. 2022) and websites like GrassBase-The Online World Grass Flora (Clayton et al. 2016), Tropicos (www.tropicos.org), IPNI (www.ipni.org), POWO (powo.science.kew.org), The Plant List (www.theplantlist.org), GBIF (www.gbif.org). After examining paratype specimen *T. H. Wen & G. Y. Sheng 79413* in N and a failed attempt of searching for it in the bamboo garden of Sun Yat-sen University during the revision of Sasinae Keng f. (Keng 1982), Li (2009) treated it as a suspicious species. Significantly, the type specimens and protologue all demonstrated that this bamboo species possessed two or three branches at upper culm nodes, which conflicted with the strictly solitary branch of *Sasa* at each node (Makino and Shibata 1901; Suzuki 1978; Kobayashi 2017; Qin 2019). Thus, *S. oblongula* should not belong to the genus *Sasa* and may be a member of *Pseudosasa* based on the evidence available.

However, the previous molecular phylogenetic analysis (Zeng et al. 2010) showed a surprising result, namely that *S. oblongula*, eight Japanese *Sasa* species (including generic type), and one *Sasaella* Makino (1929) species, formed a subclade within the Arundinaria clade. To date, most Chinese *Sasa* species except *Sasa* subg. *Sasamorpha* have been transferred to *Sinosasa* L.C.Chia ex N.H.Xia, Q.M.Qin & Y.H.Tong and *Yushania* Keng f. (Keng 1957; Qin 2019; Qin et al. 2021; Li et al. 2023). We think that the voucher specimen *Zeng & Zhang 06055* of *S. oblongula* used by Zeng et al. for the molecular analysis is probably misidentified. Thus, the phylogenetic position of *S. oblongula* needs to be further studied with correct samples.

During the field trip to Baishi Town, Yunfu City, Guangdong Province in July 2021, one bamboo species with oblong foliage leaves was found. It matched the isotype very well and shares the same key characters, such as the slightly prominent culm supranodal ridge, the white powdery infranodal region, the glabrous internodes with three branches at an upper node, the solitary secondary branch, three to six foliage leaves clustered at the top of ultimate branches, the small-medium-sized and oblong foliage leaves with glabrous blades and conspicuous transverse veins. Therefore, we are certain that the specimens we collected are *S. oblongula*. Then, our question was to test the identity of *Sasa oblongula* concerning other *Sasa* species based on morphology and molecular data.

Materials and methods

Morphology

The sample of *Sasa oblongula* was collected from Hengjing Villiage, Baishi Town, Yunfu City, Guangdong, China during a field trip in July 2021. Observations and measurements were taken using a magnifier (SZ-6) and a ruler with a scale of 0.5 mm.

Some minor characters such as indumentum on ligules of both culm leaves and foliage leaves were observed with a stereomicroscope (Mshot MZ101). The description was made based on both living and dried material as well as relevant literature (e.g. Hu 1987, 1996; Wang and Stapleton 2006; Xia and Lin 2009). Comparisons between *S. oblongula* and *Pseudosasa cantorii* were conducted based on protologue and type specimens, and relevant specimens involved in the protologue of *Arundinaria cantorii* (≡*Pseudosasa cantorii*). The descriptive terms follow Beentje (2016) and herbaria acronyms follow Thiers (2021).

Sampling

For obtaining reliable results, a reasonable proof strategy with two steps was designed to identify the systematic position of *S. oblongula*. The first step is to test whether *S. oblongula* belongs to *Sasa* based on our plastid tree. The second step is to identify which genus *S. oblongula* belongs to based on SNP tree, mainly due to low discrimination rates for those 'three-branched' genera in plastid results (Guo et al. 2021). For the plastid tree, a total of 24 species from 11 genera were sampled. *Bambusa multiplex* and *Dendrocalamus strictus* were set as the outgroups. All accession numbers and voucher information are listed in Table 1. For the SNP tree, a total of 14 species from seven genera belonging to subtribe Arundinarieae were included. *Chimonobambusa sangzhiensis* was set as outgroup. Particular emphasis in our taxon sampling was placed on the inclusion that several key generic types were all involved in this study, including *Acidosasa*, *Indosasa*, *Oligostachyum*, *Pseudosasa*, and *Sasa*.

DNA extraction and sequencing

Young leaves at the vegetative growth stage were collected in the field. Total genomic DNA was isolated from silica-dried leaves following the manufacturer's specifications TIANGEN Genomic DNA Extraction Kit (TIANGEN, Beijing, China). DNA samples of concentration up to standard (≥1 μg) were sheared into fragments using Covaris M220 (Covaris, Woburn, MA). Insert size of 350 bp fragments were enriched by PCR, and the paired-end (2 × 150 bp) libraries were constructed on NovaSeq 6000 platform. About 20G deep genome skimming (DGS) data were generated. Finally, adapters and low-quality reads were filtered from raw data using Fastp v 0.23.1 (Chen et al. 2018) software.

Plastome assembly and chloroplast DNA regions mapping

The filtered clean reads were utilized to de novo assemble complete chloroplast (cp) genomes using GetOrganelle v 1.6.2 pipeline (Jin et al. 2018). Six k-mer values, including 21, 45, 65, 85, 105,125, were set for plastid contigs connection. Subsequently, the filtered plastid reads were transferred to Bandage (Wick et al. 2015) software for visualization processing. Two opposite plastid sequences exported from Bandage were aligned with the reference sequence *Phyllostachys edulis* (GenBank accession No. HQ337796),

Table 1. List of 24 species with species names, voucher information and GenBank accession numbers for the plastid tree based on eight combined plastid sequences extracted from whole chloroplast genomes (WCG).

Taxon	Voucher information	GenBank accession								
		WCG	atpI/H	psaA-ORF170	rpl32-trnL	rpoB-trnC	rps16-trnQ	trnD/T	trnS/G	trnT/L
Ingroup										
Acidosasa purpurea (Hsueh & Yi) Keng f.	Zhang 07067 (KUN)	/	GU355020	GU355340	GU355500	GU354382	GU354540	GU354700	GU355180	GU354860
Fargesia edulis Hsueh & Yi	Li & Zhang 07051 (KUN)	/	GU355130	GU355450	GU355610	GU354490	GU354650	GU354810	GU355290	GU354970
Indocalamus sinicus (Hance) Nakai	Zeng & Zhang 06081 (KUN)	/	GU355153	GU355473	GU355633	GU354513	GU354673	GU354833	GU355313	GU354993
Pseudosasa hindsii (Munro) C.D.Chu & C.S.Chao	Zhang 07013 (KUN)	/	GU355030	GU355350	GU355510	GU354392	GU354550	GU354710	GU355190	GU354870
Pseudosasa longiligula Wen	Zhang 07021 (KUN)	/	GU355067	GU355387	GU355547	GU354429	GU354587	GU354747	GU355227	GU354907
Sasa kurilensis (Ruprecht) Makino et Shibata	Triplett 223 (KUN)	/	GU355137	GU355457	GU355617	GU354497	GU354657	GU354817	GU355297	GU354977
Sasa oblongula C.H.Hu	Zeng & Zhang 06055 (KUN)	/	GU355112	GU355432	GU355592	GU354472	GU354632	GU354792	GU355272	GU354952
Sasa palmata (Mitford) Camus	Triplett 228 (KUN)	/	GU355141	GU355461	GU355621	GU354501	GU354661	GU354821	GU355301	GU354981
Sasa senanensis (Franchet & Savatier) Rehder	Triplett 146 (KUN)	/	GU355111	GU355431	GU355591	GU354471	GU354631	GU354791	GU355271	GU354951
Sasa tsuboiana Makino	Triplett 133 (KUN)	/	GU355139	GU355459	GU355619	GU354499	GU354659	GU354819	GU355299	GU354979
Sasa veitchii (Carriere) Rehder	Triplett 126 (KUN)	/	GU355138	GU355458	GU355618	GU354498	GU354658	GU354818	GU355298	GU354978
Yushania maculata Yi	Zhang 08006 (KUN)	/	GU355084	GU355404	GU355564	GU354444	GU354604	GU354764	GU355244	GU354924
Acidosasa galuca B.M.Yang	CZY56 (IBSC)	OP850353								
Pseudosasa oblongula (C.H.Hu) N. H. Xia & X. Li	XNH187 (IBSC)	OP874594	/	/	/	/	/	/	/	/
Pseudosasa japonica (Sieb. & Zucc. ex Steu.) Maki. ex Naka.	NH028 (IBSC)	OP874595	/	/	/	/	/	/	/	/
Pseudosasa amabilis (McClure) P. C. Keng ex S. L. Chen et al.	NH032 (IBSC)	OP850358	/	/	/	/	/	/	/	/
Indosasa crassiflora McClure	BH58 (IBSC)	OK558536	/	/	/	/	/	/	/	/
Sinosasa fanjingshanensis N.H.Xia, Q.M.Qin & J.B.Ni	BH124 (IBSC)	OP850348	/	/	/	/	/	/	/	/
Sinosasa longiligulata (McClure) N.H.Xia, Q.M.Qin & J.B.Ni	CZY163 (IBSC)	OP850351	/	/	/	/	/	/	/	/
Oligostachyum sulcatum Z.P.Wang & G.H.Ye	Not provided by the author	MW190089	/	/	/	/	/			
Indosasa sinica C.D.Chu & C.S.Chao	MPF10034 (KUN)	JX513422	/	/	/	/	/	/	/	/
Oligostachyum shiuyingianum (Chia & But) Wang et Ye	DZL09122 (KUN)	JX513423	/	/	/	/	/	/	/	/
Outgroup										
Bambusa multiplex (Loureiro) Raeu. ex Schu. & J. H. Schu.	Not provided by the author	KJ722536	/	/	/	/	/	/	/	/
Dendrocalamus strictus (Roxburgh) Nees	zmy018 (KUN)	MK679802								

and one that matched the genomic direction of the reference was retained. The final cp genomes were manually corrected in Geneious 9.1.4 (Kearse et al. 2012).

After referring to previous plastid phylogeny studies of Arundinarieae (Zeng et al. 2010; Zhang et al. 2012), eight plastid DNA regions (*atpI-atpH*, *psaA-ORF170*, *rpl32-trn*L, *rpoB-trnC*, *rps16-trnQ*, *trnD-trnT*, *trnS-trnG* and *trnT-trnL*) were selected to reconstruct plastid phylogenetic tree. Our cp genomes were annotated from eight DNA regions of *Acidosasa purpurea* with ≥ 70% sequence similarity in Geneious. Then, all the annotated plastid DNA regions were extracted from whole cp genomes. Sequence directions were visualized and adjusted using Mauve v 2.4.0 (Darling et al. 2004).

SNP calling

The latest high-quality genome sequence of moso bamboo (*Phyllostachys edulis*) (Zhao et al. 2018) was selected as the chromosome-level reference genome to build an index using the software SAMtools v 1.9 (Danecek et al. 2021) and Picard v 2.27.3 (Broad Institute 2019). After filtration of low-quality data, our clean reads were processed in removal of duplicates using Fastuniq v 1.1 (Xu et al. 2012). New filtered paired reads were aligned to the reference genome by Bowtie2 v 2.4.4 (Langmead and Salzberg 2012) with the parameter of minimum acceptable alignment score for L, 0.3, 0.3. After that, SAMtools was further employed to sort alignment (BAM files). Picard was utilized to remove duplicates again with the parameter "MarkDuplicates". GATK v 4.2.2.0 (Van der Auwera and O'Connor 2020) was performed to anchor variant calling including SNP and InDel using the joint calling method "HaplotypeCaller" in the genomic variant call format (GVCF). Each sample based on reads with mapping quality was set as at least 10 and the kmer size was set as 10 to 25. After completion of variants calling, the tool "CombineGVCFs" in GATK was carried out to combine all the GVCF files. The tool "GenotypeGVCFs" was then utilized to identify joint-called variants. Subsequently, the tool "SelectVariants" was implemented to select single nucleotide polymorphic sites (SNPs). Filtration of SNPs of low quality was then conducted in the tool "VariantFiltration" with the parameter "QD < 2.0, MQ < 40.0, FS > 60.0, SOR > 3.0, MQRankSum < -12.5 and ReadPosRankSum < -8.0". Finally, the tool "SelectVariants" was run to extract filtered SNPs.

For a reliable phylogenetic tree based on SNP dataset, we considered that filtered raw SNPs with high missing genotype rates and low minor allele frequency will affect the accuracy of the phylogenetic trees and thus should be removed. Therefore, plink v 1.90b4.6 (Purcell et al. 2007) was operated to filter those low-quality SNPs with parameter "geno" set as 0.1 and "maf" set as 0.01. Filtered variants were then pruned with the parameter "indep-pairwise" set as 50, 10, 0.2, representing its window size, a variant count to shift the window and pairwise r2 threshold for SNPs, respectively. Finally, new clean SNP dataset was generated, and the GVCF format was transferred to PHYLIP format for phylogenetic analysis using the python script "vcf2phylip.py" (Ortiz 2019).

Alignments construction and phylogenetic trees inference

Chloroplast DNA regions and SNP dataset were utilized to reconstruct the phylogenetic tree, respectively. Eight plastid matrices were aligned using MAFFT v 7.450 (Katoh and Standley 2013) and concatenated as a super matrix. Maximum likelihood (ML) tree was inferred for plastid and SNP datasets using IQTREE v 1.6 in SH-aLRT test and ultrafast bootstrap (UFBoot) value (Nguyen et al. 2015). Node supports rates with SH-aLRT ≥ 80% and UFboot ≥ 95% were reliable and shown on each node. The final results were visualized with Figtree 1.4.4 (Rambaut 2018).

Result

Morphological comparison

Ssasa oblongula has leptomorph rhizome, glabrous culm internodes, white powdery infranodal region, flat or slightly prominent nodes and culm supranodal ridge, mostly solitary branch at lower culm nodes and two to three (Fig. 3E, if three branches, central slightly dominant than lateral) branches at mid and upper culm nodes, glabrous culm leaf sheath (Fig. 3G) with erect and lanceolate blades, falcate auricles and ligules with ciliolate margin, glabrous foliage leaves blades and conspicuous transverse veins. These vegetative characters mentioned above make it fit well with the circumscription of *Pseudosasa* Makino ex Nakai (1925), rather *Sasa*. After examining the specimens of similar species and referring to the related literature (Munro 1868; Chia et al. 1983), we found that *S. oblongula* is most similar to *P. cantorii* (Munro) P. C. Keng ex S. L. Chen et al. (Zhu et al. 2006) by sharing one to three branches per nodes, glabrous internodes, the white powdery infranodal region, slightly prominent supranodal ridge, culm leaf sheath with falcate auricles, erect and lanceolate blades with serrulate margin, foliage leaf sheath with ciliate margin and truncate ligules, glabrous foliage leaf blades with conspicuous transverse veins, but differs by having nearly solid (vs. hollow) culm internode with appressed (vs. patent) branches, intravaginal (vs. transferred) and glabrous (vs. setose) abaxially culm leaf sheath with ciliate upper (vs. wholly) margin and arched (vs. truncate) ligules with ciliolate (vs. glabrous) margin, 3–6 foliage leaves with irregular (vs. coplanar) arrangement clustered at the top ultimate branch, glabrous (vs. hirsute) abaxially foliage leaf sheath with 1–4 mm (vs. 5–13 mm) long length per adjacent sheath apex, small-medium-sized (7–10 × 1.5–2.6 cm vs. 12.5–25 × 2.5–3.2 cm) foliage leaf blades with 6–7-paired (vs. 7–9-paired) secondary veins. A more detailed comparison between the two species is provided in Table 2.

Phylogenetic analysis

To make clear the position of *S. oblongula* and its relationship with *P. cantorii*, phylogenetic Maximum likelihood analysis was conducted based on plastid, and SNP dataset was shown with SH-aLRT and UFboot values noted at each node. Our plastid phylo-

Table 2. Comparison of *Pseudosasa oblongula* and *Pseudosasa cantorii*.

Morphology	*Pseudosasa oblongula*	*Pseudosasa cantorii*
Culm internode	Nearly solid, with appressed branches	Hollow, with patent branches
Culm leaves	Intravaginal, glabrous abaxially	Transferrd, setose abaxially and readily deciduous when old
Margin	Ciliate on the upper	Ciliate wholly
Ligule	Arched, with ciliolate margin	Truncate, with glabrous margin
Foliage leaves	3–6, with irregular arrangement clustered at the top ultimate branch	4–7, with a coplanar arrangement at the top ultimate branch
Sheath	Glabrous abaxially, 1–4 mm long per adjacent sheath apex	Hirsute abaxially, 5–13 mm long per adjacent sheath apex
Blades	7–10 × 1.5–2.6 cm, with 6–7-paired secondary veins	12.5–25 × 2.5–3.2 cm, with 7–9-paired secondary veins

genetic tree indicated that *S. oblongula* was distantly related to those Japanese *Sasa* species (including generic type) (Fig. 4, SH-aLRT=99.5% & UFboot=100%) and those *Sinosasa* species (SH-aLRT=100% & UFboot=100%) previously assigned to *Sasa* from China (Qin et al. 2021). The SNP phylogenetic tree suggested that *S. oblongula* was sister to *P. cantorii* with strong support (Fig. 5, SH-aLRT=100% & UFboot=100%), supporting our morphological study well.

Taxonomic treatment

Pseudosasa oblongula **(C.H.Hu) N.H.Xia & X.Li, comb. nov.**
urn:lsid:ipni.org:names:77317186-1
Figs 1–3

Sasa oblongula C. H. Hu, J. Bamboo Res., 6(4):18 (1987). Basionym.

Type. China. Guangdong: type locality unknown, cultivated in Bamboo Garden, Sun Yat-sen University, 5 April 1980, *Y. L. Yang & C. H. Hu 198001* (holotype: N, photo!; isotypes: N019023154, Fig. 1A; N019023155, image!; N019023156, Fig. 1B)

Description. Shrubby bamboo, rhizomes leptomorph. Culm erect, 1–1.5 m tall, 2–7 cm in diameter; branches appressed, usually 1 branch at the lower culm nodes and 2–3 at the mid or upper nodes of culm (if 3 branches, central slightly dominant than lateral); internodes terete or slightly flattened above branches, 5–27 cm long, glabrous, nearly solid; nodes flat or slightly prominent, white powdery under nodes; supranodal ridge flat or slightly prominent; intranodes 5–8 mm high, glabrous; culm buds solitary, ovate to elliptic, light yellow, puberulent abaxially at upper part, ciliolate on the upper margin, apex obtuse. Culm leaf sheath persistent or deciduous later, intravaginal, thinly leathery, 1/3–2/3 as long as internodes, glabrous abaxially, ciliate on the upper margin and sometimes glabrescent, longitudinal ribs conspicuous; sheath scar with remains of sheath base; auricles falcate to long-elliptic, obliquely ascending, 2–4 × 1–2 mm; oral setae erect or slightly curved, 3–10 mm long; ligule entire, 0.5–1 mm high, asperous abaxially, ciliolate on the margin, apex arched; blades narrowly lanceolate to lanceolate, erect, glabrous abaxially, margin sparsely serrate. Foliage leaves 3–6

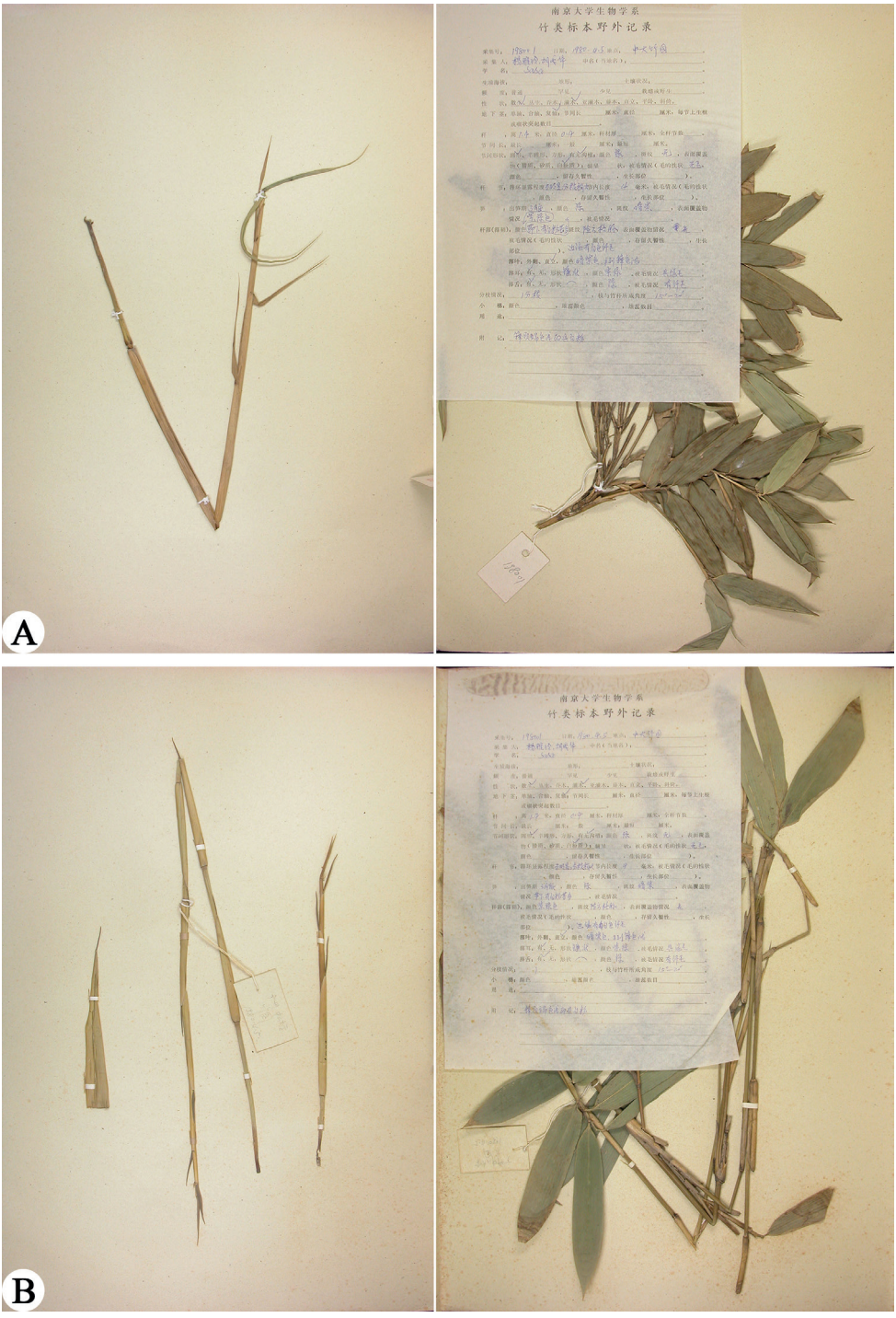

Figure 1. Isotypes of *Pseudosasa oblongula, Y.L. Yang & C.H. Hu 198001* (**A** N019023154 **B** N019023156). Photos downloaded from Chinese Virtual Herbarium (https://www.cvh.ac.cn/).

Figure 2. *Pseudosasa oblongula* (C.H.Hu) N. H. Xia & X. Li, *N. H. Xia XNH-187* (IBSC). Photo by Xing Li.

clustered at the top of ultimate branches, with irregular arrangement; sheath thinly leathery, glabrous abaxially, margins densely ciliate, sometimes glabrous, thinly white-powdery, longitudinal ribs conspicuous, length per adjacent sheath apex very short, 1–4 mm; auricles undeveloped, ovate to falcate or absent, 1–3 × 1–1.5 mm; oral setae erect or curved, 5–10 mm long, usually deciduous when old; inner ligule 0.5–1 mm high, densely ciliolate on margin, apex truncate; outer ligule ca. 0.5 mm high, ciliolate on margin; blades oblong to oblong-lanceolate, papyraceous, 7–10 × 1.5–2.6 cm,

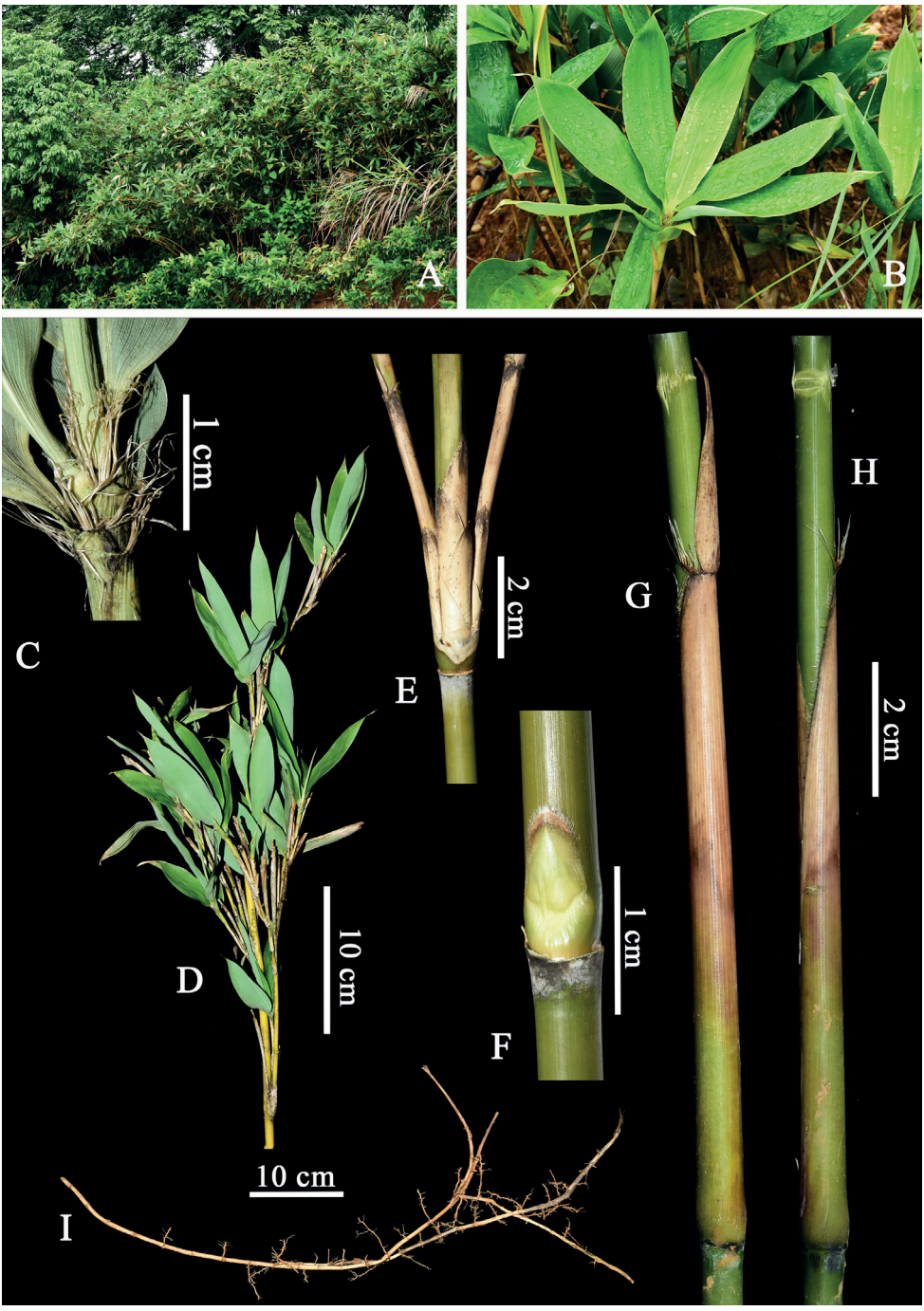

Figure 3. *Pseudosasa oblongula* (C.H.Hu) N. H. Xia & X. Li **A** habit **B** foliage leaf, showing oblong blade **C** part of terminal branch, showing sheath and ligule **D** partial culm and branches **E** nodes of the upper culm, showing three branches complement **F** culm bud **G, H** culm leaf, showing lanceolate blades, falcate auricles and glabrous sheath **I** leptomorph rhizomes. Photos **E, F** by Zhuo-yu Cai, others by Xing Li.

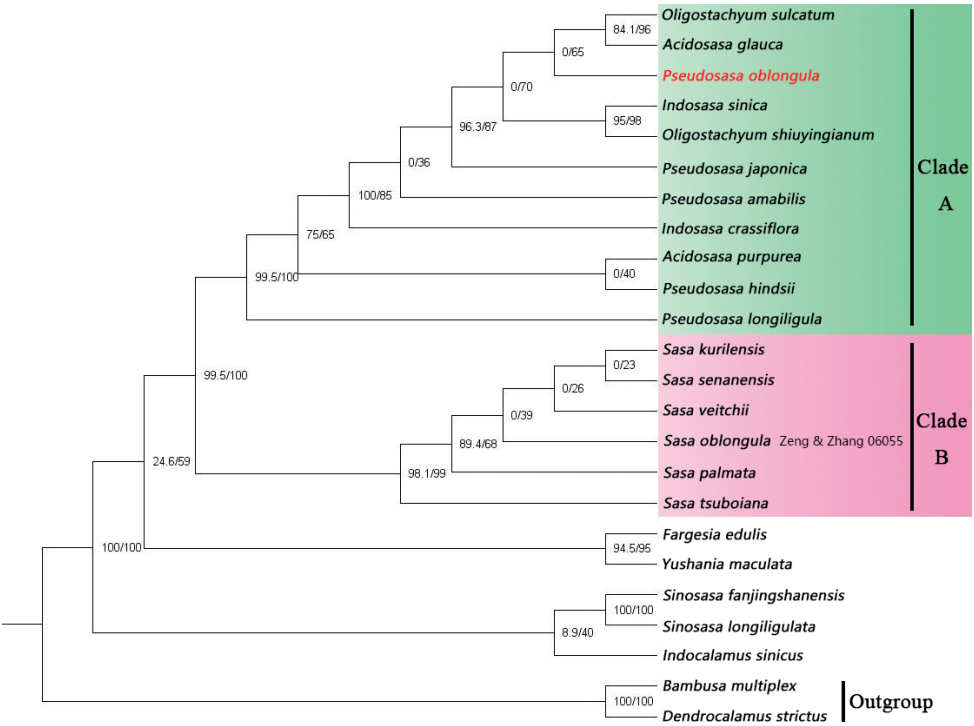

Figure 4. Phylogenetic relationships of *Pseudosasa oblongula* and other 23 species of which most taxa belong to the tribe Arundinarieae based on eight combined plastid sequences. The value of the SH-aLRT test (left) and ultrafast bootstrap (right) are indicated on each node.

glabrous adaxially and abaxially, apex acute to attenuate, base obtuse to unequal rounded, margin serrate; secondary veins 6–7 pairs, tertiary veins 6–7 pairs, transverse veins conspicuous; petioles 2–4 mm long, glabrous; Inflorescence unknown.

Phenology. New shoots were produced from March to July.

Vernacular names. Jǔ Yè Shǐ Zhú (Chinese pronunciation); 矩叶矢竹 (Chinese name).

Additional specimens examined. *Pseudosasa oblongula*: China. Guangdong: type locality unknown, cultivated in Bamboo Garden, Sun Yat-sen University, 12 April 1979, *T. H. Wen & G. Y. Sheng 79413* (JSB518673 image!); Yunfu City, Yunan County, Baishi Town, Hengjing village, 4 July 2021, *N. H. Xia XNH-187* (IBSC!); ibid. 22°52'8"N, 111°51'59"E, elev. 206 m, 11 June 2022, *J. B. Ni & X. Li LX142* (IBSC!). ***Pseudosasa cantorii*:** China. Hong Kong: Lantau Island, *Cantor s.n.*, quoad foliage leaf (K000876243, image!); Green Island, 1 May 1981, *L. C. Chia et al. Nan-zhu 2875* (US 00031256, image!); Shatin, Siu Lek Yuen, 18 Oct. 1980, *L. C. Chia et al. Nan-zhu 2823* (US00031257, image!); ibid. *L. C. Chia et al. Nan-zhu 2830* (US00031259, image!); Xinjie, Jiadaoli Farm, 22 April 1981, *Nan-zhu 2867* (IBSC!); ibid. 15 October 1980, *Nan-zhu 2810* (IBSC!).

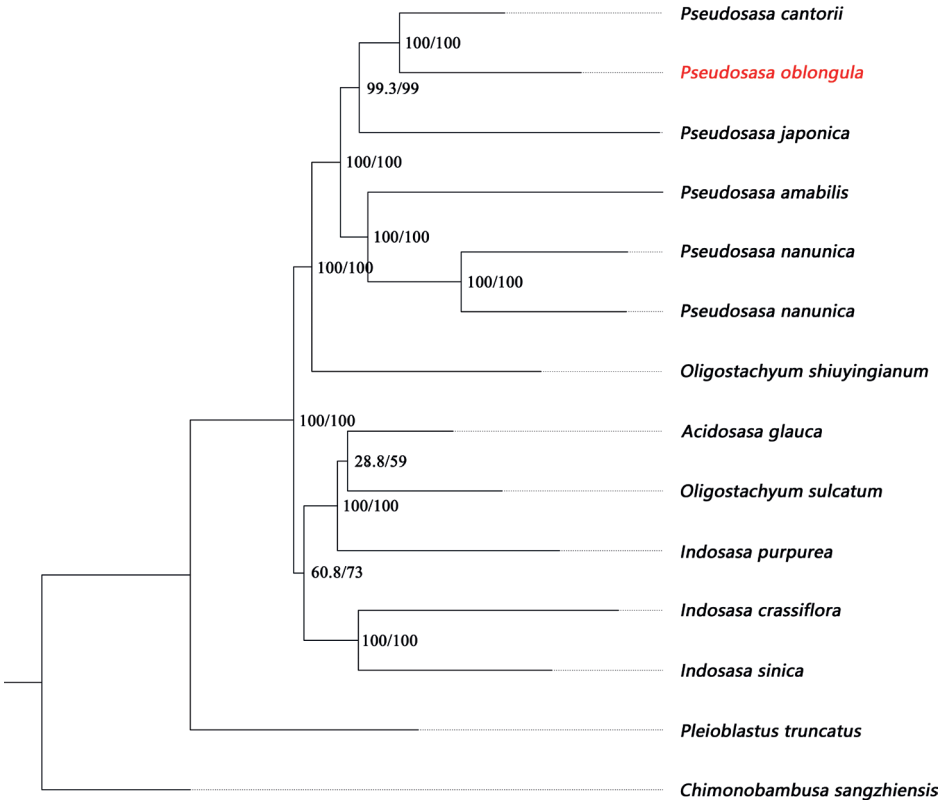

Figure 5. Phylogenetic relationships of *Pseudosasa oblongula* and other 13 species belong to the tribe Arundinarieae based on single nucleotide polymorphism dataset. The value of SH-aLRT test (left) and ultrafast bootstrap (right) are indicated on each node.

Discussion

Sasa oblongula, mainly characterized by its oblong foliage leaves, was published based on sterile materials introduced in the bamboo garden of Sun Yat-sen University. It differed from Japanese *Sasa* species by having 1–3 branches per node (vs. 1 branch) and remote geographic distribution, indicating that it was not obviously the member of *Sasa*. After the examination of the voucher specimen *Zeng & Zhang 06055* from Zeng et al. (2010), we were certain that this specimen does not represent *S. oblongula* since it possesses solitary branch at upper culm nodes, undeveloped or absent culm leaf auricles, and long-lanceolate foliage leaf blades. Our phylogenetic study revealed that the actual *S. oblongula* and those Japanese *Sasa* species are dispersed in two different clades (Fig. 4, Clade A & B). Furthermore, it and *P. cantorii* form a well-supported clade with two different branch lengths based on SNP phylogenetic tree (Fig. 5), supporting the result of morphology.

However, previous studies (Zhang et al. 2012; Guo et al. 2021) showed that *Pseudosasa* is polyphyletic, and the phylogenetic relationships between *Pseudosasa* and several other genera of subtribe Arundinariinae (Zhang et al. 2020), such as *Pleioblastus*, *Oligostachyum*, *Indosasa*, etc., have not been resolved. *Sasa oblongula* was closely related

to Chinese *Pseudosasa* species in morphology and phylogeny, and thus was congruently assigned to the genus *Pseudosasa* here. Accordingly, a new combination *Pseudosasa oblongula* (C. H. Hu) N. H. Xia & X. Li was proposed.

Acknowledgements

We thank Dr. Qiang Fan for hosting our visits to the Bamboo garden of Sun Yat-sen University and Zhuo-yu Cai for taking some photos of type specimens of *Sasa oblongula*. This research was funded by the Guangdong Basic and Applied Basic Research Foundation (grant no. 2021A1515011302) and the National Natural Science Foundation of China (grant no. 32270227).

References

Beentje H (2016) The Kew Plant Glossary, Second Edition. Royal Botanic Gardens, Kew, London, 184 pp.

Broad Institute (2019) Picard Toolkit. Broad Institute, GitHub repository.

Chen SF, Zhou YQ, Chen YR, Gu J (2018) fastp: An ultra-fast all-in-one FASTQ preprocessor. Bioinformatics 34(17): i884–i890. https://doi.org/10.1093/bioinformatics/bty560

Chia LZ, Fung HL, Paul PB (1983) Notes on Gramineae: Bambusoideae in Hong Kong. Kew Bulletin 37(4): e591. https://doi.org/10.2307/4109728

Clayton WD, Vorontsova M, Harman KT, Williamson H (2016) GrassBase-The online world grass flora. https://kew.org/data/grasses-db/index.html [accessed 19 March 2023]

Danecek P, Bonfield JK, Liddle J, Marshall J, Ohan V, Pollard MO, Whitwham A, Keane T, McCarthy SA, Davies RM, Li H (2021) Twelve years of SAMtools and BCFtools. GigaScience 10(2): giab008. https://doi.org/10.1093/gigascience/giab008

Darling ACE, Mau B, Blattner FR, Perna NT (2004) Mauve: Multiple alignment of conserved genomic sequence with rearrangements. Genome Research 14(7): 1394–1403. https://doi.org/10.1101/gr.2289704

Guo C, Ma PF, Yang GQ, Ye XY, Guo Y, Liu JX, Liu YL, Eaton DAR, Guo ZH, Li DZ (2021) Parallel ddRAD and genome skimming analyses reveal a radiative and reticulate evolutionary history of the temperate bamboos. Systematic Biology 70(4): 756–773. https://doi.org/10.1093/sysbio/syaa076

Hu CH (1987) A new species of *Sasa* from Guangdong. Journal of Bamboo Research 6(4): 18–20.

Hu CH (1996) *Sasa* Makino et Shibata. In: Geng BJ, Wang ZP (Eds) Flora Reipublicae Popularis Sinicae (Vol. 9). Science Press, Beijing, 662–675.

Jin JJ, Yu WB, Yang JB, Song Y, Yi TS, Li DZ (2018) GetOrganelle: a simple and fast pipeline for de novo assembly of a complete circular chloroplast genome using genome skimming data. bioRxiv 256479. https://doi.org/10.1101/256479

Katoh K, Standley DM (2013) MAFFT: multiple sequence alignment software version 7: improvements in performance and usability. Molecular Biology and Evolution 30(4): 772–780. https://doi.org/10.1093/molbev/mst010

Kearse M, Moir R, Wilson A, Stones-Havas S, Cheung M, Sturrock S, Buxton S, Cooper A, Markowitz S, Duran C, Tierer T, Ashton B, Meintjes P, Drummond A (2012) Geneious Basic: An integrated and extendable desktop software platform for the organization and analysis of sequence data. Bioinformatics 28(12): 1647–1649. https://doi.org/10.1093/bioinformatics/bts199

Keng PC (1957) One new genus and two new species of Chinese bamboos. Zhiwu Fenlei Xuebao 6: 355–362.

Keng PC (1982) A revision of the genera of bamboos from the world. Journal of Bamboo research 1(1): 1–19.

Kobayashi M (2017) The Illustrated Book of Plant Systematics in Color Bambusoideae in Japan. The Hokuryukan Press, 435 pp.

Langmead B, Salzberg SL (2012) Fast gapped-read alignment with Bowtie 2. Nature Methods 9(4): 357–359. https://doi.org/10.1038/nmeth.1923

Li L (2009) Systematic Studies on Sasinae. PhD Thesis, Nanjing Forestry University, China.

Li X, Ni JB, Tan F, Tong YH, Xia NH (2023) *Yushania tomentosa* (Poaceae, Bambusoideae), a new combination from Guangxi. PhytoKeys 218: 11–18. https://doi.org/10.3897/phytokeys.218.97312

Makino T (1929) A Contribution to the Knowledge of the Flora of Japan. Shokubutsu Kenkyu Zasshi 6: 1–15.

Makino T, Shibata K (1901) On *Sasa*, a new genus of Bambuseae, and its affinities. Botanical Magazine Tokyo 15(168): 18–31. https://doi.org/10.15281/jplantres1887.15.168_18

Munro W (1868) A Monograph of the Bambusaceae, including Description of all the Species. Transactions of the Linnean Society of London 26(1): e111. https://doi.org/10.1111/j.1096-3642.1968.tb00502.x

Nakai T (1925) Two new genera of Bambusaceae, with special remarks on the related genera growing in eastern Asia. Journal of the Arnold Arboretum 6: e150. https://doi.org/10.5962/bhl.part.24130

Nguyen LT, Schmidt HA, von Haeseler A, Minh BQ (2015) IQ-TREE: A fast and effective stochastic algorithm for estimating maximum likelihood phylogenies. Molecular Biology and Evolution 32(1): 268–274. https://doi.org/10.1093/molbev/msu300

Ortiz EM (2019) vcf2phylip v2.0: convert a VCF matrix into several matrix formats for phylogenetic analysis.

Purcell S, Neale B, Todd-Brown K, Thomas L, Ferreira MAR, Bender D, Maller J, Sklar P, de Bakker PIW, Daly MJ, Sham PC (2007) PLINK: A toolset for whole-genome association and population-based linkage analysis. American Journal of Human Genetics 81(3): 559–575. https://doi.org/10.1086/519795

Qin QM (2019) Taxonomic studies of *Sasa* Makino & Shibata and *Gigantochloa* Kurz ex Munro (Poaceae: Bambusoideae) from China. PhD Thesis, University of Chinese Academy of Sciences, China.

Qin QM, Tong YH, Zheng XR, Ni JB, Xia NH (2021) *Sinosasa* (Poaceae: Bambusoideae), a new genus from China. Taxon 70(1): 27–47. https://doi.org/10.1002/tax.12422

Rambaut A (2018) FigTree, version v.1.4.4. http://tree.bio.ed.ac.uk/software/figtree/ [accessed 25 October 2020]

Shi JY, Che BY, Zhang YX, Zhou DQ, Ma LS, Yao J (2022) *Sasa* Makino & Shibata. In: Yi TP, Shi JY, Zhang YX, Zhou DQ, Ma LS, Yao J (Eds) Illustrated Flora of Bambusoideae in China (Vol. 2). Science Press, Beijing & Springer Nature, Singapore, 381–396. https://doi.org/10.1007/978-981-16-2758-3_43

Suzuki S (1978) Index to Japanese Bambusaceae. Gakken Press, 384 pp.

Thiers B (2021) Index Herbariorum: A global directory of public herbaria and associated staff. New York Botanical Garden's Virtual Herbarium. http://sweetgum.nybg.org/ih

Van der Auwera GA, O'Connor BD (2020) Genomics in the Cloud: Using Docker, GATK, and WDL in Terra (1st edn). O'Reilly Media, 506 pp.

Vorontsova MS, Clark LG, Dransfield J, Govaerts R, Baker WJ (2016) World Checklist of Bamboos and Rattans. INBAR Technical Report No. 37. International Network of Bamboo & Rattan, Beijing, 454 pp.

Wang ZP, Stapleton CMA (2006) *Sasa* Makino et Shibata. In: Wu ZY, Raven P (Eds) Flora of China (Vol. 22). Science Press, Beijing & Missouri Botanical Garden Press, St. Louis, 109–112.

Wick RR, Schultz MB, Justin Z, Holt KE (2015) Bandage: Interactive visualization of *de novo* genome assemblies. Bioinformatics 31(20): 3350–3352. https://doi.org/10.1093/bioinformatics/btv383

Xia NH, Lin RS (2009) Bambusoideae. In: South China Botanical Garden, Chinese Academy of Sciences (Eds) Flora of Guangdong (Vol. 9). Guangdong Science and Technology Press, Guangzhou, 224–325.

Xu H, Qian J, Pang X, Song J, Qian G, Chen J, Chen S (2012) FastUniq: A fast de novo duplicates removal tool for paired short reads. PLoS ONE 7(12): e52249. https://doi.org/10.1371/journal.pone.0052249

Yi TP, Shi JY, Ma LS, Wang HT, Yang L (2008) Iconographia Bambusoidearum Sinicarum. Science Press, Beijing, 763 pp.

Zeng CX, Zhang YX, Triplettd JK, Yang JB, Li DZ (2010) Large multi-locus plastid phylogeny of the tribe Arundinarieae (Poaceae: Bambusoideae) reveals ten major lineages and low rate of molecular divergence. Molecular Phylogenetics and Evolution 56(2): 821–839. https://doi.org/10.1016/j.ympev.2010.03.041

Zhang YX, Zeng CX, Li DZ (2012) Complex evolution in Arundinarieae (Poaceae: Bambusoideae): Incongruence between plastid and nuclear GBSSI gene phylogenies. Molecular Phylogenetics and Evolution 63(3): 777–797. https://doi.org/10.1016/j.ympev.2012.02.023

Zhang YX, Guo C, Li DZ (2020) A new subtribal classification of Arundinarieae (Poaceae, Bambusoideae) with the description of a new genus. Plant Diversity 42(3): 127–134. https://doi.org/10.1016/j.pld.2020.03.004

Zhao HS, Gao ZM, Wang L, Wang JL, Wang SB, Fei BH, Chen CH, Shi CC, Liu XC, Zhang HL, Lou YF, Chen LF, Sun HY, Zhou XQ, Wang SN, Zhang C, Xu H, Li LC, Yang YH, Wei YL, Yang W, Gao Q, Yang HM, Zhao SC, Jiang ZH (2018) Chromosome-level reference genome and alternative splicing atlas of moso bamboo (*Phyllostachys edulis*). GigaScience 7(10): giy115. https://doi.org/10.1093/gigascience/giy115

Zhu ZD, Li DZ, Stapleton CMA (2006) *Pseudosasa* Makino ex Nakai. In: Wu ZY, Raven P (Eds) Flora of China (Vol. 22). Science Press, Beijing & Missouri Botanical Garden Press, St. Louis, 115–121.

Supplementary material 1

SNP matrix

Authors: Xing Li

Data type: phylogenetic

Explanation note: This SNP matrix contains 14 species with 36490 bp.

Link: https://doi.org/10.3897/phytokeys.226.101221.suppl1

PhytoKeys 226: 33–51 (2023)
doi: 10.3897/phytokeys.226.103500
https://phytokeys.pensoft.net

RESEARCH ARTICLE

A peer-reviewed open-access journal
PhytoKeys
Launched to accelerate biodiversity research

Morphology, taxonomy, biogeography and ecology of *Micrasterias foliacea* Bailey ex Ralfs (Desmidiales, Zygnematophyceae)

Anatoliy Levanets[1], Sanet Janse van Vuuren[1]

1 *Unit for Environmental Sciences and Management, North-West University, Private Bag X6001, Potchefstroom, 2520, South Africa*

Corresponding author: Anatoliy Levanets (20868421@nwu.ac.za)

Academic editor: W.-H. Kusber | Received 14 March 2023 | Accepted 19 April 2023 | Published 9 May 2023

Citation: Levanets A, Janse van Vuuren S (2023) Morphology, taxonomy, biogeography and ecology of *Micrasterias foliacea* Bailey ex Ralfs (Desmidiales, Zygnematophyceae). PhytoKeys 226: 33–51. https://doi.org/10.3897/phytokeys.226.103500

Abstract

Micrasterias foliacea (Desmidiales, Zygnematophyceae) is an interesting desmid species as its filamentous life form is quite different from all other species within the genus. Due to the large size of the filaments and cells, accurate species identification is easy. After its original description from Rhode Island (USA) it was recorded from five continents, but no record could be found of its presence in Europe. In this paper a review of the worldwide distribution of *M. foliacea* (Desmidiales, Zygnematophyceae) is presented, together with notes on the species' ecology. In addition to its currently known geographical distribution, the paper also records the species' presence at two new locations in southern Africa, namely Botswana (Okavango River) and Mozambique (Palma, Cabo Delgado). The paper presents a discussion of taxonomical levels of intraspecific taxa, based on morphological characteristics. It is proposed that the taxonomical status of *M. foliacea* Bailey ex Ralfs f. *nodosa* should be raised to the variety, as its nodular cell wall thickenings are unique morphological features.

Keywords

Botswana, global distribution, Mozambique, new records, taxonomy

Introduction

The genus *Micrasterias* C. Agardh ex Ralfs (1848: 48) (Desmidiales, Zygnematophyceae) accounts for 95 currently taxonomically accepted species (Guiry and Guiry 2023), however in AlgaeBase there are more than 900 species and intraspecific names (Guiry and Guiry 2023).

Species of the genus *Micrasterias* consists mostly of single cells, each divided into two symmetrical semicells which are mirror images of each other. There is only one filamentous species within the genus, namely *Micrasterias foliacea* Bailey ex Ralfs. This species was initially described from Rhode Island (United States of America) in a letter from Prof. J.W. Bailey addressed to John Ralfs in 1847, and it was published and illustrated by the latter in the British Desmidieae (Ralfs 1848: 210).

At later stages *M. foliacea* was also recorded in Asia (Bangladesh, Cambodia, China, India, Indonesia, Japan, Malaysia, Myanmar, Nepal, Papua New Guinea, Pakistan, Philippines, Russia, Singapore, South Korea, Sri Lanka, Taiwan, Thailand, and Vietnam), North America (Canada, USA), Central America (Cuba, Nicaragua, Panama) and South America (Argentina, Bolivia, Brazil, Suriname, Venezuela), Australia and Africa. Currently, this species is known from 17 countries on the African continent, mostly from tropical central Africa (Benin, Cameroon, Chad, Côte d'Ivoire, Democratic Republic of Congo, Guinea, Mali, Niger, Nigeria, Sierra Leone, Tanzania), Madagascar, and southern Africa (Botswana, Mozambique, South Africa, Zambia, Zimbabwe).

In addition to the type species, several forms and varieties were described from tropical regions of Asia and two from South America based on cell dimensions and morphology (ornamentation, size and position of the spines, cell wall thickenings).

In this paper we report on the presence of this species in two new locations in southern Africa, namely the Okavango River in Botswana and a wetland in northern Mozambique.

Material and methods

In Botswana grab samples were collected in the Okavango River near Shakawe during January 2015. The samples were fixed with 10% ethanol to preserve the algae. The water lily, genus *Nymphaea* L., dominated at the sampling site during sampling.

In Mozambique samples were collected during October 2011 near Palma, Cabo Delgado, just south of the Tanzanian border. Water samples were collected from seven sites in an inland wetland system with soft black peat-like sediment. All samples were preserved with 10% ethanol. The samples in which *M. foliacea* were found were deposited in the North-West University Diatom Collection and Herbarium (sample no. 12-140, 12-142 and 12-436).

The samples were examined using a Leica DM2500 LED compound microscope equipped with phase contrast objectives and a Flexacam C3 microscope digital camera.

An investigation of all scientific literature, phycological inventories, technical reports and internet databases (Atlas of Living Australia 2022; Guiry and Guiry 2023; The Global

Biodiversity Information Facility 2023) was carried out to account for all existing records of *M. foliacea*, including intraspecific names and nomenclatural synonyms. Where possible, the citation, along with geographical locations and ecological characteristics of the habitats, was recorded. A desktop study of all published scientific literature, mentioning the ecology of the species, was also made to determine its ecological preferences.

Results and discussion

In the following paragraphs the taxonomy, morphology, geographical distribution, habitat and ecology of the different varieties of *M. foliacea* will be discussed.

1. *Micrasterias foliacea* [var. *foliacea*] Bailey ex Ralfs, 1848

Micrasterias foliacea [var. *foliacea*] Bailey ex Ralfs, 1848. "The British Desmidiaceae": 210, tab. 35, fig. 3.

Synonyms. *M. foliacea* Bailey *in lit. cum icone* 1847; *M. foliacea* Bailey ex Ralfs f. α typica Turner, 1892. "Algae Aquae Dulcis Indiae Orientalis": 94, tab. 6, figs 12–14; *M. foliacea* Bailey ex Ralfs var. *granulifera* J.A. Cushman, 1908. "Rhodora" 10(114): 111.

The earliest description of *M. foliacea* var. *granulifera* by Cushman (1908) is doubtful, and no drawings or micrographs were provided. Cushman (1908) indicated that var. *granulifera* is similar to the type, but in addition the surface is covered with large irregularly disposed granules. Later, Krieger (1939) classified this variety as a synonym of the type variety, which is currently accepted.

Morphology. Fig. 1 illustrates the morphology of *M. foliacea* var. *foliacea* found in the Mozambique samples. It is the only species of *Micrasterias* where the cells are permanently attached to each other to form a ribbon-like chain, which may consist of 2–100 cells. The cells are nearly square (sub-quadrate) with deep constrictions at the sinus. Each semicell is sub-divided into three lobes, two of which are lateral and the third apical (polar). The lateral lobes are further sub-divided into smaller lobes and lobules by means of incisions of various depths. The polar lobes are narrow with a pair of pointed extensions at each end. The polar extensions interlock where neighbouring cells are attached to each other. The cells are 70–80 µm in length and 65–80 µm wide (isthmus 13–16 µm). The morphology of specimens in our samples corresponds to the original description by Ralfs (1848) and later descriptions, such as those provided by Kim (2013) and Ribeiro et al. (2015).

A description of Ling and Taylor (2000) of a form of *M. foliacea* recorded from the Northern Territories in Australia indicated a simpler form with less divided lateral lobes and one, instead of the usual two, triangular process on the face of the polar lobe. Cell length without processes was 66–67 µm, and with processes 91–95 µm; width was 102–109 µm; apex 38–43 µm and isthmus 14–15 µm.

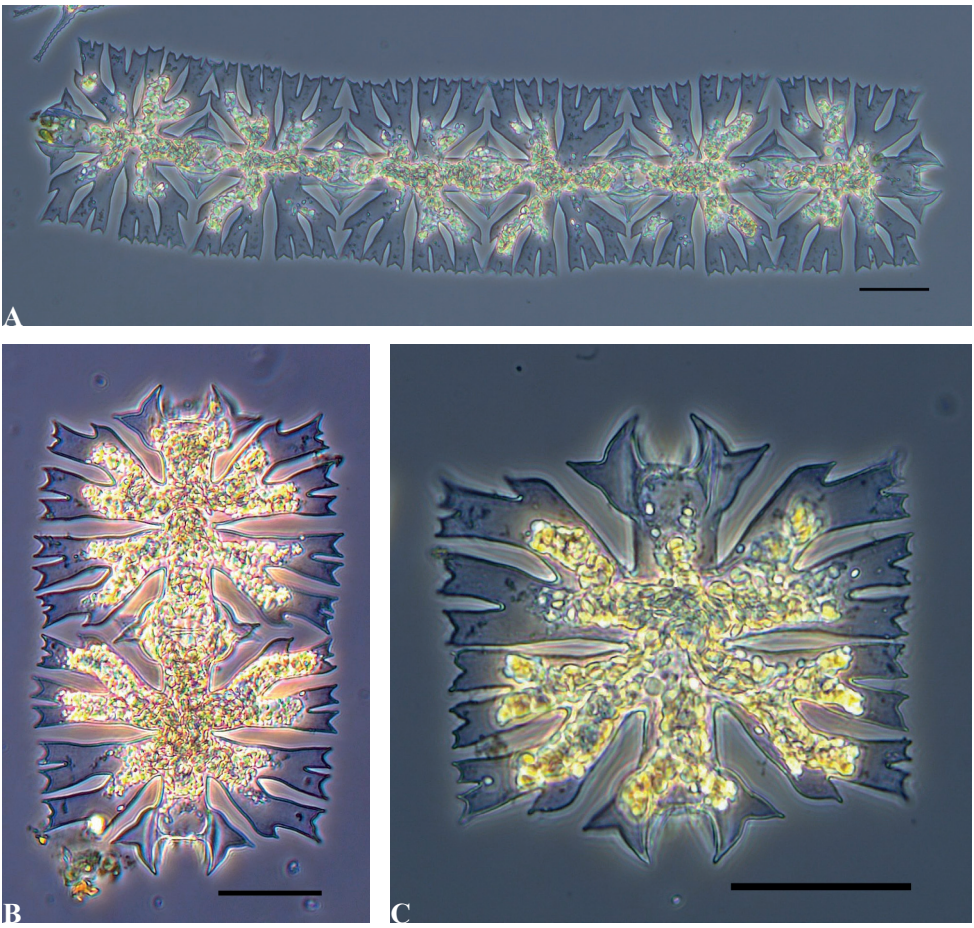

Figure 1. Morphology of *M. foliacea* var. *foliacea* found in samples from Mozambique **A** six cells illustrating chain formation **B** two adjacent cells indicating the interlocking polar extensions **C** morphology of a single cell. Scale bars: 30 µm.

Distribution. A map, illustrating the geographical distribution of *M. foliacea*, is presented in Fig. 2. This figure shows that variety *foliacea* (type) is widely distributed, being present on most continents. It is, however, only recorded from the eastern side of North America and, surprisingly, it is completely absent from European countries. Palamar-Mordvintseva (1984) speculated that this species can possibly be found in future in the rice fields of southern Ukraine, but according to the general known distribution of this species it is doubtful that this statement is true. A detailed list, with references, of all localities where this variety was found is presented in Suppl. material 1.

Habitat and ecology. From intensive literature searches it is clear that the habitats of free-living *M. foliacea* are exceptionally diverse. It can be found in plankton and periphyton of a variety of different lentic and lotic water bodies. Lentic (stagnant) water

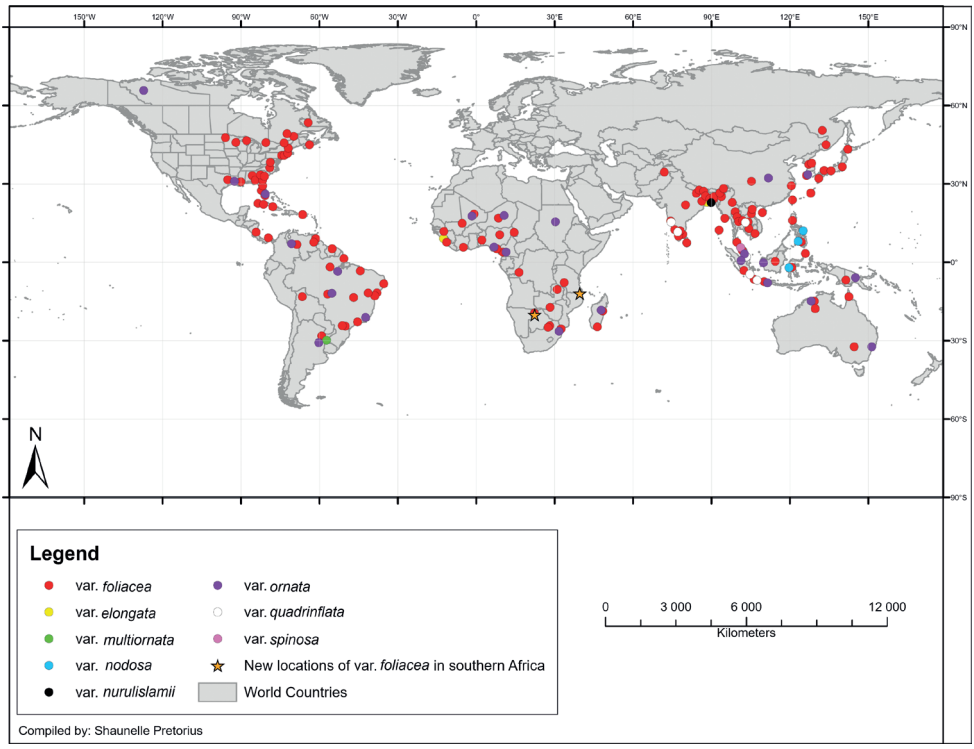

Figure 2. Worldwide distribution of different varieties of *Micrasterias foliacea.*

bodies include wetlands, marshes, various types of swamps (e.g., peat swamps) and ponds (including irrigation and oxidation ponds, rainwater ponds, rock ponds, fish-ponds, and small ponds in botanical gardens), reservoirs, deltas, floodplains, lagoons and lakes (including crater lakes), flooded savannahs and meadows, and in ditches associated with paddy (rice) fields. It is most common in small and shallow (<1 to 2 m) ponds, but it was also occasionally found at the embankments of larger standing water bodies, e.g., Lake Laguna de Bay in the Philippines (4–6 m deep; Behre 1956). Lotic habitats include cobbles, streams, rivers, and irrigation canals. In addition, it was also recorded from a tropical estuarine mangrove swamp in Nigeria with high conductivity levels (Table 1; Ubong et al. 2017). In these habitats, it often occurs between floating algal masses. In terrestrial habitats it may be found amongst moist mosses, growing on the surface of rocks, or inhabiting wet soils.

Besides being free-living, it can also be found as epiphytes on aquatic plants (Jena and Adhikary 2011). It is frequently found living on *Utricularia* species, such as *U. flexuosa* (Lütkemüller 1900; Turner 1892) and *U. fasciculata* (Turner 1892). It was also found on leaves of *Hymenachne amplexicaulis* (Salazár Pereira 1991; Salazar 2006/2007) and the stems and roots of submerged *Ipomaea reptans* (Bourrelly 1975). It was common in samples that were obtained when the roots of *Eichhornia crassipes*,

Table 1. Physico-chemical properties of waterbodies throughout the world in which *M. foliacea* var. *foliacea* was found.

Environmental variable	Value/Ranges	Country	Reference
pH	6.6	Cambodia	Hirano 1972
	4.7–5.3	Malaysia	Ratnasabapathy and Kumano 1974
	5.78±0.76, 6.10±0.44, 6.12±0.74	Malaysia	Noor et al. 2012
	8.0	Philippines	Behre 1956
	5.0–5.5	Sumatra	Scott and Prescott 1961
	6.3–6.8	Russia	Gontcharov 1997
	5.6–7.5	South Korea	Kim 2014
	5.6, 5.9	Thailand	Ngearnpat et al. 2008
	7.42±0.11	Thailand	Prasertsin and Peerepornpisal 2018
	7.6–8.3	India	Ecology and biodiversity of Lower Ganga River basin 2012
	6.5–7.0	India	Kalita et al. 2016,
	5.7–6.8 (open water), 5.2 (littoral vegetation)	Zambia	Thomasson 1966
	6.3	Congo	Van Oye 1953
	8.0	Nigeria	Ubong et al. 2017
	6.2	South Africa	Claassen 1982
	8.15	Nigeria	Ali et al. 2016
	6.0	India	Das and Keshri 2013, 2016
	6.44	Botswana	Williamson and Marazzi 2013
	5.7, 8.1	USA	Oyadomari 2013
	5.4	Brazil	Thomasson 1977
	5.5	Suriname	Leentvaar 1975
	5.26–5.83	Australia	Thomasson 1986
	6.8–7.2	USA	Ngo et al. 1986–1987
Water temperature (°C)	26.8	Cambodia	Hirano 1972
	23.8–26.9 (running water) 23.4–33.4 (still water)	Malaysia	Ratnasabapathy and Kumano 1974
	27.01±4.2, 27.22±3.96, 27.33±4.87	Malaysia	Noor et al. 2012
	8, 10, 21	India	Das and Keshri 2016
	22–26	Russia	Gontcharov 1997
	29.1, 32.2	Thailand	Ngearnpat et al. 2008
	30±0.71	Thailand	Prasertsin and Peerepornpisal 2018
	18.6–30.4	India	Ecology and biodiversity of Lower Ganga River basin 2012
	17.8–30.2	India	Kalita et al. 2016
	35	Guinea	Bourrelly 1975
	23–24	USA	Oyadomari 2013
	28.5–31.1	Australia	Thomasson 1986
	10	India	Das and Keshri 2013
	21.6	Botswana	Williamson and Marazzi 2013
	33.46	Nigeria	Ali et al. 2016
	26.17	Nigeria	Ubong et al. 2017
Conductivity (µS/cm)	31.88±17, 33.88±12, 34.75±19	Malaysia	Noor et al. 2012
	36–55, 44–108	South Korea	Kim 2014
	315, 327	Thailand	Ngearnpat et al. 2008
	15, 6	USA	Oyadomari 2013
	23–58	Australia	Thomasson 1986
	76.0	Botswana	Williamson and Marazzi 2013
	74.34	Nigeria	Ali et al. 2016
	49993.33 ± 634.09	Nigeria	Ubong et al. 2017
	94.80±2.39	Thailand	Prasertsin and Peerepornpisal 2018

Environmental variable	Value/Ranges	Country	Reference
Dissolved oxygen (mg/L)	2.35±2.62, 3.16±2.22, 3.44±2.76	Malaysia	Noor et al. 2012
	4.2, 8.0	Thailand	Ngearnpat et al. 2008
	3.69–6.67	Australia	Thomasson 1986
	1.70	Botswana	Williamson and Marazzi 2013
	5.74	Nigeria	Ali et al. 2016
	6.12	Nigeria	Ubong et al. 2017
	7.10±0.79	Thailand	Prasertsin and Peerepornpisal 2018
Alkalinity (meq/L)	0.038–0.082	Australia	Thomasson 1986
	2.53	Nigeria	Ali et al. 2016
	149.00±2.65	Thailand	Prasertsin and Peerepornpisal 2018
Total alkalinity (mg/L)	11, 11.5	Thailand	Ngearnpat et al. 2008
Phosphate-phosphorus (mg/L)	0.13±0.28 0.15±0.39 0.18±0.45	Malaysia	Noor et al. 2012
	0.66	Nigeria	Ali et al. 2016
Soluble Reactive Phosphate (mg/L)	0.52±0.28	Thailand	Prasertsin and Peerepornpisal 2018
Nitrate-nitrogen (mg/L)	0.15±0.1 0.15±0.2 0.18±0.2	Malaysia	Noor et al. 2012
	12.63	Nigeria	Ali et al. 2016
Turbidity (NTU)	1.6	Botswana	Williamson and Marazzi 2013
	0.46	Nigeria	Ali et al. 2016
	25.55	Nigeria	Ubong et al. 2017
	8.07±1.7	Thailand	Prasertsin and Peerepornpisal 2018

Pistia stratiotes, *Salvinia molesta* and submerged aquatic macrophytes were squeezed out (Bicudo and Sormus 1982; Rai et al. 2008; Paudel 2017). The species was also found in the stomachs of catfish *Synodontis schall* and *S. nigrita* (Lalèyè et al. 2006).

A variety of aquatic plants inhabit waters in which *M. foliacea* var. *foliacea* was found. Shallow water was often dominated by species of *Nymphaea* and *Utricularia* (Schumacher 1956; Thomasson 1966; Ratnasabapathy and Kumano 1974; Turner 1892; González 2009). Other dominant species include those of *Pistia* and *Salvinia* (Ngearnpat et al. 2008; González 2009). In deeper waters *Brasenia schreberi*, *Cabomba caroliniana*, *Nuphar orbiculata*, *Nymphaea odorata* and *Utricularia purpurea* were common (Schumacher 1956). During the current study *Nymphaea* dominated the macrophyte community at the sampling site in Botswana.

The abundance of *M. foliacea* var. *foliacea* may range from extremely rare, present in low to moderate quantities (Behre 1956) or it may be common (Scott and Prescott 1961; Prowse 1969; Kadiri and Opute 1989; Kadiri 2002; Islam and Ifranullah 2006). Other authors described it as abundant (Kim 2014), or sometimes dominant (Medvedeva 2007; Ekhator et al. 2013).

Variety *foliacea* can be found in a wide pH range and a literature overview, presented in Table 1, shows that it is present in both acidic (min pH 4.7; Malaysia), as well as alkaline waters (max pH 8.3; India). Results from the literature review contradict a finding made by Prescott and Scott (1943) who stated that the acidity of water in which *M. foliacea* grows, varies between pH 5.8 and 6.4 (rarely as high as 6.8), and that this species' distribution is so specifically related to the chemistry

of the water that it can be used as an indicator organism for soft and highly acid waters. After the study of Prescott and Scott (1943) the species was frequently recorded in waters with pH values around 8 (Philippines, India, Nigeria, USA; see Table 1), indicating that it can also tolerate and thrive in alkaline waters and that it is thus not suitable as an indicator organism. Table 1 also indicates alkalinity ranges of water in which the species was recorded and, in accordance with the findings of Förster (1982), several published results show that it is usually found under neutral to alkaline conditions.

It was found in both winter (Islam and Ifranullah 2006) and summer (Thomas et al. 2003; Prasertsin and Peerapornpisal 2018) seasons throughout the world. In India it was found during pre-monsoon, monsoon, post-monsoon and winter seasons (Kalita et al. 2016). Water temperature ranged between a minimum of 8 °C (India) and a maximum of 35 °C (Guinea), although it was most frequently recorded in moderate to high water temperatures, ranging from 23–27 °C (Table 1).

Typical conductivity levels of freshwater are below 1 500 µS/cm, while typical sea water has a conductivity value of about 50 000 µS/cm. *M. foliacea* was usually found in freshwater with relatively low conductivity values (< 327 µS/cm; Table 1), but cells were also found in some estuaries, archipelagos and marine waters (Chung et al. 1965; McAlice 1975; Opute 1992; Kadiri 2002; Li et al. 2011; Ecology and biodiversity of Lower Ganga River basin 2012; Silveira 2012; Opute and Kadiri 2013; Dayala et al. 2014; Mama et al. 2016; Ubong et al. 2017). Average conductivity values in the tropical estuarine mangrove swamp (Nigeria) in which it was found by Ubong et al. (2017) was in the order of 50 000 µS/cm, showing its ability to survive in saline water. It is, however, suspected that its presence in estuaries and oceans may be the result of outflows from the rivers.

Table 1 shows nutrient ranges (phosphate-phosphorus, nitrate-nitrogen) of water in which *M. foliacea* was recorded. Based on these nutrient concentrations, it was mostly found in oligotrophic to slightly mesotrophic water (Kim 2014; Ali et al. 2016).

Dissolved oxygen concentrations ranged from 1.7–8.0 mg/L in water in which *M. foliacea* was recorded. It was mostly found in low turbidity (high transparency) waters (Williamson and Marazzi 2013; Ali et al. 2016; Ubong et al. 2017; Prasertsin and Peerapornpisal 2018). However, in Thailand it was found in muddy, pale yellow-brown water with transparencies less than 1 m (Hirano 1975) and in the middle reaches of the Niger River in Mali it was found in polluted, cloudy, muddy water having a sandy substrate (Couté and Rousselin 1975).

2. *Micrasterias foliacea* var. *elongata* (W.B. Turner) Willi Krieger, 1939

Micrasterias foliacea var. *elongata* (W.B. Turner) Willi Krieger, 1939. "Rabenhorst's Kryptogamen-Flora von Deutschland", "Österreich und der Schweiz", 2 Aufl., 13 (Abt.1, Teil 2): 77.

Synonyms. *M. foliacea* Bailey ex Ralfs var. β Wallich, 1860. "Annals and Magazine of Natural History" Series 3, 5: 280, tab. XIV, figs 1–4; *M. foliacea* Bailey ex Ralfs f. β *elongata* Turner, 1892. "Aquae Dulcis Indiae Orientalis": 94.

This variety was originally described by Wallich (1860) as "var. β". A later study by Turner (1892) revealed the same alga, but he described it as "forma β *elongata*". In his monograph, Krieger (1939) indicated the same algal species as "var. *elongata* Turner".

Morphology. The prominent feature of *M. foliacea* var. *elongata* is the largely developed, triangular terminal lobe, with an outward directed base, emarginate at its angles and centre and furnished with two short stout teeth placed obliquely to each other (comparable to that of *M. baileyi*). The central emargination of this lobe is deep and rectangular and the entire lobe projects very slightly beyond the apices of the lateral lobes. The margins of the filament are parallel and direct, the fronds tabular, and divided by a very deep constriction into two dichotomously incised segments, the ultimate subdivisions of which are emarginate. In the Bengal variety, the teeth-like projections next to the terminal lobe are acutely angular, instead of being rounded and, as in the case of *Onychonema*, the projecting processes, by which cohesion is either secured or increased, overlap each other alternately in adjacent fronds. The cell length is 85–90 μm, width 70–75 μm, width of isthmus 11–13 μm, width of apex 32 μm, width of polar lobes 15 μm (Wallich 1860; Turner 1892).

Distribution. This variety seems to be endemic to southeastern tropical Asia (Lower Bengal, India; Fig. 2 and Suppl. material 2), where it was found in the 1800's by Wallich (Wallich 1860). A single record of this variety from Sierra Leone (Woodhead and Tweed 1958; Suppl. material 2) is doubtful, because descriptions and illustrations of the cell morphology, as well as information about the sampling site, are absent.

Habitat and ecology. No information is available in the literature about the habitats or ecology of this variety.

3. *Micrasterias foliacea* var. *multiornata* Zalocar de Domitrovic, 1981

Micrasterias foliacea var. *multiornata* Zalocar de Domitrovic, 1981. "Physis (Buenos Aires)", Sec.B, 40(98): 58, fig. 2: 13.

Morphology. This variety differs from the type by the presence and distribution of warts, situated in a row from the isthmus to half the length of the sinus. There is also a wart on the basis of the upper side lobes. Cells are 120–124 μm long, 115–120 μm wide, polar lobes are 53–57 μm wide, isthmus is 20–22 μm wide (Zalocar de Domitrovic 1981).

Distribution. The variety is endemic to South America and was only found in tropical areas of Argentina (Fig. 2 and Suppl. material 2 for more information).

Habitat and ecology. *M. foliacea* var. *multiornata* was found in a wetland for which no ecological data is available.

4. *Micrasterias foliacea* var. *nodosa* (Behre) Levanets & Janse van Vuuren, stat. nov.

M. foliacea f. *nodosa* Behre 1956. "Archiv für Hydrobiologie / Supplement" 23: 84, Pl. 10, fig. 5, Basionym.

Taxon depository. PhycoBank registration: http://phycobank.org/103725.

Nodular cell wall thickenings are unique morphological features of this variety and therefore it is proposed to raise taxonomical status of this form to the variety.

Morphology. This taxon was described by Karl Behre (1956) as "forma *nodosa*" based on cell morphology – it differs from the type by the presence of nodular wall thickenings. Usually, thickenings are located on the inner corners and opposed points of adjacent lobes. Sometimes adjacent lobes are connected by ridge-like thickenings. It was noted that this variety is not a teratological form, because similar wall thickenings were found in numerous cells collected in several sites. Also, no transitional forms were seen between the nodular and the typical forms and the two forms occurred side by side in some samples. Dimensions: 70–74 x 80 μm, isthmus 16 μm.

Distribution. Variety *nodosa* was rarely encountered, and only recorded from a few islands in Indonesia and the Philippines (southeastern Asia; Fig. 2 and Suppl. material 2 for more information).

Habitat and ecology. In all cases *M. foliacea* var. *nodosa* were found in lake environments. In the Philippines the water bodies were characterized by clear water, covered by plants, containing detritus and other remains of higher plants. In Indonesia it was recorded from a crater lake (Suppl. material 2). No data on physico-chemical environmental variables was present for these water bodies.

5. *M. foliacea* var. *nurulislamii* Levanets & Janse van Vuuren, 2023: 1, no fig.

Micrasterias foliacea var. *spinosa* Islam & Ashrafi, *nom. inval*. 2004. "Bangladesh Journal of Plant Taxonomy" 6, Pl. 3, figs 12–14. Basionym.

Remarks. Islam and Begum (2004) published a paper on *Micrasterias* Agardh from selected areas of Bangladesh and described a new variety of *M. foliacea* (var. *spinosa*). This varietal designation was invalid and was not designated in accordance with Art. 40.6 of ICN (Turland et al. 2018). In addition, the varietal name "*Micrasterias foliacea* var. *spinosa* Islam & Ashrafi" was invalid as *Micrasterias foliacea* var. *spinosa* Levanets and Guiry (2021) had priority. A new name, in honor of National Professor of Bangladesh, Abul Khayer Mohammed Nurul Islam, was therefore proposed for this variety (Levanets and Janse van Vuuren 2023).

Morphology. This variety differs from the type because there are numerous spines on the cell wall. The cell wall is covered with many stout, curved spines, unequal in size. The incision between the lobes is usually wide open. Cell length 33–76 μm, width 34.5–77 μm, isthmus 5.0–11.5 μm (Islam and Begum 2004).

Distribution. *M. foliacea* var. *nurulislamii* was found only once in Bangladesh (Suppl. material 2).

Habitat and ecology. It was found in a ditch. No ecological information is available.

6. *Micrasterias foliacea* var. *ornata* Nordstedt, 1869

Micrasterias foliacea var. *ornata* Nordstedt, 1869. "Videnskabelige Meddelelser fra den Naturhistorisk Forening i Kjøbenhavn for Aaret" 21: 221, Taf. 2, fig. 16.

Morphology. Each semicell is rectangular and the cell wall bears one to three small spines along the sinus, as well as on the upper margin of the upper lateral lobe near its base and the lower margin of the lower lateral lobes near the isthmus (Kim 2013, 2014). The presence of the spines on the upper and lower margins of the lateral lobes, as well as the incision which separates the polar lobe, is regarded as the major difference between this variety and the type (Nordstedt 1869; Zalocar de Domitrovic 1981).

In Asian specimens of both the specific form and var. *ornata* a peculiar phenomenon, never seen in any American specimens, was observed. This is a warping of the surface of the filament, resulting in the twisting of the side (edge) view of the chains into a sinusoidal curve which is sometimes quite pronounced. It is caused by the curving and dishing in opposite directions of the right and left lateral lobes of one semicell, those of the other semicell being curved and dished in the reverse manner (Scott and Prescott 1961). Illustrations of these twisting of the chains can be found in Scott and Prescott (1961).

Distribution. Although variety *ornata* is less widespread than var. *foliacea*, it is also widely distributed throughout the world. Similar to the type, it was not recorded anywhere in Europe and in North America it was only recorded from northwestern Canada and two eastern states of the USA. It is more abundant in South America, Africa, and Asia and it was also recorded from Australia. The distribution of var. *ornata* is illustrated in Fig. 2 and more details regarding its patterns of distribution are presented in Suppl. material 3.

Habitat and ecology. Variety *ornata* was recorded from a wide range of different ecological niches – it was found in different types of freshwaters, both standing (rainwater pools, rock ponds, rice fields, reservoirs, lakes, swamps, wetlands, flooded savannahs and lagoons) and flowing (creeks, moderate to rapidly flowing rivers). It was growing on the leaves of *Hymenachne amplexicaulis* (Poaceae) by Salazár Pereira (1991) and Salazar (2006/2007). It was also found in a coastal area in Nigeria (Kadiri 2002).

According to Kim (2013) this variety occurs mostly in oligo-mesotrophic, neutral-alkaline water bodies. The variety had a rare abundance in a natural oligotrophic pond on Jeju Island (South Korea), with pH ranging between 6.1 and 7.5 and conductivity between 44 and 108 μS/cm (Kim 2014). In Venezuela it was found in a flooded savannah which was acidic, with a low salinity and a high biomass of macrophytes (Salazár Pereira 1991; Salazar 2006/2007).

7. *M. foliacea* var. *quadrinflata* Scott & Prescott, 1961

M. foliacea var. quadrinflata Scott & Prescott, 1961. "Hydrobiologia" 17(1–2): 48, Pl. 15, figs 5–8.

Morphology. *M. foliacea* var. *quadrinflata* differs from the type in having two large, prominent semi-ellipsoidal hollow swellings at the base of the lateral lobes, each bearing a long spine at the narrow ends. In addition, there may or may not be, four other long spines on each semicell, two adjacent to each of the swellings. Cells are 69–72 μm long and 63–72 μm wide. The isthmus is 12 μm wide and the teeth are 15–18 μm long (Scott and Prescott 1961).

Distribution. The distribution of this variety is plotted in Fig. 2 (with more detailed information in Suppl. material 2). It is limited to the Hindustan and Indochina peninsulas and Indonesian archipelago and was recorded from India, Indonesia, Malaysia and Thailand.

Habitats and ecology. Variety *quadrinflata* was found in freshwater lakes, rivers, reservoirs, swamps and wetlands (India, Indonesia and Malaysia), as well as in a rice paddy field in Thailand.

In Malaysia, the shallow parts and edges of the Tasek Bera swamp lake were covered with *Lepironia articulata* associations. Aquatic plants such as *Utricularia* spp., *Hydrilla* sp., *Nymphoides indica* and *Pandanus helicopus* were present in still water areas, while *Utricularia* sp., *Cryptocoryne griffithii*, *Scirpus confervoides* and *Pandanus helicopus* were present in running water (Ratnasabapathy and Kumano 1974). At the time of sampling the temperatures ranged between 23.4 and 33.4 °C (in still water) and between 23.8 and 26.9 °C (in running water) and the pH ranged between 4.7 and 5.3 Ratnasabapathy and Kumano 1974). In South Sumatra it was also found in acidic waters in Lebak Danau (pH between 5.0 and 5.5; Scott and Prescott 1961).

8. *M. foliacea* var. *spinosa* G.A. Prowse ex Levanets & Guiry, 2021: 2.

Micrasterias foliacea var. *spinosa* G.A. Prowse, *nom. inval*. 1969. "Gardens' Bulletin", Singapore 24: 341, Pl. 4, text-fig. 2(a). Basionym.

Morphology. The variety differs from all other forms because the isthmus is widely opened and due to the large width of the gap between the subterminal and terminal lobes. Pairs of prominent sharp teeth are borne on either side of the isthmus and on both sides of the base of terminal lobes. Cells 72–75 μm long., 68–70 μm wide, isthmus 8 μm wide (Prowse 1969).

Distribution. Its current known distribution is limited to only one location in the Malayan peninsula (Suppl. material 2 and Fig. 2).

Habitat and ecology. Variety *spinosa* was commonly found, together with var. *quadrinflata*, in the Tasek Bera forest swamp lake for which ecological conditions are described in the paragraph on var. *quadrinflora* above.

Conclusions

Chain forming cells of *M. foliacea* were found in water samples from Botswana and Mozambique. The morphology of cells of *M. foliacea* found in these samples corresponded to that given in earlier descriptions of the type species. The species is easily distinguished from other species of the genus by its peculiar apex, interlocking the cells to form chains of up to more than 100 cells. Research on this species resulted in a review of the taxonomy, morphology, worldwide distribution, and ecology of the different varieties of *M. foliacea*, presented in this paper.

During research on the species, it was noted that doubtful records exist for different varieties of *M. foliacea*, mainly as a result of the lack of drawings (or micrographs) and new description of previously described varieties. This paper attempted to correct these mistakes and a new status is proposed, namely:

- *Micrasterias foliacea* var. *nodosa* (Behre) Levanets et Janse van Vuuren, stat. nov. – It is proposed to raise the taxonomical status of this form, described by Behre as *M. foliacea* Bailey ex Ralfs f. *nodosa*, to the variety, as its nodular cell wall thickenings are unique morphological features.

Detailed analysis of the distribution of *M. foliacea* and its varieties presented an interesting and clear picture, collated in a distribution map. Despite the wide geographical distribution of varieties *foliacea* (type) and *ornata*, they are completely absent from Europe and the majority of North America; both these varieties were only recorded from the eastern side of the latter continent. During this study *M. foliacea* var. *foliacea* was observed in two new locations in southern Africa, namely Botswana and northern Mozambique. In general, most other varieties (*elongata*, *nodosa*, *spinosa*, *nurulislamii* and *quadrinflata*) are much more limited regarding their distribution and were observed and recorded mostly from southeastern tropical Asia (e.g., Indonesia, Malaysia, Philippines). Only var. *multiornata* is endemic to tropical South America.

A review on physico-chemisty of waterbodies in which *M. foliacea* was found, indicated that it may be present in a variety of different types of habitats in both standing and flowing water. It can tolerate a wide range of water temperature and pH. It was found in both acidic, neutral and alkaline waters all over the world. Conductivity values measured in waterbodies containing *M. foliacea* indicated that it is mostly prevalent in fresh waters and findings in estuaries and oceans may be coincidental as the result of washout during runoff. This species occurs mostly in oligo-mesotrophic conditions under conditions of relatively low turbidity.

Acknowledgements

Thank you to Prof. Louis du Preez (North-West University, South Africa) for samples collected in Okavango Delta (Botswana) and Prof. Jonathan Taylor (North-West University, South Africa) for providing samples from Northern Mozambique. The authors

would also like to thank Yolanda Zalocar de Domitrovic (Centro de Ecología Aplicada del Litoral (CONICET), Argentina), Ms. Lara Jakson (University of Toronto, Canada) and Dr. Olaf Polmann (SCENSO – Scientific Environmental Solutions, Germany) for help with obtaining rare and old literature inaccessible in South Africa. A special thank you to the reviewers for their positive and useful comments – they really walked the extra mile to improve the quality of the paper.

References

Ali AD, Abiem I, Alisha EB, Musa PJ (2016) Floristic Composition of soft-bodied Algae of Pandam Lake (Pandam Wildlife Park, Nigeria). International Journal of Pure & Applied Bioscience 4(4): 39–49. https://doi.org/10.18782/2320-7051.2328

Atlas of Living Australia (2022) Atlas of Living Australia. http://www.ala.org.au/ [Accessed 20 January 2022]

Behre K (1956) Die Süβwasser-Algen der Wallacea-Expedition (ohne die Diatomeen und Peridineen). Archiv für Hydrobiologie Supplement 23(1): 1–104.

Bicudo CEM, Sormus L (1982) Desmidioflórula paulista, 2: Gênero *Micrasterias* C. Agardh ex Ralfs. Bibliotheca Phycologica 57: 1–230.

Bourrelly P (1975) Quelques algues d'eau douce de Guinée. Bulletin du Muséum national d'Histoire naturelle, 3ᵉ série, n.276, 20: 1–72.

Chung YH, Shim JH, Lee MJ (1965) A study on the microflora of the Han River. 1. The phytoplanktons and the effect of the marine water in the lower course of the Han River. Korean Journal of Botany 8(4): 7–29. [In Korean]

Claassen MI (1982) 'n Taksonomiese studie van Transvaalse varswater Euglenophyceae en Chlorophyceae. PhD Thesis, University of Pretoria, South Africa. [In Afrikaans]

Couté A, Rousselin G (1975) Contribution à l'étude des algues d'eau douce du Moyen Niger (Mali). Bulletin du Muséum national d'Histoire naturelle, 3ᵉ série, n.277, 21: 73–175.

Cushman JA (1908) A synopsis of the New England species of *Micrasterias*. Rhodora 10(114): 97–111.

Das D, Keshri JP (2013) Desmids from South Sikkim, India. Nelumbo 55: 172–180.

Das D, Keshri JP (2016) Desmids of Eastern Himalaya. J. Cramer in Borntraeger Science Publishers, Stuttgart: 1–260. Bibliotheca Phycologica: e119.

Dayala VT, Salas PM, Sujatha CH (2014) Spatial and seasonal variations of phytoplankton species and their relationship to physicochemical variables in the Cochin estuarine waters, Southwest coast of India. Indian Journal of Geo-Marine Sciences 43(6): 937–947.

Ecology and biodiversity of Lower Ganga River basin (2012) Ganga river basin environment management plan, indian institutes of technology. Report Code: 026_GBP_IIT_ENB_DAT_04_Ver_Jun 2012: 1–48.

Ekhator O, Ihenyen JO, Okooboh GO (2013) Desmids of Osse River, Edo state, Nigeria. International Journal of Modern Botany 3(2): 25–31. https://doi.org/10.5923/j.ijmb.20130302.03

Förster K (1982) Conjugatophyceae, Zygnematales und Desmidiales (excl. Zygnemataceae). In: Huber-Pestalozzi G (Ed.) Das Phytoplankton des Süβwassers. Systematik und Biologie.

8. Teil, 1. Hälfe. (Die Binnengewässer, Band XVI). E. Schweizerbart'sche Verlagsbuchhandlung, Stuttgart, 543 pp.

Gontcharov AA (1997) Contribution to the desmid flora of the Primorsky Territory, Russia. Bulletin of National Science Museum, Ser. B., Tokyo 23(2): 59–80.

González AC (2009) Catálogo de las Algas y Cianoprocariotas Dulciacuícolas de Cuba. Impreso en Universidad de Cienfuegos, Cuba, 147 pp.

Guiry MD, Guiry GM (2023) AlgaeBase. World-wide electronic publication, National University of Ireland, Galway. http://www.algaebase.org [Accessed 24 February 2022]

Hirano M (1972) Desmids from Cambodia, with special reference to Phytoplankton of Lake Grands Lacs (Tonle Sap). Contributions from the Biological Laboratory. Kyoto University 22(3–4): 123–157.

Hirano M (1975) Phytoplankton from Lake Boraphet in the central Plain of Thailand. Contributions from the Biological Laboratory. Kyoto University 24(4): 187–203.

Islam AKM, Begum A (2004) Desmids from some selected areas of Bangladesh: 1. Genus *Micrasterias* Agardh. Bangladesh Journal of Plant Taxonomy 11(2): 1–14.

Islam AKMN, Ifranullah HM (2006) Hydrobiological studies within the tea gardens at Srimangal, Bangladesh. V. Desmids (*Euastrum*, *Micrasterias*, *Actinotaenium* and *Cosmarium*). Bangladesh Journal of Plant Taxonomy 13(1): 1–20. https://doi.org/10.3329/bjpt.v13i1.589

Jena M, Adhikary SP (2011) Algal diversity of Loktak Lake, Manipur. Nelumbo 53: 21–48.

Kadiri MO (2002) A checklist of desmids in Nigeria. Global Journal of Pure and Applied Sciences 8(2): 223–237. https://doi.org/10.4314/gjpas.v8i2.16036

Kadiri MO, Opute FI (1989) A rich flora of *Micrasterias* from the Ikpoba Reservoir, Nigeria. Archiv für Hydrobiologie 116(3): 391–399. https://doi.org/10.1127/archiv-hydrobiol/116/1989/391

Kalita SR, Ahmed R, Das M (2016) Physico-Chemical Characteristics and Phytoplanktonic Diversity of Urpod Beel, Goalpara Assam (India). Series a Thesis Conceptual Magazine 3(7): 10–14.

Kim HS (2013) Algal Flora of Korea (Vol. 6, Number 3). Charophyta: Conjugatophyceae (Desmids II). Desmidiales: Closteriaceae II, Desmidiaceae II. Freshwater Green Algae. Sang Pal Lee Publisher, 103 pp.

Kim HS (2014) Desmids from Korea; 1. *Desmidiaceae* 1 (*Micrasterias*). Journal of Ecology and Environment 37(4): 285–298. https://doi.org/10.5141/ecoenv.2014.032

Krieger W (1939) Die Demidiaceen Europas mit Berücksichtigung der auβereuropäischen Arten. Rabenhorst's Kryptogamen-Flora von Deutschland, Österreich und der Schweiz 13(2). Akademische Verlagsgesellschaft M.B.H., Leipzig, 1–117.

Lalèyè P, Chikou A, Gnohossou P, Vandewalle P, Philippart JC, Teugels G (2006) Studies on the biology of two species of catfish *Synodontis schall* and *Synodontis nigrita* (*Ostariophysi: Mochokidae*) from the Ouémé River, Bénin. Belgian Journal of Zoology 136(2): 193–201.

Leentvaar P (1975) Hydrobiological observations in Surinam with special reference to the manmade Brokopondo Lake. Studies of the fauna of Suriname and other Gayanas 56: 1–173. https://doi.org/10.1007/978-94-017-7106-1_1

Levanets A, Guiry MD (2021 [May 28]) Validation of desmid names (*Desmidiales*, *Zygnematophyceae*) described by G.A. Prowse from Malaysia and Singapore. Notulae Algarum 193: 1–3.

Levanets A, Janse van Vuuren S (2023 [February 1]) *Micrasterias foliacea* var. *nurulislamii* Levanets & Janse van Vuuren, nom. nov. (≡"*Micrasterias foliacea* var. *spinosa* Islam & Ashrafi", nom. inval.) (Desmidiaceae, Zygnematophyceae). Notulae Algarum 270: 1.

Li WKW, Andersen RA, Gifford DJ, Incze LS, Martin JL, Pilskaln CH, Rooney-Varga JN, Sieracki ME, Wilson WH, Wolff NH (2011) Planktonic Microbes in the Gulf of Maine Area. PLoS ONE 6(6) e20981. https://doi.org/10.1371/journal.pone.0020981

Ling HU, Taylor PA (2000) Australian Freshwater Algae (exclusive of diatoms). J. Cramer in der Gebrüder Borntraeger Verlagsbuchhandlung, Berlin, Stuttgart, 643 pp. [Bibliotheca Phycologica 105.]

Lütkemüller J (1900) Desmidiaceen aus den Ningpo-Mountains in Centralchina. Annalen des K.K. Naturhistorischen Hofmuseums 15(2): 115–126.

Mama AC, Mbeng OL, Dongmo ChT, Moto I, Ngoupayou NJR, Ohondja ALM (2016) Tidal variations and its impacts on the abundance and diversity of phytoplankton in the Nyong Estuary of Cameroon. Journal of Multidisciplinary Engineering Science and Technology 3(1): 3667–3675.

McAlice BJ (1975) Preliminary checklist of planktonic microalgae from the Gulf of Maine. Maine Sea Grant Information Leaflet 9, March 1975 (MEU-H-75-001), Cooperative Extension Service, University of Maine, Orono, Maine, 17 pp.

Medvedeva LA (2007) Results of algological study of middle part of River Bureya basin. In: Medvedeva LA, Teslenko VA, Tiunova TM (Eds) Hydro-ecological monitoring in Bureyskaya Hydro-Electric Power Station zone influences. Institute of Water and Ecological Problems of Far East Branch of Russian Academy of Sciences, Khabarovsk, 64–79. [In Russian]

Ngearnpat N, Coesel PFM, Peerapornpisal Y (2008) Diversity of desmids in three Thai peat swamps. Biologia 63(6): 897–902. https://doi.org/10.2478/s11756-008-0140-x

Ngo H, Prescott GW, Czarnecki DB (1986–1987) Additions and confirmations to the algal flora of Itasca State Park. I. Desmids and diatoms from North Deming Pond. Journal of the Minnesota Academy of Science 52(2): 14–26. https://doi.org/10.2216/i0031-8884-26-2-293.1

Noor S, Salleh A, Nasrodin S (2012) Desmid flora in Tasik Sungai Semuji, Kuantan, Pahang, Malaysia. Proceedings of the 2nd International Conference on Arts, Social Sciences & Technology, Penang, Malaysia, 3rd-5th March 2012, Paper Code No. I2040: I2040-1-I2040-10.

Nordstedt CFO (1869) Desmidiaceae. In: Warming E (Ed.) Symbolae ad floram Brasiliae centralis cognoscendam. Videnskabelige Meddelelser fra den Naturhistorisk Forening i Kjøbenhavn for Aaret 14, 15: 195–234.

Opute FI (1992) Contribution to the knowledge of algae of Nigeria. 1. Desmids from the Warri / Forcados Estuaries. Part II. The genera *Euastrum* and *Micrasterias*. Algological Studies 65: 73–92.

Opute FI, Kadiri MO (2013) Phytoplankton algae of Nigeria. A Practical & Theoretical Guide (Vol. 1): The desmids. Mindex Publishing Company Limited, Benin City, 304 pp.

Oyadomari J (2013) Keweenaw Algae. http://www.keweenawalgae.mtu.edu/gallery_pages/charophyceans3.htm [Accessed: 20 April 2015]

Palamar-Mordvintseva GM (1984) Identification guide of the freshwater algae of Ukrainian SSR. VIII. Conjugatophyceae. Part 1. *Mesotaeniales*, *Gonatozygales*, *Desmidiales*. Naukova Dumka Publishing House, Kiev, 512 pp. [In Ukrainian]

Paudel N (2017) New record of desmids from Ramwell-Rhino Lake, Chitwan, Nepal. International Journal of Scientific Research 6(8): 523–526. https://doi.org/10.21275/ART20175881

Prasertsin T, Peerapornpisal Y (2018) Distribution and isolation of microalgae for lipid production in selected freshwater reservoirs of northern Thailand. Biodiversitas (Surakarta) 19(1): 343–350. https://doi.org/10.13057/biodiv/d190147

Prescott GW, Scott AM (1943) The desmid genus *Micrasterias* Agardh in southeastern United States. Papers of the Michigan Academy of Science, Arts and Letters 28: 67–82.

Prowse GA (1969) Some new desmid taxa from Malaya and Singapore. Gardens' Bulletin (Singapore) 24: 337–346.

Rai SK, Rai RK, Paudel N (2008) Desmids from Bees-hazaar Lake, Chitwan, Nepal. Our Nature 6(1): 58–66. https://doi.org/10.3126/on.v6i1.1656

Ralfs J (1848) The British Desmidieae. Reeve, Benham & Reeve, London, 226 pp.

Ratnasabapathy M, Kumano S (1974) Desmids from Tasek Bera, West Malaysia. The Bulletin of the Japanese Society of Phycology (Sôrui) 22(1): 22–28. [In Japanese]

Ribeiro CA, Ramos GJP, Oliveira IB, Moura CWN (2015) *Micrasterias* (Zygnematophyceae) de duas áreas do Pantanal dos Marimbus (Baiano e Remanso), Chapada Diamantina, Bahia, Brasil. Ciências Biológicas, Sitientibus série 15: 1–12. https://doi.org/10.13102/scb578

Salazar C (2006/2007) Desmidiaceae (Zygophyceae) asociadas a *Hymenachne amplexicaulis* (Poaceae) en una sabana tropical inundable, Venezuela. Memoria de la Fundación La Salle de Ciencias Naturales 166: 95–131.

Salazár Pereira CV (1991) Estudio sistemático de la ficoflora perifítica (Desmidiales y Euglenaceae) asociada a *Himenachne amplexicaulis* en una sabana inundable de Venezuela. Doctorado en Ciencias Naturales, Universidad Nacional de La Plata, Facultad de Ciencias Naturales y Museo, La Plata, 237 pp.

Schumacher G (1956) A qualitative and quantitative study of the plankton algae in southwestern Georgia ponds. American Midland Naturalist 56(1): 88–115. https://doi.org/10.2307/2422446

Scott AM, Prescott GW (1961) Indonesian Desmids. Hydrobiologia 17(1–2): 1–132. https://doi.org/10.1007/BF00040416

Silveira Jr AM (2012) Composição e biomassa microfitoplanctônica associadas a variáveis fisico e químicas em dois transectos da zona estuarinado Rio Amazonas (Amapá, Amazônia, Brasil). Dissertação apresentada ao Programa de Pós-Graduação em Ciências da Saúde da Universidade Federal do Amapá – UNIFAP, como parte dos requisitos necessários para a obtenção do título de Mestre em Ciências da Saúde; Área de Concentração, Ensaios Biológicos, Macapá, 92 pp.

The Global Biodiversity Information Facility (2023) GBIF Home Page. https://www.gbif.org [Accessed 17 April 2023]

Thomas JK, Sreekumar S, Jaya Cheriyan (2003) Muriyad Wetlands: ecological changes and human consequences. Project report submitted to Kerala Research Programme on Local Development, Centre for Developmental Studies, Thiruvanandapuram, 83 pp.

Thomasson K (1966) Le phytoplancton du lac Shiwa Ngandu: Phytoplankton of Lake Shiwa Ngandu. Exploration hydrobiologique du bassin du lac Bangweolo et du Luapula, v.4, fasc.2: 1–91.

Thomasson K (1977) Two conspicuous desmids from Amazonas. Botaniska Notiser, Stockholm 130: 41–51.

Thomasson K (1986) Algal Vegetation in North Australian Billabongs. Nova Hedwigia 42(204): 301–378.

Turland NJ, Wiersema JH, Barrie FR, Greuter W, Hawksworth DL, Herendeen PS, Knapp S, Kusber W-H, Li D-Z, Marhold K, May TW, McNeill J, Monro AM, Prado J, Price MJ, Smith GF [Eds] (2018) International Code of Nomenclature for algae, fungi, and plants (Shenzhen Code) adopted by the Nineteenth International Botanical Congress Shenzhen, China, July 2017. Regnum Vegetabile (Vol. 159). Koeltz Botanical Books, Glashütten, 253 pp. https://doi.org/10.12705/Code.2018

Turner WB (1892) Algae Aquae Dulcis Indiae Orientalis. The Fresh-Water Algae (principally Desmidieae) of East India. Kongl. Boktryckeriet, Stockholm, 187 pp.

Ubong G, Aniema I-E, Ndueso I (2017) Bio-monitoring and diversity of phytoplankton in a tropical estuarine mangrove swamp in Akwa Ibom State, South-South, Nigeria. European Journal of Biotechnology and Bioscience 5(4): 71–79.

Van Oye P (1953) Contribution à la connaissance des Desmidiées du Congo belge. Hydrobiologia 5(3): 239–308. https://doi.org/10.1007/BF00024300

Wallich GC (1860) Description of Desmidieae from Lower Bengal. Annals and Magazine of Natural History, Series 3, 5: 184–197. [273–285.] https://doi.org/10.1080/00222936008697200

Williamson DB, Marazzi L (2013) A new *Cosmarium* (*Chlorophyta*, *Desmidiaceae*) variety from the Okavango Delta, Botswana. Quekett Journal of Microscopy 42: 35–37.

Woodhead N, Tweed RD (1958) A check-list of tropical West African algae. Hydrobiologia 11(3–4): 299–395. https://doi.org/10.1007/BF00018696

Zalocar de Domitrovic Y (1981) Desmidiales (*Chlorophyta*) de la provincia de Corrientes (Argentina). II. El género *Micrasterias*. Physis (Buenos Aires). Sec. B 40(98): 55–62.

Supplementary material 1

Geographical distribution of *M. foliacea* var. *foliacea* throughout the world.

Authors: Anatoliy Levanets, Sanet Janse van Vuuren

Data type: Distribution, references

Explanation note: Habitat types and locations are indicated, together with the reference stating its presence.

Link: https://doi.org/10.3897/phytokeys.226.103500.suppl1

Supplementary material 2

Geographical distribution of *M. foliacea* var. *elongata*, *multiornata*, *nodosa*, *nurulislamii*, *quandrinflata* and *spinosa* throughout the world

Authors: Anatoliy Levanets, Sanet Janse van Vuuren

Data type: Distribution, references

Explanation note: Habitat types and locations are indicated, together with the reference stating its presence.

Link: https://doi.org/10.3897/phytokeys.226.103500.suppl2

Supplementary material 3

Geographical distribution of *M. foliacea* var. *ornata* throughout the world

Authors: Anatoliy Levanets, Sanet Janse van Vuuren

Data type: Distribution, references

Explanation note: Habitat types and locations are indicated, together with the reference stating its presence.

Link: https://doi.org/10.3897/phytokeys.226.103500.suppl3

Supplementary material 4

Supplementary references

Authors: Anatoliy Levanets, Sanet Janse van Vuuren

Data type: references

Link: https://doi.org/10.3897/phytokeys.226.103500.suppl4

PhytoKeys 226: 53–63 (2023)
doi: 10.3897/phytokeys.226.101164
https://phytokeys.pensoft.net

RESEARCH ARTICLE

A peer-reviewed open-access journal
PhytoKeys
Launched to accelerate biodiversity research

Sinosasa gracilis (Poaceae, Bambusoideae), a new combination supported by morphological and phylogenetic evidence

Xing Li[1,2,3], Jing-Bo Ni[1,3], Zhuo-Yu Cai[1,2,3], Yi-Hua Tong[1,3], Nian-He Xia[1,3]

1 *Key Laboratory of Plant Resources Conservation and Sustainable Utilization & Guangdong Provincial Key Laboratory of Applied Botany, South China Botanical Garden, Chinese Academy of Sciences, CN-510650, Guangzhou, China* **2** *University of Chinese Academy of Sciences, CN-100049, Beijing, China* **3** *South China National Botanical Garden, CN-510650, Guangzhou, China*

Corresponding authors: Yi-Hua Tong (yh-tong@scbg.ac.cn); Nian-He Xia (nhxia@scbg.ac.cn)

Academic editor: Weilim Goh | Received 29 January 2023 | Accepted 7 April 2023 | Published 9 May 2023

Citation: Li X, Ni J-B, Cai Z-Y, Tong Y-H, Xia N-H (2023) *Sinosasa gracilis* (Poaceae, Bambusoideae), a new combination supported by morphological and phylogenetic evidence. PhytoKeys 226: 53–63. https://doi.org/10.3897/phytokeys.226.101164

Abstract

The results of phylogenetic analysis, based on the whole chloroplast genome and morphological study support the transfer of a long ignored bamboo species, *Sasa gracilis*, to the recently established genus, *Sinosasa*, in this study. Morphologically, this species differs from all the other known *Sinosasa* species by having very short (2–3 mm) foliage leaf inner ligules, which is unusual in this genus. A revised description of its morphology and colour photos are also provided.

Keywords

bamboo, phylogeny, *Sinosasa*, taxonomy

Introduction

Sinosasa L.C.Chia ex N.H.Xia, Q.M.Qin & Y.H.Tong was recently segregated from *Sasa* Makino and Shibata (1901) to accommodate some species previously placed in *Sasa* subg. *Sasa* from China, based on morphological and phylogenetic evidence (Qin et al. 2021). This genus differs from *Sasa* in having raceme-like (vs. panicle-like) synflorescences, two to three (vs. four to ten) florets per spikelet with a rudimentary terminal floret, three (vs. six) stamens and two (vs. three) stigmas per floret, wavy

(vs. usually flat) foliage leaf blades when dry and relatively long (> 1 cm) (vs. short) foliage leaf inner ligules (Qin et al. 2021). Up to now, *Sinosasa* contains seven species endemic to subtropical areas of China and usually found growing along the river valley or in moist areas under evergreen broad-leaved forests at elevations of 700–1200 m (Qin et al. 2021).

Sasa gracilis B.M.Yang (1990) was described based on the only collection *B. M. Yang 06774* from Shangmuyuan, Jiangyong County, Hunan Province, China. After its publication, it is only recognised in 'Bamboos of Hunan' (Yang 1993), edited by the author of this name, 'Iconographia Bambusoidearum Sinicarum' (Yi et al. 2008) and its English version 'Illustrated Flora of Bambusoideae in China' (Shi et al. 2022). However, because of the narrow circulation of the publication Acta Scientiarum Naturalium Universtis Normalis Hunanensis (later the name was changed to Journal of Natural Science of Hunan Normal University) at that time in China (Deng and Xia 2014), this species was ignored by the widely distributed monographs, such as 'Flora Reipublicae Popularis Sinicae', 'Flora of China', 'World Checklist of Bamboos and Rattans' (Hu 1996; Wang and Stapleton 2006; Vorontsova et al. 2016), the well-known database GrassBase-The Online World Grass Flora (Clayton et al. 2016) and some important websites like http://www.ipni.org, http://www.tropicos.org and http://www.theplantlist.org. In the protologue, this species was described to possess a suite of vegetative characters, such as solitary branches at each branching node, strongly raised supranodal ridges and wavy foliage leaf blades when dry, which fit well with the circumscription of *Sinosasa*. However, this species has very short foliage leaf inner ligules that are only 2–3 mm long, while all hitherto known *Sinosasa* species typically have more than 1 cm long inner ligules. Therefore, the taxonomic position of *Sasa gracilis* needs a further study.

Materials and methods

The specimens of *Sasa gracilis* were collected from its type locality during a field trip in September 2022. Fresh foliage leaves were deposited in silica gel for DNA extraction. Type specimens of *Sasa gracilis* deposited in the Herbarium of Hunan Normal University (HNNU) were examined. Observations and measurements were taken using a magnifier and a ruler with a scale of 0.5 mm. Some minor characters like the indumentum were observed with a stereomicroscope (Mshot MZ101). The morphological terms follow McClure (1966) and Beentje (2016). Herbarium acronyms follow Thiers (2022, continuously updated).

To study the phylogenetic position of *Sasa gracilis* within the tribe Arundinarieae, the whole chloroplast genomes were used for building the phylogenetic tree. A total of 24 representatives belonging to all the five subtribes of the tribe Arundinarieae (Zhang et al. 2020a) were sampled and *Bambusa multiplex* (Lour.) Raeusch. ex Schult. f. from the tribe Bambuseae was used as outgroup. All the sampled taxa, as well as their voucher information and GenBank accession numbers, are listed in Table 1.

Table 1. List of 25 bamboo taxa sampled in the present study with the related voucher and GenBank accession information.

Taxon	Voucher information	Accession number
Ingroup		
Acidosasa glauca B.M.Yang	CZY56 (IBSC)	OP850353
Ampelocalamus actinotrichus (Merr. & Chun) S.L.Chen, T.H.Wen & G.Y.Sheng	MPF10003 (KUN)	MF066245
Chimonobambusa tumidissinoda Ohrnb.	MPF10083 (KUN)	MF066244
Fargesia edulis Hsueh f. & T.P.Yi	D418 (SANU)	MH988735
Gaoligongshania megalothyrsa (Hand.-Mazz.) D.Z.Li, Hsueh & N.H.Xia	MPF10056 (KUN)	JX513419
Gelidocalamus stellatus T H.Wen	BH102 (IBSC)	OP850347
Hsuehochloa calcareus (C.D.Chu & C.S.Chao) D.Z.Li & Y.X.Zhang	MPF10050 (KUN)	KJ496369
Indocalamus longiauritus Hand.-Mazz.	MPF10168 (KUN)	HQ337795
Indocalamus sinicus (Hance) Nakai	ZMY037 (KUN)	MF066250
Indosasa crassiflora McClure	BH58 (IBSC)	OK558536
Oligostachyum sulcatum Z.P.Wang & G.H.Ye	Not provided by the author	MW190089
Phyllostachys edulis (Carriere) J.Houzeau	MPF10163 (KUN)	HQ337796
Pleioblastus maculatus (McClure) C.D.Chu & C.S.Chao	MPF10161 (KUN)	JX513424
Pseudosasa cantorii (Munro) Keng f.	MPF10006 (KUN)	MF066255
Pseudosasa japonica (Siebold & Zucc. ex Steud.) Makino ex Nakai	Pjc-1 (ZJFC)	KT428377
Ravenochloa wilsonii (Rendle) D.Z.Li & Y.X.Zhang	MPF10146 (KUN)	JX513421
Sasa veitchii Rehder	LC1325 (ISC)	KU569975
Sasa gracilis B.M.Yang	LX153 (IBSC)	*OP973764
Shibataea chiangshanensis T.H.Wen	ZLN-2011080 (KUN)	MF066257
Sinosasa fanjingshanensis N.H.Xia, Q.M.Qin & J.B.Ni	BH124 (IBSC)	OP850348
Sinosasa longiligulata (McClure) N.H.Xia, Q.M.Qin & J.B.Ni	CZY163 (IBSC)	OP850351
Sinosasa sp.	CZY173 (IBSC)	OP850352
Sinobambusa tootsik (Makino) Makino ex Nakai	NH031 (IBSC)	OP850357
Yushania niitakayamensis (Hayata) Keng f.	Not provided by the author	MN310560
Outgroup		
Bambusa multiplex (Lour.) Raeuschel ex Schult. & Schult. f.	Not provided by the author	KJ722536

DNA extraction, sequencing, assembly and annotation

Total genomic DNA was extracted from leaves dried in silica gel using the Plant Genomic DNA Kit and then sent to Novogene (Tianjin, China) for DNA quality assessment. The qualified DNA fragments with 350 bp insert size were enriched by PCR experiment. Paired reads were sequenced on an Illumina NovaSeq 6000 platform. A total of 40 G genome skimming data (150 bp read length) were generated for each sample. These sequenced data were used to assemble the whole chloroplast genome by GetOrganelle v. 1.7.4 pipeline (Jin et al. 2018) using *Phyllostachys edulis* (GenBank accession number: HQ337796) set as the reference, with k-mer values of 45, 65, 85, 105 and 125. The complete assembly graph was visualised for plastid contig in Bandage software (Wick et al. 2015). Finally, the sequence editing was manually operated in Geneious v. 9.1.4 (Kearse et al. 2012) with the structure of LSC-IRa-SSC-IRb.

Phylogenetic analysis

All the whole chloroplast genomes were aligned with MAFFT v. 7.490 (Katoh and Standley 2013) and combined as a data matrix. Phylogenetic analyses were conducted using Maximum Likelihood (ML) and Bayesian Inference (BI) implemented in the PhyloSuite v.1.2.2 platform (Zhang et al. 2020b). The best substitution model (K81 + GTR) for the combined data was determined using the Bayesian Information Criterion (BIC) in ModelFinder (Kalyaanamoorthy et al. 2017). A standard Maximum Likelihood tree search was performed using IQ-TREE v.1.6.8 (Nguyen et al. 2015). Nodal support (bootstrap support; BS) was assessed using 1000 standard bootstrap replicates. Bayesian phylogenetic inference was performed using MrBayes v.3.2.6 (Ronquist et al. 2012). Posterior Probability (PP) was obtained from Metropolis-coupled Markov Chain Monte Carlo simulations (two independent runs; four chains; 40,000,000 generations, sampling frequency of once every 4000 generations; 25% burn-in). Visualisation of ML and BI trees was done in FigTree v. 1.4.4 (Rambaut 2018).

Result

The chloroplast genome size of *Sasa gracilis* is 140,013 bp and those of all the samples ranged from 139,394 bp (*Bambusa multiplex*) to 140,064 bp (*Gaoligongshania megalothyrsa* (Hand.-Mazz.) D.Z.Li, Hsueh & N.H.Xia) with an alignment of 144,169 bp. The data matrix was characterised by sequence divergence with 3,688 variable sites (2.56%), including 773 parsimony informative sites (0.54%) and 2,915 singleton variable sites (2.02%). The phylogenetic trees, generated by the ML and BI methods, were generally consistent in topology, so only the ML tree was shown with nodal support values from both methods labelled on each node (Fig. 1). As shown in the phylogenetic tree, *Sasa gracilis* is distantly related to *Sasa veitchii* Rehder (= *Sasa albomarginata* (Miq.) Makino & Shibata, the type of *Sasa*), but forms a monophyletic clade with three *Sinosasa* species with strong nodal support (BS = 100% and PP = 1.00).

Discussion

Our phylogenetic analysis and previous studies of Zeng et al. (2010), Zhang et al. (2012), Guo et al. (2021) and Qin et al. (2021) all demonstrated that *Sinosasa* is monophyletic. Molecular evidence, based on plastid genomic data, further confirmed that *Sasa gracilis* should be a member of *Sinosasa* rather than *Sasa*. Morphologically, the characters of this species also match well with those of *Sinosasa* species as mentioned above. The short inner ligule (2–3 mm) of *Sasa gracilis* can easily differentiate this species from all the other *Sinosasa* species. Consequently, the previous circumscription of

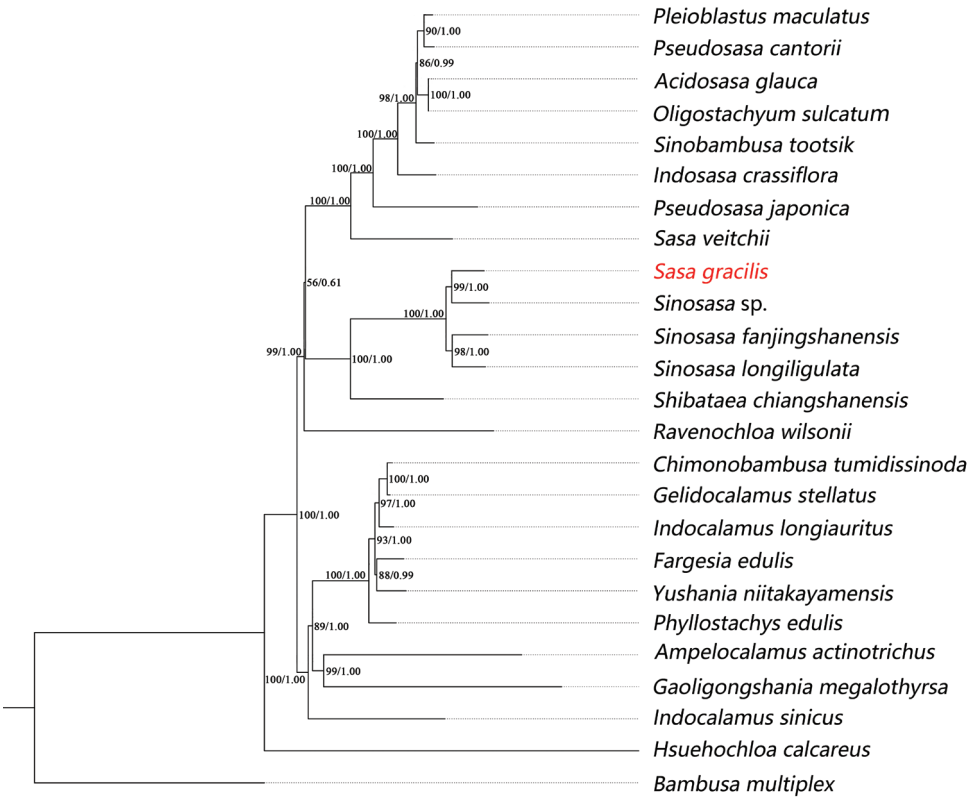

Figure 1. Phylogenetic tree reconstruction for *Sasa gracilis*, based on plastid genome dataset with Maximum Likelihood and Bayesian analyses. Bootstrap values and posterior probabilities are indicated at each node.

Sinosasa on the length of foliage leaf inner ligule should be modified. In other words, *Sinosasa* does not always have long (typically > 1 cm) foliage leaf inner ligules as we knew previously. If this character is excluded, *Sasa gracilis* is somewhat similar to two other *Sinosasa* species also with culm leaf auricles, viz. *Sinosasa magninoda* (T.H.Wen & G.L.Liao) N.H.Xia, Q.M.Qin & X.R.Zheng and *Sinosasa guangxiensis* (C.D.Chu & C.S.Chao) N.H.Xia, Q.M.Qin & X.R.Zheng. It further differs from *Sinosasa guangxiensis* by the glabrous (vs. densely strigose) abaxially mid- and upper part of the culm leaf sheath with short (0.5–1 mm vs. 1–3 mm) ligules and the glabrous (vs. puberulent) foliage leaf sheath and from *Sinosasa magninoda* by having culm leaf with shorter (0.5–1 mm vs. 1–3 mm) ligules, larger (2–4 × 1–2 mm vs. 1–1.5 × 1 mm) auricles and (vs. absent) oral setae and foliage leaf with more (7–12 vs. 1–4) and longer (8–20 mm vs. 5–10 mm) oral setae. A more detailed comparison amongst the three species is provided in Table 2. Based on the above evidence, it is concluded that *Sasa gracilis* represents a distinct species of *Sinosasa* and a new combination of it under *Sinosasa* should be made.

Table 2. Comparison of *Sasa gracilis*, *Sinosasa guangxiensis* and *Sinosasa magninoda*.

Characters	*Sasa gracilis*	*Sinosasa guangxiensis*	*Sinosasa magninoda*
Culm leaf			
Sheath	Glabrous on the mid- and upper part	Densely strigose	Glabrous or sparsely strigose
Auricles	Elliptic to falcate, 2–4 × 1–2 mm	Ovate or oblong, 2–3 × 1–2 mm	Ovate, 1–1.5 × 1 mm
Oral setae	Present, 2–10 mm long	Present, 3–10 mm long	Absent
Ligule	0.5–1 mm	1–3 mm	1–3 mm
Foliage leaf			
Sheath	Glabrous	Puberulent	Glabrous
Oral setae	7–12, 8–20 mm	Ca. 10, 6–10 mm long	1–4, 5–10 mm
Inner ligule	2–3 mm	10–15 mm	8–12 mm

Taxonomic treatment

Sinosasa gracilis **(B.M.Yang) N.H.Xia, Y.H.Tong, J.B.Ni & X. Li, comb. nov.**
urn:lsid:ipni.org:names:77318864-1
Figs 2, 3

Basionym. *Sasa gracilis* B. M. Yang, Acta Sci. Nat. Univ. Norm. Hunan. 13 (supplement): 1 (1990).

Type. China. Hunan: Jiangyong County, Dayuan Township, Shangmuyuan, elev. 620 m, 28 October 1987, *B. M. Yang 6774* (Holotype: HNNU00053209!)

Description. Shrubby bamboos. Rhizomes leptomorph, internodes 4–5.5 cm long, 2–3.5 mm in diameter, solid. Culms pluricaespitose, 0.2–1.5 m tall, 1.5–7 mm in diameter; internodes terete, 2–15 cm long, upper part initially densely white puberulent, glabrescent when old, hollow; supranodal ridge 5–9 mm in diameter, strongly raised; intranode ca. 3 mm long, glabrous, densely puberulous in infranodal region; branches extravaginal, solitary at each branching node. Culm bud solitary, trullate, sunken into supranodal ridge, ciliate on the margin. Culm leaf sheath persistent or tardily deciduous, 1/2–1/3 as long as internodes, glabrous abaxially, except for the base with a 2–3 mm wide brown and downward-appressed hispid band, glabrous on the margin; sheath scar flat or slightly prominent; auricles elliptic to falcate, 2–4 × 1–2 mm, oral setae curved, 2–10 mm long; ligule truncate, 0.5–1 mm high, ciliolate on the margin; blade triangular to lanceolate, erect or reflexed, 5–10 mm long, glabrous, serrulate along the margin. Foliage leaves 5–12 per ultimate branch; sheath glabrous, green or purple-green, 8–12 mm long, margin glabrous, longitudinal ribs conspicuous; auricles elliptic to falcate, 1–2 × 1–1.5 mm, oral setae developed, 7–12, erect or curled, 8–20 mm long; inner ligule 2–3 mm high, slightly arcuate to truncate, glabrous; outer ligule ca. 1 mm high, abaxially puberulous, white ciliate on the margin; pseudopetioles glabrous, 4–8 mm long; blades oblong-lanceolate to lanceolate, 7–29 × 1.5–5 cm, papery, wavy when dry, both surfaces glabrous, apex long-attenuate, base cuneate to obtuse, margin serrulate; secondary veins 3–8 pairs, transverse veins conspicuous. Inflorescence unknown.

Figure 2. Holotype of *Sinosasa gracilis* (B.M.Yang) N.H.Xia, Y.H.Tong, J.B.Ni & X.Li (≡ *Sasa gracilis* B.M.Yang), *B. M. Yang 06774* (HNNU, barcode: 00053209). Photo by Zhuo-Yu Cai.

Figure 3. *Sinosasa gracilis* **A** habit **B** foliage leafy branch **C** culm bud and strongly raised supranodal ridge **D** culm leaf sheath base **E** partial culm, showing solitary branch **F** dried foliage leafy branch, showing wavy blades and a close-up view of glabrous sheath, short inner ligules, auricles and oral setae **G** culm leaf blade, auricles and oral setae **H** glabrous abaxial surface of culm leaf sheath. All photos by Xing Li.

Phenology. New shoots from April to May.

Distribution and habitat. It is endemic to Shangmuyuan Mountain in Jiangyong County, Hunan, China. It grows in moist places along the river banks in the valley at elevations of 600–1000 m.

Chinese name. 纤细华赤竹 (Chinese pronunciation: xiān xì huá chì zhú).

Additional specimens examined. *Sinosasa gracilis*: China. Hunan: Jiangyong County, Dayuan Township, Shangmuyuan, 18 September 2022, 25°24'24.7"N, 111°16'17.9"E, elev. 838 m, *X. Li & J. B. Ni LX153* (IBSC).

Sinosasa guangxiensis: China. Guangxi: Rongshui County, Jiuwan Mountain, Gema, elev. 800 m, 23 April 1979, *C. D. Chu & Z. Wang 7906* (isotypes: PE0008644, image, N019023145, image); Lingchuan County, Dajing Township, Qifen Mountain, 30 July 2006, *C. X. Zeng & Y. X. Zhang 06179* (KUN0720003, image, KUN0719374, image, KUN0719386, image, KUN0719166, image, KUN0719167, image, KUN0719168, image, KUN0719169, image).

Sinosasa magninoda: China. Jiangxi: Jinggang Mountain, Longtan, Zhenzhutan, 26 May 1985, *Liao et Xu 85017* (ZJFI); ibid. 28 May 1990, elev. 700 m, *T. H. Wen & G. L. Liao 90551* (Holotype: ZJFI); ibid. 27 Aug 2017, *X. R. Zheng 25* (IBSC).

Acknowledgements

We thank Xing-Min Zhou for his assistance in the fieldwork. This research was funded by the Guangdong Basic and Applied Basic Research Foundation (grant no. 2021A1515011302) and National Natural Science Foundation of China (grant no. 32270227).

References

Beentje H (2016) The Kew Plant Glossary, Second Edition. Royal Botanic Gardens, Kew, London, 1–184.

Clayton WD, Vorontsova M, Harman KT, Williamson H (2016) GrassBase-The online world grass flora. https://kew.org/data/grasses-db/index.html [Accessed 21 December 2022]

Deng YF, Xia NH (2014) *Acidosasa* (Poaceae: Bambusoideae): Publication by description generico-specifica and typification. Taxon 63(2): 400–402. https://doi.org/10.12705/632.10

Guo C, Ma PF, Yang GQ, Ye XY, Guo Y, Liu JX, Liu YL, Eaton DAR, Guo ZH, Li DZ (2021) Parallel ddRAD and genome skimming analyses reveal a radiative and reticulate evolutionary history of the temperate bamboos. Systematic Biology 70(4): 756–773. https://doi.org/10.1093/sysbio/syaa076

Hu CH (1996) *Sasa* Makino et Shibata. In: Keng PC, Wang ZP (Eds) Flora Reipublicae Popularis Sinicae (Vol. 9). Science Press, Beijing, 662–675.

Jin JJ, Yu WB, Yang JB, Song Y, Yi TS, Li DZ (2018) GetOrganelle: a simple and fast pipeline for de novo assembly of a complete circular chloroplast genome using genome skimming data. bioRxiv 256479. https://doi.org/10.1101/256479

Kalyaanamoorthy S, Minh BQ, Wong T, von Haeseler A, Jermiin LS (2017) ModelFinder: Fast model selection for accurate phylogenetic estimates. Nature Methods 14(6): 587–589. https://doi.org/10.1038/nmeth.4285

Katoh K, Standley DM (2013) MAFFT: multiple sequence alignment software version 7: improvements in performance and usability. Molecular Biology and Evolution 30(4): 772–780. https://doi.org/10.1093/molbev/mst010

Kearse M, Moir R, Wilson A, Stones-Havas S, Cheung M, Sturrock S, Buxton S, Cooper A, Markowitz S, Duran C, Thierer T, Ashton B, Meintjes P, Drummond A (2012) Geneious Basic: An integrated and extendable desktop software platform for the organization and analysis of sequence data. Bioinformatics (Oxford, England) 28(12): 1647–1649. https://doi.org/10.1093/bioinformatics/bts199

Makino T, Shibata K (1901) On *Sasa*, a new genus of Bambuseae, and its affinities. Botanical Magazine Tokyo 15(168): 18–31. https://doi.org/10.15281/jplantres1887.15.168_18

McClure FA (1966) The bamboos: A fresh perspective. Harvard University Press, Cambridge, 1–347. https://doi.org/10.4159/harvard.9780674428713

Nguyen LT, Schmidt HA, Haeseler V, Minh BQ (2015) IQ-TREE: A fast and effective stochastic algorithm for estimating Maximum-Likelihood phylogenies. Molecular Biology and Evolution 32(1): 268–274. https://doi.org/10.1093/molbev/msu300

Qin QM, Tong YH, Zheng XR, Ni JB, Xia NH (2021) *Sinosasa* (Poaceae: Bambusoideae), a new genus from China. Taxon 70(1): 27–47. https://doi.org/10.1002/tax.12422

Rambaut A (2018) FigTree, version v.1.4.4. http://tree.bio.ed.ac.uk/software/figtree/ [Accessed 25 October 2020]

Ronquist F, Teslenko M, Mark VDP, Ayres DL, Darling A, Höhna S, Larget B, Liu L, Suchard MA, Huelsenbeck JP (2012) MrBayes 3.2: Efficient Bayesian phylogenetic inference and model choice across a large model space. Systematic Biology 61(3): 539–542. https://doi.org/10.1093/sysbio/sys029

Shi JY, Che BY, Zhang YX, Zhou DQ, Ma LS, Yao J (2022) *Sasa* Makino & Shibata. In: Yi TP, Shi JY, Zhang YX, Zhou DQ, Ma LS, Yao J (Eds) Illustrated Flora of Bambusoideae in China (Vol. 2). Science Press, Beijing & Springer Nature Singapore Pte Ltd., Singapore, 381–396. https://doi.org/10.1007/978-981-16-2758-3_43

Thiers B (2022[continuously updated]) Index Herbariorum: A global directory of public herbaria and associated staff. http://sweetgum.nybg.org/ih [Accessed 21 December 2022]

Vorontsova MS, Clark LG, Dransfield J, Govaerts R, Baker WJ (2016) World checklist of bamboos and rattans. INBAR Technical Report No. 37. Beijing: International Network of Bamboo & Rattan, 1–454.

Wang ZP, Stapleton CMA (2006) *Sasa* Makino et Shibata. In: Wu ZY, Raven P (Eds) Flora of China (Vol. 22). Science Press, Beijing & Missouri Botanical Garden Press, St. Louis, 109–112.

Wick RR, Schultz MB, Justin Z, Holt KE (2015) Bandage: Interactive visualization of de novo genome assemblies. Bioinformatics (Oxford, England) 31(20): 3350–3352. https://doi.org/10.1093/bioinformatics/btv383

Yang BM (1990) Fourteen new bamboo species from Hunan. Acta Scientiarum Naturalium Universtis Normalis Hunanensis 13(supplement): 1–14.

Yang BM (1993) Bamboos of Hunnan. Hunan Science & Technology Press, Changsha, 1–281.

Yi TP, Shi JY, Ma LS, Wang HT, Yang L (2008) Iconographia Bambusoidearum Sinicarum. Science Press, Beijing, 1–766.

Zeng CX, Zhang YX, Triplettd JK, Yang JB, Li DZ (2010) Large multi-locus plastid phylogeny of the tribe Arundinarieae (Poaceae: Bambusoideae) reveals ten major lineages and low rate of molecular divergence. Molecular Phylogenetics and Evolution 56(2): 821–839. https://doi.org/10.1016/j.ympev.2010.03.041

Zhang YX, Zeng CX, Li DZ (2012) Complex evolution in Arundinarieae (Poaceae: Bambusoideae): Incongruence between plastid and nuclear GBSSI gene phylogenies. Molecular Phylogenetics and Evolution 63(3): 777–797. https://doi.org/10.1016/j.ympev.2012.02.023

Zhang YX, Guo C, Li DZ (2020a) A new subtribal classification of Arundinarieae (Poaceae, Bambusoideae) with the description of a new genus. Plant Diversity 42(3): 127–134. https://doi.org/10.1016/j.pld.2020.03.004

Zhang D, Gao FL, Jakovlić I, Zou H, Zhang J, Li WX, Wang GT (2020b) PhyloSuite: An integrated and scalable desktop platform for streamlined molecular sequence data management and evolutionary phylogenetics studies. Molecular Ecology Resources 20(1): 348–355. https://doi.org/10.1111/1755-0998.13096

PhytoKeys 226: 65–77 (2023)
doi: 10.3897/phytokeys.226.103975
https://phytokeys.pensoft.net

RESEARCH ARTICLE

A peer-reviewed open-access journal
PhytoKeys
Launched to accelerate biodiversity research

Marsupella brasiliensis sp. nov. (Gymnomitriaceae, Marchantiophyta) from Brazil – the distribution of sect. *Stolonicaulon* in Neotropics is now confirmed

Vadim A. Bakalin[1], Yulia D. Maltseva[1], Alfons Schäfer-Verwimp[2], Seung Se Choi[3]

1 *Laboratory of Cryptogamic Biota, Botanical Garden-Institute FEB RAS, Makovskogo Street 142, 690024 Vladivostok, Russia* **2** *Mittlere Letten 11, 88634 Herdwangen-Schönach, Germany* **3** *Team of National Ecosystem Survey, National Institute of Ecology, Seocheon 33657, Republic of Korea*

Corresponding authors: Vadim A. Bakalin (vabakalin@gmail.com); Seung Se Choi (hepaticae@jbnu.ac.kr)

Academic editor: Peter de Lange | Received 23 March 2023 | Accepted 29 April 2023 | Published 12 May 2023

Citation: Bakalin VA, Maltseva YD, Schäfer-Verwimp A, Choi SS (2023) *Marsupella brasiliensis* sp. nov. (Gymnomitriaceae, Marchantiophyta) from Brazil – the distribution of sect. *Stolonicaulon* in Neotropics is now confirmed. PhytoKeys 226: 65–77. https://doi.org/10.3897/phytokeys.226.103975

Abstract

The specimen previously identified as *Marsupella microphylla* from Brazil is reassessed and described as a new species, *M. brasiliensis*. The new species is characterized by paroicous inflorescence, bispiral elaters, scale-like, commonly unlobed leaves and very small leaf cells. Descriptions and drawings are provided along with a corresponding discussion of the morphological peculiarity of the new species. *Marsupella brasiliensis* belongs to sect. *Stolonicaulon*, and the distribution of *Marsupella* sect. *Stolonicaulon* in the New World is confirmed. The infrageneric position of *M. microphylla* remains unresolved, and whether it belongs to the same section is still unclear.

Keywords

Distribution patterns, endemics, Latin America, Marchantiophyta, *Marsupella*, molecular-genetic

Introduction

Marsupella sect. *Stolonicaulon* (N. Kitag.) Váňa is a mysterious section that includes the smallest taxa of the genus and is characterized by a disjunct range, mainly in the tropical and subtropical mountains of Asia to Melanesia, as well as in the Venezuelan Andes and the mountain range of SE Brazil of Latin America (Bakalin et al. 2022). This section

possesses a number of distinctive morphological features that are not characteristic of other members of the genus, such as regular underleaves and scale-like unlobed leaves. A recent revision of this section (Bakalin et al. 2022) showed that it contains sterile morphotypes similar to those in other families; for example, the regular underleaves and remote leaves resemble *Cephaloziella* (*Marsupella praetermissa* Bakalin & Vilnet, *M. taiwanica* Mamontov, Vilnet & Schäf.-Verw.) or deeply dissected conduplicate leaves, resemble small *Schizophyllopsis* Váňa & L. Söderstr. (*Marsupella anastrophylloides* Bakalin, Vilnet & Maltseva). The cited revision (Bakalin et al. 2022) was limited by the integrative study of Asian taxa of the section. Therefore, the question arose whether it is correct to refer to sect. *Stolonicaulon Marsupella microphylla* R.M. Schust., as suggested by Bakalin et al. (2019). Moreover, the latter taxon was originally placed in its own monotypic subgenus: *Marsupella* subg. *Nanocaulon* R.M. Schust. (Schuster 1996) and then transferred to sect. *Boeckiorum* Müll. Frib. ex R.M. Schust. (Váňa 1999).

One of the authors (A.S.-V.) collected a specimen identified by J. Váňa as *Marsupella microphylla* in the Brazilian state of Rio de Janeiro. This specimen is now being investigated in our integrative research. The purpose of this account is to resolve the taxonomic position of this specimen and a review of the genetic relationships within *Marsupella* sect. *Stolonicaulon*.

Materials and methods

Taxon sampling

The specimen identified by J. Váňa as *Marsupella microphylla* (referred to in the report as specimen ASV15033) was studied by traditional morphological techniques, and plant morphology was compared with other taxa of sect. *Stolonicaulon* (N. Kitag.) Váňa, originally described and well known in Asia, and further treatments of *Marsupella microphylla* by Schuster (1978, 1996).

To compile the dataset for molecular phylogenetic analysis, we sequenced two loci (ITS 1−2 and *trn*L−F) from the specimen ASV15033 and added these sequences to the dataset from Bakalin et al. (2022). The outgroup for tree rooting remained unchanged (*Eremonotus myriocarpus* (Carrington) Lindb. & Kaal.). Specimen voucher details, including GenBank accession numbers, are listed in Table 1.

DNA isolation, amplification, and sequencing

DNA was extracted from dried liverwort tissue using the NucleoSpin Plant II Kit (Macherey-Nagel, Germany). Amplification was performed using an Encyclo Plus PCR kit (Evrogen, Moscow, Russia) with the primers listed in Table 2.

The polymerase chain reaction was performed in a total volume of 20 μl, including 1 μl of template DNA, 0.4 μl of Encyclo polymerase, 4 μl of Encyclo buffer, 0.4 μl of

Table 1. The list of voucher details and GenBank accession numbers for the specimens used in the phylogenetic analysis in the present paper. The newly obtained sequences are marked in bold.

Taxon	Specimen voucher	GenBank accession number	
		ITS 1–2 nrDNA	trnL–F cpDNA
Eremonotus myriocarpus (Carrington) Lindb. & Kaal. ex Pearson	Russia, Karachaevo-Cherkessian Rep., N. Konstantinova, K446-6-05, 109, 615 (KPABG)	EU791839	EU791716
Gymnomitrion brevissimum (Dumort.) Warnst.	Russia, Murmansk Prov., N. Konstantinova, G 8171 (KPABG)	EU791833	EU791711
Gymnomitrion corallioides Taylor ex Carrington	Norway, Svalbard, N. Konstantinova, K155-04, 110, 103 (KPABG)	EU791826	EU791705
Marsupella aleutica Mamontov, Vilnet, Konstant. & Bakalin	USA, Alaska, Schofield, 103, 958 (MO)	MH826408	MH822632
Marsupella anastrophylloides Bakalin, Vilnet & Maltseva	Vietnam, Hà Giang Prov., V.A. Bakalin & K.G. Klimova, V-15-6-20 (VBGI)	OM480746	OM489480
Marsupella apertifolia Steph.	Russia, Sakhalin Prov., V.A. Bakalin, K-79-2-15 (VBGI), 123, 501 (KPABG)	MH539834	MH539891
Marsupella apiculata Schiffn.	Norway, Svalbard, N. Konstantinova, K93-1-06, 111, 840 (KPABG)	EU791819	EU791699
Marsupella aquatica (Lindenb.) Schiffn.	Russia, Murmansk Prov., N. Konstantinova, 152/5-87, 6090 (KPABG)	EU791813	AF519201
Marsupella arctica (Berggr.) Bryhn & Kaal.	Norway, Svalbard, N. Konstantinova, 128-04 (KPABG)	EU791815	EU791695
Marsupella boeckii (Austin) Lindb. ex Kaal.	Russia, Murmansk Prov., N. Konstantinova, 367-2-00, 8184 (KPABG)	EU791816	EU791696
Marsupella bolanderi (Austin) Underw. **2**	USA, California Monterey CO, (KPABG)	MF521464	MF521476
Marsupella bolanderi (Austin) Underw. **1**	USA, Santa Yen Mts. St. Barbara, 38802 (KPABG)	MF521463	MF521475
Marsupella brasiliensis Bakalin, Maltseva & Schäf.-Verw. sp. nov.	Brazil, Rio de Janeiro, Serra de Itatiaia, Schäfer-Verwimp & Verwimp, 15033, 15.10.1991	**OQ398709**	**OQ408447**
Marsupella condensata (Ångstr. ex C.Hartm.) Lindb. ex Kaal.	Russia, Kamchatka Terr., V.A. Bakalin, K-60-30-15 (VBGI)	MH539844	MH539901
Marsupella disticha Steph.	Japan, Deguchi, Yamaguchi, Bryophytes of Asia 170 (2000) (KPABG)	EU791824	EU791703
Marsupella emarginata (Ehrh.) Dumort.	Russia, Buryatia Rep., N. Konstantinova, 23-4-02, 104, 411 (KPABG)	EU791811	EU791692
Marsupella funckii (F. Weber & D. Mohr) Dumort.	Russia, Karachaevo-Cherkessian Rep., N. Konstantinova, K516-1-05, 109, 804 (KPABG)	EU791820	EU791700
Marsupella koreana Bakalin & Fedosov	Republic of Korea, KyongNam Province, V.A. Bakalin, Kor-23-18-15 (VBGI)	MH539850	MH539907
Marsupella patens (N.Kitag.) Bakalin & Fedosov	Japan, Fukuoka Pref., V.A. Bakalin, J-7-26a-14 (VBGI)	MH539846	MH539903
Marsupella pseudofunckii S.Hatt.	Japan, Yamanashi Pref., V.A. Bakalin, J-7-10-14 (VBGI)	MH539852	MH539909
Marsupella sphacelata (Giesecke ex Lindenb.) Dumort.	Russia, Kemerovo Prov., N. Konstantinova, 65/1-00 (KPABG)	EU791821	AF519200
Marsupella sprucei (Limpr.) Bernet	Russia, Kemerovo Prov., N. Konstantinova, 54-1-00, 101, 850 (KPABG)	EU791823	HQ833031
Marsupella stoloniformis N.Kitag.	Vietnam, Lao Cai Prov., V.A. Bakalin & K.G. Klimova, V-11-11-17 (VBGI)	MH539859	MH539916
Marsupella subemarginata Bakalin & Fedosov	Japan, Yamanashi Pref., V.A. Bakalin, J-89-31-15 (VBGI), 123, 468 (KPABG)	MH539836	MH539893
Marsupella taiwanica Mamontov, Vilnet & Schäf.-Verw. **2**	China, Taiwan, Nantou Co., A. Schäfer-Verwimp 37663 (MHA, TAIE, JE, VBGI), 123, 642 (KPABG)	OM509627	OM515126
Marsupella taiwanica Mamontov, Vilnet & Schäf.-Verw. **1**	China, Taiwan, Chiayi Co., A. Schäfer-Verwimp 39136 (MHA, TAIE, JE, VBGI), 123, 545 (KPABG)	OM509628	OM515127
Marsupella tubulosa Steph.	Russia, Kamchatka Terr., V.A. Bakalin, K-66-7-15 (VBGI)	MH539860	MH539917

Taxon	Specimen voucher	GenBank accession number	
		ITS 1–2 nrDNA	trnL–F cpDNA
Marsupella vermiformis (R.M.Schust.) Bakalin & Fedosov **2**	Republic of Korea, Jeju Prov., S.S. Choi, 120911-1 (VBGI)	MH539858	MH539915
Marsupella vermiformis (R.M. Schust.) Bakalin & Fedosov **1**	Republic of Korea, Jeju Prov., S.S. Choi, 120911-2 (VBGI)	MH539857	MH539914
Marsupella vietnamica Bakalin & Fedosov	Vietnam, Lao Cai Prov., V.A. Bakalin, V-2-101-16 (VBGI)	MH539862	MH539919
Marsupella yakushimensis (Horik.) S.Hatt.	Republic of Korea, Gangwon Prov., S.S. Choi, 8347 (VBGI)	MH539864	MH539921
Nardia compressa (Hook.) Gray	Canada, British Columbia, N. Konstantinova, A 97/1-95 (KPABG)	EU791837	AF519188
Prasanthus suecicus (Gottsche) Lindb.	Norway, Svalbard, N. Konstantinova, K121-5-06, 111, 821 (KPABG)	EU791825	EU791704

Table 2. Primers used in polymerase chain reaction (PCR) and cycle sequencing.

Locus	Sequence (5'-3')	Direction	Annealing temperature (°C)	Reference
ITS 1–2 nrDNA	CGGTTCGCCGCCGGTGACG	forward	68	Groth et al. 2002
ITS 1–2 nrDNA	CGTTGTGAGAAGTTCATTAAACC	forward	64	Feldberg et al. 2016
ITS 1–2 nrDNA	TCGTAACAAGGTTTCCGTAGGTG	forward	68	Hsiao et al. 1994
ITS 1–2 nrDNA	GATATGCTTAAACTCAGCGG	reverse	58	Milyutina et al. 2010
*trn*L–F cpDNA	CGAAATTGGTAGACGCTGCG	forward	62	Bakalin et al. 2021
*trn*L–F cpDNA	TGCCAGAAACCAGATTTGAAC	reverse	60	Bakalin et al. 2021

dNTP-mixture (included in Encyclo Plus PCR Kit), 13.4 µl (for *trn*L–F)/12.4 µl (for ITS 1–2) of double-distilled water (Evrogen, Moscow, Russia), 1 µl of dimethylsulfoxide/DMSO (for ITS 1–2) and 0.4 µl of each primer (forward and reverse, at a concentration of 5 pmol/µl). Polymerase chain reactions were carried out using the following program: 180 sec initial denaturation at 94 °C, followed by 35 cycles of 30 sec denaturation at 95 °C, 20 (for *trn*L–F) – 30, 35 sec (for ITS 1–2) annealing at 58 °C (*trn*L–F and ITS 1–2) and 60 °C (ITS 1–2) and 30 sec elongation at 72 °C. Final elongation was carried out in one 3-min step at 72 °C. Amplified fragments were visualized on 1% agarose TAE gels by EthBr staining and purified using the Cleanup Mini Kit (Evrogen, Moscow, Russia). The DNA was sequenced using the ABI PRISM BigDye Terminator Cycle Sequencing Ready Reaction Kit (Applied Biosystems, Waltham, MA, USA) with further analysis of the reaction products following the standard protocol on an automatic sequencer 3730 DNA Analyzer. (Applied Biosystems, Waltham, MA, USA) in the Genome Center (Engelhardt Institute of Molecular Biology, Russian Academy of Sciences, Moscow).

Phylogenetic analyses

The alignments were compiled for the ITS 1–2 and *trn*L–F loci and aligned using MAFFT (Katoh and Standley 2013) with standard settings and then edited manually

in BioEdit ver. 7.2.5 (Hall 1999). All positions of the final alignment were included in the phylogenetic analyses. Absent data at the ends of regions and missing loci were coded as missing data. Both datasets revealed congruence after preliminary phylogenetic analysis, so we combined them into a single ITS 1–2+*trn*L–F alignment for further analysis.

Phylogenetic trees were reconstructed using two approaches: maximum likelihood (ML) with IQ-tree ver. 1.6.12 (Nguyen et al. 2015) and Bayesian inference (BA) with MrBayes ver. 3.2.7 (Ronquist et al. 2012).

For the ML analysis, the best fitting evolutionary model of nucleotide substitutions according to the BIC value was TIM2e+R2 determined by ModelFinder (model-selection method which is implemented in IQ-tree) (Kalyaanamoorthy et al. 2017). Consensus trees were constructed with 1000 bootstrap replicates.

Bayesian analyses were performed by running two parallel analyses using the GTR+I+G model. The analysis consisted of four Markov chains. Chains were run for five million generations, and trees were sampled every 500th generation. The first 2,500 trees in each run were discarded as burn-in; thereafter, 15,000 trees were sampled from both runs to produce a resulting tree. Bayesian posterior probabilities were calculated from the trees sampled after burn-in. The average standard deviation of split frequencies between two runs reached 0.0021 before the analysis was stopped.

To visualize molecular relationships within the *Marsupella* sect. *Stolonicaulon* we used TCS network inference method (Clement et al. 2002) in the PopART package (http://popart.otago.ac.nz/), accessed on 08 November 2019 (Leigh and Bryant 2015). The PopART program automatically removes positions having at least one N or a gap value from the consideration.

Results

Newly obtained ITS 1−2 and *trn*L−F sequences from specimen ASV15033 were deposited in GenBank. The combined ITS 1−2+*trn*L−F alignment of the 33 specimens consisted of 1409 character sites: conservative sites − 944 (67%); variable sites − 420 (29.81%); and parsimony-informative sites − 205 (14.55%).

The ML criterion recovered a bootstrap consensus tree with a log-likelihood = -6121.943. The arithmetic means of the log likelihoods in Bayesian analysis for each sampling run were -6145.17 and -6144.03.

On the Bayesian phylogenetic tree (Fig. 1), which demonstrates the ML topology with an indication of bootstrap support values (BS) and Bayesian posterior probabilities (PP), specimen ASV15033 formed a clade within sect. *Stolonicaulon* with high support of BS = 96% and PP = 1 (or 96/1). The TCS haplotype network (Fig. 2) revealed five haplotypes separated from each other by many nucleotide substitutions (at least 10), and specimen ASV15033 formed a separate group.

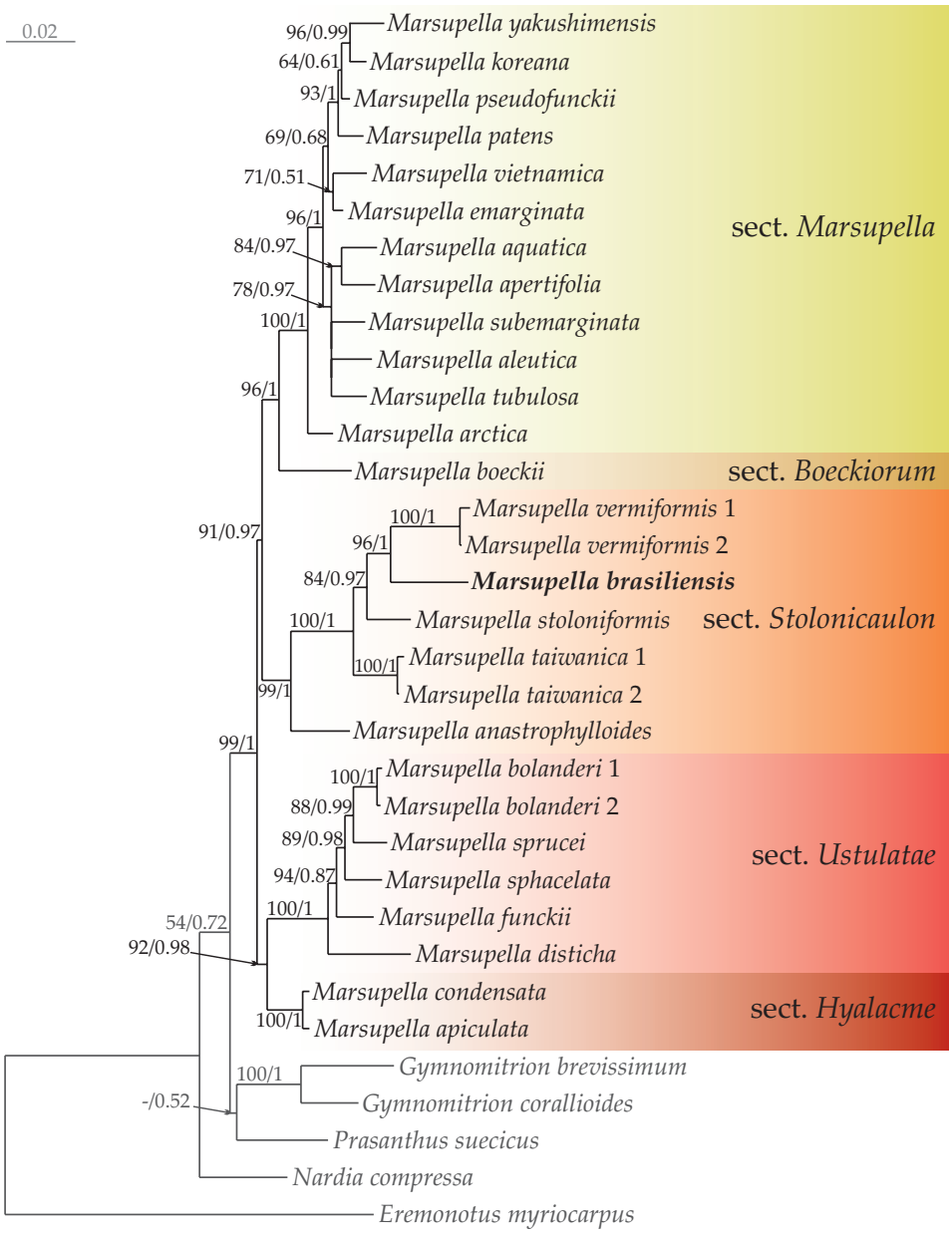

Figure 1. Phylogram obtained in a Bayesian analysis for the genus *Marsupella* based on the ITS 1–2+*trn*L–F dataset. The values of bootstrap support from the ML analysis and Bayesian posterior probabilities greater than 0.50 (50%) are indicated. The newly obtained sequences are marked in bold. Specimen voucher details and GenBank accession numbers are listed in Table 1.

The morphological comparison confirmed many traits indicating that the studied specimen belongs to sect. *Stolonicaulon*. Along with the latter, the comparison showed some features that do not fit well with the morphology of *M. microphylla* (Schuster

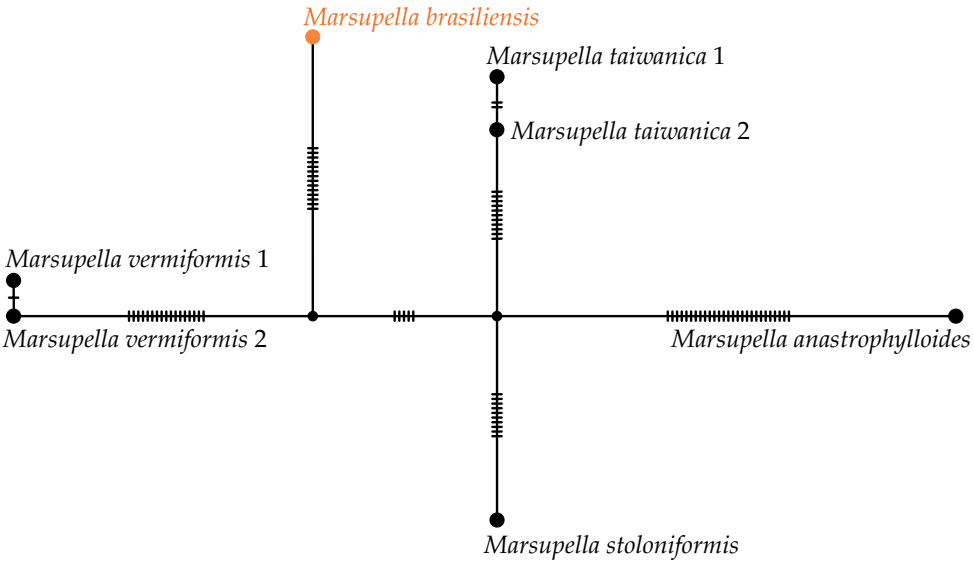

Figure 2. TCS haplotype network of ITS 1−2+*trn*L−F sequences for *Marsupella* sect. *Stolonicaulon*. Dashes indicate the number of nucleotide substitutions. Specimen voucher details and GenBank accession numbers are listed in Table 1.

1978, 1996); the most valuable features are stem cross-section, leaf and sporophyte characteristics. The latter, along with the results of molecular genetic comparison, led to the conclusion that the studied specimen belongs to *Marsupella* sect. *Stolonicaulon*; however, it is not conspecific with 'true' *M. microphylla*, as it was originally identified. Below, we provide the corresponding description of the specimen along with a discussion on its morphological traits.

Taxonomy

***Marsupella brasiliensis* Bakalin, Maltseva & Schäf.-Verw., sp. nov.**

Description. Plants wiry, ascending in loose patches, densely intermixed with *Cephaloziella* sp. and *Metasolenostoma* sp., perianthous plants strongly clavate, from densely branched and rhizomatous base, sterile branches 120–200 μm wide with leaves, in perichaetium zone to 900 μm wide, rusty to brownish and grading to whitish brown in older parts, with red tint in the leaf apices in the apical part of shoot. Rhizoids virtually absent in leaved shoots, in rhizomatous base sparse and colorless, separated (not united to the fascicles). Stem 70–90 μm in diameter, branching ventral, but new branch always arose near to the ventral base of the leaf and may be regarded as deeply postical-intercalary; cross section nearly orbicular, outer cells with outer wall thin, other slightly thickened (10-)12–14 μm in diameter, inward cell walls become thicker, with large triangular trigones, while cell size become smaller, 8–10 μm in diameter. Leaves obliquely to suberect spreading, slightly narrower to twice wider than stem,

50–180×60–190 μm, reniform to widely ovate, smaller constantly entire, sometimes with obtuse apex, larger divided by U-shaped sinus descending to 1/10–1/5 of leaf length, lobes acute. Underleaves absent. Midleaf cells strongly collenchymatous with large and slightly convex trigones, 10–14 μm in diameter to shortly oblong 10–16×8–12 μm, cuticle virtually smooth. Paroicous. Perianthous branches distinctly clavate, perigynium high, ca. 1250×550 μm, with 3 pairs of leaves whose lower pair composed by strongly ventricose bracts containing antheridia; perianth hidden within bracts, conical, eroding from the mouth, and completely disappearing after sporophyte emergence. Female bracts slightly wider than long, to 500×550 μm with gamma-shaped sinus descending to 1/4–1/3 of bract length, lobes triangular, acute, with somewhat diverging apices; bracteoles absent. Androecial bracts in 1(-2) pairs in lower part of perigynium, monandrous. Capsule wall bistratose, outer cells with nodular thickenings present on vertical walls and only sometimes present in horizontal walls; inner layer of rectangular cells with small nodular (not semicircular) thickenings. Spores brownish, 8–10 μm in diameter, faintly papillose, elaters bispiral, (-75)100–130×7–8 μm brown, with narrow, but never homogenous ends.

Type. Brazil, Rio de Janeiro, ca. 22°24'S, 44°41'W, Serra de Itatiaia, Hochgebirgsvegetation auf der Hochfläche bei Abrigo Rebouças, an exponierter, zeitweise sickerfeuchter Felswand [Serra de Itatiaia, high alpine vegetation on the plateau near Abrigo Rebouças, on exposed, intermittently dripping cliff], 2420 m, 15. Oct. 1991, leg. Schäfer-Verwimp & Verwimp 15033 (holotype JE!; isotype VBGI!, PRC, SP (not restudied in the preparation of the present account)).

Illustration in present paper. Fig. 3.

Discussion

The newly described *Marsupella brasiliensis* seems to be a rather rare species, hitherto known only from the Itatiaia mountains of Southeast Brazil between 2300–2420 m. Váňa (1999) reported this specimen for the first time in Brazil under the name *M. microphylla* (type of *M. brasiliensis*), and subsequently, a second specimen was cited from the same region by Gradstein and Costa (2003), who found it growing together with *Cephaloziella divaricata* (Sm.) Schiffn. In the type specimen, shoot fragments of a *Metasolenostoma* Bakalin & Vilnet species have been detected (confirmed genetically as the new species of the latter genus, unpublished). *Marsupella brasiliensis* was found only along the main road in the National Park on exposed rock faces, and further associated species are not known to us. It may have been overlooked due to its very small size and may rarely occur elsewhere around Itatiaia or Serra da Mantiqueira. Climate change may pose a threat to high-altitude bryophytes confined to Southeast Brazil.

The present study showed that this specimen identified as *Marsupella microphylla* previously and treated here as *M. brasiliensis* belongs to *Marsupella* sect. *Stolonicaulon*; therefore, the distribution of the section in Latin America is definitely confirmed. At the same time, the morphological study of the material revealed that the plants are

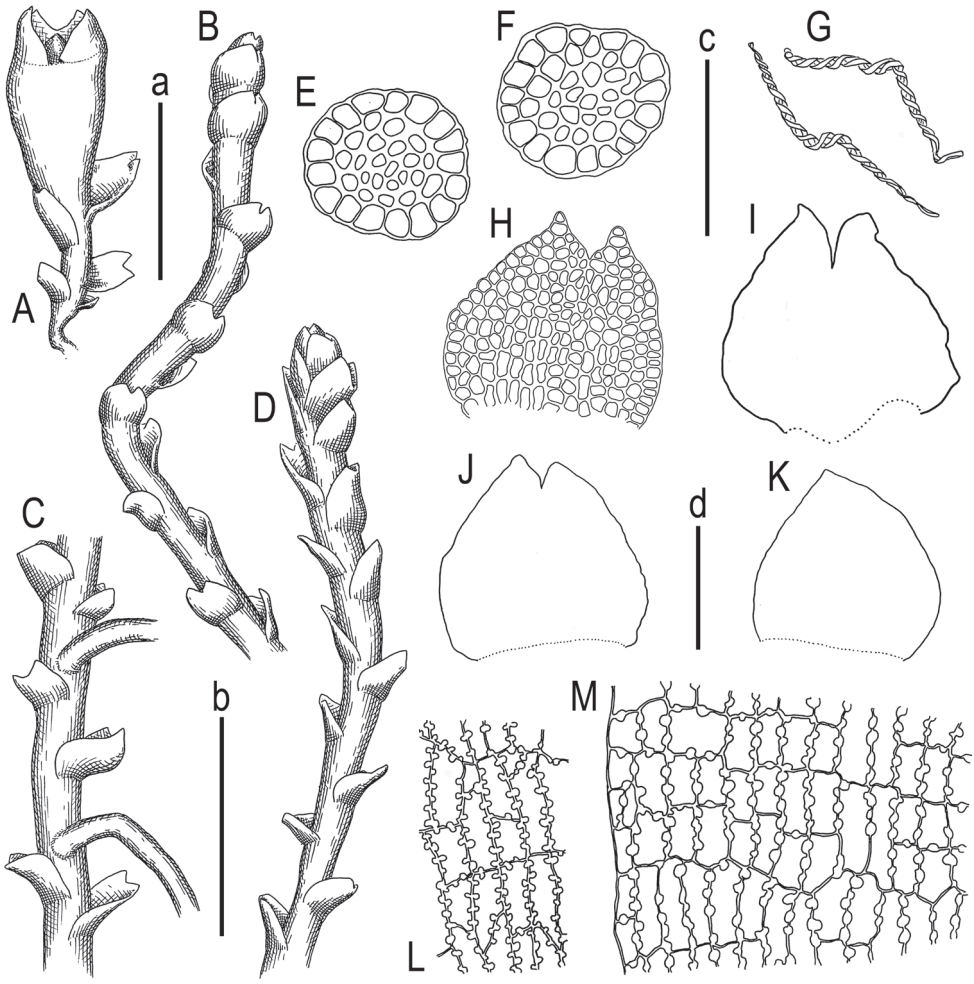

Figure 3. *Marsupella brasiliensis* Bakalin, Maltseva et Schäf.-Verw. sp. nov. **A** perianth bearing shoot, fragment **B** plant habit, fragment, lateral view **C** plant habit, fragment, ventral view **D** plant habit, fragment, dorsal view **E, F** stem cross-section **G** elaters **H–K** leaves **L** capsule, inner layer **M** capsule, outer layer. Scale bars: 1 mm (a: **A**); 500 μm (b: **B–D, I**); 100 μm (c: **E–G, L, M**); 100 μm (d: **H–K**). All from 15033 (isotype VBGI).

not conspecific with *M. microphylla*, which has been described from the Venezuelan Andes (Estado Merida, Sierra Nevada de Merida ca 4160 m a.s.l.). On one side, the high peaks of Itatiaia and the "páramo" characteristic of the "Campos de Altitude" benefit the establishment of large numbers of Andean species, such as *Aureolejeunea fulva* R.M. Schust., *Diplasiolejeunea pauckertii* (Nees) Steph. (also present in Central America), *Drepanolejeunea granatensis* (J.B. Jack & Steph.) Bischler, *Herbertus oblongifolius* (Steph.) Gradst. et Cleef, and others (Gradstein and Costa 2003; Costa et al. 2015, 2018). Macroclimatic congruities form the basis for strong Andean-southeast

Brazilian biogeographic connections, which was also confirmed by Frahm (1991) in the moss genus *Atractylocarpus* Mitt. and *Campylopus* Brid. On another side, the Serra da Mantiqueira, including the Itatiaia region, is famous for its high number of endemic species, including *Colura itatyana* Steph. and *Brachydontium notorogenes* W.R. Buck & Schäf.-Verw., as well as the genera *Cladastomum* Müll. Hal., *Crumuscus* W.R. Buck & Snider, and *Itatiella* Smith (Costa et al. 2018). Therefore, the nonspecificity of the Brazilian plant with the type of *Marsupella microphylla* is not truly surprising. Váňa (1999) mentioned differences in some sporophyte characters; however, he failed to describe a new species based on different seta structures alone. During investigation of the type specimen, some additional morphological differences came to light. Schuster (1996: 76) notes, "Elaters [in *M. microphylla*] very short rather stiff and sinuous, 6–7×60–70 μm, with 3 narrow spirals", in addition, as seen in fig. 14:11 in l.c., the elater endings are abruptly rounded. Whereas *M. brasiliensis* described here possesses distinctly bispiral elaters, they are narrowed at the end. Second, although the general tendency of the stem structure characteristic for several taxa of sect. *Stolonicaulon* (as well as many *Marsupella* Dumort. species in general) is retained: larger and thin-walled (or thinner-walled) cells on the outer layer and smaller and thick-walled cells inward, the cell size of *M. brasiliensis* is much smaller. In the latter, the outer cells are 12–14 μm in diameter and the inner cells are 8–10 μm in diameter, versus 12–25 μm in the outer layer and 12–15 μm in the inner layer in *M. microphylla*. Third, the leaves of *M. microphylla* are consistently bilobed, while in our species, they are entire on smaller shoots and are only shortly incised on larger shoots. In addition, Váňa (1999) noted the difference in the seta cross section between the *M. microphylla* type and the specimens described here as *M. brasiliensis*. He found that the seta cross section consists of 10–14(-16) rows of cells in the outer layer with 4–8 rows in the inner layer, whereas that of *M. microphylla* possesses 8–10 outer rows and 3–4 inner rows. Váňa (1999) treated this variability in seta cross section as hardly valuable for the taxonomy of *Marsupella*.

Within *Marsupella* sect. *Stolonicaulon*, based on taxa whose position within the section is genetically confirmed, sporophytes are only known in *M. stoloniformis* N. Kitag. The elaters of this species are 2–3-spiral (Bakalin et al. 2022). Elaters of *Marsupella brasiliensis* are strictly 2-spiral. It is worth mentioning that Váňa (1999: 226) wrote about the specimen discussed in the present study: "some elaters are 2-spiral (Schuster (1996) described as 3-spiral in *M. microphylla*)". Therefore, it is unclear if Váňa actually saw the 3-spiral elaters or was referring to the 3-spiral elaters previously described by Schuster (1996). The capsule structure is very similar to that described for *M. microphylla*: capsule wall bistratose, with nodular thickening in both the outer and inner layers. Within sect. *Stolonicaulon*, *M. brasiliensis* is distinguished from other species by paroicous inflorescence (shares this feature with conditionally referred to sect. *Stolonicaulon M. microphylla*, from which it immediately differs in bispiral elaters presence). The morphology of sterile plants of *M. brasiliensis* is similar to that of *M. vermiformis* (R.M. Schust.) Bakalin & Fedosov and *M. microphylla*; the haplotype network (Fig. 2) also shows the genetic relationship with *M. vermiformis*. *Marsupella brasiliensis* differs from both species in its less deep and inconsistently incised leaves.

The cell size of the leaves and the leaf cell network are similar in *M. brasiliensis* to those observed in *M. vermiformis* but not similar to those in *M. microphylla* (the cells are much smaller, as noted above). The stem cross-section characteristics of *M. vermiformis* are distinctly different from those of *M. brasiliensis* (smaller toward the margin versus distinctly larger toward the margin (cf. (Bakalin et al. 2019)), but somewhat similar to the stem cross-section characteristics of *M. microphylla*, *M. praetermissa* Bakalin et Vilnet and *M. anastrophylloides* Bakalin, Vilnet & Maltseva (cf. (Bakalin et al. 2022)).

Therefore, the present study has confirmed the occurrence of *Marsupella* sect. *Stolonicaulon* in Latin America, but was unable to determine whether *M. microphylla* belongs to sect. *Stolonicaulon*. Taking into account that the number of elater spirals and the shape of the elaters may be a rather important taxonomic feature, there are doubts that *M. microphylla* can be referred to as the same section, and the subgenus *Nanocaulon* may require re-evaluation, at least at the rank of section. *Marsupella* subg. *Nanocaulon* was synonymized with *M.* sect. *Boeckiorum* Müll. Frib. ex R.M. Schust. (*M*. sect. *Boeckiae* Müll. Frib.) in Váňa (1999: 226), based on the fact that the differences between two sections are not sufficient to maintain them as separate entities: "At the moment I do not agree with the separation of infrageneric taxa only on the basis of a different seta structure". This question also remained unanswered in the present research because we did not study molecularly 'true' *M. microphylla*. However, taking into account data in an integrative systematic study by Bakalin et al. (2019, 2022), where sect. *Boeckiorum* is strictly different from sect. *Stolonicaulon*, and considering the distribution pattern, we suggest that even if *M. microphylla* does not belong to sect. *Stolonicaulon* it also seems hardly possible that *M. microphylla* belongs to sect. *Boeckiorum*, which contains north Holarctic taxa and has a sister position to the *Marsupella* sect. *Marsupella*, which is also composed of North Holarctic species.

Marsupella brasiliensis is thus far the only known species of the sect. *Stolonicaulon* with paroicous inflorescence and occurring in Latin America whose position has been confirmed genetically. All other species are dioicous (with adjustment for the fact that the inflorescences are not known for *M. praetermissa* and *M. anastrophylloides*). Finally, we may assume that the mountain systems of Latin America may hide additional taxa belonging to *Marsupella* sect. *Stolonicaulon*, and purposeful research in this field should be continued.

Acknowledgements

Line-art figures were kindly prepared by Matvei Bakalin, to whom the authors are sincerely grateful. Authors are deeply indebted to Dr. Lars Söderström and Dr. Matthew Renner for critical evaluation of the manuscript and helpful comments.

The work of V.A.B. and Y.D.M. is within the frame of the institutional research project "Cryptogamic Biota of Pacific Asia" (no. 122040800088-5). The work of S.S.C. was supported by the Korean National Institute of Ecology, grant number NIE-A-2023-01.

References

Bakalin VA, Fedosov VE, Fedorova AV, Nguyen VS (2019) Integrative Taxonomic Revision of *Marsupella* (Gymnomitriaceae, Hepaticae) Reveals Neglected Diversity in Pacific Asia. Cryptogamie, Bryologie 40(7): 59–85. https://doi.org/10.5252/cryptogamie-bryologie2019v40a7

Bakalin V, Maltseva Y, Vilnet A, Choi SS (2021) The transfer of *Tritomaria koreana* to *Lophozia* has led to recircumscription of the genus and shown convergence in Lophoziaceae (Hepaticae). Phytotaxa 512(1): 41–56. https://doi.org/10.11646/phytotaxa.512.1.3

Bakalin VA, Vilnet AA, Mamontov YS, Schäfer-Verwimp A, Maltseva YD, Klimova KG, Nguyen VS, Choi SS (2022) *Stolonicaulon*: A Section-Puzzle within *Marsupella* (Gymnomitriaceae, Marchantiophyta). Plants 11(12): e1596. https://doi.org/10.3390/plants11121596

Clement M, Snell Q, Walke P, Posada D, Crandall K (2002) TCS: Estimating Gene Genealogies. Proceedings of the Proceedings 16th International Parallel and Distributed Processing Symposium, Washington, DC, USA, 15–19 April 2002. IEEE: Fort Lauderdale, FL, USA, 2002, 33. https://doi.org/10.1109/IPDPS.2002.1015467

Costa DP, Santos ND, Rezende MA, Buck WR, Schäfer-Verwimp A (2015) Bryoflora of the Itatiaia National Park along an elevation gradient: Diversity and conservation. Biodiversity and Conservation 24(9): 2199–2212. https://doi.org/10.1007/s10531-015-0979-4

Costa DP, Couto GP, Siqueira MF, Churchill SP (2018) Bryofloristic affinities between Itatiaia National Park and tropical Andean countries. Phytotaxa 346(3): 203–220. https://doi.org/10.11646/phytotaxa.346.3.1

Feldberg K, Váňa J, Krusche J, Kretschmann J, Patzak SDF, Pérez-Escobar OA, Rudolf NR, Seefelder N, Schäfer-Verwimp A, Long DG, Schneider H, Heinrichs J (2016) A phylogeny of Cephaloziaceae (Jungermanniopsida) based on nuclear and chloroplast DNA markers. Organisms, Diversity & Evolution 16(4): 727–742. https://doi.org/10.1007/s13127-016-0284-4

Frahm J-P (1991) Dicranaceae: Campylopodioideae, Paraleucobryoideae. Flora Neotropica. Monograph 54: 1–237.

Gradstein SR, Costa DP (2003) The Hepaticae and Anthocerotae of Brazil. Memoirs of the New York Botanical Garden, 87 pp.

Groth H, Helms G, Heinrichs J (2002) The systematic status of *Plagiochila* sects. *Bidentes* Carl and *Caducilobae* Inoue (Hepaticae) inferred from nrDNA ITS sequences. Taxon 51(4): 675–684. https://doi.org/10.2307/1555022

Hall TA (1999) BioEdit: A User-Friendly Biological Sequence Alignment Editor and Analysis Program for Windows 95/98/NT. Nucleic Acids Symposium Series 41: 95–98. https://doi.org/10.1021/bk-1999-0734.ch008

Hsiao C, Chatterton NJ, Asay KH, Jensen KB (1994) Phylogenetic relationships of 10 grass species: An assessment of phylogenetic utility of the internal transcribed spacer region in nuclear ribosomal DNA in monocots. Genome 37(1): 112–120. https://doi.org/10.1139/g94-014

Kalyaanamoorthy S, Minh BQ, Wong TKF, von Haeseler A, Jermiin LS (2017) ModelFinder: Fast model selection for accurate phylogenetic estimates. Nature Methods 14(6): 587–589. https://doi.org/10.1038/nmeth.4285

Katoh K, Standley DM (2013) MAFFT Multiple Sequence Alignment Software Version 7: Improvements in Performance and Usability. Molecular Biology and Evolution 30(4): 772–780. https://doi.org/10.1093/molbev/mst010

Leigh JW, Bryant D (2015) Popart: Full-feature software for haplotype network construction. Methods in Ecology and Evolution 6(9): 1110–1116. https://doi.org/10.1111/2041-210X.12410

Milyutina IA, Goryunov DV, Ignatov MS, Ignatova EA, Troitsky AV (2010) The phylogeny of *Schistidium* (Bryophyta, Grimmiaceae) based on the primary and secondary structure of nuclear rDNA internal transcribed spacers. Molecular Biology 44(6): 883–897. https://doi.org/10.1134/S0026893310060051

Nguyen L-T, Schmidt HA, Haeseler A, Minh BQ (2015) IQ-TREE: A Fast and Effective Stochastic Algorithm for Estimating Maximum-Likelihood Phylogenies. Molecular Biology and Evolution 32(1): 268–274. https://doi.org/10.1093/molbev/msu300

Ronquist F, Teslenko M, Mark P, Ayres DL, Darling A, Höhna S, Larget B, Liu L, Suchard MA, Huelsenbeck JP (2012) MrBayes 3.2: Efficient Bayesian Phylogenetic Inference and Model Choice Across a Large Model Space. Systematic Biology 61: 539–542. https://https://doi.org/10.1093/sysbio/sys029

Schuster RM (1978) Studies on Venezuelan Hepaticae. I. Phytologia 39: 239–251. https://doi.org/10.5962/bhl.part.7614

Schuster RM (1996) Studies on antipodal Hepaticae. XII. Gymnomitriaceae. The Journal of the Hattori Botanical Laboratory 80: 1–147.

Váňa J (1999) Notes on the genus *Marsupella* s. lat. (Gymnomitriaceae, Hepaticae) 1–10. Bryobrothera 5: 221–229.

PhytoKeys 226: 79–87 (2023)
doi: 10.3897/phytokeys.226.104110
https://phytokeys.pensoft.net

RESEARCH ARTICLE

A peer-reviewed open-access journal
PhytoKeys
Launched to accelerate biodiversity research

Lectotypification and nomenclature notes of the name *Caragana opulens* (Fabaceae, Papilionoideae) and its synonyms

Shabir A. Rather[1], Anand Kumar[2], Hongmei Liu[1]

1 *Center for Integrative Conservation & Yunnan Key Laboratory for Conservation of Tropical Rainforests and Asian Elephants, Xishuangbanna Tropical Botanical Garden, Chinese Academy of Sciences, Mengla, Menglun 666303, Yunnan, China* **2** *Central National Herbarium, Botanical Survey of India, P.O. Botanic Garden, Howrah-711 103, West Bengal, India*

Corresponding author: Shabir A. Rather (shabir@xtbg.ac.cn)

Academic editor: Patrick Herendeen | Received 27 March 2023 | Accepted 17 April 2023 | Published 12 May 2023

Citation: Rather SA, Kumar A, Liu H (2023) Lectotypification and nomenclature notes of the name *Caragana opulens* (Fabaceae, Papilionoideae) and its synonyms. PhytoKeys 226: 79–87. https://doi.org/10.3897/phytokeys.226.104110

Abstract

Morphological characters currently used to differentiate *Caragana opulens* as a species have been found to be insufficient and inconsistent. Through extensive research and comparisons of specimens, it has been revealed that *C. opulens* and its synonyms have overlapping geographical distributions, and that typification is necessary for *C. opulens*. Therefore, a lectotype is designated for the name *C. opulens*, with comments on its typification. Additionally, the current typification status is discussed for all its synonyms, accompanied by substantive notes.

Keywords

Lectotype, Leguminosae, opulens complex, overlapping traits, taxonomy

Introduction

The legume genus *Caragana* Fabr. (Fabaceae, Papilionoideae) is ecologically and pharmacologically important, comprising approximately 100 species distributed in temperate arid and semi-arid areas of the Northern Hemisphere (Polhill 1981; Zhang et al. 2009; Rather et al. 2021). China alone hosts more than 70% of the species diversity of these legumes, with about 66 species (Li and Ni 1985). The Euro-Asian range, which

includes 80 species, extends towards Japan, Korea, and Siberia in the north and northeast, towards Central Asia and Europe in the west, and along the Himalaya towards Northern India, Bhutan, and Nepal in the south (Polhill 1981; Lock 2005; Liu et al. 2010; Rather et al. 2021).

Identifying closely related species in *Caragana* has been challenging through the alpha taxonomic approach, as some species have overlapping morphological traits. One such case is of the *C. opulens* species complex, consisting of three species, namely *C. opulens*, *C. kansuensis* and *C. licentiana*. Although diagnostic characters have been identified, such as ovary/fruit pubescence, leaf shape, bract shape, and leaf pubescence, these traits have been found to be variable and labile (Moore et al. 2010). To make matters worse, several specimens housed in major herbaria in China have been misidentified (Zhao 1993). Extensive investigation of literature and comparison of specimens has revealed that these species have overlapping geographical distribution and require lectotypification.

During our ongoing revisionary studies of the genus *Caragana* in the Pan-Himalaya region, we found the typification of *C. opulens* Kom. requires clarification by designating a lectotype. By carefully studying the protologue and the material arguably studied by Komarov, we designated the lectotype for the above name. Furthermore, we discussed the types of all synonyms of this species, including *C. kansuensis* Pojark., *C. licentiana* Hand.-Mazz., *C. opulens* var. *angustifolia* Y.Z. Zhao ex Zhao Y. Chang & F.C. Shi., *C. opulens* var. *perforata* Merrgen & Ma., and *C. opulens* var. *trichophylla* Z.H. Gao & S.C. Zhang. Nomenclatural notes discussing the selection of type specimens are given for each name, and known isotypes are also cited.

Material and method

This study is based on the examination of relevant literature on the floristics of China and adjacent nations, and the examination of specimens held in the following herbaria: LE, P, PE, and W (Brach and Song 2006). We made special efforts to examine material studied by Komorov by reaching out to the curators of the Komarov Botanical Institute (LE) and the Naturhistorisches Museum Wien (W) to inquire about the availability of type specimens. To select types, we compared images and specimens with protologues, and the most complete and representative specimens were selected as lectotype for the name, according to Art. 9.3 of the "Shenzhen Code" (Turland et al. 2018).

Taxonomic treatment

Types of *Caragana opulens* and its synonyms

***Caragana opulens* Kom., Trudy Imp. S.-Peterburgsk. Bot. Sada. 29: 208. 1908.**

Type. China. Kansu: Bara-Topra, 26 April 1880, *N.M. Przewalski 42* (***lectotype*** LE [barcode LE01024209, image!], designated here, Fig. 1). Remaining syntypes: China. Kan-

Figure 1. Lectotype of *Caragana opulens* Kom. (LE01024209). Komarov Botanical Institute, St. Petersburg, Russia (LE).

su: Bara-Topra, 11 May 1880, *N.M. Przewalski s.n.* (LE [barcode LE01024210, image!]). China. Thibet [Tibet]: route de Lhassa à Batang, May 1890, *Henry D'Orléans s.n.* (P [barcode P02767097, image!]).

Caragana licentiana **Hand.-Mazz., Oesterr. Bot. Z. 82: 249. 1933.**

Type. China. Kansu, 16 June 1918, *Licent 3932* (***holotype*** W [barcode W0196552, image!, Fig. 2]; isotypes K [barcode K000511783, image!], P [barcode P02767130, image!]). China. Kansu: Kiangra, 9 October 1918, *Licent 4908* (paratypes W [barcode W0016458, image!], P [barcode P02767129, image!]).

Caragana kansuensis **Pojark., Bot. Mater. Gerb. Bot. Inst. Komarova Akad. Nauk S.S.S.R. 13: 138. 1950.**

Type. China. Kansu [Gansu]: Tjan-lo-ba dicto, 14 July 1908, *S. Czetyrkin s.n.* (***holotype*** LE [barcode LE01024198, image!, Fig. 3]).

Caragana opulens **var.** ***perforata*** **Merrgen & Ma, Acta Sci. Nat. Univ. Intramongol. 20: 554. 1989.**

Type. China. Nei Mongol: Hohhot, Daqing Shan, 31 May 1973, *Y.C. Ma & C.J. Wu 32* (***holotype*** HIMC [barcode HIMC0017878, image!] [https://www.cvh.ac.cn/spms/detail.php?id=e33a1be3]). ***Paratypes*****:** China. Nei Mongol: Baotou, Wudang Zhao, 8 July 1959, *Y.C. Ma et al. 4-47* (HIMC [barcode HIMC0017877, image!]). China. Ulanqab Meng, Helinger, 19 July 1959, *Y.C. Ma et al. 1-173* (HIMC [barcode HIMC0017879, image!]).

Caragana opulens **var.** ***trichophylla*** **Z.H. Gao & S.C. Zhang, Bull. Bot. Res., Harbin 9(3): 63. 1989.**

Type. China. Gansu: Minqinxian (Cultivated in Garden of Minqin Desert Botanica), 13 May 1988, *Z.H. Gao & S.C. Zhang 88001* (MQ, *n.v.*). Paratype: China. Gansu: Qilianshan, Qilianlinchang, *Z.H. Gao 86002* (MQ, *n.v.*).

Caragana opulens **var.** ***angustifolia*** **Y.Z. Zhao ex Zhao Y. Chang & F.C. Shi, Bull. Bot. Res., Harbin 31: 136. 2011.**

Type. China. Shaanxi: Suide, Jiuyuangou, near Wujiapan, 20 May 1956, *Huanghe Exped. 6879* (***holotype*** WUK [barcode WUK0086537, image!] [https://www.cvh.ac.cn/spms/detail.php?id=bfd87e11]; isotype PE [barcode PE00180919, image!]). ***Paratypes*****:** China. Shanxi: Wuzhai, Hanjialou, on a slope, alt. 1400 m, 13 June 1965, *J.X. Yang*

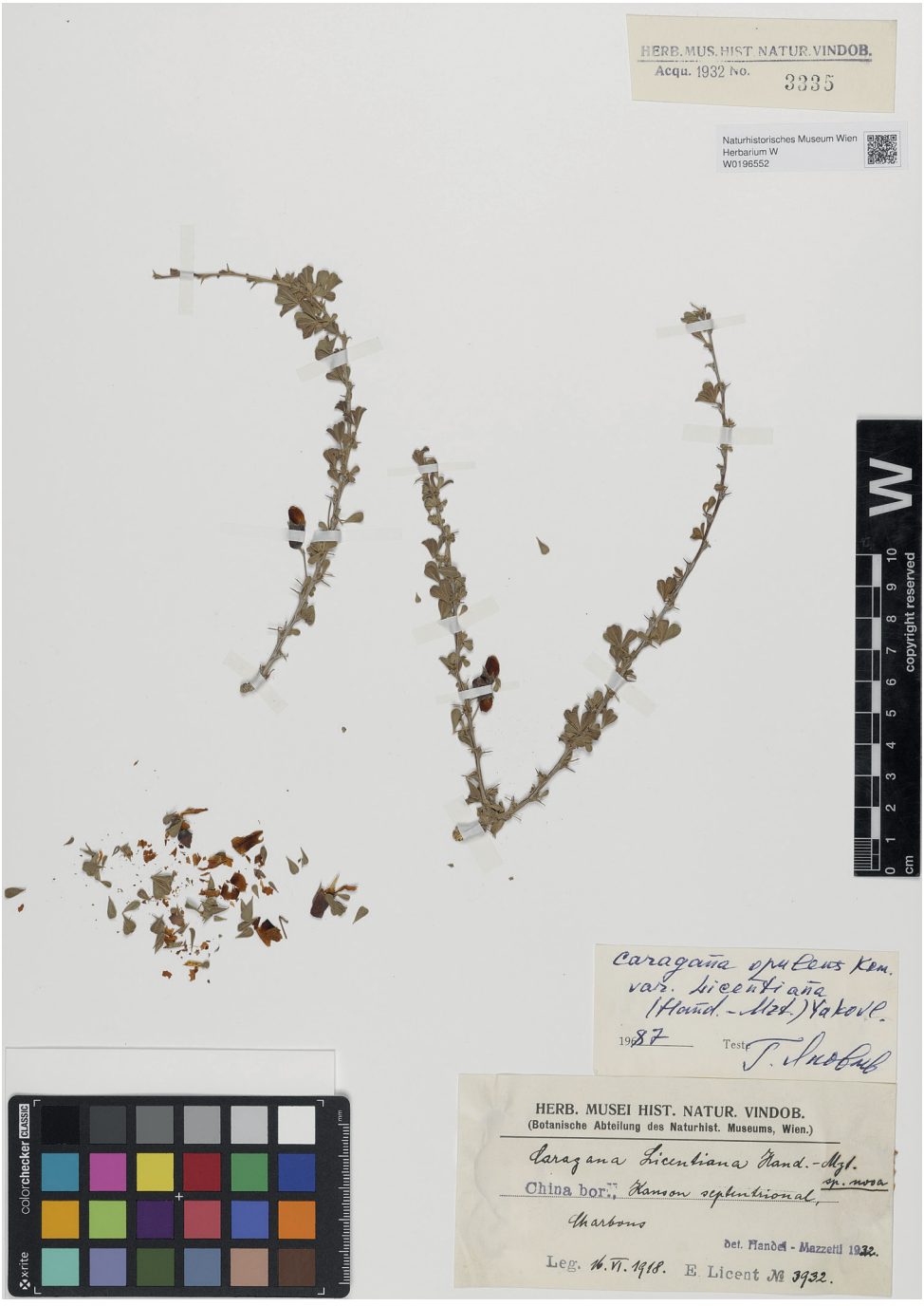

Figure 2. Holotype of *Caragana licentiana* Hand.-Mazz. (W0196552). Natural History Museum, Vienna-Herbarium (W).

Figure 3. Holotype of *Caragana kansuensis* Pojark. (LE01024198) Komarov Botanical Institute, St. Petersburg, Russia (LE).

3303 (WUK [barcode WUK024889, image!], HNWP [barcode HNWP86481, image!]). China. Shanxi province: Xingxian, Caijiaya, on a slope, 22 August 1955, *Huanghe Exped. 2074* (PE [barcode PE01580673, image!]) China. Shaanxi: Yanchuan, near Suyahe, alt. 580 m, 5 September 1955, *K.T. Fu 7857* (WUK, *n.v.*).

Nomenclature notes

Caragana opulens was described by the famous Russian botanist Vladimir Leontyevich Komarov (1869–1945) in 1908, who cited accessions from three major provinces: Gansu, Mongolia, and Tibet (Komarov 1908). The protologue included a total of eleven accessions, including four syntypes from Mongolia, six from Gansu, and one from Tibet. We were able to retrieve three specimens, namely two specimens at LE and one at P. Additionally, we found one specimen at PE with a label indicating 'Paratypus', but it lacked any herbarium collection label. Most importantly, there was no annotation by Komarov. Thus, no evidence supported that Komarov studied this specimen when he described *C. opulens*. Therefore, we excluded this specimen from our study. As Komarov worked at St. Peterburg, many accessions studied by him are expected to be held at the institute now named after him, the Komarov Botanical Institute at St. Petersburg, Russia (LE). Therefore, we gave preference to designate a lectotype from the collection maintained at LE. Two syntype specimens were present at LE, but the specimen was collected by the Russian explorer N.M. Przewalski (1839–1888) from Gansu, with the barcode number LE01024209, was the closest match to the protologue. Additionally, the specimen also bore pencil line drawings of dissected parts of flowers and fruit. Although the specimen bore the annotation 'Lectotypus' by N. Imch, this designation was never published. Here, we proposed to accept N. Imch's selection and designated this specimen as the lectotype of *Caragana opulens*, according to Art. 9.3 of the "Shenzhen Code" (Turland et al. 2018).

In 1933, the Austrian botanist Heinrich Raphael Eduard Handel-Mazzetti (1882–1940) described *Caragana licentiana* Hand.-Mazz. based on two collections, *Licent 3932* and *Licent 4908*, from the Gansu Province of China (Handel-Mazzetti 1933). In the protologue, *Licent 3932* was cited as the type. Furthermore, Handel-Mazzetti (1931) stated, "Die Exemplare befinden sich im Herbar des Naturhistorischen Museums in Wien" [The specimens are in the Herbarium of the Natural History Museum in Vienna]. We corresponded with the curator of the W and received one image of *Licent 3932* and one image of *Licent 4908*. Thus, the holotype *Licent 3932* was confirmed to be housed at W, while the duplicates at K and P represented isotypes. *Licent 4908* housed at W and P were assigned to be paratypes.

The name *Caragana kansuensis* Pojark. was described based on a collection by S. Czetyrkin obtained from the Gansu Province of China (Pojarkova 1950). We traced a single specimen of S. Czetyrkin at LE bearing Pojarkova's annotation '*Caragana kansuensis* sp. nov.' in her own handwriting. The specimen also comprised the dissected parts of flowers. Each and every part of the drawing of the protologue was also prepared from this specimen by the author. Therefore, we found conclusive evidence that this specimen represented the holotype.

Acknowledgements

We would like to express our gratitude to Dr. Irina Illarionova, Dr. Alisa Grabovskaya, and Dr. Leonid Averyanov at the Komarov Botanical Institute (RAS), Herbarium of Higher Plants (LE), St. Petersburg, Russia, for providing us with the high-resolution images of type specimens. We also thank Dr. Christian Bräuchler and Dr. Heimo Rainer of the Natural History Museum, Vienna-Herbarium (W), for granting us access to the highly valuable specimens held in their herbarium. The second author (AK) is thankful to the Director of the Botanical Survey of India (BSI) and the Head of Office, Central National Herbarium, BSI, for providing the facilities. We would also like to express our gratitude to Prof. Harald Schneider for reviewing the manuscript and improving its quality. We are grateful to the anonymous reviewer for their helpful comments and suggestions.

We acknowledge the financial support of the National Natural Science Foundation of China (Grant No. 32250410305) and the Yunnan Postdoctoral Research Project funded by the Yunnan Science and Technology Department (Grant No. Y8B-SH11008) for this study.

References

Brach AR, Song H (2006) eFloras: New directions for online floras exemplified by the Flora of China Project. Taxon 55(1): 188–192. https://doi.org/10.2307/25065540

Handel-Mazzetti H (1931) Kleine Beitrage zur Kenntnis der Flora von China. Oesterreichische botanische Zeitschrift 80: 337–343. https://doi.org/10.1007/BF01246111

Handel-Mazzetti H (1933) Kleine Beiträge zur Kenntnis der Flora von China. Oesterreichische botanische Zeitschrift 82: 245–253. https://doi.org/10.1007/BF01246320

Komarov VL (1908) Prolegomena ad floras Chinae nec non Mongoliae. Generis Caraganae mongraphia. Cum 16 tabulis et icone in textu. Trudy Imperatorskago S.-. Peterburgskago Botaniceskago Sada 29: 179–388.

Li PC, Ni CC (1985) *Chesneya* and *Gueldenstaedtia*. In: Wu CY (Ed.) Flora Xizangica. Science Press, Beijing, 789–797.

Liu YX, Chang ZY, Yakovlev GP (2010) *Caragana*. In: Wu ZY, Hong DY, Raven PH (Eds) Flora of China (Vol. 10). Science Press, Beijing & Missouri Botanical Garden Press, St Louis, 528–545.

Lock JM (2005) Tribe Hedysareae. In: Lewis G, Schrire B, MacKinder B, Lock M (Eds) Legumes of the World. Kew Publishing, London, 489–495.

Moore MJ, Soltis PS, Bell CD, Burleigh JG, Soltis DE (2010) Phylogenetic analysis of 83 plastid genes further resolves the early diversification of eudicots. Proceedings of the National Academy of Sciences of the United States of America 107(10): 4623–4628. https://doi.org/10.1073/pnas.0907801107

Pojarkova AI (1950) Araliaceae. Flora USSR (Vol. 16). Moscow–Leningrad, 646 pp.

Polhill RM (1981) Carmichaelieae, Galegeae, and Hedysareae. In: Polhill, RM, Raven PH (Eds) Advances in Legume Systematics, part. 1. Royal Botanic Garden, Kew, 357–370.

Rather SA, Wang S, Dwivedi MD, Chang ZY (2021) Molecular phylogeny and systematic evaluationof the *Caragana opulens* species complex (Fabaceae, Papilionoideae) based on molecular and morphological data. Phytotaxa 478(2): 179–200. https://doi.org/10.11646/phytotaxa.478.2.1

Turland NJ, Wiersema JH, Barrie FR, Greuter W, Hawksworth DL, Herendeen PS, Knapp S, Kusber WH, Li DZ, Marhold K, May TW, Mcneill J, Monro AM, Prado J, Price MJ, Smith GF (2018) International Code of Nomenclature for algae, fungi, and plants (Shenzhen Code) adopted by the Nineteenth International Botanical Congress, Shenzhen, China, July 2017. Regnum Vegetabile 159. Koeltz Botanical Books, Glashütten, 254 pp. https://doi.org/10.12705/Code.2018

Zhang ML, Fritsch PW, Cruz BC (2009) Phylogeny of *Caragana* (Fabaceae) based on DNA sequence data from *rbc*L, trnS–trnG, and ITS. Molecular Phylogenetics and Evolution 50(3): 547–559. https://doi.org/10.1016/j.ympev.2008.12.001

Zhao YZ (1993) Taxonomic study of the genus *Caragana* from China. Acta Scientiarum Naturalium Universitatis Intramongolicae 24: 631–653.

PhytoKeys 226: 89–100 (2023)
doi: 10.3897/phytokeys.226.100062
https://phytokeys.pensoft.net

SHORT COMMUNICATION

A peer-reviewed open-access journal
PhytoKeys
Launched to accelerate biodiversity research

Independent origins of *Spiranthes* ×*kapnosperia* (Orchidaceae) and their nomenclatural implications

Matthew C. Pace[1]

1 *New York Botanical Garden, 2900 Southern Blvd., Bronx, New York, 10348, USA*

Corresponding author: Matthew C. Pace (mpace@nybg.org)

Academic editor: Timothée Le Péchon | Received 8 January 2023 | Accepted 28 April 2023 | Published 19 May 2023

Citation: Pace MC (2023) Independent origins of *Spiranthes* ×*kapnosperia* (Orchidaceae) and their nomenclatural implications. PhytoKeys 226: 89–100. https://doi.org/10.3897/phytokeys.226.100062

Abstract

Spiranthes Rich. (Orchidaceae) is a commonly encountered but systematically and nomenclaturally challenging component of the North American orchid flora. Here, the evolutionary history and hybrid origin of the recently described *S. sheviakii* Hough and Young are critically examined. The available molecular data unambiguously support a hybrid origin of *S. cernua* (L.) Rich. × *S. ochroleuca* (Rydb.) Rydb. for *S. sheviakii*, the same parentage as the priority name *S.* ×*kapnosperia* M.C. Pace. As hybrid formulas can have only one correct name, *S. sheviakii* is a synonym of *S.* ×*kapnosperia*. It is likely that *S.* ×*kapnosperia* evolved independently at least twice in at least two widely disjunct locations.

Keywords

hybrid speciation, Interior Lowlands, nomenclatural priority, species complex, *Spiranthes cernua*, *Spiranthes ochroleuca*

Species complexes continue to present some of the most impenetrable systematic challenges for evolutionary biology and conservation biology, and the challenges associated with their study are amplified when species within a complex hybridize (e.g., Arnold 2001; Fu et al. 2020), with challenging implications for nomenclature. Although Orchidaceae have been long seen as a model family for pre-zygotic barriers to hybridization, primarily due to documented or inferred pollinator specificity (Ackerman et al. 2023), a growing body of literature makes clear that reproductive barriers are often porous, and that hybridization plays an important role in the speciation of many orchid genera (e.g., *Dactylorhiza* Neck. ex Nevski (e.g., Pillon et al. 2007), *Epidendrum* (e.g., Pinheiro et al. 2010), *Ophrys* L. (e.g., Soliva and Widmer 2003), *Orchis* Tourn. ex L. (e.g., Jacquemyn

et al. 2012), *Platanthera* Rich. (e.g., Wettewa et al. 2020), and *Tolumnia* Raf. (e.g., Ackerman and Galarza-Pérez 1991)), making for 'fuzzy' species boundaries.

Spiranthes is one such orchid genus where renewed systematic attention has supported many previous hypotheses of hybridization (e.g., Dueck et al. 2014), in addition to the discovery of new hybrid taxa (e.g., Pace and Cameron 2017). Of the 44 currently accepted *Spiranthes* species (including nothospecies), 10 have molecular evidence to support a hybrid origin (Sun 1996; Arft and Ranker 1998; Szalanski et a. 2001, Dueck et al. 2014; Pace 2015, 2021; Pace and Cameron 2017, 2019; Surveswaran et al. 2018; Pace et al. 2019). These hybrid species do not only occur within complexes of closely related species (e.g., *S.* ×*stellata* P.M.Br., Dueck and K.M.Cameron), but between clades of species complexes that are often distantly related (e.g., *S. diluvialis* Sheviak). The *S. cernua* (L.) Rich. species complex has traditionally been regarded as systematically "intractable" (Sheviak 1982, 1991; Sheviak and Brown 2002), primarily due to the frequency of hybridization and cryptic speciation (Pace and Cameron 2017) and the variability of all taxa involved. Within the *S. cernua* species complex, the identity of *S. ochroleuca* (Rydb.) Rydb. has contributed significantly to systematic and nomenclatural challenges. For example, primarily due to the nature of the *Gyrostachys ochroleuca* Rydb. holotype (*Mrs Long s.n.*, drawing, NY barcode 9463, Fig. 1), and morphological similarities to other members of the complex, *S. ochroleuca* has either been treated as a synonym or variety of *S. cernua* for much of the last 90 years (e.g., Gleason and Cronquist 1963). It was only after the detailed work of Sheviak and Catling (1980), that *S. ochroleuca* was widely accepted as a species fully distinct from *S. cernua* (e.g., Pace and Freudenstein 2018). Despite this distinction, *S. cernua* s.s. and *S. ochroleuca* were still hypothesized to engage in frequent and widespread hybridization and introgression (Sheviak 1982; Sheviak and Brown 2002). Pace and Cameron (2017) presented the first molecular evidence for hybridization between *S. ochroleuca* and *S. cernua* s.s. in the southern Appalachians, describing this hybrid taxon as *S.* ×*kapnosperia* M.C. Pace.

The name *S. sheviakii* Hough and Young (2021) was recently described as a species of hybrid origin distributed from central New York to the greater Ohio River Valley, but Hough and Young (2021) were unusually vague about the parentage of *S. sheviakii*, writing "[this is] apparently the result of hybridization of *S. ochroleuca* with another member of the *S. cernua* species complex" (pg. 47). They included comparisons to *S. cernua*, *S. ochroleuca*, and *S.* ×*kapnosperia* in the diagnosis and throughout the discussion, noting that *S. sheviakii* is "intermediate in form" between *S. cernua* and *S. ochroleuca* (pg. 37), but did not give a full parentage to their newly proposed species. Curiously, Hough originally identified the type specimens of *S. sheviakii* as "*S.* ×*kapnosperia*, *S. cernua* × *S. ochroleuca*" (Fig. 1), indicating he was aware of its full parentage, or that he thought these plants were morphologically similar to *S.* ×*kapnosperia*.

After reviewing the relevant type specimens (Fig. 1) and the publicly available molecular data presented in Pace and Cameron (2017) and Hough and Young (2021), it is clear that both *S.* ×*kapnosperia* and *S. sheviakii* share a hybrid ancestry of *S. cernua* × *S. ochroleuca*, although the genetic patterns are differently expressed in the resulting regional hybrids. Appalachian *S.* ×*kapnosperia* displays a discordance between nuclear and chloroplast datasets: the chloroplast data (including *ndhJ*)

Figure 1. Comparison of type specimens **A** holotype of *Spiranthes* ×*kapnosperia* (*M.C. Pace 1030,* NY) **B** holotype of *Spiranthes sheviakii* (*M. Hough and M.A. Young s.n.*, BH) **C** holotype of *Gyrostachys ochroleuca* Rybd. (*Mrs Long s.n.*, NY); this image is a composite of two images to show the front and back of the drawing plate **D** lectotype of *Ophrys cernua* L. (*P. Kalm s.n.*, LINN) **A** and **C** courtesy of the C. V. Starr Virtual Herbarium (http://sweetgum.nybg.org/science/vh/) **B** courtesy of the Liberty Hyde Bailey Hortorium, Cornell University **D** courtesy of the Linnean Society of London.

indicates a maternal parent of *S. ochroleuca*, whereas the nuclear data (*ACO* and nrITS) indicate a paternal parentage of *S. cernua* (Table 2; Pace and Cameron 2017). The *ACO* dataset for Appalachian *S.* ×*kapnosperia* lacks major nucleotide ambiguities at points of differentiation between the parental species, sharing all of the unique molecular synapomorphies of *S. cernua* vs. *S. ochroleuca*. *Spiranthes sheviakii* also displays a discordance between nuclear and chloroplast data, although the discordance is slightly different than in Appalachian *S.* ×*kapnosperia*. The available *ndhJ* data for *S. sheviakii* clearly indicate a maternal parentage of *S. cernua*, as the samples share all of the same nucleotide patterns as *S. cernua* and are clearly different from *S. ochroleuca* (or any other member of the *S. cernua* species complex). However, *S. sheviakii* displays *ACO* nucleotide ambiguities at all of the exact and unique points of molecular differentiation between *S. cernua* and *S. ochroleuca* (Fig. 2). These ambiguities in the *ACO* dataset indicate a hybrid origin between *S. cernua* and *S. ochroleuca* for

Table 1. Comparison of *Spiranthes cernua*, *S.* ×*kapnosperia*, and *S. ochroleuca*.

Taxon	Distribution	Flower color	Flower position	Labellum color (Adaxial / Abaxial)	Abaxial gland shape	Lateral sepal position
S. cernua	Maritime Canada s. to n. FL, west to central PA, the interior lowland plateaus, and e. Texas	White	Perpendicular to stem to strongly nodding	White to very pale yellow / white	Conical, reduced	Sepal base held in-line with the profile of the flower, sepals ascending
S. ×*kapnosperia*	Southern Appalachian Mountains of NC, SC, and TN; southern Great Lakes Basin from central NY to IL, s. to Ohio River Valley	White to ivory	Nodding to slightly ascending	Pale yellow / pale yellow	Rounded	Sepal base held just below the profile of the flower, sepals ascending
S. ochroleuca	Maritime Canada s. to w. NC, west through the Southern Great Lakes Basin, disjunct in s. IL, IN, central KY, and TN	Ivory to ochroleucous	Slightly to strongly ascending	Deep yellow / deep yellow	Rounded (sometimes reddish)	Sepal base held below the profile of the flower, held low against the profile of the flower, downwardly falcate to ascending

Table 2. Inferred genetic contributions for *S.* ×*kapnosperia* sensu nov. Chloroplast regions include *matK*, *ndhJ*, *trnL-F*, *trnS-M*, and *ycf1 3*' (Pace and Cameron 2017). The only chloroplast region sampled in Hough and Young (2021) for a priori *S. sheviakii* is *ndhJ*.

Hybrid taxa	ACO (nuclear)	nrITS	Chloroplast
S. ×*kapnosperia* (Appalachian *S.* ×*kapnosperia*)	*S. cernua* s.s.	*S. cernua* s.s.	*S. ochroleuca*
S. sheviakii (Interior Lowland *S.* ×*kapnosperia*)	*S. cernua* s.s. + *S. ochroleuca*	[not sampled]	*S. cernua* s.s.

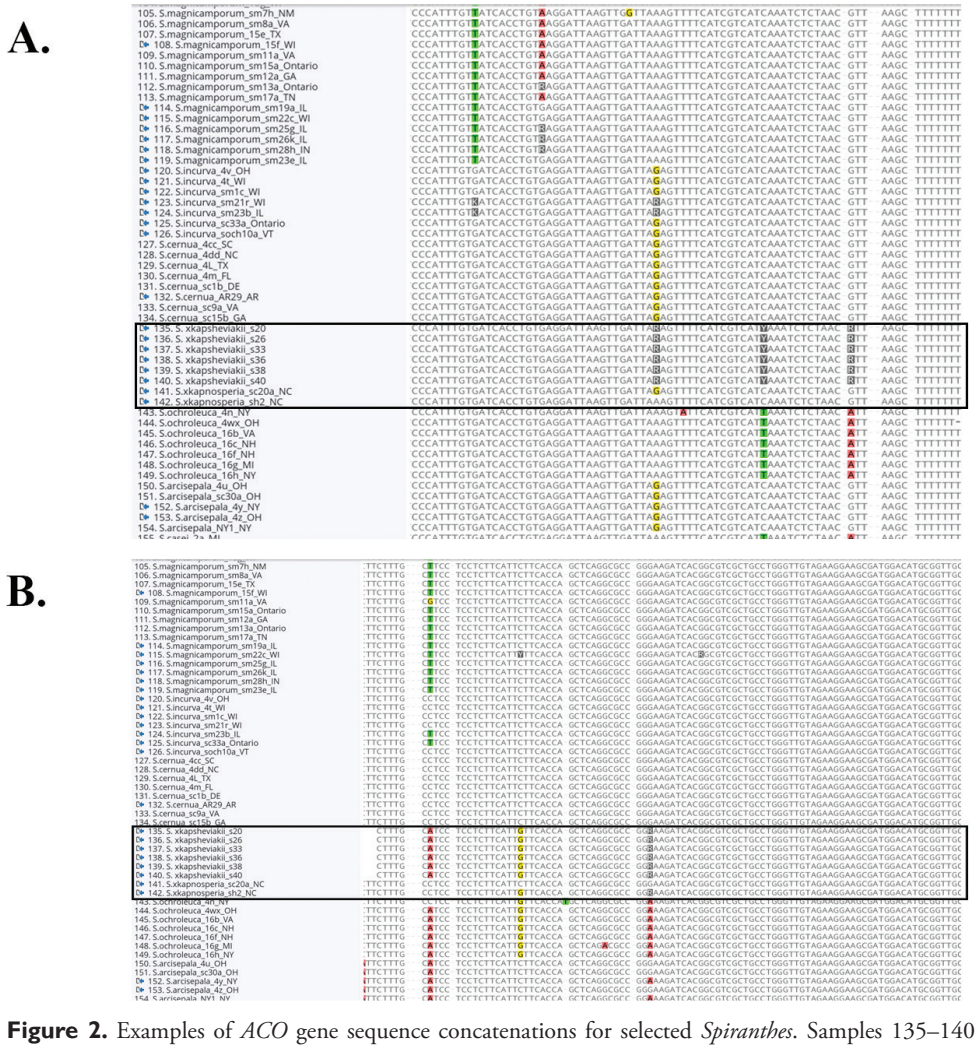

Figure 2. Examples of *ACO* gene sequence concatenations for selected *Spiranthes*. Samples 135–140 labeled "S. ×kapsheviakii" represent *a priori* interior lowland *S. sheviakii* from Hough and Young (2021), all other samples are from Pace and Cameron (2017). Samples 141 & 142 represent Appalachian *S.* ×*kapnosperia*. Samples of *S. cernua* s.s. are included immediately above the highlighted box and samples of *S. ochroleuca* are included immediately below the highlighted box **A** examples of ambiguities in *a priori S. sheviakii* that correspond to nucleotide differences between *S. cernua* and *S. ochroleuca* (e.g., G, R, A) **B** examples of nucleotide states that are shared with *S. ochroleuca* but not *S. cernua* (e.g., left-most highlighted A & G), and additional examples of ambiguous states in *a priori S. sheviakii* that correspond to nucleotide differences between *S. cernua* and *S. ochroleuca* (e.g., G, R, and A).

S. sheviakii. Additionally, the *ACO* nucleotide ambiguity patterns for *S. sheviakii* are distinct from those of regionally sympatric *S. incurva* (Jenn.) M.C. Pace, *S. magnicamporum* Sheviak, or any other member of the *S. cernua* species complex (Fig. 2), indicating these species are not involved in the evolution of *S. sheviakii*. The nucleo-

tide ambiguity and nuclear/chloroplast discordant patterns are consistent across all samples of *S.* ×*kapnosperia* and *S. sheviakii* included in Pace and Cameron (2017) and Hough and Young (2021). Thus, *S.* ×*kapnosperia* and *S. sheviakii* share the same ancestral hybrid parentage of *S. cernua* × *S. ochroleuca*, but this parentage is expressed differently within the genomes of the two resulting regionally distinct hybrid populations (Table 2). Nomenclaturally, per The Code (Article H.4.1):

When all the parent taxa can be postulated or are known, a nothotaxon is circumscribed so as to include all individuals recognizably derived from the crossing of representatives of the stated parent taxa (i.e. not only the F1 but subsequent filial generations and also back-crosses and combinations of these). There can thus be only one correct name corresponding to a particular hybrid formula; this is the earliest legitimate name (Art. 6.5) at the appropriate rank (Art. H.5), and other names corresponding to the same hybrid formula are synonyms of it.

Thus, any recognizably intermediate individual or population that results from the hybridization of *S. cernua* and *S. ochroleuca* must be recognized by the priority name *S.* ×*kapnosperia*, even if different hybridization events between the parental species occurred at different geologic times, in different places, resulting in different genomic expressions, and different morphologies. Based on the available *ndhJ* and *ACO* molecular data of Hough and Young (2021), *S. sheviakii* is unambiguously of hybrid origin between *S. cernua* and *S. ochroleuca*, and is thus synonymous with *S.* ×*kapnosperia*. It should be noted that species and nothospecies are the same nomenclatural rank, and the use of the multiplication symbol (×) is simply to emphasize the hybrid origin of nothospecies. Because Hough and Young (2021) appear to have been aware of the full hybrid parentage of their newly proposed name when they described *S. sheviakii* (based on the label of the type specimens, *Hough s.n.*, Fig. 1), this name is likely superfluous, although it is not illegitimate as they did not include the type of *S.* ×*kapnosperia* within the circumscription of *S. sheviakii*.

The evolutionary history of *S.* ×*kapnosperia* in its newly expanded understanding (*S.* ×*kapnosperia* sensu nov.) is perhaps one of the more unusual within the entire genus, having formed from the same two parental species (at least) two times, in widely disjunct locations, displaying different molecular signals between the parents. Additionally, the parental species likely played different maternal vs. paternal roles in the formation of the regionally disjunct *S.* ×*kapnosperia* populations (Table 2). The resulting differences in ambiguity patterns (or the lack of ambiguities) are likely due to differences in the hybridization and introgression histories of these regional populations. As Appalachian *S.* ×*kapnosperia* lacks *ACO* and nrITS ambiguities, it may be the result of chloroplast capture. This is a process through which an initial F1 hybridization event between paternal *S. cernua* and maternal *S. ochroleuca* is then followed by several backcrossing events with *S. cernua* as the pollen (paternal) parent, until the entire nuclear genome is only represented by *S. cernua*, but the chloroplast genome retains the original chloroplast contribution of *S. ochroleuca*. By contrast, the ambiguities present in the *ACO* locus of Interior Lowland *S.* ×*kapnosperia* (previously referred to as *S. sheviakii*) indicate it likely resulted from an initial F1 hybridization without exten-

sive (or only limited) backcrossing. Elsewhere in *Spiranthes*, Arft and Ranker (1998) hypothesized that at least two separate hybridization events between *S. magnicamporum* and *S. romanzoffiana* Cham. led to the formation of *S. diluvialis*, with subsequent localized dispersal in Utah and Colorado. However, the examined molecular signals from all sampled populations were the same (at the time of their study *S. diluvialis* was known from Colorado, Montana, Nevada, Utah, and Wyoming, but their study focused on samples from Colorado and Utah; Arft and Ranker 1998). Additional molecular phylogenetic study has not found major molecular differentiation between different populations of *S. diluvialis* (Dueck et al. 2014; Pace 2015).

Spiranthes ×*kapnosperia* was originally known to occur diffusely over a small region of the greater Smoky Mountain region and southern Blue Ridge Mountains, in the southern Appalachian Mountains of North Carolina, South Carolina, and Tennessee (Pace and Cameron 2017). The expanded understanding of *S.* ×*kapnosperia* sensu nov. discussed here extends the known distribution of this nothospecies throughout the distributional contact zone between *S. cernua* and *S. ochroleuca* along the northern limit of *S. cernua* in the area of the Interior Lowlands, Ohio River Valley, and southern Great Lakes Basin, an area that was not heavily sampled in the molecular work of Pace and Cameron (2017). Ecologically, populations in the southern Appalachians occur in more mesic sites vs. less mesic habitat of the Interior Lowlands populations; habitat variability is not uncommon across the genus. Morphologically, both disjunct populations are readily identifiable as intermediate hybrids of *S. cernua* × *S. ochroleuca*. However, they display slightly different morphological affinities to their parents, with southern Appalachian *S.* ×*kapnosperia* being more similar to *S. ochroleuca*, and Interior Lowland *S.* ×*kapnosperia* being more similar to *S. cernua*. The flowers of southern Appalachian *S.* ×*kapnosperia* are generally slightly ascending (as is common in *S. ochroleuca*). The flowers of Interior Lowlands *S.* ×*kapnosperia* are generally very similar in overall size and appearance to *S. cernua* s.s., commonly with a nod to the flowers, but sharing the yellowish labellum coloration and rounded abaxial labellum glands with *S. ochroleuca* (Table 1).

Within the *S. cernua* species complex, molecular data have supported hybridization as a strong driver of speciation, with four of the seven non-hybrid species within the complex involved in the evolution of six species of hybrid origin or nothospecies (Table 3, Pace and Cameron 2017). *Spiranthes cernua* is the most frequently involved species, giving rise to the evolution of four hybrid taxa, and is typically the inferred maternal parent. The frequent involvement of *S. cernua* in the evolution of hybrid taxa may be due to its broad geographic distribution, stretching from Maritime Canada south to northern Florida and west through the mid- and southern-Appalachian Mountains to Texas. The repeated evolution of hybrid taxa such as *S.* ×*kapnosperia*, in addition to the cryptic morphological nature of the species within the complex, has contributed to the systematic and nomenclatural challenges commonly associated with the genus. The repeated evolution of *S.* ×*kapnosperia* and complicated hybridization history of the wider *S. cernua* species complex also highlight the need for slow and careful study when deciding to name and describe new taxa within the genus (Ames

Table 3. Ancestry of known hybrid taxa derived from members of the *S. cernua* species complex, as supported by combined molecular and morphological evidence.

Hybrid taxa	Inferred paternal species	Inferred maternal species	Literature source
S. bightensis	*S. odorata*	*S. cernua*	Pace (2021)
S. casei	*S. lacera* (var. *lacera*)	*S. ochroleuca*	Pace (2015); Pace unpublished data
S. diluvialis	*S. magnicamporum*	*S. romanzoffiana*	Arft and Ranker (1998)
S. incurva	*S. magnicamporum*	*S. cernua*	Pace and Cameron (2017)
S. ×kapnosperia sensu nov.	*S. cernua* (southern Appalachian populations) or *S. ochroleuca* (Interior Lowland populations)	*S. cernua* (Interior Lowland populations) or *S. ochroleuca* (southern Appalachian populations)	Pace and Cameron (2017); Hough and Young (2021)
S. niklasii	*S. cernua*	*S. ovalis*	Pace and Cameron (2017)

1921), with particular attention given to nomenclatural rules and priority. Although they do not provide any molecular data, Hough and Young (2021), using terminology from Sheviak (1982), also place emphasis on the potential distinction of "low prairie race" and "southern prairie complex" populations currently contained within the circumscription of *S. cernua* s.s. Moving forward, researchers should keep in mind the priority names for taxa that involve hybridization between *S. cernua* and other members of the *S. cernua* species complex (Table 3). Additionally, not all individuals or populations of hybrid ancestry should be named, as genomic data increasingly shows complex hybridization and introgression patterns make for cryptically complex genetic ancestries and species relationships in groups with porous reproductive barriers (e.g., Evans et al. 2023).

A few additional notes related to Hough and Young (2021) are discussed here: 1) Hough and Young (2021) discuss the "holotype for *S. incurva*." As detailed in Pace and Cameron (2017), the name *S. incurva* is a nomenclatural combination based on the basionym *Ibidium incurvum* Jenn.:

Since Jennings selected a suite of specimens, "Aug. 24–26, 1905", housed at CM as "the type specimens", and not a specific specimen, collection number, or sheet, the specimen designated by Catling as the holotype, via an annotation label, is more properly designated as the lectotype. All other specimens collected on Aug. 26, 1905 must then be isolectotypes, and all other specimens collected within "the type specimens" collection range designated as syntypes.

The lectotype of *I. incurvum* is the *Jennings s.n.* specimen collected on 26 August 1905, from Fog Whistle (CM). However, this specimen is not discussed or examined in Hough and Young (2021), which only discusses the remaining syntypes. 2) Hough and Young (2021) note "at least within the range of this study, we have not observed *S. incurva* growing in xeric sites. The typical habitats appear to be mostly moist to wet and mediacid to calcareous." It should be noted that *S. incurva* is found in a wide variety of habitats, from hot, dry, sandy lake beach dunes, old fields, and roadside embankments, to standing in shallow water of fens and lake beach dune swales (Pace and Cameron 2017). This is inclusive of locations within the study range of Hough and Young (2021). 3) Hough and Young (2021) make much of apparent ambiguities

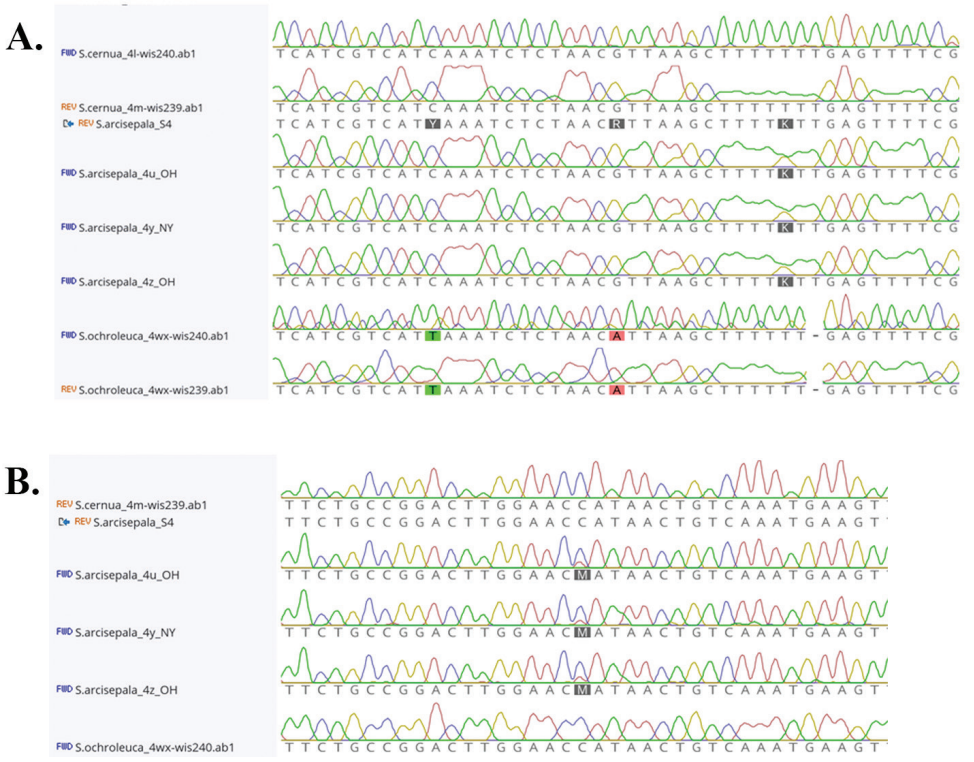

Figure 3. Examples of *ACO* gene nucleotide ambiguities for selected *Spiranthes*. The sample "S.arcisepala_S4" is from Hough and Young (2021), all other samples are from Pace and Cameron (2017) **A** examples of ambiguities present in Hough and Young (2021), but not present in Pace and Cameron (2017) (Y and R), and an ambiguity present in Hough and Young (2021) but overlooked in Pace and Cameron (2017) (K) **B** example of ambiguity present in Pace and Cameron (2017) (M), but not present in Hough and Young (2021).

in the nuclear *ACO* data for their accessions of *S. arcisepala* M.C. Pace, claiming that Pace and Cameron (2017) misinterpreted their data. After comparing the GenBank data of Hough and Young (2021) to the raw sequence data of Pace and Cameron (2017) (Fig. 3), there was a single instance where Pace and Cameron (2017) missed an ambiguity that is present in the data of Hough and Young (2021). However, the overwhelming majority of supposed *S. arcisepala* ambiguities present in Hough and Young (2021) are simply not present in our data, which are unambiguously a single nucleotide. Furthermore, I found an additional ambiguity in the *ACO* data of Pace and Cameron (2017) that is not present in the *ACO* data of Hough and Young (2021), and this point of ambiguity does not correspond to a point of molecular differentiation between any other member of the *S. cernua* species complex (Fig. 3). Based on this reexamination and comparison, I reassert that *S. arcisepala* is not of hybrid origin, although it may be an autopolyploid. Genomic examination of hybridization across the genus is obviously needed, and is currently underway.

Nomenclature

***Spiranthes* ×*kapnosperia* M.C. Pace [*S. cernua* × *S. ochroleuca*], Syst. Bot. 42: 659. 2017.**

= *Spiranthes sheviakii* M. Hough and M.A. Young. Native Orchid Conf. J. 18.3: 35. 2021. Type: U.S.A. New York: Onondaga County, town of Lysander, Three Rivers WNA, 19 Sep 2020, *M. Hough and M.A. Young s.n.* (holotype: BH! [BH 000298396]; isotype: CORT! (×2)).

Type. U.S.A. North Carolina: Transylvania County, Great Smoky Mountains, Pisgah National Forest, ca 7.5 km NW of Balsam Grove, north side of 215, below a steep seeping cliff, growing in moss and lichen hummocks, 2 Oct 2016, *M.C. Pace 1030* (holotype: NY! [01392730]; isotype: NCU! [NCU00332163], US!).

Acknowledgements

Thank you to Kanchi Gandi (Harvard University) for helpful conversations regarding the nomenclature of hybrids while this manuscript was in preparation; two anonymous reviewers for their helpful comments; Anna M. Stalter (BH) and Michael Hough (CORT) for sending images of the *S. sheviakii* types. James (Jim) Fowler (1947–2021) provided samples that led to the description of *S.* ×*kapnosperia*.

References

Ackerman JD, Galarza-Pérez M (1991) Patterns and maintenance of extraordinary variation in the Caribbean orchid, *Tolumnia* (*Oncidium*) *variegata*. Systematic Botany 16(1): 182–194. https://doi.org/10.2307/2418982

Ackerman JD, Phillips RD, Tremblay RL, Karremans A, Reiter N, Peter CI, Bogarín D, Pérez-Escobar OA, Liu H (2023) Beyond the various contrivances by which orchids are pollinated: global patterns in orchid pollination biology. Botanical Journal of the Linnean Society XX: 1–30. https://doi.org/10.1093/botlinnean/boac082

Ames O (1921) Notes on New England orchids. I. *Spiranthes*. Rhodora 23: 3–85.

Arft AM, Ranker TA (1998) Allopolyploid origin and population genetics of the rare orchid *Spiranthes diluvialis*. American Journal of Botany 85(1): 110–122. https://doi.org/10.2307/2446560

Arnold ML (2001) Anderson's paradigm: Louisiana Irises and the study of evolutionary phenomena. Molecular Ecology 9(11): 1687–1698. https://doi.org/10.1046/j.1365-294x.2000.01090.x

Dueck LA, Aygoren D, Cameron KM (2014) A molecular framework for understanding the phylogeny of *Spiranthes* (Orchidaceae), a cosmopolitan genus with a North American center of diversity. American Journal of Botany 101(9): 1551–1571. https://doi.org/10.3732/ajb.1400225

Evans SA, Whigham DF, Hartvig I, McCormick MK (2023) Hybridization in the Fringed Orchids: An Analysis of Species Boundaries in The Face of Gene Flow. Diversity (Basel) 15(3): 384. https://doi.org/10.3390/d15030384

Fu PC, Sun SS, Khan G, Dong XX, Tan JZ, Favre A, Zhang FA, Chen ZL (2020) Population subdivision and hybridization in a species complex of *Gentiana* in the Qinghai-Tibetan Plateau. Annals of Botany 125(4): 677–690. https://doi.org/10.1093/aob/mcaa003

Gleason HA, Cronquist A (1963) Manual of vascular plants of Northeastern United States and adjacent Canada. D. Van Nostrand Company.

Hough M, Young MA (2021) A systematic survey of the *Spiranthes cernua* species complex (Orchidaceae) in New York. The Native Orchid Conference Journal 18(3): 22–56.

Jacquemyn H, Brys R, Honnay O, Roldán-Ruiz I, Lievens B, Wiegand T (2012) Nonrandom spatial structuring of orchids in a hybrid zone of three *Orchis* species. The New Phytologist 193(2): 454–464. https://doi.org/10.1111/j.1469-8137.2011.03913.x

Pace MC (2015) Evolution, species boundaries, and biogeography of *Spiranthes* (Orchidaceae): Uncoiling Ames's "most perplexing orchid genus in our flora". Ph.D. dissertation. University of Wisconsin, Madison, WI.

Pace MC (2021) *Spiranthes bightensis* (Orchidaceae), a New and Rare Cryptic Hybrid Species Endemic to the U. S. Mid-Atlantic Coast. Phytotaxa 498(3): 159–176. https://doi.org/10.11646/phytotaxa.498.3.2

Pace MC, Cameron KM (2017) The systematics of the *Spiranthes cernua* species complex (Orchidaceae): Untangling The Gordian Knot. Systematic Botany 42(4): 640–669. https://doi.org/10.1600/036364417X696537

Pace MC, Cameron KM (2019) The evolutionary and systematic significance of hybridization between taxa of *Spiranthes* (Orchidaceae) in the California Sierra Nevada and Cascade Range. Taxon 68(2): 199–217. https://doi.org/10.1002/tax.12034

Pace MC, Freudenstein JV (2018) Orchidaceae, the orchid family. In: Naczi RFC, et al. (Eds) New Manual of Vascular Plants of Northeastern United States and Adjacent Canada, online edition 2016 onward. NYBG Press, New York. https://doi.org/10.21135/893275471.096

Pace MC, Giraldo G, Frericks J, Lehnebach CA, Cameron KM (2019) Illuminating the systematics of the *Spiranthes sinensis* species complex (Orchidaceae): Ecological speciation with little morphological differentiation. Botanical Journal of the Linnean Society 189(1): 36–62. https://doi.org/10.1093/botlinnean/boy072

Pillon Y, Fay MF, Hedrén M, Bateman RM, Devey DS, Shipunov AB, van der Bank M, Chase MW (2007) Evolution and temporal diversification of western European polyploid species complexes in *Dactylorhiza* (Orchidaceae). Taxon 56(4): 1185–1208. https://doi.org/10.2307/25065911

Pinheiro F, De Barros F, Palma-Silva C, Meyer D, Fay MF, Suzuki RM, Lexer C, Cozzolino S (2010) Hybridization and introgression across different ploidy levels in the Neotropical orchids *Epidendrum fulgens* and *E. puniceoluteum* (Orchidaceae). Molecular Ecology 19(18): 3981–3994. https://doi.org/10.1111/j.1365-294X.2010.04780.x

Sheviak CJ (1982) Biosystematic study of the *Spiranthes cernua* complex. Bulletin of the New York State Museum Science Service, Bulletin Number 448. https://doi.org/10.5962/bhl.title.135544

Sheviak CJ (1991) Morphological variation in the compliospecies *Spiranthes cernua* (L.) Rich.: Ecologically-limited effects of gene flow. Lindleyana 6: 228–234.

Sheviak CJ, Brown PM (2002) *Spiranthes*. In: Flora of North America Editorial Committee (Eds) Flora of North America vol. 26. Oxford University Press, New York, 530–545.

Sheviak CJ, Catling PM (1980) The identity and status of *Spiranthes ochroleuca* (Rydberg) Rydberg. Rhodora 82: 525–562.

Soliva M, Widmer A (2003) Gene flow across species boundaries in sympatric, sexually deceptive *Ophrys* (Orchidaceae) species. Evolution; International Journal of Organic Evolution 57(10): 2252–2261. https://doi.org/10.1111/j.0014-3820.2003.tb00237.x

Sun M (1996) The allopolyploid origin of *Spiranthes hongkongensis* (Orchidaceae). American Journal of Botany 83(2): 252–260. https://doi.org/10.1002/j.1537-2197.1996.tb12702.x

Surveswaran S, Gowda V, Sun M (2018) Using an integrated approach to identify cryptic species, divergence patterns and hybrid species in Asian ladies' tresses orchids (*Spiranthes*, Orchidaceae). Molecular Phylogenetics and Evolution 124: 106–121. https://doi.org/10.1016/j.ympev.2018.02.025

Szalanski AL, Steinauer G, Bischof R, Petersen J (2001) Origin and conservation genetics of the threatened Ute ladies'-tresses, *Spiranthes diluvialis* (Orchidaceae). American Journal of Botany 8(1): 177–180. https://doi.org/10.2307/2657138

Wettewa E, Bailey N, Wallace L (2020) Comparative Analysis of Genetic and Morphological Variation within the *Platanthera hyperborea* Complex (Orchidaceae). Systematic Botany 45(4): 767–778. https://doi.org/10.1600/036364420X16033962925303

PhytoKeys 226: 101–108 (2023)
doi: 10.3897/phytokeys.226.103005
https://phytokeys.pensoft.net

RESEARCH ARTICLE

A peer-reviewed open-access journal
PhytoKeys
Launched to accelerate biodiversity research

Amentotaxus × *hybridia* (Taxaceae), a new natural *Amentotaxus* hybrid from southeast Yunnan province, China

Lian-Ming Gao[1,2], Gui-Liang Zhang[3], Zhi-Qiong Mo[1,4], Philip Thomas[5]

1 *CAS Key Laboratory for Plant Diversity and Biogeography of East Asia, Kunming Institute of Botany, Chinese Academy of Sciences, Kunming 650201, China* **2** *Lijiang Forest Diversity National Observation and Research Station, Kunming Institute of Botany, Chinese Academy of Sciences, Lijiang 674100, Yunnan, China* **3** *Hekou Branch of Administration Bureau of Daweishan National Nature Reserve, Hekou, Yunnan 661399, China* **4** *University of Chinese Academy of Sciences, Beijing 10049, China* **5** *Royal Botanic Garden Edinburgh, 20A Inverleith Row, Edinburgh EH3 5LR, Scotland, UK*

Corresponding author: Lian-Ming Gao (gaolm@mail.kib.ac.cn)

Academic editor: Dennis Stevenson | Received 5 March 2023 | Accepted 12 April 2023 | Published 23 May 2023

Citation: Gao L-M, Zhang G-L, Mo Z-Q, Thomas P (2023) *Amentotaxus* × *hybridia* (Taxaceae), a new natural *Amentotaxus* hybrid from southeast Yunnan province, China. PhytoKeys 226: 101–108. https://doi.org/10.3897/phytokeys.226.103005

Abstract

During floristic surveys of Taxaceae in Hekou County, Yunnan Province, China, a putative natural hybrid between *A. yunnanensis* H.L. Li and *A. hekouensis* L.M. Gao was collected. Morphological and molecular evidence confirms its status as a natural hybrid. *Amentotaxus* × *hybridia* L.M. Gao has linear or linear-lanceolate leaves 6–13 cm × 1.0–1.5 cm, white stomatal bands with 34–40 rows on abaxial side, 2.5–3.5 mm, slightly wider than leaf margins; 3–6 seeds borne at the base of the branchlet, peduncle 1.3–1.6 cm long with 3–4 rows of persistent basal bracts.

Keywords

Amentotaxus × *hybridia*, molecular evidence, natural hybridisation, new hybrid, Taxaceae

Introduction

The genus *Amentotaxus* Pilg. (1916) in the family Taxaceae comprises five or six species (Fu et al. 1999; Farjon 2010; Yang et al. 2017). Southeast Yunnan (China) and adjacent areas of Vietnam and Laos are the centre of diversity for this genus with more than half of the known species recorded (Nguyen et al. 2004; Averyanov et al. 2014; Gao et al. 2019).

In February 2016, surveys were undertaken in the mountains near Nanxi town, Hekou county, Yunnan province, China to collect fertile material of the recently described species *Ametotaxus hekouensis* L.M. Gao. This taxon was initially identified as a potential new species based on DNA barcoding data (Gao et al. 2017) and then subsequently formally described (Gao et al. 2019). During the 2016 surveys, a tree with vegetative morphology intermediate between *A. yunnanensis* H.L. Li and *A. hekouensis* but with seed cones resembling *A. hekouensis*, was found growing with several trees identified as either *A. yunnanensis* or *A. hekouensis*. Its intermediate characters indicated that it may represent a hybrid between *A. yunnanensis* and *A. hekouensis*. Initial sequencing of two DNA barcodes, the plastid DNA (ptDNA) *trnL-F* and the internal transcribed spacer of nuclear ribosomal DNA (nrITS), previously used for species identification within *Amentotaxus* (Gao et al. 2017) indicated that the paternally inherited (Collins et al. 2013) ptDNA *trnL-F* sequence was identical to that of *A. hekouensis* (GenBank accession number: KX059381). The ITS sequence of the hybrid individual (including the whole length of ITS1 and 5.8S, and a partial sequence of ITS2) was also identical to that of *A. hekouensis* (GenBank accession number: JF975885). However, we found many mixed nucleotide sites in the ITS sequence where they are polymorphic between *A. yunnanensis* and *A. hekouensis* ITS sequences. These sites had double peaks but with different heights in the Sanger sequencing trace file, which suggested the presence of interspecific hybridisation but required further research.

Materials and methods

All measurements of the new hybrid of *Amentotaxus* were taken from dried herbarium specimens of the hybrid individual *GLM164267*. All measurements of *A. hekouensis* and *A. yunnanensis* were based on literature (Fu et al. 1999; Farjon 2010; Gao et al. 2019) and our collections and observations.

To confirm that the individual (*GLM164267*) is a hybrid between *A. hekouensis* and *A. yunnanensis*, we generated approximately 2.5GB (gigabase) of genome skimming data to assemble the complete plastid genome and nrITS region. The methods of DNA extraction, genome skimming sequencing, the plastome and nrITS sequences assembly, and gene annotation are detailed in Fu et al. (2022). We mapped the genome skimming reads back to the nrITS sequence to show the nucleotide composition of polymorphic sites of the hybrid individual along with the ITS sequence of *A. hekouensis* and *A. yunnanensis* (Gao et al. 2017).

Results and discussion

The morphological trait comparison among the three taxa showed that several traits of the hybrid (*Amentotaxus* × *hybridia*), such as texture of leaves, width of stomatal bands, and number of rows of each stomatal band, are intermediate between *A. hekouensis* and *A. yunnanensis*, but with more similarity to *A. hekouensis*. The hybrid differs from its parental species by having linear or linear-lanceolate leaves, white stomatal bands with 34–40 rows that are slightly wider than the marginal bands in width; 3–6 seeds borne at the base of the branchlet, and 3–4 rows of persistent basal bracts at the peduncle (Table 1).

The nrITS sequence of the hybrid individual *de novo* was assembled using the GetOrganelle toolkit (Jin et al. 2020), which is identical to that of *A. hekouensis* (AM24). There are 6,891 clean reads mapped to the nrITS region with a mean sequencing coverage of 494×. The mapping reads of the ITS region showed that a total of 17 polymorphic sites of ITS sequence were consistent with the polymorphic nucleotide sites between *A. hekouensis* (AM24) and *A. yunnanensis* (AM21); 15 were point mutation and two mononucleotide indels (Table 2). The result confirmed that the individual is the result of interspecific hybridisation between *A. hekouensis* and *A. yunnanensis*. The dominant nucleotides of the hybrid individual are same as those of *A. hekouensis* (AM24), and the ratio of the polymorphic nucleotide sites between the parental species ranged from 1.7 to 3.2 with an average of 2.2 (Table 2). This closely corresponds to the results from the direct sequencing of ITS sequence for the hybrid individual by Sanger sequencing. The trace file showed double peaks with different height at the polymorphic sites, and resulted in a messy sequence for primer ITS4 trace file after the occurrence of an indel in the ITS2. These results also indicated that the hybrid may not represent an F1 generation of the hybrid.

The length of the plastome of the hybrid (*GLM164267*) is 137,786 bp with 35.8% GC content. A total of 198,855 reads were mapped to the assembled plastome with an average sequencing coverage of 215×. The whole plastome included 118 unique genes, comprising 4 rRNA genes, 31 tRNA genes (three tRNA have two copies: *trnI-CAU*, *trnN-GUU* and *trnQ-UUG*) and 83 protein-coding genes. The plastid genome phylogenetic tree of *Amentotaxus* showed that the hybrid individual fell in the clade of *A. hekouensis* (data not shown). As the plastid genome is paternally inherited in *Amentotaxus*, the results demonstrate that *A. hekouensis* is the paternal parent with *A. yunnanensis* as the maternal parent. In our previous DNA barcoding study (Gao et al. 2017), we also found a hybrid individual (Coll. No.: *P11120*) from Thai Phin Tung Commune Dong Van, Ha Giang Province, Vietnam, which, at the time, was the first evidence of an interspecific hybridisation in natural populations of *Amentotaxus*. In that case, the paternal species was *A. yunnanensis* rather than *A. hekouensis*, and the hybrid was morphologically more similar to the paternal species *A. yunnanensis*. Both results demonstrate natural hybridisation between *A. yunnanensis* and *A. hekouensis* when they occur sympatically. The hybrids are morphologically more similar to the paternal species. The results also indicate that bidirectional hybridisation does occur.

Table 1. Morphological character comparison of the three *Amentotaxus* taxa.

Characters	*A. hekouensis*	*A. × hybridia*	*A. yunnanensis*
Leaf Length (cm)	8–12.5 cm	6–13 cm	3.5–10 cm
Leaf width (cm)	9–14 mm	10–15 mm	8–12 mm
Leaf texture	thin, leathery	moderately thick, leathery	thick, leathery
Leaf apex	long acuminate	acuminate	obtuse or tapered
Width of stomatal bands	2.1–3.0 mm	2.5–3.5 mm	3–4 mm
No. rows of each stomatal band	25–30	34–40	c. 40
Ratio of stomatal band/marginal band	0.75–1	1.10–1.25	> 2
Marginal band colour in fresh leaves	bright green	green	yellowish green
No. of bract rows on peduncle	unknown	3–4	2

Table 2. Sequence variation and polymorphisms of nrITS among the parent species and the hybrid.

nrITS	ITS1											ITS2					
Position	**179**	**200**	**268**	**307**	**355**	**366**	**368**	**425**	**461**	**516**	**816**	**833**	**856**	**861**	**910**	**964**	**969**
A. yunnanensis AM21 (female)	C	T	G	T	C	A	G	T	G	T	C	C	T	G	C	T	C
A. hekouensis AM24 (male)	T	C	A	C	T	T	T	C	C	C	T	–	C	A	G	–	G
A. × hybridia AM51	T/C	C/T	A/G	C/T	T/C	T/A	T/G	C/T	C/G	C/T	T/C	-/C	C/T	A/G	G/C	-/T	G/C
Nucleotide rate of polymorphic mapping sites#	2.0	2.2	2.2	2.3	2.5	2.0	2.0	2.1	2.2	2.3	3.2	2.6	2.6	2.1	2.0	1.9	1.7

The nucleotide rate is AM24/AM21 of the polymorphic mapping sites for the *A. × hybridia* individual (AM51) with genome skimming data.

Taxonomic treatment

***Amentotaxus* × *hybridia* L.M.Gao & G.L.Zhang, sp. nov.**
urn:lsid:ipni.org:names:77319909-1
Figs 1, 2, Table 1

Diagnosis. *Amentotaxus* × *hybridia* L.M. Gao & G.L. Zhang resembles *A. hekouensis* L.M. Gao, but differs by its larger linear or linear-lanceolate leaves of 6–13 cm × 1.0–1.5 cm, stomatal bands with 34–40 rows on abaxial side, 2.5–3.5 mm wide, slightly wider than the green leaf margins; 3–6 seeds borne at the base of the branchlets, peduncle 1.3–1.6 cm long, 3–4 rows of persistent basal bracts (Table 1).

Type. China. Yunnan: Qincaitang Mt., Longbao village, Nanxi Town, Hekou County, Honghe, 22°39'49"N, 104°01'17"E, elevation 1100 m, 15 February 2016 (with mature seeds), *Zhang GL*, *GLM164267* (Holotype: KUN, isotype: KUN).

Morphological description. Small tree up to 5 m tall, bark brown gray; branch cylindric or subtetragonal, yellowish green; leafy branchlets ascending, broadly rectangular to oblong-elliptic in outline, axis green in 1st year, greenish yellow in 2nd and 3rd years, quadrangular or subterete in cross section. Leaves borne at 40–70° to the branchlet axis, distichous, twisted at the short petiolate or nearly sessile base, subsessile or petiolate, petiole to 2 mm long, almost opposite, 5–7 leaf pairs on each branchlet;

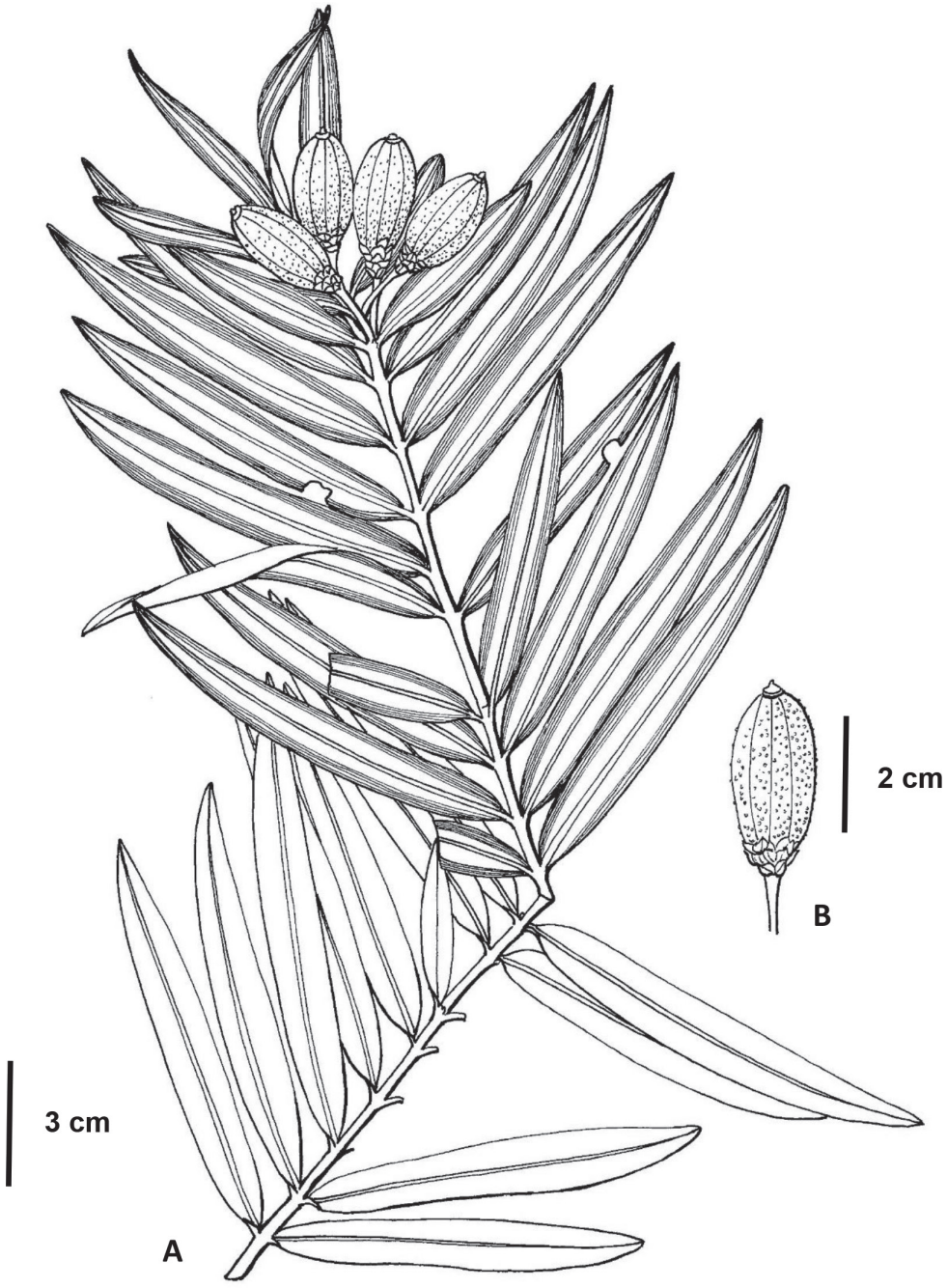

Figure 1. *Amentotaxus* × *hybridia* L.M. Gao & G.L. Zhang (from the holotype, drawn by Ling Wang) **A** branchlet with seeds **B** seed with peduncle and bracts.

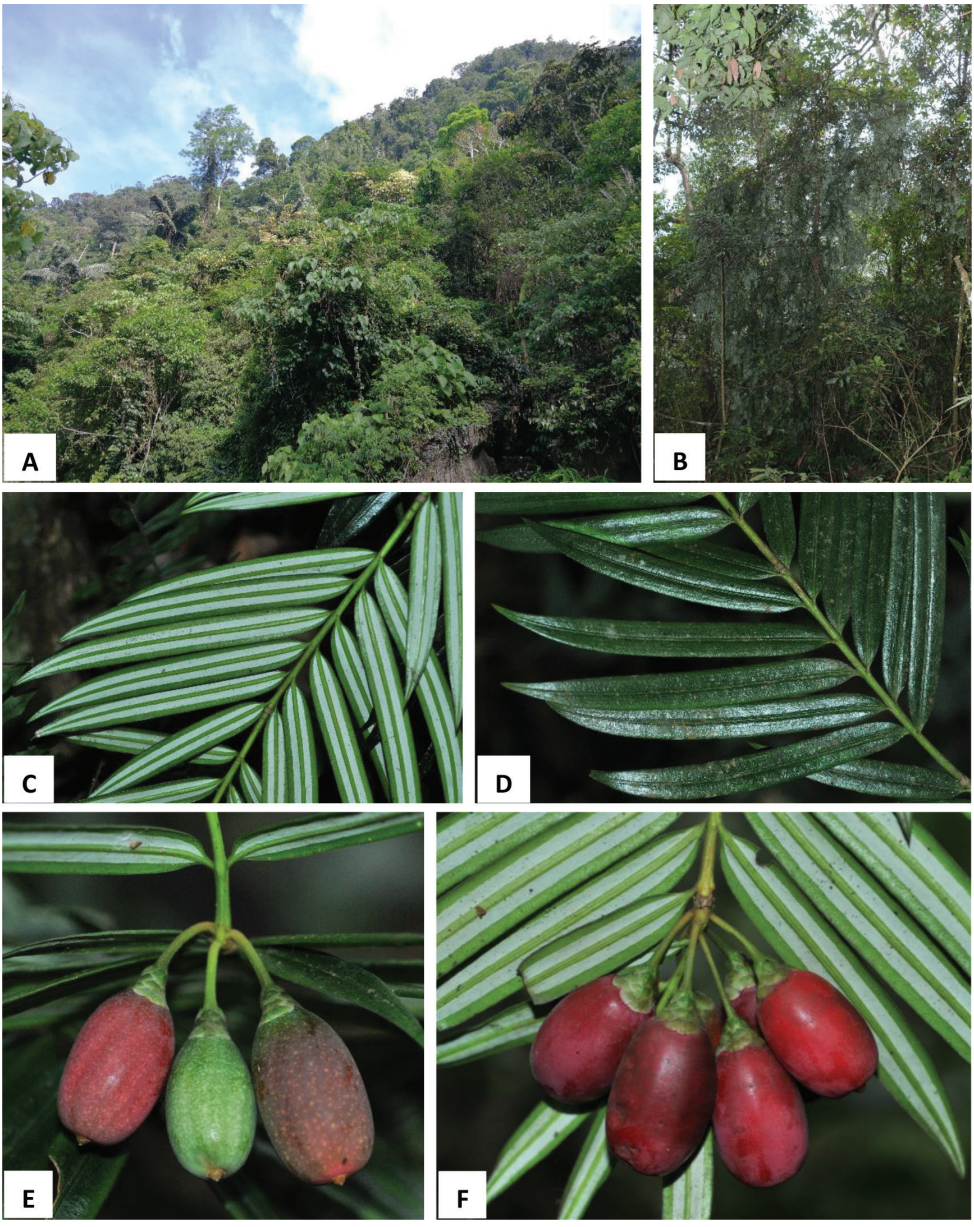

Figure 2. *Amentotaxus* × *hybridia* L.M. Gao & G.L. Zhang **A** habitat **B** habit **C** branchlet with abaxial leaves **D** branchlet with adaxial leaves **E** seeds bearing branchlet and seeds with mucronate apex **F** seed-bearing structure with peduncle and bracts.

Leaves leathery, linear or linear-lanceolate, 6–13 cm × 1.0–1.5 cm, straight, sometimes slightly falcate, cuneate at base, asymmetric, apex acuminate, leaf margin narrowly revolute, sometime flat; leaf marginal band green when fresh, yellowish green when

dry, 2.0–3.0 mm wide; stomatal bands white when fresh and yellow white when dry, 2.5–3.5 mm wide, slightly wider than green leaf margins, stomata in 34–40 rows of each band, densely arranged; midvein slightly sunken or flat adaxially, raised abaxially, 1.5–2.0 mm wide, narrower than the stomatal and marginal bands, yellowish green, same color as the branchlet. Seed-bearing structures in clusters of 3–6 at the base of the branchlet, not from subtending leaf. Aril reddish purple when ripe. Mature seed reddish purple, obovoid-ellipsoid, 2.5–3.0 cm × 1.4–1.6 cm, mucronate at apex, naked; peduncle 1.3–1.6 cm long, compressed-quadrangular, slightly dilated below bracts; 3–4 rows of persistent basal bracts on peduncle, four bracts per row, imbricate, obovate or obovate-oblong, with a ridge in middle. Seed maturity February. Pollen cone not seen.

Distribution and ecology. *Amentotaxus* × *hybridia* has only been found in the karst montane monsoon evergreen forest in southeast Yunnan province along the border between China (Hekou, Yunnan) and Vietnam occurring at an elevation around 1100 m.

Phenology. Seed matures in February.

Etymology. The specific epithet is derived from the natural hybridisation between *A. yunnanensis* and *A. hekouensis*.

Conservation status. As a natural hybrid, *Amentotaxus* × *hybridia* is not eligible for listing under the current IUCN Categories and Criteria (IUCN Standards and Petitions Committee 2022). However, as it occurs in areas where *A. yunnanensis* and *A. hekouensis* are sympatric, hybridisation could lead to a loss of genetic diversity for those species. In addition, the lack of a reproductive barrier between *A. hekouensis* and *A. yunnanensis* has implications for ex-situ conservation programs, especially if collections are intended to be used as a source of material for reintroduction or for long term conservation in cultivation.

Acknowledgements

We are grateful to Ms. Ling Wang from KUN for drawing the illustration of the holotype. This work was supported by the Strategic Priority Research Program of the Chinese Academy of Sciences (XDB31000000) and the Key Basic Research Program of Yunnan Province, China (202101BC070003). The Royal Botanic Garden Edinburgh is funded by the Rural and Environment Science and Analytical Services division of the Scottish Government.

References

Averyanov LV, Nguyen TH, Sinh KN, Pham TV, Lamxay V, Bounphanmy S, Lorphengsy S, Phan LK, Lanorsavanh S, Chantthavongsa K (2014) Gymnosperms of Laos. Nordic Journal of Botany 32(6): 765–805. https://doi.org/10.1111/njb.00498

Collins D, Mill RR, Möller M (2003) Species separation of *Taxus baccata*, *T. canadensis*, and *T. cuspidata* (Taxaceae) and origins of their reputed hybrids inferred from RAPD and cpDNA data. American Journal of Botany 90(2): 175–182. https://doi.org/10.3732/ajb.90.2.175

Farjon A (2010) A handbook of the world's conifers, Vol. 1. Brill, Leiden and Boston, 1073–1111. https://doi.org/10.1163/9789047430629

Fu LK, Li N, Mill RR (1999) Taxaceae. In: Wu ZY, Raven PH, Hong DY (Eds) Flora of China. Beijing: Science Press; St. Louis: Missouri Botanical Garden Press 4: 89–96.

Fu CN, Mo ZQ, Yang JB, Cai J, Ye LJ, Zou JY, Qin HT, Zheng W, Hollingsworth PM, Li DZ, Gao LM (2022) Testing genome skimming for species discrimination in the large and taxonomically difficult genus *Rhododendron*. Molecular Ecology Resources 22(1): 4049–4414. https://doi.org/10.1111/1755-0998.13479

Gao LM, Li Y, Phan LK, Yan LJ, Thomas P, Long KP, Möller M, Li DZ (2017) DNA barcoding of East Asian *Amentotaxus* (Taxaceae): Potential new species and implications for conservation. Journal of Systematics and Evolution 55(1): 16–24. https://doi.org/10.1111/jse.12207

Gao LM, Tan SL, Zhang GL, Thomas P (2019) A new species of *Amentotaxus* (Taxaceae) from China, Vietnam, and Laos. PhytoKeys 130: 25–32. https://doi.org/10.3897/phytokeys.130.33956

IUCN Standards and petitions committee (2022) Guidelines for Using the IUCN Red List Categories and Criteria. Version 15. Prepared by the Standards and petitions committee. https://www.iucnredlist.org/resources/redlistguidelines [Accessed on 9 May 2022]

Jin JJ, Yu WB, Yang JB, Song Y, Depamphilis CW, Yi TS, Li DZ (2020) GetOrganelle: A fast and versatile toolkit for accurate de novo assembly of organelle genomes. Genome Biology 21(1): 1–31. https://doi.org/10.1186/s13059-020-02154-5

Nguyen TH, Phan KL, Nguyen NDTL, Thomas PI, Farjon A, Averyanov L, Regalado J (2004) *Amentotaxus*. Vietnam Conifers: Conservation Status Review. Fauna and Flora International, Vietnam Program, Hanoi, 102–109.

Yang Y,Wang ZH, Xu XT (2017) Taxonomy and Distribution of Global Gymnosperms. Shanghai Science and Technology Press, Shanghai, 1039 pp.

PhytoKeys 226: 109–158 (2023)
doi: 10.3897/phytokeys.226.99316
https://phytokeys.pensoft.net

RESEARCH ARTICLE

A peer-reviewed open-access journal
PhytoKeys
Launched to accelerate biodiversity research

Insect herbivore and fungal communities on *Agathis* (Araucariaceae) from the latest Cretaceous to Recent

Michael P. Donovan[1,2,3,4], Peter Wilf[4], Ari Iglesias[5], N. Rubén Cúneo[6], Conrad C. Labandeira[3,7,8]

1 *Geological Collections, Gantz Family Collections Center, Field Museum of Natural History, Chicago, IL 60605, USA* **2** *Department of Paleobotany and Paleoecology, Cleveland Museum of Natural History, Cleveland, OH 44106, USA* **3** *Department of Paleobiology, National Museum of Natural History, Smithsonian Institution, Washington, DC 20013, USA* **4** *Department of Geosciences, Pennsylvania State University, University Park, Pennsylvania, 16802, USA* **5** *Instituto de Investigaciones en Biodiversidad y Medioambiente, CONICET-Universidad Nacional del Comahue, San Carlos de Bariloche, Río Negro 8400, Argentina* **6** *CONICET-Museo Paleontológico Egidio Feruglio, Trelew, Chubut 9100, Argentina* **7** *Department of Entomology and Behavior, Ecology, Evolution, and Systematics Program, University of Maryland, College Park, Maryland 20742, USA* **8** *College of Life Sciences, Capital Normal University, Beijing, 100048, China*

Corresponding author: Michael P. Donovan (mdonovan@fieldmuseum.org)

Academic editor: D. Stevenson | Received 30 December 2022 | Accepted 21 April 2023 | Published 26 May 2023

Citation: Donovan MP, Wilf P, Iglesias A, Cúneo NR, Labandeira CC (2023) Insect herbivore and fungal communities on *Agathis* (Araucariaceae) from the latest Cretaceous to Recent. PhytoKeys 226: 109–158. https://doi.org/10.3897/phytokeys.226.99316

Abstract

Agathis (Araucariaceae) is a genus of broadleaved conifers that today inhabits lowland to upper montane rainforests of Australasia and Southeast Asia. A previous report showed that the earliest known fossils of the genus, from the early Paleogene and possibly latest Cretaceous of Patagonian Argentina, host diverse assemblages of insect and fungal associations, including distinctive leaf mines. Here, we provide complete documentation of the fossilized *Agathis* herbivore communities from Cretaceous to Recent, describing and comparing insect and fungal damage on *Agathis* across four latest Cretaceous to early Paleogene time slices in Patagonia with that on 15 extant species. Notable fossil associations include various types of external foliage feeding, leaf mines, galls, and a rust fungus. In addition, enigmatic structures, possibly armored scale insect (Diaspididae) covers or galls, occur on *Agathis* over a 16-million-year period in the early Paleogene. The extant *Agathis* species, throughout the range of the genus, are associated with a diverse array of mostly undescribed damage similar to the fossils, demonstrating the importance of *Agathis* as a host of diverse insect herbivores and pathogens and their little-known evolutionary history.

Keywords
Araucariaceae, Gondwana, herbivory, plant-insect associations

Introduction

Agathis (Araucariaceae) is a genus of broadleaved conifers with ca. 17 extant species that are historically dominant in many areas of lowland to upper montane rainforests from Sumatra to New Zealand (Farjon 2010). The first South American and earliest known members of the genus occur as well-preserved vegetative and reproductive fossils in floras from the early Paleocene (ca. 64 Ma), early and middle Eocene (52.2 and 47.7 Ma), and possibly terminal Cretaceous (66–67 Ma) of Patagonian Argentina (Wilf et al. 2014; Escapa et al. 2018). The Paleocene species, *A. immortalis*, resolves as a stem lineage (Wilf et al. 2014; Escapa et al. 2018), and the approximately 12-million-year younger Eocene species, *A. zamunerae*, belongs to the crown lineage of *Agathis* based on the presence of many of the derived characters of the genus (Wilf et al. 2014; Escapa et al. 2018). Rich insect feeding damage on all the fossil *Agathis* species from Patagonia suggests that the species hosted diverse herbivore communities (Labandeira and Wappler 2023; but also see Root 1973) of specialized insects, as presented earlier in a paper that emphasized leaf mines (Donovan et al. 2020). The abundant damage provides a rare opportunity to study how insect herbivore communities developed on a host genus in the process of evolving its modern characteristics.

The earlier study (Donovan et al. 2020) found similar suites of insect damage, including leaf mines, external foliage feeding, and galls, on Patagonian *Agathis* fossils across four time slices spanning 18 million years from the latest Cretaceous to middle Eocene, and on extant *Agathis*. Two non-exclusive hypotheses were proposed to explain the pattern of persistent damage types on *Agathis* through time (Donovan et al. 2020): The first hypothesis is that similar damage-type morphology represents convergence, possibly due to the relatively unchanged leaf architecture and chemistry of *Agathis*, wherein unrelated groups of insects with similar feeding behaviors colonized *Agathis* repeatedly over time. Second, the evolutionarily conservative morphology and habitat preferences of *Agathis* (Kooyman et al. 2014; Wilf et al. 2014; Merkhofer et al. 2015) may have provided stability for ecological guilds or possibly herbivore communities containing the same insect lineages to persist on the genus over geologic time. A combination of these two scenarios likely contributed to the pattern of multiple persistent associations observed on *Agathis* through time (Donovan et al. 2020). By the early Eocene, diversified, modern-aspect *Agathis* probably ranged throughout Gondwanan rainforest biomes (Wilf et al. 2014). The genus may have been restricted to rainforest environments throughout its history, tracking suitable habitat during changing climates (Kooyman et al. 2014, 2022; Wilf et al. 2014; Merkhofer et al. 2015). Extant *Agathis* leaves have accessory xylem tissues adjacent to the veins (Kausik 1976). These tissues can collapse during periods of drought (Brodribb and Holbrook 2005), which underscores the necessity of elevated moisture availability.

In this study, we provide complete documentation of all the herbivore communities associated with fossil *Agathis* from the latest Cretaceous to middle Eocene of Patagonian Argentina as a follow-up to our previous study that focused on leaf mines (Donovan et al. 2020). We examined insect and fungal damage on cf. *Agathis* fossils from the latest Cretaceous part of the Lefipán Formation, *Agathis immortalis* from the early Paleocene (early Danian) Salamanca Formation, and *Agathis zamunerae* from the early Eocene Laguna del Hunco and middle Eocene Río Pichileufú sites (Huitrera Formation). Together, these assemblages represent four time slices spanning discontinuously an approximately 18 million-year-long interval from the latest Cretaceous to middle Eocene in which the evolution of the herbivore communities on *Agathis* was examined. We also document representative insect and pathogen damage on 15 species of extant *Agathis* from herbarium collections for comparisons with the fossils. We provide detailed descriptions of insect and fungal damage and discuss the biology of these associations and their extant analogs.

Methods

We compared insect and fungal damage on Patagonian *Agathis* fossils (482 specimens), including isolated leaves, leafy branches, and cone scales, from four latest Cretaceous to early middle Eocene fossil assemblages described below. We described all insect and fungal damage, except for previously described blotch mines (Donovan et al. 2020). Damage type numbers (DTs) were assigned with the "Guide to Insect (and Other) Damage Types on Compressed Fossil Plants" (Labandeira et al. 2007) and subsequent published and unpublished supplements. *Agathis* fossils from the Late Cretaceous Lefipán Formation, the early Paleocene Palacio de los Loros 2 (PL2) site, and the early Eocene Laguna del Hunco (LH) flora are housed at the Museo Paleontológico Egidio Feruglio (**MPEF-Pb**) in Trelew, Chubut Province, Argentina. Recent Río Pichileufú (RP) collections are curated at the Museo Paleontológico Bariloche (**BAR**), San Carlos de Bariloche, Río Negro Province (examined while on loan at MPEF), and the type material from RP first published by Berry (1938, under the name "*Zamia tertiaria*") is housed at the Smithsonian Institution, National Museum of Natural History (**USNM**), in Washington, DC, United States of America. Specimen numbers beginning with LefE, LefL, LefW, and PL2 are unique field numbers not yet assigned repository numbers, and these specimens are curated at MPEF.

The Lefipán Formation is a tidally dominated delta deposit in northwest Chubut, Argentina (Scasso et al. 2012; Vellekoop et al. 2017), which preserves a diverse Maastrichtian macroflora and Maastrichtian–Danian microfloras and marine invertebrates (67–66 Ma based on biostratigraphic age constraints; Kiessling et al. 2005; Barreda et al. 2012; Scasso et al. 2012; Vellekoop et al. 2017). As detailed elsewhere (Scasso et al. 2012; Donovan et al. 2017), three fossil plant localities (LefE, LefL, LefW) are located in close proximity. LefE and LefW are located

approximately 1000 m from each other on opposite sides of a ridge, and LefL is ~500 m to the east of LefE at the same stratigraphic level. Although no reproductive organs or in situ cuticles have been found, cf. *Agathis* leaves (10 specimens) from the Lefipán Formation exhibit characters associated with extant members of the genus, including a symmetrical, lanceolate shape, parallel venation, and a short, constricted petiole. The Lefipán flora is dominated by angiosperms (Stiles et al. 2020; Cunéo et al. 2021) and associated with diverse insect damage (Donovan et al. 2017, 2018). Besides likely *Agathis*, other conifers from the formation include *Araucaria lefipanensis* (Araucariaceae; Andruchow-Colombo et al. 2018), *Patagotaxodia lefipanensis* (Cupressaceae; Andruchow-Colombo et al. 2022), and *Retrophyllum superstes* (Podocarpaceae; Wilf et al. 2017).

Danian *Agathis immortalis* Escapa, Iglesias, Wilf, Catalano, Caraballo, and Cúneo fossils (319 specimens) are from Palacio de los Loros 2 (PL2), a fossil plant locality in the estuarine Salamanca Formation in southern Chubut (Iglesias et al. 2007, 2021; Stiles et al. 2020) deposited during chron C28n (64.67–63.49 Ma) (Gradstein et al. 2012; Clyde et al. 2014; Comer et al. 2015). *Agathis immortalis* specimens from PL2 (leaves, cone scales, winged seeds, and pollen cones with in situ pollen) have similar morphology to extant and fossil *Agathis*, with reproductive features that suggest a basal position within the lineage (Escapa et al. 2018). The PL2 flora is angiosperm dominated (Iglesias et al. 2007, 2021), and other well-described elements of the flora include Cunoniaceae flowers (Jud et al. 2018a; Jud and Gandolfo 2021), Menispermaceae endocarps and leaves (Jud et al. 2018b), a podocarpaceous conifer (Andruchow-Colombo et al. 2019), and *Azolla* (Salviniaceae) sporophytes (Hermsen et al. 2019).

Agathis zamunerae Wilf fossils (Wilf et al. 2014), including leaves, leafy branches, pollen cones, and cone scales with in-situ seeds, occur at two Eocene caldera-lake deposits in the Huitrera Formation, Laguna del Hunco (LH; 121 specimens; ^{40}Ar-^{39}Ar dated tuff from the fossiliferous interval with age 52.22 ± 0.22 Ma; Wilf et al. 2005b; Wilf 2012) and Río Pichileufú (RP; 32 specimens; ^{40}Ar-^{39}Ar dated tuff immediately above the main fossiliferous horizon of 47.74 ± 0.05 Ma; Wilf et al. 2005b; Wilf 2012), located in northwest Chubut and western Río Negro provinces, Argentina, respectively. Numerous paleontological studies have been conducted on fossil plants, insects, frogs, and fish from these localities, as summarized by Wilf et al. (2013, 2014) and (Barreda et al. 2020).

We also surveyed insect and fungal damage on extant *Agathis* specimens from several herbaria (in person), including nearly all *Agathis* collections at the Arnold Arboretum Herbarium (**A**) and Gray Herbarium (**GH**) of the Harvard University Herbaria, Royal Botanic Garden Edinburgh (**E**), Royal Botanic Gardens Kew (**K**), United States National Herbarium (**US**), Australian National Herbarium (**CANB**), National Herbarium of New South Wales (**NSW**), and the Singapore Botanic Gardens Herbarium (**SING**). From these collections, we documented representative insect and pathogen damage on 15 species of *Agathis*. Extant leaf mines associated with *Agathis* were covered in depth in the supplement of Donovan et al. (2020) and are re-illustrated and briefly described in the text here for the sake of completeness. Extant species taxonomy followed Farjon (2010).

Macro- and microphotographic methods for fossil and extant specimens were detailed previously (Donovan et al. 2020). We applied DT keywords to specimen photographs with Adobe Bridge to facilitate rapid comparisons between fossil and extant specimens (Rossetto-Harris et al. 2022). We used Adobe Photoshop CC 2017 to compose images and Adobe Camera Raw Editor to change temperature, white balance, contrast, and other features on whole images as needed.

Results: Insect herbivory on fossil *Agathis*

Latest Cretaceous, Lefipán Formation

Latest Cretaceous (Maastrichtian) cf. *Agathis* leaves from the Lefipán Formation are preserved with hole feeding, margin feeding, surface feeding, piercing and sucking, mining, galling, and oviposition damage. External foliage feeding (Fig. 1A–C) includes circular holes measuring 0.4–1.0 mm in diameter (DT1; Fig. 1A). The holes are surrounded by a 0.1–0.2 mm wide reaction rim, and the margins of the holes are not influenced by leaf venation. A shallow, semicircular excision into the leaf margin (DT12; Fig. 1B) measures 1.1 mm wide by 0.4 mm deep with a 0.3 mm wide reaction rim. Circular to polylobate patches of surface feeding (DT29; Fig. 1C) measure 1.4–3.9 mm in diameter.

A cluster of black marks probably represents piercing-and-sucking damage (DT46; Fig. 1D). The marks, or punctures, measure 0.1–0.2 mm in diameter. Some of these punctures are composed of a black rim that surrounds lighter tissue, interpreted as a reaction rim surrounding a pinpoint feeding site.

An oblong blotch mine lacking frass, occurring along the central axis of a leaf, was previously described by Donovan et al. 2020 (Fig. 1K). A serpentine mining association, characterized by a linear path largely confined by parallel venation (DT139; Fig. 1H–J), is also associated with a cf. *Agathis* leaf. The mine varies in width between 0.5–0.7 mm with no obvious directional width increase. The origin and overall trajectory of the mine, or possibly multiple mines, is difficult to discern because the entire leaf was not recovered, and some detail is obscured by poor preservation (Fig. 1I). Linear mine paths lie between adjacent parallel veins (Fig. 1J), although the mine sporadically crosscuts or straddles the veins. The central frass trail measures 0.3–0.4 mm wide (35–80% of the mine width) and is densely packed. The moderately to tightly sinusoidal frass trail is intermittent and may consist of spheroidal pellets. The lateral margins of the mine are smooth and parallel-sided (Fig. 1J).

Carbonized, oval galls measure 1.0–1.1 mm in maximum diameter by 0.8–0.9 mm in minimum diameter (DT32; Fig. 1E). The long axes of the galls are parallel to the leaf veins. The galls have a slight positive relief relative to the leaf surface.

Oviposition lesions are composed of inner elliptical, disturbed tissues surrounded by scar tissue, such as callus (Fig. 1F, G). The inner disturbed tissue areas measure 0.6 mm long by 0.2 mm wide, and the reaction tissue is 0.1–0.4 mm wide. The oviposition lesions are oriented parallel to major venation.

Figure 1. Insect damage on cf. *Agathis* leaves from the Lefipán Formation **A** circular hole with dark reaction rim (DT1; MPEF-Pb 9835) **B** small excision into the leaf margin (DT12) **C** patches of surface feeding (DT29) **D** cluster of circular piercing and sucking marks (DT46; MPEF-Pb 9837) **E** dark circular galls (DT32; MPEF-Pb 9829) **F** elliptical oviposition mark (DT101; MPEF-Pb 9841) **G** elliptical oviposition mark (DT101) **H** linear serpentine mines following leaf venation (DT139; MPEF-Pb 9836) **I** close-up of mines in (**H**) **J** detail of frass trail in (**H**) **K** oblong blotch mine (DT88; MPEF-Pb 9839).

Early Paleocene, Palacio de los Loros 2

Insect feeding on early Paleocene (Danian) *Agathis immortalis* at PL2 in the Salamanca Formation includes hole feeding, margin feeding, surface feeding, piercing and sucking, mining, and galling. External foliage feeding (Fig. 2A–F) includes circular holes measuring 0.3–3.4 mm in diameter (DT1, DT2; Fig. 2A, B) surrounded by 0.2 mm

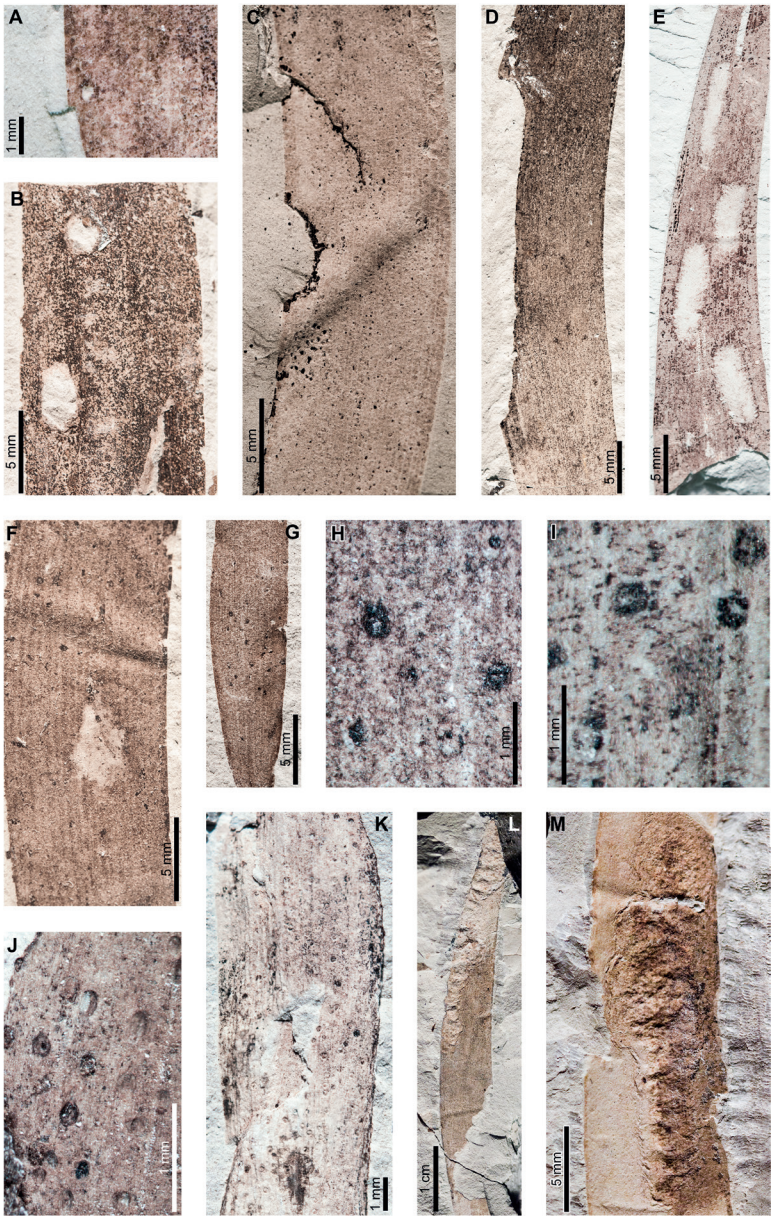

Figure 2. External foliage feeding, piercing and sucking, and leaf mining on *Agathis immortalis* from Palacio de los Loros 2 **A** small, circular hole (DT1; MPEF-Pb 6010) **B** circular and elliptical holes (DT2; MPEF-Pb 6042) **C** semicircular excision into the leaf margin (DT12; MPEF-Pb 6091) **D** elongate excision into the leaf margin (DT12; MPEF-Pb 9768) **E** zones of surface feeding (DT29; MPEF-Pb 9774) **F** patch of surface feeding (DT29; MPEF-Pb 6030) **G** cluster of piercing and sucking marks (DT46; MPEF-Pb 9766) **H** detail of piercing and sucking marks in (**G**) with central depressions **I** detail of piercing and sucking marks in (**G**) (DT46; MPEF-Pb 5959) **J** detail of piercing and sucking marks with central depressions in (**K**) (DT46; MPEF-Pb 9779) **K** clusters of piercing and sucking marks (DT46; MPEF-Pb 5959) **L** *Frondicuniculum flexuosum* blotch mine (DT421; paratype MPEF-Pb 6001) **M** *F. flexuosum* blotch mine (DT421; holotype MPEF-Pb 5970).

wide reaction rims. Shallow, approximately circular excisions into the leaf margin (DT12; Fig. 2C, D) measure 5.2–33.0 mm long by 1.0–1.8 mm deep into the leaf blade. Reaction tissue surrounding the excisions measures 0.1–0.3 mm wide. Circular to oblong surface feeding zones lack reaction rims (DT29; Fig. 2E, F) and measure 5.0–8.5 mm long by 1.3–2.7 mm wide. Leaf veins within the surface feeding zones are faintly visible or locally not visible.

Circular piercing-and-sucking marks (DT46; Fig. 2G–K) measure 0.1–0.3 mm in diameter. Some punctures have a depression at their centers (Fig. 2H–J). The punctures are typically clustered on a leaf.

Agathis immortalis is associated with *Frondicuniculum flexuosum*, an elongate-ellipsoidal blotch mine with undulatory margins with a wrinkled appearance (DT421; Donovan et al. 2020). The mines are positioned along leaf margins with their long-axes parallel to leaf veins. Frass is deposited as distinct pellets or more amorphous packets, either along one margin of the mine or throughout (Fig. 2L, M). We assign *F. flexuosum* to DT421 (Suppl. material 1) for use in future versions of the "Guide to Insect (and Other) Damage Types on Compressed Fossil Plants" (Labandeira et al. 2007), and detailed descriptions and an ichnotaxonomic treatment of *F. flexuosum* were provided by Donovan et al. 2020.

Agathis immortalis is associated with three gall DTs. Distinctive ellipsoidal to near-circular galls with thickened walls (DT115; Fig. 3A–J) measure (1.0) 2.0–5.0 (9.9) mm long by (0.9) 1.5–3.0 (3.9) mm wide. The galls are oriented with their long axes parallel to the leaf veins. The outer walls of the galls are composed of a thickened layer of woody tissue (Fig. 3I, J) preserved as carbonized material and measuring 0.2–0.9 mm wide. The hardened outer wall surrounds unthickened tissue where the internal chamber was located. The galls are situated on epidermal tissue, and epidermal cells are visible in the center of some galls (Fig. 3B–D). However, leaf veins are not visible within the galls. For those galls that preserve epidermal tissue, a small, black splotch, possibly representing the position of the larval chamber or an exit hole, is located near the center (Fig. 3B–D). The thickened outer rims of the galls may have extended over the entire surfaces of these structures (Fig. 3E). Circular galls with an outer rim of thickened tissue surrounding a zone of unthickened tissue (DT11; Fig. 3K) measure 0.7–1.6 mm in diameter. The thickened rim, 0.2–0.4 mm wide, is striated and carbonized. Although common at PL2, this gall type is not found on *Agathis* at any other locality.

The third gall DT associated with *Agathis immortalis* is defined as a columnar gall protruding above the leaf surface (DT116; Fig. 4A–L). The galls measure 1.1–1.8 mm in diameter and are ornamented with rounded or pointed bumps (Fig. 4E–K), which appear to be arranged concentrically. Some galls have a substantial oval depression near their center (Fig. 4I–L), which may be a feature of the standard morphology of the galls, analogous to extant galls made by *Neuroterus numismalis* (Hymenoptera, Cynipidae) on oak leaves (Jankiewicz et al. 2017), an exit hole, or a fungal ostiole. Each gall is surrounded by a thin rim of tissue (Fig. 4F–H), which wraps around the top of the gall on some specimens. The tissue rims measure 0.02–0.12 mm wide and approximately 0.3–0.4 mm tall, marked by horizontal and vertical striations (Fig. 4F–H).

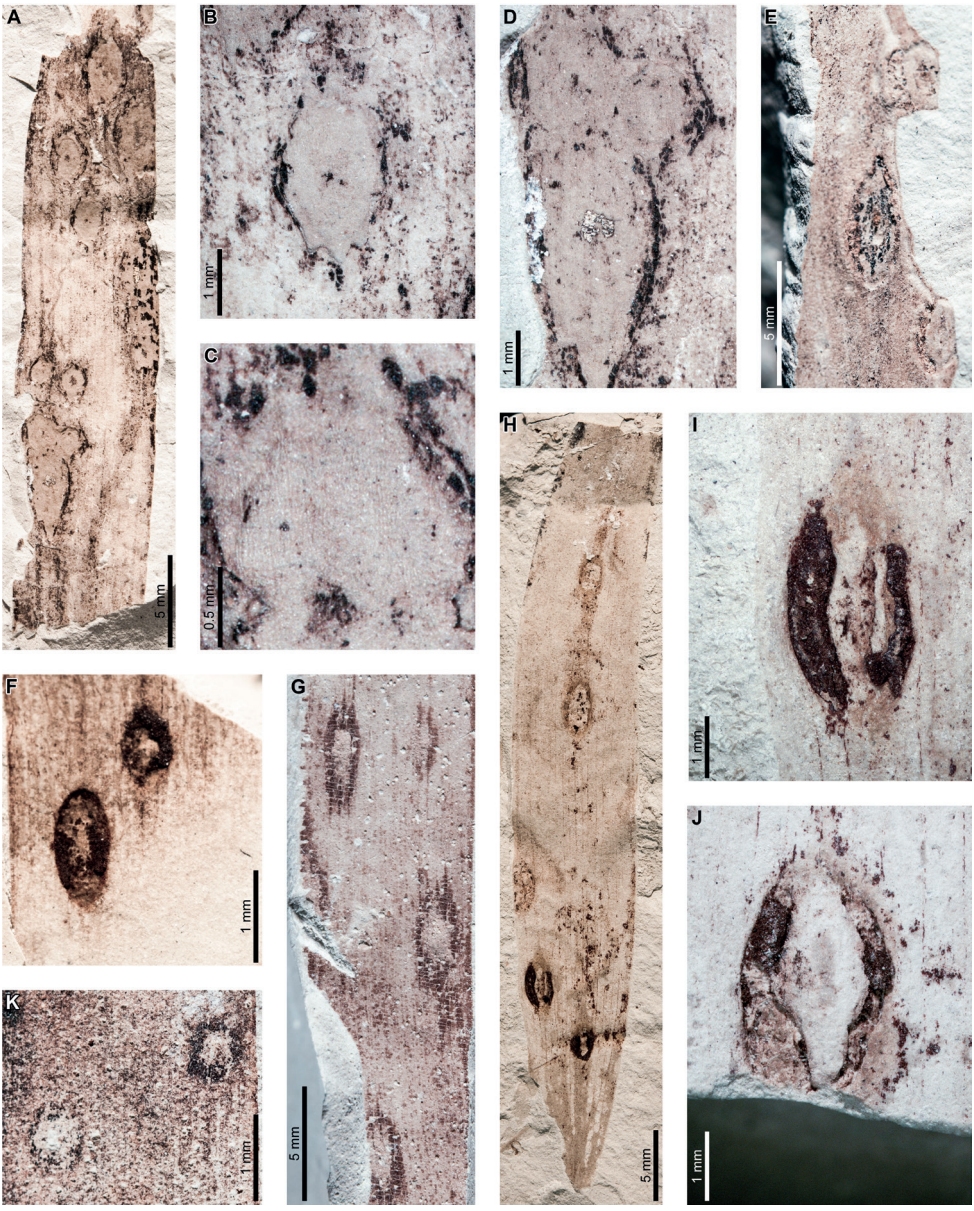

Figure 3. Galls on *Agathis immortalis* from Palacio de los Loros 2 (**A–K**) **A** elliptical galls with thickened outer walls surrounding epidermal tissue (DT115; MPEF-Pb 9767) **B** detail of oval gall with thickened walls in (**A**) **C** detail of gall in (**B**) showing files of epidermal cells and a dot representing the larval chamber or exit hole **D** detail of cluster of elliptical and circular galls in (**A**) **E** elliptical gall covered in carbonized, thickened tissue (DT115; MPEF-Pb 5977) **F** galls with thickened outer walls and central larval chamber (DT115; MPEF-Pb 6029) **G** galls with thickened outer walls (DT115; MPEF-Pb 6027) **H** five galls with carbonized, thickened walls (DT115; MPEF-Pb 9773) **I** detail of elliptical gall with carbonized, thickened walls in (**H**) **J** detail of elliptical gall with carbonized, thickened walls in (**H**) **K** circular galls with thickened outer tissue surrounding unthickened inner area (DT11; MPEF-Pb 5983).

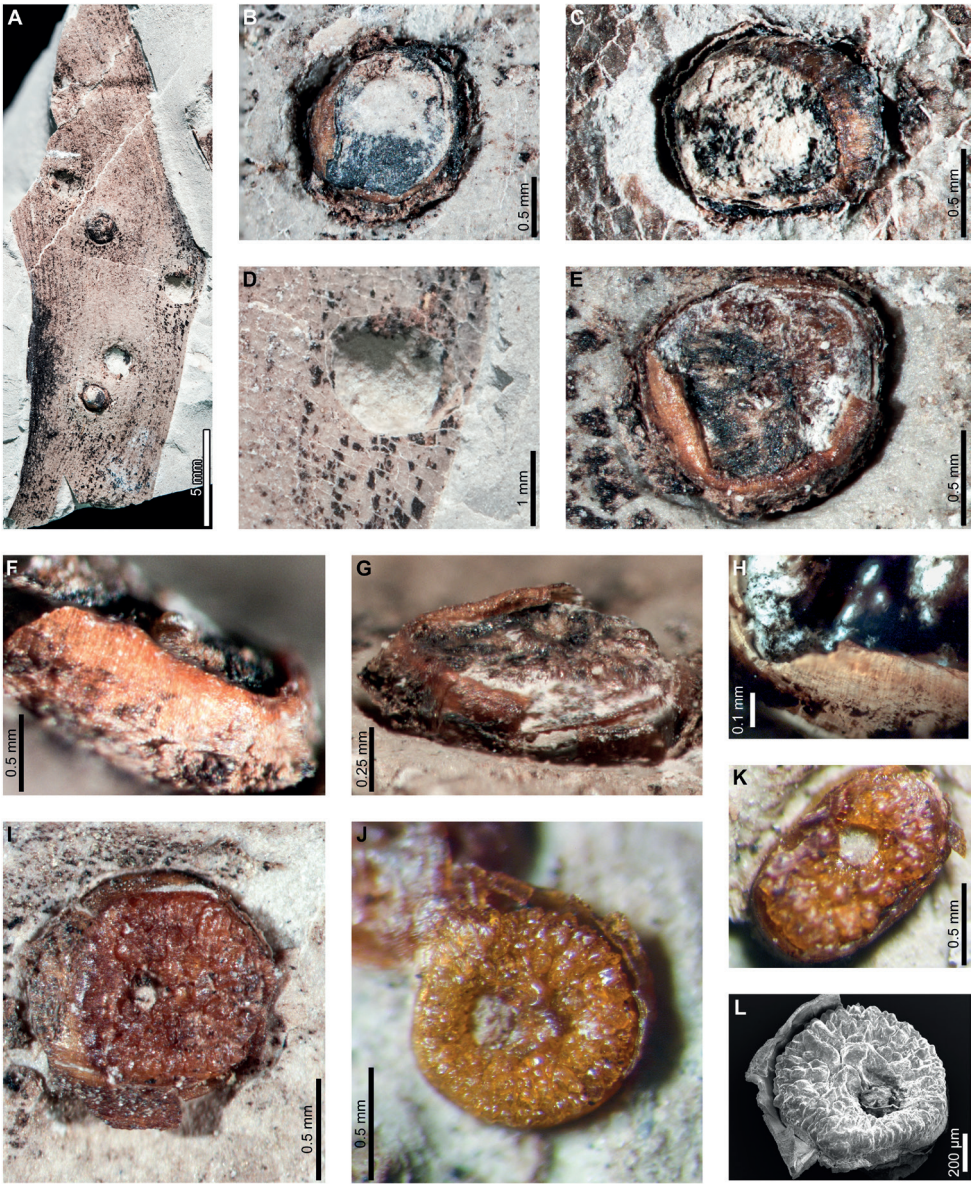

Figure 4. Galls (DT116) on *Agathis immortalis* from Palacio de los Loros 2 **A** columnar galls and pits where galls were not preserved (MPEF-Pb 6023) **B** detail of gall in (**A**) **C** columnar gall with striated side (MPEF-Pb 6088) **D** detail of pit in (**A**) **E** columnar scale with striated side overlapping the top (MPEF-Pb 5995) **F** side view of gall in (**E**) showing horizontal and vertical striations on the ventral cover **G** side view of gall in (**E**) **H** detail of gall in (**E**) under epifluorescence showing vertical and horizontal striations **I** columnar gall (MPEF-Pb 5960) **J** columnar gall preserved as amber (MPEF-Pb 9750) **K** columnar gall preserved as amber (MPEF-Pb 9750) **L** SEM image of gall in (**J**) showing texture (MPEF-Pb 9750).

These columnar galls appear to be deeply set in the leaf tissue and result in a concave pit when removed (Fig. 4A, D). Most specimens are replaced by or filled in with amber derived from ambient leaf resins.

Enigmatic structures possibly representing armored scale-insect covers (Diaspididae) are associated with leaves (Fig. 5A–G, I–O) and a cone scale (Fig. 5H). The structures, which we refer to as "covers" in the description, may be preserved as amber casts of the dorsal cover and/or ventral cover or "collar" (Fig. 5A–D, F, G, H); impressions of the dorsal covers (Fig. 5E, F, I–M); or impressions where the ventral covers were once located. The dorsal covers are approximately circular to oval, more or less flattened, marked with concentric growth rings, and are surrounded by an attached ventral cover (DT86). Dorsal covers measure 0.87–1.65 mm in maximum diameter by 0.77–1.5 mm in minimum diameter. Concentric growth rings on dorsal covers (Fig. 5A, C, D, K–N) are spaced 0.02–0.08 mm apart. The concentric rings may represent instar growth increments, although the boundaries between the first and second instar and adult phases of the dorsal covers are unclear. An ovoidal bump or pustule (Fig. 5K–N) near the center of the covers in the area presumably made by the first instar nymph may be present, possibly marking the location of the first instar exuviae or the position of stylets from the piercing-and-sucking insects into the subjacent targeted tissues. The ovoidal bumps measure 0.17–0.20 by 0.13–0.16 mm in dimension. On one specimen, rod-like structures radiate from the center of the cover (Fig. 5N, O). The ventral covers that surround the dorsal covers measure 0.06–0.20 mm wide and typically have greater relief than the surrounding unaffected area. The covers share similarities to the galls illustrated in Fig. 4, including the ventral collar and concentric rings, and ovoidal bump or hole on the dorsal side, suggesting that these structures may be related.

Early Eocene, Laguna del Hunco

Insect and pathogen damage on early Eocene *A. zamunerae* at LH in the Huitrera Formation includes hole feeding, margin feeding, surface feeding, piercing and sucking, mining, galling, and a rust fungus. External foliage feeding (Fig. 6A–G) includes circular to elliptical holes measuring 0.2–1.1 mm in length and 0.1–0.7 mm in width (DT1; Fig. 6A). The holes are surrounded by thin reaction rims, which measure <0.1 mm wide. A slot-feeding hole (DT8; Fig. 6B) measures 2.8 mm long and 0.3–0.6 mm wide with a 0.1 mm wide reaction rim. The long axis of the hole is parallel to the leaf veins. Shallow, approximately circular excisions into the leaf margins (DT12, Fig. 6C–F) measure 1.0–28.2 mm long and 0.2–2.8 mm deep. Flaps of unconsumed, apparently necrotic tissue measure 0.1–0.5 mm wide, and veinal stringers may be present (Fig. 6F). Polylobate surface feeding zones with reaction rims (DT30; Fig. 6G) measure 1.3–3.0 mm long by 0.2–1.3 mm wide. Reaction rims measure 0.2 mm wide.

Circular to elliptical piercing-and-sucking punctures (DT46; Fig. 6H) are characterized by a black spot or a rim encircling an inner circle of lighter tissue where the

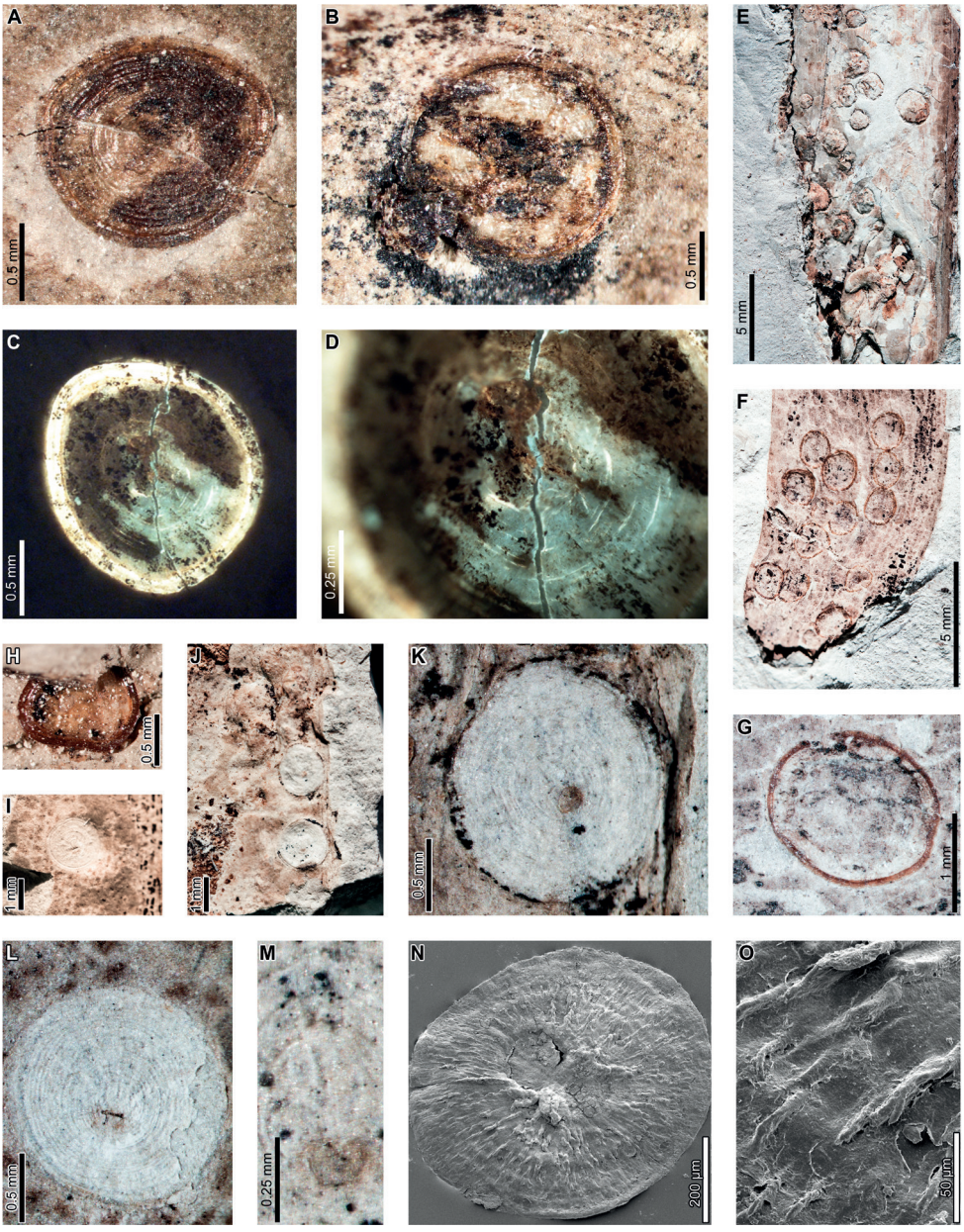

Figure 5. Enigmatic structures, possibly armored scale insect (Diaspididae) covers, (DT86) on *Agathis* leaves (**A–G, I–M**) and a cone scale (**H**) from Palacio de los Loros 2 **A** cover with concentric growth rings (MPEF-Pb 6096) **B** cover with concentric growth rings (MPEF-Pb 6096) **C** cover in (**A**) under epifluorescence **D** detail of (**C**) showing concentric growth rings **E** clusters of cover impressions (MPEF-Pb 6113) **F** embedded ventral cover (MPEF-Pb 6020) **G** embedded ventral cover (MPEF-Pb 5985) **H** cover preserved as amber (MPEF-Pb 5861) **I** impression of cover (MPEF-Pb 5996) **J** impressions of two covers (MPEF-Pb 5996) **K** detail of upper cover impression in (**J**) **L** detail of cover impression in (**I**) **M** detail of lower cover in (**J**) showing concentric growth rings **N** cover showing rod-like structures (MPEF-Pb 9750) **O** close-up of rod-like structures in (**N**).

puncture was located. These piercing-and-sucking punctures measure 0.11–0.18 mm in minimum and 0.14–0.22 in maximum diameter.

Agathis zamunerae is associated with the ichnotaxon *Frondicuniculum lineacurvum*, an oblong blotch mine with smooth, gently curving margins described previously (Donovan et al. 2020). The mines follow the leaf axis, and their long axes are parallel to leaf veins. Frass, including amorphous matter and spherical to hemispherical pellets locally replaced by amber, is deposited mostly along the mine margin when present (Fig. 6I). Putative linear blotch mines with smooth margins and breached epidermal tissue are also found on *A. zamunerae* (DT251; Fig. 6J–L). Epidermal tissue was breached on most specimens, leaving flaps of tissue along the internal margin of the mine, although epidermal tissue is still preserved across the width of some mines (Fig. 6L). Detailed descriptions of these mines, including the ichnotaxomic treatment of *F. lineacurvum*, were provided by Donovan et al. 2020.

A dark, oval gall measures 3.4 mm long by 2.8 mm wide (DT32; Fig. 6M). The long axis of the gall is parallel to the leaf venation. The gall has slight relief above the leaf surface and is characterized by a smooth, carbonized texture.

Enigmatic structures, possibly representing female diaspidid covers, are flattened, approximately circular to oval, and measure 0.90–1.63 mm in diameter (DT86; Figs 7–9). In our descriptions, we use the term "covers" to refer to these structures. The dorsal covers are marked by concentric rings (Figs 7B–D, H–K, 8H, I, 9F, G), which may represent cover growth increments during the first and second instar and adult phases. The first instar covers measure 0.31–0.44 mm minimum by 0.29–0.57 mm maximum diameter. The covers constructed by the first instars are marked by an ovoid depression along the edge of the cover, which may indicate the position of the remnant of the first instar exuviae or the stylet fascicle as it penetrated subjacent epidermal and deeper tissues (Figs 7H–K, 8G–I). The ovoid depressions measure 0.22–0.24 mm long by 0.14–0.18 mm wide, with the long axes typically parallel to the maximum diameter of the entire dorsal cover. Material added by second instars increases the diameters of the dorsal covers to 0.58–0.92 mm by 0.62–0.75 mm, and the fully formed adult dorsal covers measure 0.7–1.47 mm by 0.7–1.33 mm. Each dorsal cover is surrounded by a ventral cover (Figs 8J–L, 9C–E), which is deeply embedded in the leaf tissue and measures 0.04–0.15 mm wide. The tops of the ventral covers typically protrude above the leaf surface and the dorsal covers. Although the entire heights of the ventral covers are not usually visible, measured heights are 0.55–0.75 mm. Some scales are only represented by pits (Fig. 8E) or depressed rims where the ventral cover was originally positioned but subsequently detached (Figs 7E, 9I, J).

A probable rust fungus (Fig. 6K, N–P) developed as a gall on which nearly concentric rings of circular to oval aecia (aeciospore-producing structures) are embedded. The aecia are 0.45–1.28 mm in diameter and have slight relief relative to the leaf surface (Fig. 6P). A depressed rim, 0.10–0.25 mm wide, surrounds each aecium, suggesting that the aecia were deep-set in the host tissue and/or that the aecia were cupulate. The circular gall in which the aecia are embedded is delimited by a depressed rim (0.3 mm wide), most clearly visible on the basal side of the gall as oriented in Fig. 6P. Leaf veins within the spot are distorted, possibly caused by thickened tissue growth. The gall measures 13.2 mm in the direction parallel to the leaf veins, and it spans the width of the leaf (15.6 mm).

Figure 6. External foliage feeding, leaf mining, and rust fungus damage on *Agathis zamunerae* from Laguna del Hunco **A** oval hole (DT1; MPEF-Pb 6328) **B** parallel-sided slot feeding (DT8; MPEF-Pb 6368) **C** excision into the leaf margin (DT12; MPEF-Pb 6329) **D** adjacent, shallow excisions into the leaf margin (DT12; MPEF-Pb 6311) **E** shallow excision into the leaf margin with veinal stringers (DT12; MPEF-Pb 6361) **F** detail of veinal stringers and reaction tissue in (**E**) **G** small zone of surface feeding (DT29; MPEF-Pb 6356) **H** circular to elliptical piercing and sucking marks (DT46; MPEF-Pb 6303) **I** *Frondicuniculum lineacurvum* blotch mine (holotype MPEF-Pb 6336) **J** probable blotch mine with breached epidermal tissue (DT251; MPEF-Pb 6361) **K** two probable blotch mines with breached epidermal tissue (DT251) and a rust fungus (MPEF-Pb 6303) **L** detail of blotch mine in (**K**) **M** dark, circular gall with slight relief (DT32; MPEF-Pb 6346) **N** concentric rings of aecia on a rust fungus spot (MPEF-Pb 6303) **O** detail of rust fungus in (**N**) **P** detail of two aecia in (**N**).

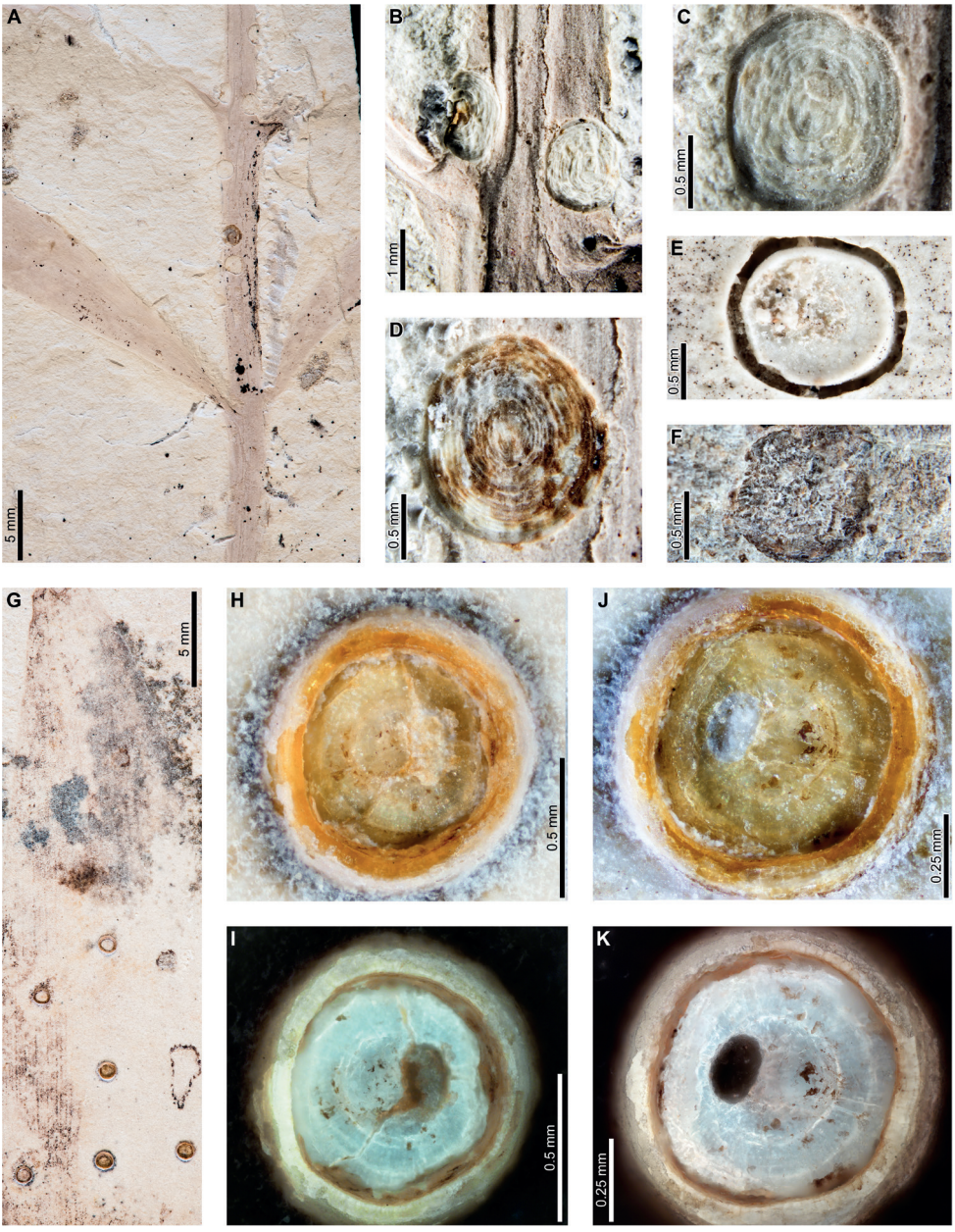

Figure 7. Enigmatic structures, possibly armored scale insect (Diaspididae) covers (DT86) on *Agathis zamunerae* branches (**A–D**) and leaves (**E–K**) from Laguna del Hunco **A** impressions of covers (MPEF-Pb 6307) **B** two covers on a branch in (**A**) **C** detail of cover with concentric growth rings in (**A**) **D** detail of cover with concentric growth rings in (**A**) **E** depression where ventral cover was positioned (MPEF-Pb 6349) **F** depression where cover was probably located (MPEF-Pb 6360) **G** possible scale insect covers (MPEF-Pb 6383) **H** detail of cover in (**G**) **I** cover in (**H**) under epifluorescence showing concentric growth rings **J** detail of cover in (**G**) **K** cover in (**J**) under epifluorescence showing concentric growth rings.

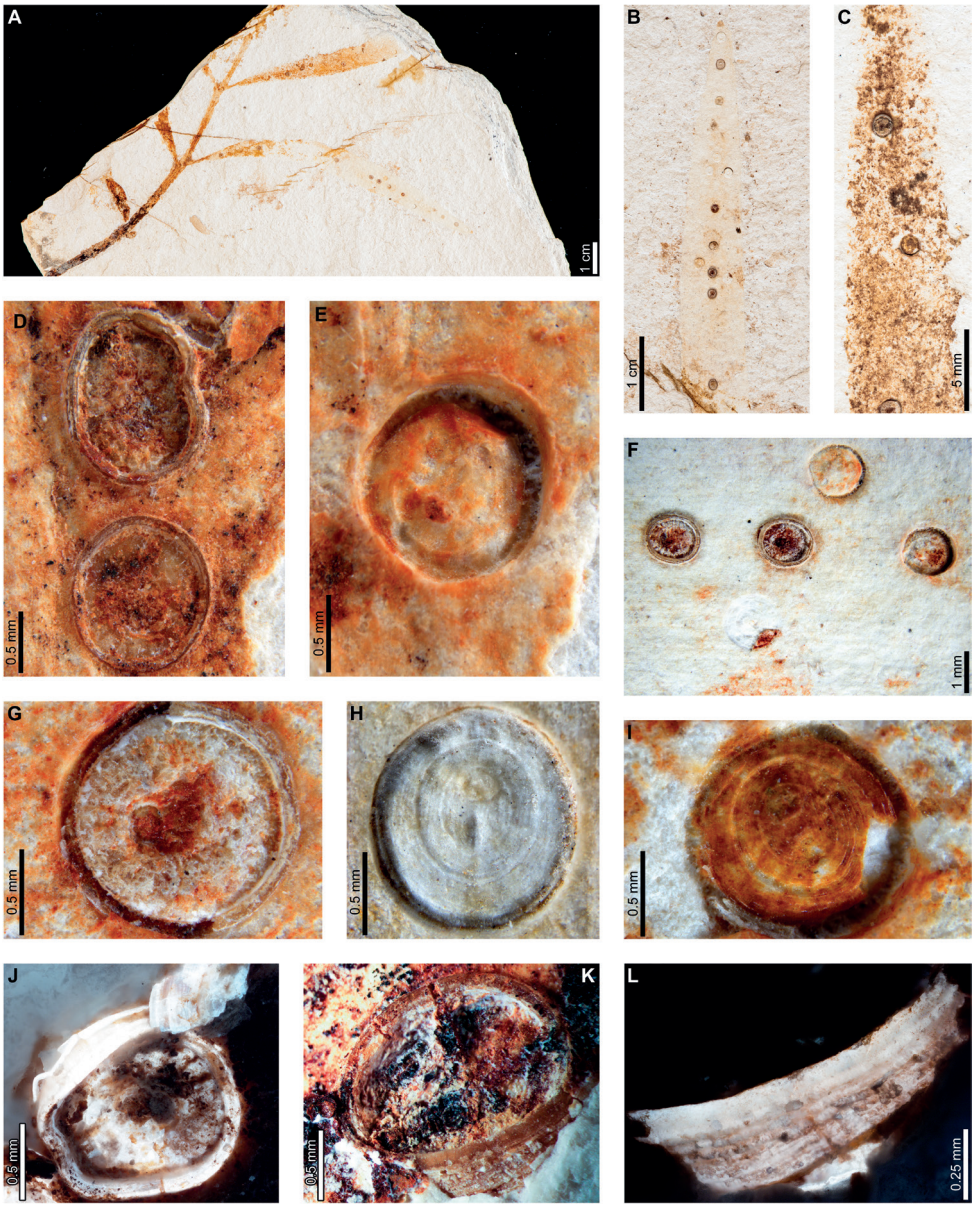

Figure 8. Enigmatic structures, possibly armored scale insect (Diaspididae) covers (DT86) on *Agathis zamunerae* from Laguna del Hunco (MPEF-Pb 6324) **A** covers on leaves and a branch **B** row of covers along the central axis of a leaf **C** four covers **D** dorsal and ventral covers **E** impression of cover **F** five covers **G** ventral cover and poorly preserved dorsal cover **H** impression of dorsal cover with concentric growth rings **I** dorsal cover with concentric growth rings **J** view of ventral cover under epifluorescence **K** protruding ventral cover with horizontal and vertical striations **L** ventral cover with horizontal and vertical striations under epifluorescence.

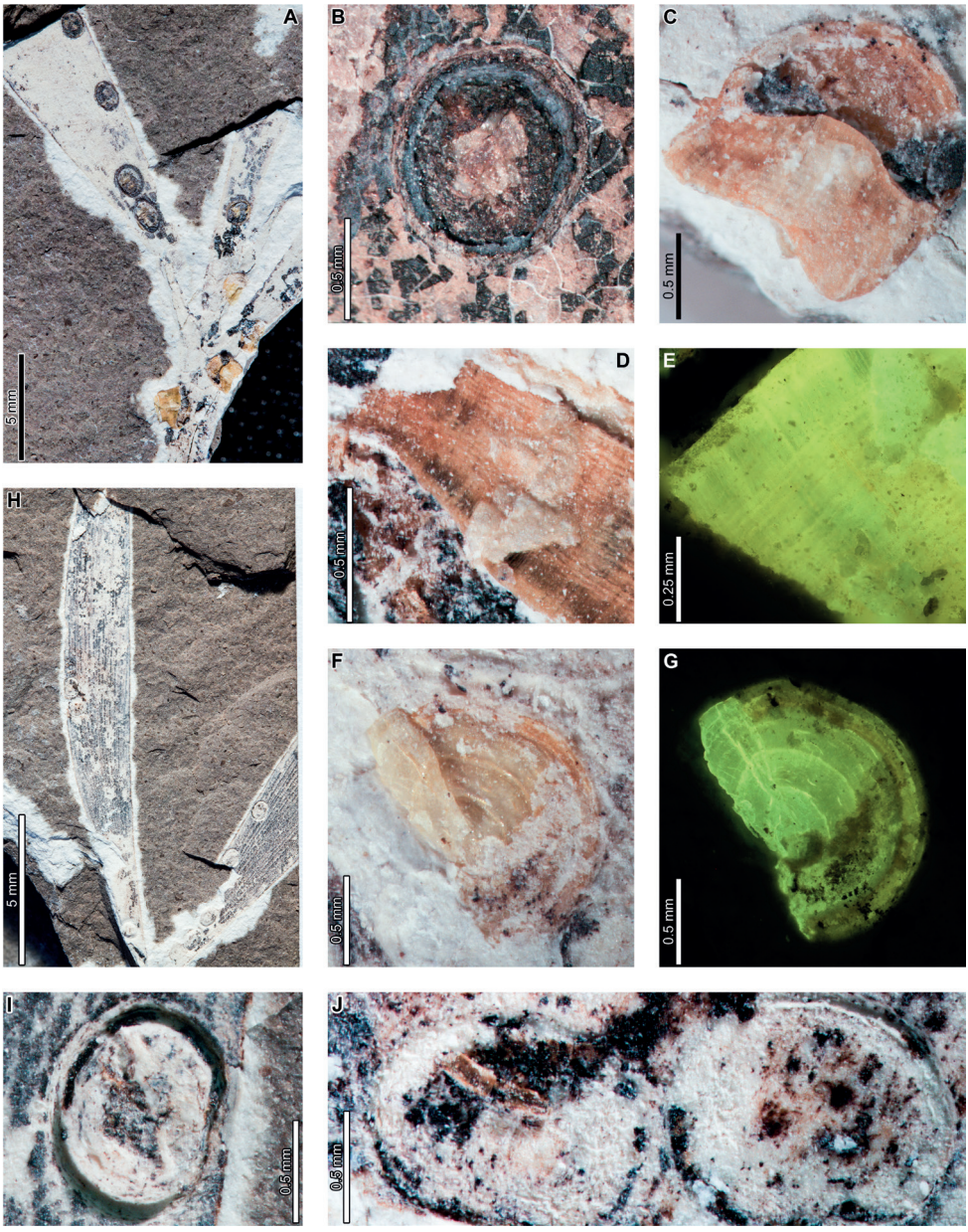

Figure 9. Enigmatic structures, possibly armored scale insect (Diaspididae) covers on *Agathis zamunerae* from Laguna del Hunco (MPEF-Pb 9842) **A** cover impressions and amber casts on leaves and a branch **B** raised ventral cover **C** dorsal cover surrounded by exposed, vertically-oriented ventral cover **D** detail of ventral cover showing horizontal and vertical striations **E** ventral cover in (**D**) under epifluorescence **F** dorsal cover with concentric growth rings **G** dorsal cover in (**F**) **H** counterpart to (**A**) **I** impression of ventral cover in (**H**) **J** impressions of ventral covers in (**H**).

Middle Eocene, Río Pichileufú

Insect damage on early middle Eocene *A. zamunerae* at RP in La Huitrera Formation includes margin feeding, skeletonization, and mining. External foliage feeding (Fig. 10A, B) includes an excision into the leaf margin composed of two, adjacent, approximately circular feeding areas (DT12; Fig. 10A) that measure 13 mm across and are incised 1.8 and 3.7 mm, respectively. Ragged reaction tissue with visible vein stringers measures 0.6–0.8 mm wide. A patch of skeletonized tissue composed of multiple, closely spaced, holes with some leaf veins intact is surrounded by a dark reaction rim (DT17; Fig. 10B) measuring 0.3–0.5 mm wide.

The ichnotaxon *Frondicuniculum lineacurvum*, an elongate-ellipsoidal blotch mine with smooth margins, occurs on *A. zamunerae* at both RP and LH, as previously reported (Donovan et al. 2020). The best-preserved example occupies approximately 85% of a leaf surface (Fig. 10C). Putative oblong blotch mines with flaps of unconsumed tissues along the rims of the mines are also found on *A. zamunerae* at RP (DT251; Fig. 10D, E). Detailed descriptions of these mines were provided by Donovan et al. 2020.

Enigmatic structures resembling female diaspidid covers (Figs 11, 12) are similar to those found at LH. Dorsal covers measure 0.70–1.08 mm in diameter and are marked by two concentric rings (0.40 by 0.38 mm and 0.53–0.55 by 0.55–0.57 mm wide, respectively), possibly representing instar growth increments (DT86; Fig. 11). The first instar covers are usually associated with an oval or semicircular depression (0.22–0.23 mm long by 0.15–0.16 mm wide; Fig. 11D–I) surrounded by a raised rim or flange (0.02–0.06 mm wide; Fig. 11H). Dorsal covers are marked by small circular

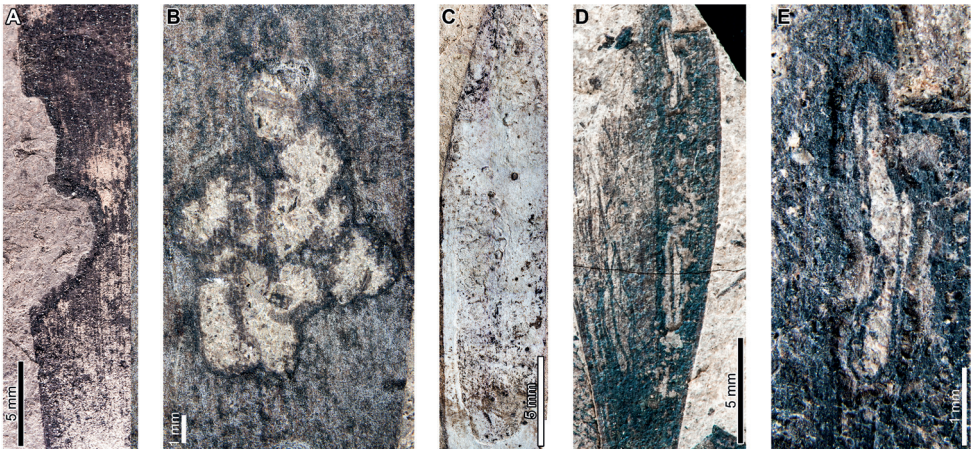

Figure 10. External foliage feeding and leaf mines on *Agathis zamunerae* leaf from Río Pichileufú **A** arcuate excisions into the leaf margin (DT12; BAR 5002-20) **B** zone of skeletonized tissue with reaction rims (DT17; USNM 545229) **C** *Frondicuniculum lineacurvum* blotch mine (paratype USNM 545226) **D** probable blotch mines with breached epidermal tissue (DT251; USNM 545227) **E** detail of blotch mine in (**D**).

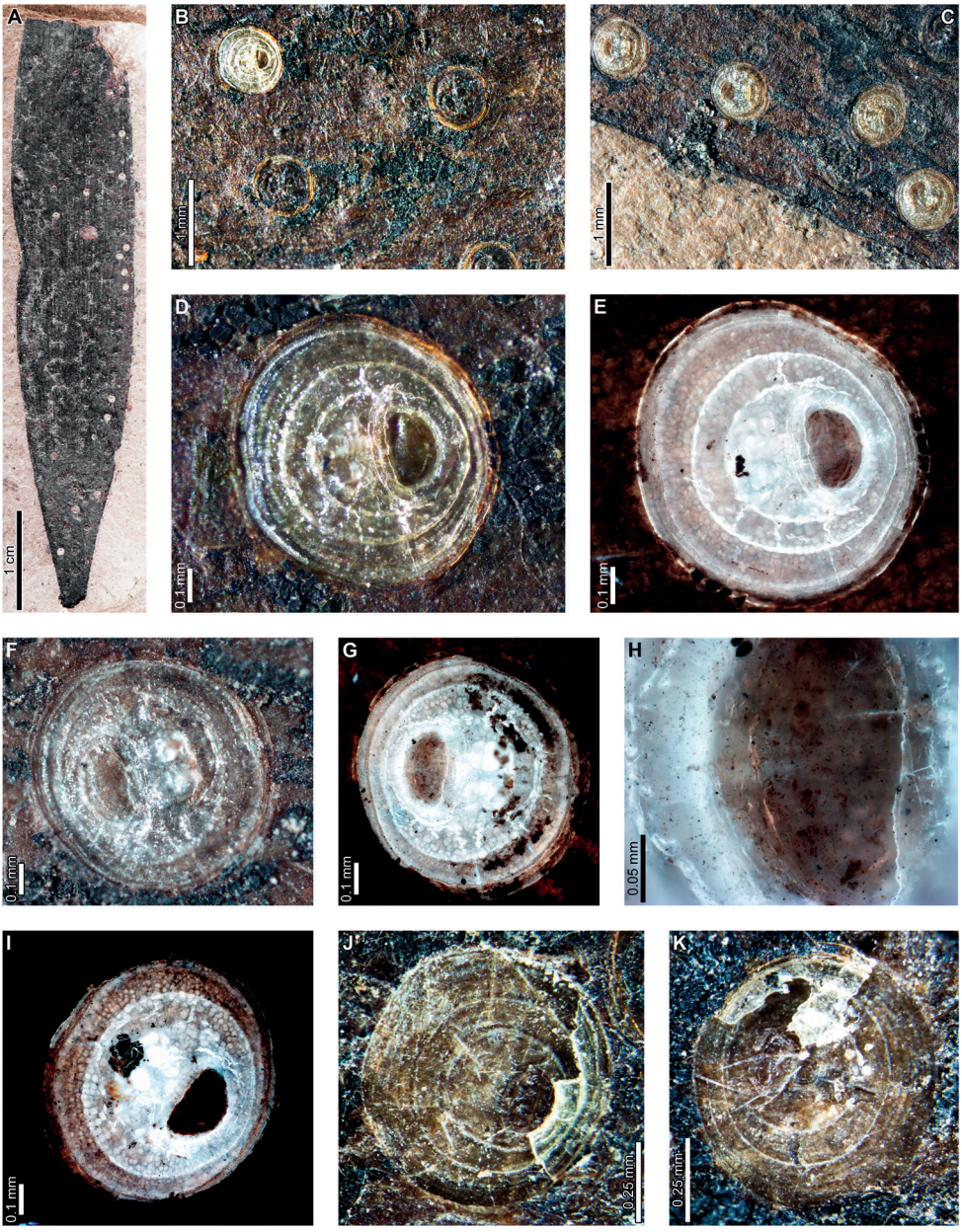

Figure 11. Enigmatic structures, possibly armored scale insect (Diaspididae) covers (DT86) on an *Agathis zamunerae* leaf from Río Pichileufú (USNM 545228) **A** leaf with covers **B** dorsal covers **C** dorsal covers **D** dorsal cover with concentric growth rings **E** cover in (**E**) under epifluorescence **F** dorsal cover with concentric growth rings **G** cover in (**F**) under epifluorescence **H** detail of rim surrounding semicircular impression in (**G**) **I** dorsal cover under epifluorescence showing concentric growth rings **J** dorsal cover with concentric growth rings **K** dorsal cover with concentric growth rings.

to ellipsoidal shapes visible under epifluorescence (Fig. 11E, G, I), which correspond to bumps on the surface. The bumps measure 0.01–0.02 mm in diameter and decrease in size moving from the first instar through the adult portions of the scales. The first instar covers appear to be thicker than the material added by second instars and adults (Fig. 11E, G, I), probably attributable to the presence of exuviae. A deeply-set ventral cover (0.02–0.06 mm wide) surrounds each dorsal cover (Fig. 12A–C). Ovoid pits may represent where covers were originally positioned (Fig. 12D–G).

Extant *Agathis* herbivory

Relatively few herbivorous insect associations with extant *Agathis* have been documented in the literature, as summarized by Donovan et al. (2020). Here, we provide brief descriptions of insect and fungal damage that we observed on *Agathis* herbarium specimens. Although not intended to be a comprehensive survey, the damage is representative of the diversity we found while looking for analogs to the fossil damage on thousands of herbarium sheets in several major herbaria. Much of this extant damage diversity that resembles the fossils is from unknown culprits, representing a major opportunity to discover living insect diversity and evolutionary history based on fossil analogs. Some of the leaf mines were previously illustrated by Donovan et al. (2020) but are re-illustrated and briefly mentioned in the text here for completeness. Extant *Agathis* species delimitations and range information follows (Farjon 2010). See the following section for comparisons of the fossil and extant damage.

On *Agathis australis* (Fig. 13; from the North Island of New Zealand), we observed external foliage feeding, including arcuate margin feeding (DT12; Fig. 13A) and removal of the leaf apex (DT13; Fig. 13B). A flap of dead tissue bordered by a black reaction rim forms at the sites of external foliage feeding damage (Fig. 13A, B). Galls are black, circular to ellipsoidal, with minor relief compared to the leaf surface (Fig. 13C–E). Most galls are single-chambered, but some are conjoined or are multichambered with exit holes. Galls were found on the adaxial leaf surfaces, and the long axes of the galls tend to be oriented parallel to leaf veins. Finally, *Parectopa leucocyma* (Lepidoptera, Gracillariidae) (Wise 1962) mines are common, typically characterized by an initial blotch phase transitioning into a serpentine trail. The mines follow the leaf margin and end in a gall near the petiole (Fig. 13F, G).

Agathis lanceolata (New Caledonia; Fig. 14A–E) is associated with external foliage feeding, including semicircular excisions into the leaf margin (DT12) and removal of the leaf apex (DT13). Galls on *A. lanceolata* include ellipsoidal blisters oriented parallel to leaf veins (Fig. 14A). Houard (1914, 1922) briefly described ellipsoidal blister galls on the upper surfaces of *A. lanceolata* leaves. The galls were not illustrated, but he may have been referring to galls similar to those in Fig. 14A. A dark, circular gall with a flattened top and a central indentation was found on a cultivated tree in New Caledonia (Fig. 14B). A curved serpentine mine with smooth margins is packed with frass (Fig. 14C). Two blotches of indeterminate origins, possibly induced by pathogens

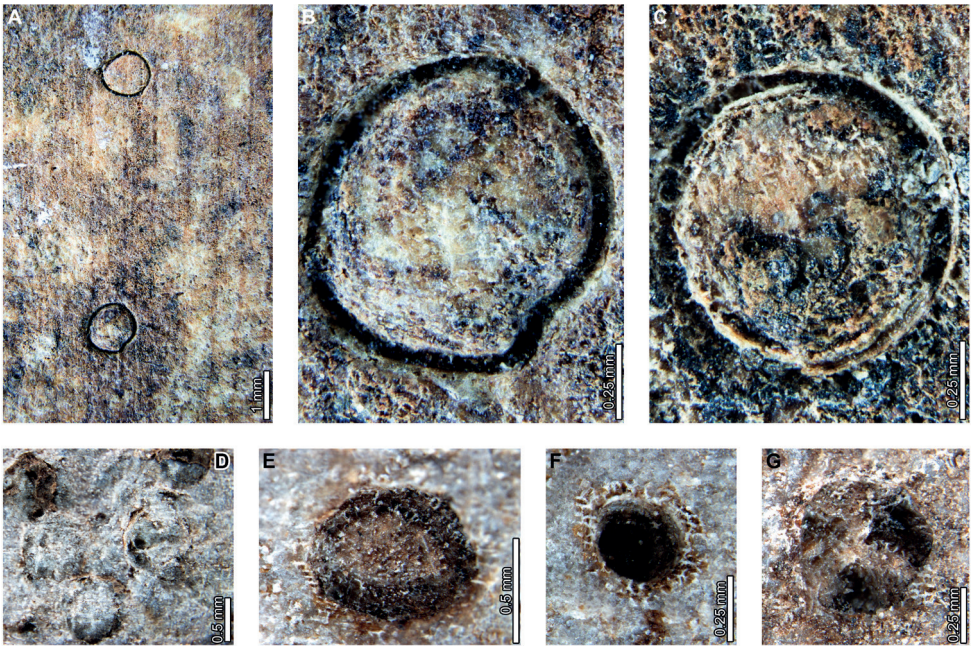

Figure 12. Enigmatic structures, possibly armored scale insect (Diaspididae) cover impressions (DT86) on *Agathis zamunerae* from Río Pichileufú **A** depressions where ventral covers were positioned (USNM 545223) **B** detail of lower depression in (**A**) **C** rim where ventral cover was positioned (USNM 545223) **D** pits where scale insects were possibly positioned (USNM 545226) **E** pit where scale insect was possibly located (USNM 545226) **F** pit surrounded by reaction tissue where scale insect was possibly positioned (USNM 545226) **G** Pit where scale insect was possibly located (USNM 545226).

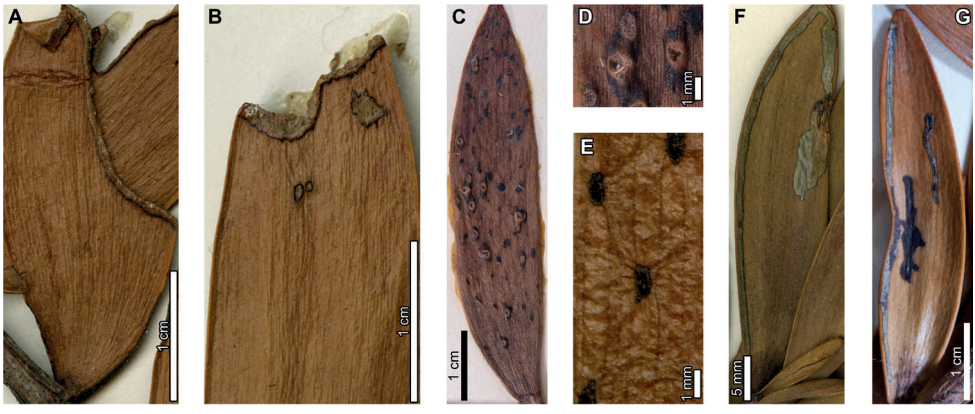

Figure 13. Insect damage on *Agathis australis* from New Zealand **A** excision into the leaf margin (Capt. Wilkes, U.S.N., 1838-42 (GH)) **B** excision through the leaf apex (Capt. Wilkes, U.S.N., 1838-42 (GH)) **C** blister galls with exit holes (K 0000230) **D** detail of blister galls in (**C**) **E** black, ellipsoidal galls (E.H. Wilson, February 2, 1921 (A)) **F** *Parectopa leucocyma* (Gracillariidae) moth mine (Capt. Wilkes, U.S.N., 1838-42 (GH)) **G** *Parectopa leucocyma* mines (K 000553313).

Figure 14. Insect and pathogen damage on *Agathis lanceolata* (**A–E**), *A. montana* (**F**), *A. moorei* (**G–K**), *A. ovata* (**L–P**) from New Caledonia **A** ellipsoidal blister galls with exit holes (K 000553125) **B** black columnar gall (E 00119757) **C** Serpentine mine (K 000553127) **D** teardrop-shaped blotch damage (K 0000305) **E** linear blotch damage (GH 2372 B) **F** elongate mine along the leaf margin (A 8571) **G** excision into the leaf margin surrounded by reaction tissue and exuding resin (E 00106192) **H** circular gall (K 0000357) **I** linear blotch mines with breached epidermal tissue on the right mine (K 000553352) **J** blotch mines (K 000553352) **K** blotch mine (K 000553352) **L, M** galls with thickened margins surrounding epidermal tissue with circular exit holes (E 00399687) **N** *Chrysomphalus aonidum* (Diaspididae) scale insects (E 00036880) **O** diaspidid scale insect covers (K 0000291) **P** diaspidid scale insect covers (K 00053124).

(fungi, viruses, or bacteria), were found on *A. lanceolata*. First, a teardrop shaped blotch with raised epidermal tissue that measures 15.1 mm long by 7.7–8.7 mm in width (Fig. 14D) has an acuminate upper margin and is surrounded by a wrinkled reaction rim 0.3–0.4 mm wide. The second blotch is oblong and is positioned along the leaf edge (Fig. 14E). The blotch is 14.4 mm long by 1.4–3.1 mm wide.

On *Agathis montana* (New Caledonia), we observed an elongate mine following the margin of a single leaf (Fig. 14F). The mine measures 59.7 mm long by 0.2–4.3 mm wide and is surrounded by a 0.1 mm wide reaction rim. The mine begins near the base of the leaf and follows the leaf margin, terminating at the leaf apex. The mine gradually widens as the miner consumed leaf tissue, except for two expanded protrusions, and spans the width of the leaf at the apex. The lateral margins of the mine are smooth, and linear to gently undulous frass appears to be composed of spheroidal pellets.

Agathis moorei (New Caledonia; Fig. 14G–K) is associated with shallow, arcuate margin-feeding excisions (DT12; Fig. 14G) flanked by lighter colored dead tissue and dark reaction rims. The wounded edges may exude resin. Galls are circular with minor relief and a raised black rim (Fig. 14H). Full-depth blotch mines are falcate or linear and smooth with parallel margins (Fig. 14I–K). Epidermal tissue was weathered away in some specimens (Fig. 14I, J).

Agathis ovata (New Caledonia; Fig. 14L–P) is associated with ellipsoidal to ovate galls with a dark, thickened rim (Fig. 14L, M). The tops of the galls are flat and consist of epidermal tissue with distinct files of cellular proliferations and a circular exit hole. Diaspidids, including *Chrysomphalus aonidum* (Fig. 14N) and unidentified species (Fig. 14O, P) also occur on this species.

Agathis macrophylla (Fiji, Vanuatu, and the Solomon Islands; Fig. 15A–O) is associated with semicircular excisions into the leaf margin (DT12; Fig. 15A) and feeding through the leaf apex (DT13) with flaps of dead tissue bordered by a rim of darkened tissue. Surface feeding consists of thin, fairly linear files of damaged tissue (Fig. 15B). Galls include hemispherical, black protrusions from the adaxial surface (Fig. 15C) of leaves and small, circular blister galls with central exit holes. Serpentine mines are curved and end in an elliptical terminal chamber (Fig. 15D) or travel in a zigzag pattern and terminate with a gall at the leaf base (Fig. 15E, F). The terminal gall is similar to mines made by *Parectopa leucocyma* on *Agathis australis* in New Zealand, although *P. leucocyma* mines have an initial blotch phase (Wise 1962) and do not mine in a zigzag pattern. Elongate, oblong to elliptical blotch mines are positioned along leaf margins with their long axes parallel to leaf veins (Fig. 15G–I). Diaspidid scale insects cause piercing-and-sucking damage, leaving a discolored orange mark where the scale cover was located (Fig. 15L, M). Pit-gall-inducing diaspidids are also associated with leaves of *A. macrophylla* (Fig. 15N, O). The only other gall-inducing diaspidid that has been documented on conifers is *Leucaspis podocarpi*, which makes leaf margin rolls on *Prumnopitys taxifolia* (Podocarpaceae) in New Zealand. *Leucaspis podocarpi* is also associated with *Podocarpus cunninghamii* Colenso and *Podocarpus totara* G.Benn ex D.Don (Podocarpaceae), but it does not induce galls on these species (Henderson and Martin 2006). A blotch, probably fungal-induced, occurs along the leaf margin (Fig. 15J). Kauri rust (*Aecidium fragiforme*) fungal galls are also common (Fig. 15K).

Figure 15. Insect and fungal damage on *Agathis macrophylla* (**A–M**) **A** semicircular excision into the leaf margin (K 0000265) **B** adjacent rows of surface feeding (Fiji, K B40) **C** round, black gall (New Caledonia, E 00131862) **D** serpentine mine with elliptical terminal chamber (Fiji, E 0000340) **E** serpentine mine terminating in a gall (Fiji, K 0000346) **F** serpentine mine terminating in a gall (Fiji, K 0000346) **G** possible blotch mine along leaf margin (Fiji, K 0000322) **H** elongate blotch mine (Fiji, K 0000327) **I** blotch mine along the leaf margin (Fiji, K 0000327) **J** fungal blotch along the leaf margin (Fiji, K 16421) **K** Kauri rust (*Araucariomyces fragiformis*) (Vanuatu, S.F. Kajewski 282 (K)) **L** armored scale insect (Diaspididae) (Fiji, K 350) **M** diaspidid scale insect (Fiji, E 00127892) **N, O** pit gall-inducing scale insects (Fiji, GH 01153259).

Agathis atropurpurea (Queensland, Australia; Fig. 16A–C) is associated with slot feeding (DT8; Fig. 16A) characterized by a thin rim of necrotic tissue along the inside of the hole. Ovoid to elliptical and polylobate blister galls are positioned on the adaxial sides of leaves and are marked by centrally located circular exit holes (Fig. 16B). An oblong blotch mine with smooth, gently curving margins is positioned near the leaf margin (Fig. 16C).

Agathis microstachya (Queensland, Australia; Fig. 16D–F) is associated with elongate-ellipsoidal blotch mines that have smooth margins positioned with their long axes parallel to the leaf veins. In one specimen (Fig. 16E), the epidermal tissue was removed due to weathering, revealing an abraded inner texture caused by insect feeding.

Agathis robusta occurs in both Queensland, Australia (Fig. 16G–K) and New Guinea (Fig. 16L–O). In the Australian material, we found semicircular excisions along the leaf margin (DT12) and apex feeding (DT13). Probable blotch mines with breached epidermal tissue have a slot-like appearance. Ellipsoidal blister galls are characterized by a central exit hole and are surrounded by black rims (Fig. 16I). Serpentine mines are tightly wound (Fig. 16J, K) and some end in an elliptical terminal chamber (Fig. 16K). Ovate blotches caused by pathogens are positioned near the central axes of leaves (Fig. 16L, M) and measure 17.7–20.5 mm long by 8.6–8.9 mm at their widest diameter. The margins of the blotches are minutely ragged and surrounded by 0.1–0.2 mm wide reaction rims. Elongate fungal blotches occur along the leaf margin (Fig. 16N). In New Guinea specimens, *A. robusta* is associated with small circular holes (DT2). Blister galls on *A. robusta* in New Guinea (Fig. 16O, P) are indistinguishable from those found on Australian members of the species (Fig. 16I). Globose, black galls (Fig. 16Q) and a single coccid scale insect (Fig. 16R) were also found on the leaf surface.

Agathis labillardieri (New Guinea; Fig. 17A–E) is associated with external foliage feeding, including small circular holes (DT2), slot feeding (DT8; Fig. 17A), semicircular excisions into the leaf margin (DT12), apex feeding (DT13), and linear traces of surface feeding that parallel the leaf veins. Galls include densely packed blisters with single or multiple chambers (Fig. 17B, D) and elliptical galls composed of brown, thickened tissue (Fig. 17C). Sinusoidal serpentine mines also occur on *A. labillardieri* (Fig. 17E).

On *Agathis dammara* (eastern Malesia; Fig. 17F–U), external foliage feeding includes circular (DT2) and polylobate (DT5) holes, slot feeding (DT8; Fig. 17N, Q), arcuate excisions (DT12), feeding through the leaf apex (DT13; Fig. 17F), and trenched excisions into the leaf margin that expand towards the center of the leaf (DT15; Fig. 17R). Elongate, squiggly rows of surface feeding run parallel to each other (Fig. 17M). Circular to polylobate blister galls with central circular exit holes (Fig. 17G, H, U) and a globose woody gall (Fig. 17T) are found on the adaxial surfaces of leaves. Various serpentine mine morphologies occur on *A. dammara*, including overlapping (Fig. 17I), forking (Fig. 17K), or linear trails (Fig. 17S) that end in an elongate blotch (Fig. 17L), polylobate terminal chamber (Fig. 17O), or a gall (Fig. 17P). Elongate-ellipsoidal blotch mines also occur (Fig. 18J).

Agathis borneensis (Borneo to Sumatra; Fig. 18A–L) is associated with external foliage feeding, including arcuate margin feeding (DT12; Fig. 18A) and apex feeding (DT13) with a thin band of thickened reaction tissue. Galls on the adaxial leaf surface

Figure 16. Insect damage on *Agathis atropurpurea* (**A–C**), *A. microstachya* (**D–F**), and *A. robusta* (Fig. I–R) **A** slot feeding (Australia, K 000553290) **B** blister galls with circular exit holes (Australia, K 000553290) **C** elongate blotch mine (Mount Bartle Frere leaf litter, Queensland, Australia) **D** ellipsoidal blotch mine (Australia, K 0000199) **E** blotch mine lacking epidermal tissue (Australia, K 0000199) **F** ellipsoidal blotch mine (Australia, E 00210640) **G** ellipsoidal blotch mines (Australia, K 111455) **H** blotch mine (Queensland, Australia; A.K. Irvine 00417 (A)) **I** ellipsoidal blister galls with exit holes (Queensland, Australia, K 000553277) **J** serpentine mine (Australia, CANB 590252) **K** serpentine mine with ellipsoidal terminal chamber (Australia, K 000553286) **L** ovate blotch, probable pathogen damage (Australia, NSW 381650) **M** ovate blotch, probable pathogen damage (Australia, NSW 381650) **N** elongate fungal blotch (Queensland, Australia, A 01153261) **O** ellipsoidal blister galls with exit holes (New Guinea, K 000553264) **P** circular blister galls with exit holes (New Guinea, E 00127882) **Q** globose, black gall (New Guinea, E 00127880) **R** coccid scale insect (New Guinea, K 000553265).

Figure 17. Insect damage on *Agathis labillardieri* (**A–E**) and *A. dammara* (**F–U**) **A** slot feeding (New Guinea, K 0000171) **B** densely-packed blister galls (New Guinea, K 0000161) **C** elliptical galls composed of brown, thickened tissue (New Guinea, A 63040) **D** circular blister galls with exit holes (New Guinea, E 00036878) **E** sinusoidal serpentine mine (New Guinea, SING NIFS bb.30358) **F** feeding along the leaf apex (Maluku Islands, K 000553215) **G** polylobate blister galls with exit holes (Maluku Islands, A 106) **H** blister gall with circular exit hole (Maluku Islands, A 106) **I** serpentine mine with thin frass trail (Maluku Islands, A 121) **J** ellipsoidal blotch mine (Maluku Islands, A 121) **K** serpentine mine (Maluku Islands, K 0000041) **L** serpentine mine ending in blotch (Maluku Islands, K 0000078) **M** elongate rows of parallel surface feeding (Brunei, A 4330) **N** slot feeding (Sulawesi, Indonesia, K 0000067) **O** serpentine mine terminating in a blotch (Sulawesi, Indonesia, K 0000067) **P** serpentine mine with oval terminal chamber (Sulawesi, Indonesia, K 516) **Q** slot feeding (Philippines, K 0000137) **R** excision into the leaf margin that expands towards the center of a leaf (Philippines, K 3091) **S** linear serpentine mine (Philippines, K 3091) **T** globose woody gall (Philippines, K 000553230) **U** blister gall with central exit hole and darkened rim (Java, Indonesia, E 00420594).

Figure 18. Insect damage on *Agathis borneensis* (**A–L**), *A. lenticula* (**M–P**), *A. kinabaluensis* (**Q–S**), *A. flavescens* (**T–W**) **A** arcuate margin feeding (Sarawak, Malaysia, K 17672) **B** ellipsoidal to polylobate blister galls with exit holes (Kalimantan, Indonesia, A B1468) **C** hardened, cylindrical galls with flat tops (Brunei, K 000553181) **D** coccid scale insect (Kalimantan, Indonesia, E 00032242) **E** serpentine mine (Penang Island, Malaysia, K 000553157) **F** sinusoidal serpentine mine (Penang Island, Malaysia, SING 90799) **G** serpentine mine with terminal chamber (Sulawesi, Indonesia, A 4109) **H** elongate blotch mine (Sarawak, Malaysia, K 000553188) **I** blotch mine with silk (Brunei, K 000553179) **J** detail of silk in mine in (**I**) **K** blotch mine containing frass (Brunei, SING 91231) **L** close-up of frass in blotch mine in (**K**) **M** arcuate margin feeding (Sabah, Malaysia, K 000553185) **N** adjacent rows of surface feeding (Sabah, Malaysia, K 000553187) **O** circular to polylobate galls with flat tops and exit holes (Sabah, Malaysia, K 000553185) **P** elongate blotch mine along the leaf margin (Sabah, Malaysia, K 000553187) **Q** circular to ellipsoidal galls with exit holes (Sabah, Malaysia, K 000553243) **R** circular, raised galls (Sabah, Malaysia, K 000553243) **S** tightly overlapping serpentine mine (Sabah, Malaysia, K P644) **T** shallow excisions into the leaf margin **U** blister galls surrounded by a thin black rim (Malaysia, A P544) **V** serpentine mines packed with frass (Malaysia, A P542) **W** overlapping serpentine mine (Malaysia, A P542).

include ellipsoidal to polylobate blister-like bumps with circular exit holes (Fig. 18B) and hardened, cylindrical protrusions with flat tops (Fig. 18C). A coccid scale insect or psyllid (Fig. 18D) was found associated with *A. borneensis*. Mines include winding or overlapping serpentine trails (Fig. 18E, F), serpentine mines transitioning into an oval terminal chamber (Fig. 18G), and oblong to elliptical blotch mines (Fig. 18H–L). The presence of silk in one of the blotch mines suggests that it was created by a lepidopteran caterpillar (Fig. 18I, J).

On *Agathis lenticula* (Sabah, Malaysian Borneo; Fig. 18M–P), external foliage feeding includes arcuate excisions into the leaf margin (DT12; Fig. 18M) and curved, adjacent rows of surface feeding (Fig. 18N). Galls are circular to polylobate with flat tops, consist of one or two chambers, and have circular exit holes (Fig. 18O). A possible elongate, elliptical blotch mine or path of pathogen damage occurs along the leaf margin (Fig. 18P) measures 30.7 mm long by 1.0–4.7 mm wide. The miner targeted upper leaf tissue, leaving a thin layer of epidermal tissue intact. The mine has smooth margins, and a 0.1 mm wide enveloping reaction rim. The specimen was damaged, and much of the inner tissue was lost. No evidence of frass is present in the mine.

Agathis kinabaluensis (Mt. Kinabalu, Sabah, and Mt. Murud, Sarawak, Malaysian Borneo; Fig. 18Q–S) is associated with galls characterized by hemispherical eminences (Fig. 18Q, R), typically with their long axes oriented parallel to the leaf veins. Some galls are surrounded by a black rim and many have a central circular to elliptical exit hole. The galls appear to be single-chambered. Serpentine mines are characterized by an overlapping path filled with frass in some portions (Fig. 18S).

Agathis flavescens, restricted to two mountains in Peninsular Malaysia (Fig. 18T–W), is associated with shallow excisions into leaf margins with black reaction rims (DT12; Fig. 18T). Blister galls surrounded by a thin, black rim and associated with a central, circular exit hole (Fig. 18U) occur on the adaxial surfaces of leaves. Serpentine mines are characterized by densely packed frass, slightly increasing width, and either a curvilinear (Fig. 18V) or overlapping trajectory (Fig. 18W).

Comparison of insect damage on fossil and living *Agathis*

Both fossil and extant *Agathis* species are associated with similar, diverse suites of insect and pathogen damage, including external foliage feeding, piercing and sucking, mining, and galling damage. Below, we provide comparisons of damage on *Agathis* across space and time.

External foliage feeding

Overall, similar external-feeding damage is found at all four Cretaceous–middle Eocene fossil sites (Table 1). Small, circular holes (DT1) are associated with *Agathis* leaves during the Late Cretaceous (Lef; Fig. 1A), early Paleocene (PL2; Fig. 2A, B), and early Eocene (LH; Fig. 6A). Arcuate excisions into the leaf margins (DT12) occur at Lef (Fig. 1B), PL2 (Fig. 2C, D), LH (Fig. 6C–F), and middle Eocene RP (Fig. 10A);

Table 1. Presence and absence of insect damage types on fossil *Agathis* from Maastrichtian Lefipán localities (Lef), Danian Palacio de los Loros 2 (PL2), early Eocene Laguna del Hunco (LH), middle Eocene Río Pichileufú (RP), and extant *Agathis* from Australasia and Southeast Asia (Donovan et al. 2020).

Functional feeding group	DT	Lef	PL2	LH	RP	Extant analog
Hole feeding						
Circular, <1 mm diam.	1	x	x	x		x
Circular, 1–5 mm diam.	2		x			x
Parallel sided slots	8			x		x
Margin feeding						
Arcuate excision	12	x	x	x	x	x
Skeletonization						
Interveinal tissue removed, reaction rim	17				x	
Surface feeding						
Surface abrasion, weak reaction rim	29	x	x	x		x
Polylobate abrasion, strong reaction rim	30			x	x	
Piercing and sucking						
Circular punctures, <2 mm diam.	46	x	x	x		x
Scale cover, concentric growth rings	86		x	x	x	x
Oviposition						
Ovate scar, prominent reaction rim	101	x				
Mining						
Elongate-ellipsoidal blotch, smooth margins	88	x		x	x	x
Serpentine mine, follows parallel veins	139	x				
Linear blotch, breached epidermal tissue	251			x	x	x
Elongate-ellipsoidal blotch, wavy margins	421		x			
Galling						
Unhardened central chamber, thickened outer rim	11		x			x
Nondiagnostic, dark, circular	32	x		x		x
Epidermal center, hardened outer walls	115		x			x
Columnar gall	116		x			
Pathogen						
Circular epiphyllous rust fungus with concentric aecia	66			x		x

An earlier version of Table 1 was published in Donovan et al. (2020).

and zones of surface abrasions are found at Lef (Fig. 1C), PL2 (Fig. 2E, F), and LH (Fig. 6G). External foliage feeding damage is made by insects with mandibulate, chewing mouthparts across orders such as Lepidoptera, Coleoptera, and Orthoptera, many of which can produce comparable damage types (Carvalho et al. 2014). Although the presence of similar external foliage feeding damage on *Agathis* at multiple fossil localities does not necessarily suggest that related insects inflicted the damage, the diversity of damage at all fossil sites suggests that *Agathis* species hosted an array of externally feeding herbivores, similar to extant members of the genus (Donovan et al. 2020). Previously documented, extant, external foliage-feeding insects on *Agathis* include chrysomelid and curculionid beetles (Ecroyd 1982), geometrid and tortricid moths (Ecroyd 1982; Nuttall 1983), and phasmids (Plant-SyNZ database 2017) on *Agathis australis* in New Zealand. In addition, we found numerous examples of external foliage feeding on herbarium specimens throughout the range of the genus (Figs 13A, B, 14G, 15A, B, 16A, 17A, F, M, N, Q, R, 18A, M, N, T).

Piercing and Sucking (fluid feeding)

We found similar circular piercing and sucking marks (DT46) in fossil assemblages spanning the latest Cretaceous to early Eocene (Lef – Fig. 1D; PL2 – Fig. 2G–J; and LH – Fig. 6H), suggesting long-term associations of *Agathis* with hemipteran insects. Evidence for piercing and sucking is common on angiosperms from Lef, PL2 (Donovan et al. 2017), and LH (Wilf et al. 2005a), and on the conifer *Retrophyllum* (Podocarpaceae) from Lef and LH (Wilf et al. 2017). On extant *Agathis*, all known hemipteran associations are scale insects (Figs 14N–P, 15L–N, 16R; Cohic 1958; Williams 1985; Brun and Chazeau 1986; Cox 1987; Williams and Watson 1990; Ben-Dov 1994; Mille et al. 2016), although undocumented associations involving other hemipteran and thysanopteran groups are probable. In addition, kauri thrips, *Oxythrips agathidis* Morison (Thysanoptera, Thripidae), probe *A. robusta* leaves in Queensland, Australia, and can cause major defoliation (Morison 1941; Heather and Schaumberg 1966).

Mining

A serpentine mine occurs on a single cf. *Agathis* leaf from the Cretaceous Lefipán Formation (Fig. 1H–J), but we did not find similar mines on *Agathis* in any of the Paleogene assemblages. Therefore, this association may have gone extinct regionally, possibly in relation to the end-Cretaceous impact, which caused a decrease in leaf-mining associations in Patagonia and Western Interior North America for ca. 4 and 9 million years, respectively (Wilf et al. 2006; Donovan et al. 2014, 2017, 2018; Labandeira et al. 2002a). Although serpentine mines occur on extant *Agathis* (Fig. 13F, G; Wise 1962), mostly made by unknown insects (Figs 15D–F; 16J, K; 17E, I, K, L, O, P, S; 18E–G, S, V, W), none of the extant mines has strong associations with veins comparable to the Cretaceous specimen (Donovan et al. 2020).

Elongate-ellipsoidal blotch mines occur on *Agathis* in all four fossil assemblages (Figs 1K, 2L–M, 6I, 10C), discontinuously spanning ca. 18 myr. The mines share an overall similar morphology, including an oblong shape, long axis parallel to leaf venation, distorted leaf veins within the mine, and frass composed of spheroidal pellets surrounded by amorphous matter, commonly deposited closer to one mine margin. The mines mainly differ in the structure of their margins (Donovan et al. 2020). *Frondicuniculum flexuosum* mines from PL2 have wrinkled margins that undulate (Fig. 2L, M), and *Frondicuniculum lineacurvum* mines from LH (Fig. 6I) and RP (Fig. 10C) have smooth, gently curving margins. A blotch mine similar to *F. lineacurvum* on cf. *Agathis* from Lef (Fig. 1K) also has smooth, gently curving margins, but lacks frass. The overall similarities between blotch mines on the same genus from the latest Cretaceous and early Paleogene provide the first evidence for a possible Cretaceous–Paleogene boundary-crossing leaf mine association (Donovan et al. 2014, 2017, 2018). Based on a survey of herbarium specimens, at least six extant *Agathis* species covering much of the modern range of the genus are associated with similar blotch mines (Figs 14I–K, 15H, 16C–H, 17J, 18H–L), suggesting possible long-term associations spanning time and space (Donovan et al. 2020).

Putative linear blotch mines with breached epidermal tissue (DT251), described by Donovan et al. (2020), occur in the Eocene at LH (Fig. 6J–L) and RP (Fig. 10DE). Similar damage occurs on *Agathis immortalis* from the early Paleocene at PL2 (Fig. 2F), although margins of the damage are much less well defined, which may indicate surface feeding. Unlike the breached epidermal tissues characterizing the DT251 mines at LH and RP, the epidermal tissue of the damaged area of the PL2 specimen (Fig. 2F) is apparently intact based on color and texture differences between the damaged areas, undamaged areas, and rock matrix. Morphologically similar leaf mines that are commonly breached due to weathering occur on *Agathis robusta* in Australia (Fig. 16G, H; Donovan et al. 2020).

Galling

Galls occur on Cretaceous to early Eocene *Agathis* fossils (Lef, PL2, and LH). We found carbonized circular to oval galls (DT32) on cf. *Agathis* leaves at Lef (Fig. 1E) and LH (Fig. 6M), although they lack diagnostic features. At PL2, ellipsoidal to near-circular galls with thickened walls (DT115; Fig. 3A–H) are associated with *A. immortalis*. We did not find DT115 galls on fossil *Agathis* at other localities, but analogous ellipsoidal galls with thickened outer walls surrounding epidermal tissue are associated with *A. ovata* in New Caledonia (Fig. 14L, M; Donovan et al. 2020). Columnar galls typically replaced by or filled in with amber (DT116; Fig. 4) are found exclusively at PL2. These galls, initially defined by Labandeira et al. (2007), share features with the enigmatic structures tentatively interpreted as diaspidid scale covers (Figs 5, 7–9, 11, 12; see discussion below). With the exception of two galls on *A. ovata* and *lanceolata* briefly described by Houard (1914, 1922), documentation of galls on extant *Agathis* is rare, although we found numerous galls on herbarium specimens (Figs 13C–E, 14A, B, H, L, M, 15C, 16B, I, O–Q, 17B–D, G–H, T, U, 18B, C, Q, R, U).

Oviposition

We found oviposition lesions on cf. *Agathis* leaves from the Cretaceous Lefipán Formation (Fig. 1F, G). However, we did not find similar marks on *Agathis* at any other fossil locality or on extant *Agathis* (Donovan et al. 2020). Note added in proof: a single specimen of *Agathis zamunerae* from Laguna del Hunco is associated with an arcuate pattern of ca. 15 subparallel rows of oviposition lesions (DT54; specimen curated at Museo Jorge H. Gerhold (MJHG), Ingeniero Jacobacci, Río Negro, Argentina).

Enigmatic structures: possible armored scale insect (Diaspididae) covers or galls

Enigmatic structures, possibly representing wax coverings constructed by female armored scale insects (Diaspididae) are present on *Agathis* at PL2 (Fig. 5), LH (Figs 7–9), and RP (Figs 11, 12), spanning approximately 16 million years from the early Paleocene to middle Eocene (Suppl. material 1). These structures share many similarities at different fossil sites, including shape and size, concentric growth rings on the dorsal cover, presence of an oval hole or depression near the center of the cover, and a prominent ven-

tral cover (collar). We will first discuss similarities between the enigmatic structures and diaspidid covers and then provide an alternative interpretation of the structures as galls.

The general size and shape of the covers, as well as the presence of concentric rings, are comparable to extant diaspidid covers. The fossil covers are mostly similar in size at all sites but covers at RP are the smallest. The covers are all circular to oval, shapes that tend to be made by female scale insects with near circular bodies (Takagi and Tippins 1972). Interestingly, we found little evidence of first or second instar covers because most of the well-preserved covers with clearly defined growth rings show evidence of three instars. Exceptions include a specimen from PL2 (Fig. 5E) that is associated with varied scale diameters, although growth rings are not preserved. In addition, no evidence for male scale covers was found; as these are usually smaller than the female covers and have an elongate-oval shape (Foldi 1990b), suggesting the likelihood that the possible diaspidids associated with *Agathis* may have been uniparental. Although most diaspidids have sexual mating, some species are hermaphroditic, uniparental (not producing males), or have both uniparental and biparental populations (Miller and Davidson 2005).

Female armored scale insects have three instar stages, including the adult stage. As the insects grow, they add material to their covers, causing an increase in size. The different phases of cover formation can commonly be recognized by distinct rings, indicating the addition of new wax filaments and embedding cement and the incorporation of shed skins (Stoetzel 1976; Foldi 1990b). On well-preserved covers on Paleogene *Agathis* in Patagonia, concentric growth rings are visible on the dorsal covers with prominent rings, indicating distinct instar growth phases. At PL2, scale covers have well-preserved concentric growth rings on some specimens (Fig. 5A–D, I–N), although the transitions between instars are not clear. At LH and RP, impressions (Figs 7C, D, 8H, I) and amber casts (Figs 7H–K, 9F, G, 10) of the covers exhibit distinct growth rings, and some specimens have prominent demarcations of instar transitions.

The surface texture of the dorsal covers varies among fossil localities. At PL2, scale covers are fairly flat and smooth, but the concentric rings are marked with shallow grooves (Fig. 5A). Impressions of scale covers at LH (Figs 7C, D, 8H, I) are also marked with concentric growth rings similar to the covers at PL2 (Fig. 5 I–N), although the transitions between instar stages are much more prominent at LH. However, grooves between growth rings are less prominent on some specimens at LH (Fig. 7H–K), particularly those preserved as amber. Dorsal covers at RP have a slight bumpy surface (Fig. 11), which appears as white round areas under epifluorescence (Fig. 11E, G, I). The RP covers have fewer growth rings overall compared to PL2 and LH, but instar transitions are distinctly visible.

Most dorsal covers at PL2, LH, and RP are associated with a prominent oval, circular, or semicircular hole or impression that is slightly off center. At RP, the edges of the holes are well defined and surrounded by a raised rim (Fig. 11H). The structure is not found on extant diaspidid covers, but possibilities include the position of the white cap constructed by the first instar, which was lost during preservation; the position of unpreserved larval exuviae; or the point where the styletal fascicle was inserted into leaf tissue. Holes on morphologically similar scale covers from the Early Cretaceous of Australia and Late Cretaceous of New Zealand were suggested to have been caused

by hymenopteran parasitoids (Tosolini and Pole 2010), which are commonly associated with extant diaspidids and used today as a pest management method (Miller and Davidson 2005). However, the consistent shape, size, and position across the fossil scale-cover morphotypes suggest that parasitoid emergence holes are an unlikely cause. The holes on the fossil covers are positioned along the edges of the first instar covers, but the positions of exit holes on extant scales are less consistent. Every well-preserved dorsal cover is associated with a hole, but usually only a portion of a scale insect population would have been parasitized. Finally, some parasitoid emergence holes have ragged edges, but the holes on the fossils are consistently smooth.

An important shared character between scale covers at PL2, LH, and RP is the presence of a prominent ventral cover (collar), either embedded in leaf tissue (Fig. 7E, H–K) or protruding above the leaf surface (Figs 6, 8J–L, 9C–E). This feature is not directly comparable to features of typical covers made by most extant diaspidids. A possible analog for the construction of the scale covers on fossil *Agathis* is *Cryptaspidiotus barbusano* (Disapididae: Aspidiotinae), which feeds on *Apollonias barbujana* (Lauraceae) in the Canary Islands (Porcelli et al. 2012). After the female molts for the last time, the cover is near circular, flat, and with a slightly conical top (Porcelli et al. 2012). After mating, the adult female constructs a ventral cover, which raises the dorsal cover up, giving the entire scale a cup-like profile. The ventral cover is constructed by the adult female by repeatedly secreting material in a ring pattern (Porcelli et al. 2012). The margins of the ventral cover are raised slightly relative to the dorsal cover at the point where they are connected. Finally, the adult female of *C. barbusano* constructs an exit tunnel for crawlers (Porcelli et al. 2012), which is not found in the fossils.

Female diaspidids on fossil *Agathis* from Patagonia also probably first constructed the dorsal cover during all three instar phases, as evidenced by growth ring patterns. The ventral cover must have been constructed by the adult female after completion of the dorsal cover because it wraps completely around the dorsal cover. The sides of the ventral covers are only visible at LH (Figs 8J–L, 9C–E) and are marked with horizontal and vertical striations (Figs. 6H, 9E). The ventral covers are not plant reaction tissue, because they are clearly attached by a joint to the dorsal covers at LH (Fig. 9C) and are composed of the same material as the dorsal covers (amber). There is no evidence of plant cells on the ventral covers, but instead, horizontal striations may indicate where the insects added sequential rings of secretory material. Because ventral covers were constructed last and embedded in plant tissue, first and second instars may not have been strongly attached to the plant. Therefore, they may have been less likely to be preserved, explaining why almost all the intact covers were constructed by third instars.

The Diaspididae (armored scale insects) are the most diverse family of scale insects (Coccoidea), with ca. 2400 known extant species in 380 genera (Miller and Davidson 2005). The taxonomy of Diaspididae is mostly based on morphological characters of adult females (Takagi 1990). The two most common subfamilies of Diaspididae, Aspidiotinae and Diaspidinae, can generally be identified by their cover shape. Typically, aspidiotines produce a circular or oval cover, similar to the fossils on *Agathis*, and diaspidines construct an elongate cover (Miller and Davidson 2005).

Armored scale insects are recognizable by the detachable waxy covering that they construct over their bodies. Female diaspidids have two immature instars before the adult stage, and males have four (first and second instar, prepupal, and pupal). The first instars of both males and females (crawlers) have legs and can disperse, either actively by walking or passively by wind. All other stages are sessile, except for adult males. Adult female diaspidids are characterized by a sac-like body with fused head, thorax, and abdomen, working piercing-and-sucking mouthparts, rudimentary antennae, and absence of legs and wings (Takagi 1990). Posterior abdominal segments of the female are fused into a pygidium with wax glands and anal pores (Takagi 1990). Adult males have a pair of wings and functional legs but lack mouthparts and, therefore, do not feed (Giliomee 1990).

Armored scale insect covers are constructed by all three female instars and the first two out of five male instars. Glands on the pygidium produce wax filaments used to construct the cover, and the anal opening exudes a cementing material (Foldi 1982, 1983, 1990b). Diaspidid species that construct circular or oval scale covers, like the fossils associated with *Agathis*, typically incorporate shed skins in the central or subcentral region of the cover. Detailed treatments of cover formation have been provided in multiple publications (Matsuda 1927; Metcalf and Hockenyos 1930; Dickson 1951; Disselkamp 1954; Foldi 1990a).

The fossil record of Diaspididae is currently rather sparse, with fewer species described than any other scale insect family (Koteja 2000b). The record has been summarized elsewhere (Koteja 1990, 2000a, 2001; Koteja and Ben–Dov 2003; Harris et al. 2007; Wappler and Ben-Dov 2008) and is updated here. Diaspidid covers have been recorded in sediment samples from the Early Cretaceous of Australia and Late Cretaceous of New Zealand (Tosolini and Pole 2010). Aspidiotinae covers attached to angiosperm leaves, including Arecaceae (palms) and unidentified dicots, occur in the middle Eocene of Germany (Wappler and Ben-Dov 2008). Fourteen aspidiotine covers are associated with an angiosperm leaf, possibly Elaeocarpaceae, from the Early Miocene of New Zealand (Harris et al. 2007). *Aspidiotus crenulatus*, a female body compression fossil found in a Late Miocene deposit from Sicily, Italy, was the first diaspidid fossil described (Pampaloni 1902). Undescribed male specimens occur in middle Eocene Baltic amber (similar to *Lepidosaphes*), middle Miocene Mexican amber, and middle Miocene Dominican amber (Koteja 1990). A putative male diaspidid, *Normarkicoccus cambayae*, was described from the early Eocene of India (Vea and Grimaldi 2015). The species has a short penial sheath compared to extant diaspidid males, which use their elongated penial sheaths to reach female scales under their covers during mating. The difference in morphology suggests the possibility that some female diaspidids from the Eocene or earlier may not have constructed covers (Vea and Grimaldi 2015), although the presence of possible diaspidid covers in sediment samples from the Early Cretaceous (Tosolini and Pole 2010) and unequivocal covers on leaves from the Eocene (Wappler and Ben-Dov 2008) indicates that some members of the family had evolved the behavior.

The possible fossil diaspidid covers associated with Patagonian *Agathis* discussed here are very similar to those reported from the Cretaceous of Australia and New Zealand by Tosolini and Pole (2010). Similarities with the Patagonian fossils include a flat dorsal cover

with concentric growth rings and a ventral cover with horizontal and radial striations (Tosolini and Pole 2010), wrinkled folds arranged in a radial pattern (similar to the bumpy ornamentation on the columnar galls on *Agathis immortalis*; Fig. 4J–L), and an oval hole slightly off center on the dorsal cover (Tosolini and Pole 2010). Tosolini and Pole (2010) noted a possible relationship between the fossil scales and Araucariaceae based on their co-occurrence in Cretaceous beds in a K–Pg boundary section, the lack of scales in Paleocene sediments, and the extinction of some Araucariaceae species at the end of the Cretaceous in New Zealand (Pole 2008; Pole and Vajda 2009). Taken together, these morphologically similar fossils from the Cretaceous of Australia and New Zealand and early Paleogene of Patagonia, if representing diaspidid scale insect covers, suggest that some lineages of Diaspididae had a Gondwanan distribution early in the history of the family and that host-specialization with members of Araucariaceae may have extended outside of Patagonia.

Diaspidids on extant *Agathis* include *Chrysomphalus aonidum* on *A. lanceolata*, *A. moorei* (Brun and Chazeau 1986; Williams and Watson 1990; Mille et al. 2016), and *A. ovata* (Fig. 14N). *Leucaspis portaeaureae* on *A. australis* in New Zealand, *Hemiberlesia rapax* on *Agathis* sp. (Miller and Davidson 2005), and unidentified diaspidids on *A. ovata* in New Caledonia (Fig. 14P) and *A. macrophylla* in Fiji (Fig. 15N, O; Donovan et al. 2020). Females of the unidentified diaspidid species associated with *A. macrophylla* in Fiji induce pit galls (Fig. 15N, O; Donovan et al. 2020), which is the most common method for gall induction in diaspidids (Gullan et al. 2005). A depression is formed around the flat scale cover, and a rim of deformed tissue surrounds the exposed dorsal surface of each cover, similar to the responses of the fossil *Agathis* species. Gall-inducing diaspidids associated with conifers are very rare, and only one other gall-inducing diaspidid has been documented out of 39 species in 28 genera known to induce galls (Gullan et al. 2005). The only other gall-inducing diaspidid on conifers, *Leucaspis podocarpi*, causes leaf margin rolls on *Prumnopitys taxifolia* (Podocarpaceae) in New Zealand (Gullan et al. 2005; Henderson and Martin 2006).

The presence of a gall-inducing diaspidid species on extant *Agathis* (Donovan et al. 2020) is interesting because the possible fossil scales on Patagonian *Agathis* may also have caused similar deformation of the host plant tissue. One *Agathis* specimen at RP is associated with pits (Fig. 12D–G), possibly where covers were positioned. Many other *Agathis* specimens at PL2 (Fig. 5E), LH (Figs 7E, 9I), and RP (Fig. 12A–C) are associated with depressed rims where ventral covers were deeply set. However, we found no evidence of cell hypertrophy or hyperplasia in the areas surrounding the fossil diaspidids.

Other fossil scale insects have shown evidence of host deformation. Diaspidid (Aspidiotinae) scale covers on dicotyledenous leaves from the middle Eocene of Germany are surrounded by a ring of raised tissue, presumably a reaction to insect feeding (Wappler and Ben-Dov 2008). Depressed circular to oval rings on primary veins of *Erlingdorfia montana* (Platanaceae) from the Late Cretaceous (Maastrichtian) of North Dakota, USA were possibly made by an unidentified coccoid (Labandeira et al. 2002b).

Although the structures share many aspects of general morphology with diaspidid covers (size, shape, concentric growth rings, low domal structure), some features of the Patagonian fossil structures differ from those associated with extant scales. One, the prominent hole, called a parasitoid emergence hole in Tosolini and Pole (2010), is

not a normal feature of modern scale insects. The size, shape, and position of the holes are much more consistent than typical parasitoid emergence holes. Secondly, the sizes of covers on a leaf are consistent. If they were scale covers, we would expect to see differences in size representing different larval growth stages and cover sizes, unless early instars were not strongly attached to the plants and not preserved or alternatively these were new populations of diaspidids. The only specimen with notable differences in sizes among individual scales is on *Agathis immortalis* from PL2 (Fig. 5E). In addition, there is no evidence of sexual dimorphism in scale covers. Finally, the collar-like structure of the ventral cover, which surrounds the scale covers, is atypical for most extant scales.

A second possible explanation for the enigmatic structures is galling. There are many similarities between the fossil columnar gall at PL2 (DT116; Fig. 4) and the possible diaspidid scale covers. Both the galls and covers have a "collar" (ventral cover) marked by vertical striations (Figs 4F–H, 9C–E). However, the "collars" tend to wrap around the top of the galls (Fig. 4J), instead of neatly encircling the dorsal covers (Fig. 9C). In addition, some of the galls have a center to off-center hole (Fig. 4J–L), interpreted as an exit hole, fungal ostiole, or standard shape of the gall, which corresponds to a similar structure on the covers (Figs 5L, 7H–K, 11B–I). Both the galls and covers are preserved as amber. Concentric rings on the galls, if present, are vaguely defined, and marked by rounded bumps or pointy ornamentation (Fig. 4J–L). Dorsal covers at RP have a slightly bumpy texture (Fig. 11D), which may correspond to the ornamentations on the galls. Alternatively, DT116 at PL2 may not be a gall, but instead a preservational form of a scale cover that has been altered in some way before fossilization. Overall, the similarities between the fossil galls and covers, in addition to the atypical features discussed in the previous paragraph, complicate the interpretation of the structures as being made by diaspidids. Although their origin remains inconclusive, the enigmatic structures demonstrate persistence across an impressive spatial and temporal range, occurring on early Paleocene–middle Eocene *Agathis* in Patagonia (Donovan et al. 2020) and in sediment samples from the Cretaceous of Australia and New Zealand (Tosolini and Pole 2010).

Rust fungus (Pucciniales)

Rust fungi (Pucciniales) are obligate parasites associated with ferns, gymnosperms, and angiosperms. Their common name comes from the spores that they produce, typically yellow or orange, which germinate on plant hosts, leading to a rust-like appearance. Rusts can cause deformation of plant hosts in various ways, including inducing galls, witch's brooms, and cankers. Extant *Agathis* hosts diverse fungal communities (McKenzie et al. 2002), including two species of the recently named rust fungus genus *Araucariomyces* (Araucariomycetaceae; the species were formerly placed in *Aecidium*; Aime & McTaggart, 2021), which parasitizes *Agathis* through much of its range. *Araucariomyces fragiformis* (previously *Aecidium fragiforme*; Fig. 15K) is associated with *Agathis* in Australia, the Solomon Islands, Fiji, Vanuatu, New Guinea, Borneo, and Malaysia, and *Araucariomyces balansae* (previously *Aecidium balansae*) is restricted to New Caledonia (Punithalingam and Jones 1971; McKenzie et al. 2002). Aeciospores can

travel long distances by wind, which probably facilitated *A. fragiformis* to track *Agathis* through a large portion of its extant range. *Araucariomyces* on extant *Agathis* produce galls covered in yellow aecia with pycnia embedded in the opposite surface (Peterson 1968; Punithalingam and Jones 1971). The species are differentiated by the morphology of the aeciospores. The surfaces of aeciospores produced by *A. balansae* are covered in coarse warts, and the surfaces of aeciospores produced by *A. fragiformis* are covered in spines (Punithalingam and Jones 1971). Aecia tend to be deeply-set in swollen tissue on the abaxial leaf surface for *A. balansae* and the adaxial leaf surface for *A. fragiformis* (Punithalingam and Jones 1971). Although rusts on plant species co-occurring with *Agathis* in Australasia and Southeast Asia have been sampled extensively, the telial state for both *Araucariomyces* species is unknown, leading to speculation that *Araucariomyces* may not have a sporothallus stage and instead systemically infects *Agathis* (Aime and McTaggart 2021). Recent phylogenetic analyses of Pucciniales show *Araucariomyces* as a separate lineage from the rest of the order (Aime and McTaggart 2021). The morphological similarity between the fossil rust fungus on *Agathis zamunerae* from LH and *A. fragiformis* and *A. balansae* on extant *Agathis*, including concentric rings of deep-set aecia in swollen leaf tissue, suggests the possibility of ancient coevolutionary relationships between these groups (Donovan et al. 2020).

The evolutionary history of rust fungi is poorly understood (Tiffney and Barghoorn 1974; Pirozynski 1976). The earliest probable rust, *Teleutosporites* (*Uromyces*), is associated with *Lepidodendron*, an extinct representative of lycopsids, from the Pennsylvanian subperiod (Renault 1893; Tiffney and Barghoorn 1974). The earliest rust accepted by Tiffney and Barghoorn (1974), *Puccinites*, is associated with a monocot leaf from the Eocene of western Tennessee (Dilcher 1965). Past estimates of the most recent common ancestor of rust fungi vary between 300 to 113 Ma, and whether the main driver of rust diversification was convergence and coevolution with major plant lineages, or host switching, or a combination of both is debated (Leppik 1965; Savile 1976; Wingfield et al. 2004; Aime 2006; McTaggart et al. 2016; Aime et al. 2018). The relationships between plant hosts of rust fungi gametothalli, the stage visible on the fossil, appear to be related to the systematic relationships of Pucciniales, highlighting the role of coevolution and biological specialization in the diversification of Pucciniales (Aime et al. 2018). Fossil spores, not preserved here, are needed for finer taxonomic resolution of the fossil rust fungus on *Agathis zamunerae* (Fig. 6N–P). However, based on overall morphological similarity to *Araucariomyces* species on extant *Agathis*, the fossil fungus suggests possible long-term coevolutionary relationships between the aecial stage of a rust fungus and its host genus.

Persistence of plant-insect interactions on *Agathis* through time

Ecological guilds and possibly herbivore communities on Patagonian fossil *Agathis* exhibit remarkable host-fidelity and evolutionary conservatism across sites through time, during the process of evolving modern characteristics of the genus during the Cretaceous and early Paleogene (Wilf et al. 2014; Escapa et al. 2018). Persistence of

these ecological guilds also occurred through major environmental changes, such as the Cretaceous–Paleogene extinction, early Eocene warming (Wilf et al. 2003, 2005b; Donovan et al. 2017), and 45 million years of post-Gondwana events. Most strikingly, similar enigmatic structures, possibly covers made by armored scale insects (DT86) or galls, occur in all early Paleogene assemblages, linear blotch mines with breached epidermal tissue (DT251) occur in both Eocene assemblages, and elongate-ellipsoidal blotch mines occur in all assemblages (DT88 and DT421); Donovan et al. 2020), crossing the Cretaceous-Paleogene boundary. Associations that are unique to one time period, suggesting possible extirpation, extinction, or undersampling, include serpentine mines influenced by leaf veins (DT139) and elliptical oviposition marks (DT101) at LefE.

Persistent associations on latest Cretaceous to early Paleogene fossil *Agathis* tend to have extant analogs on *Agathis* in Australasia to Southeast Asia, raising the possibility that some of these associations may have tracked the genus through major range shifts, continental breakup, and environmental change (Donovan et al. 2020). Possible armored scale insects associated with early Paleogene *Agathis* caused deformation to the host tissue, leaving pits or depressed rims (DT86; Fig. 8E). On *A. macrophylla* in Fiji, a diaspidid causes host tissue deformation by inducing pit galls on the leaves (Fig. 15N, O; Donovan et al. 2020). Linear blotch mines with breached epidermal tissue (DT251; Figs 6J–L, 10D, E) from the early Eocene assemblages resemble mines on *A. robusta* in Queensland, Australia. Elongate-ellipsoidal blotch mines (DT88; Figs 1K, 6L, M, I, 10C) on *Agathis*, described by Donovan et al. (2020), span the latest Cretaceous to early Paleogene, and similar mines are associated with eight species of extant *Agathis* through much of its range. External foliage feeding, such as hole feeding (DT1; Fig. 1A, 2A, B, 6A), margin feeding (DT12; Figs 1B, 2C, D, 6C–F, 10A), and surface feeding (DT29; Figs 1C, 2F, 6G) are found on *Agathis* at multiple Patagonian fossil localities and are common on extant *Agathis*, although similarities in these damage morphologies do not necessarily imply common tracemakers (Carvalho et al. 2014). The pattern of persistence to the modern day observed in the previous examples was not always found for associations that only appeared during a single time slice, such as a serpentine mine (Fig. 1H–J) or oviposition lesions (Fig. 1F, G) from the latest Cretaceous, for which we have not found clear modern analogs. Exceptions include the rust fungus fossil, found on one *A. zamunerae* leaf from the early Eocene (LH; Fig. 6N–P), which is similar to two species of *Araucariomyces* associated with extant *Agathis*. Overall, most of the extant associations we found on extant *Agathis* are previously undocumented, and the insects that made the damage are unknown. Consequently, taxonomic and ecological observations of the extant plants and insects are needed to understand these patterns first observed in the fossil record.

The persistence of plant-insect associations over geologic timescales has previously been observed in the paleobotanical record (Opler 1973; Labandeira et al. 1994; Wilf et al. 2000; Winkler et al. 2010; Leckey and Smith 2015; Su et al. 2015; Adroit et al. 2020), although the recurring presence of multiple components of the insect herbivore and fungal communities on a single genus for millions of years and into the modern day is rare (Donovan et al. 2020). Other examples of persistent associations include surface feeding damage made by hispine beetles on Zingiberales fossils from latest Cretaceous and Eocene deposits in Western Interior North America, an association

that still occurs in the modern Neotropics (Wilf et al. 2000). On oaks, a minimum Miocene age has been suggested for eleven leaf mines based on morphological similarity between fossil and extant mines (Opler 1973), galls similar to those made by Cynipini wasps are found associated with two oak species from the Oligocene to Pliocene (Leckey and Smith 2015), and nearly all DTs on oak leaves from a Pliocene fossil assemblage in southwestern China occur on extant oaks in local forests (Su et al. 2015). Distinct curvilinear zones of skeletonized tissue have been associated with *Parrotia* (Hamamelidaceae) leaves for at least 15 million years, from the Miocene of China and Pliocene of Germany to modern Iran and China (Adroit et al. 2020). The study of fossil plant-insect associations is necessary to address fundamental issues concerning patterns of insect host use over time, including the prevalence of evolutionarily conservative, long-term associations (Labandeira et al. 1994; Wilf et al. 2000; Labandeira 2002; Labandeira and Wappler 2023), host-switching (Labandeira 2002), and extinct associations (Labandeira 2002; Winkler et al. 2010).

The case study of *Agathis* and its herbivore communities presented here and earlier (Donovan et al. 2020) provides some insights into potential causes of persistent interactions between plants and associated insects and fungi. *Agathis* appears to be conservative in both its morphology and habitat preferences (Kooyman et al. 2014; Wilf et al. 2014), tracking rainforest environments throughout its history. Niche conservatism, the tendency for closely related species to occupy similar niches (Pyron et al. 2015), has been observed at local and regional scales (Losos et al. 2003; Silvertown et al. 2006), and across continents (Crisp et al. 2009). Tracking of everwet rainforest biomes appears to be a common pattern for extant members of many of the plant groups present in early Paleogene fossil deposits from Patagonia (Kooyman et al. 2014; Merkhofer et al. 2015). The environmental stability caused by plant biome tracking may have provided suitable environments for ecological guilds and possibly herbivore communities, including those on *Agathis*, to establish long-term, coevolutionary relationships with their hosts (Donovan et al. 2020) that are now endangered due to habitat loss and climate change (Kooyman et al. 2022).

Agathis has evolved numerous defenses against insect herbivores. *Agathis* leaves are tough and leathery, contain copious resin (Langenheim 1990, 1996), tannins (Arbicheva and Pautov 2018) and phenolic compounds (Gadek et al. 1984), and are coated with epicuticular waxes (Dragota and Riederer 2008). When injured, *Agathis* leaves produce true wound periderm (Arbicheva and Pautov 2018). *Agathis robusta* leaves produce stomatal wax plugs, which have been shown experimentally to block fungal hyphae from entering stomatal pores (Mohammadian et al. 2009).

The presence of *Agathis* in Patagonia before the final breakup of Gondwana (Wilf et al. 2014; Escapa et al. 2018) suggests that the genus probably reached its extant range through a combination of vicariance and dispersal over water. Several plant groups represented by fossils at Laguna del Hunco are older than recent molecular clock estimates, underscoring the importance of fossils for understanding Gondwanan legacies in modern distributions (Wilf and Escapa 2015). Insect herbivores on *Agathis australis* in New Zealand are better documented than on *Agathis* in other regions. However, distinct insect damage on *A. australis*, such as mines made by *Parectopa leu-*

cocyma (Wise 1962), have not been found in other parts of the extant range of the genus or on fossils (Donovan et al. 2020). Notably, Donovan et al. (2020) did not find any types of blotch mines on *A. australis*, and *Araucariomyces* rust fungus is not associated with *A. australis* in New Zealand despite the wide range of the association (McKenzie et al. 2002). *Agathis* fossils have been described from the late Paleocene to early Miocene of Australia and the late Oligocene–Miocene of New Zealand (Hill et al. 2008; Pole 2008). Insect damage has not been reported on *Agathis* and *Agathis*-like fossils from Australia and New Zealand, and besides a possible gall on *Agathis* sp. aff. *A. robusta* from the middle Miocene of New South Wales, Australia (Holmes and Andereson 2019), we did not observe any insect damage on published images of fossil *Agathis* leaves from these regions (Cookson and Duigan 1951; Hill and Bigwood 1987; Cantrill 1992; Hill and Merrifield 1993; Pole et al. 1993; McLoughlin and Hill 1996; McLoughlin et al. 2001; Hill et al. 2008; Pole 2008; Holmes and Andereson 2019). Future discoveries of well-preserved *Agathis* macrofossils with insect damage from the current range of the genus may provide further insight into the biogeographic history of phytophagous insects associated with *Agathis*.

Conclusions

Our documentation of fossilized *Agathis* herbivore communities from the latest Cretaceous to middle Eocene of Patagonia illustrates several persistent forms of damage, including external foliage feeding, leaf mines, enigmatic structures (possibly scale insect covers or galls), and a rust fungus. *Agathis* remains an important host genus for insect herbivores and pathogens today, as evidenced by the diverse array of damage that we found on 15 extant species across their Australasian and Southeast Asian range. Most of the extant damage on *Agathis* is undescribed and much of it is similar to the fossils, demonstrating the importance of integrating fossil and extant plant-insect associational data to explore long-term evolutionary and ecological patterns of host-plant use.

Acknowledgements

We thank A.-M. Tosolini and an anonymous reviewer for helpful reviews that significantly improved the manuscript; L. Canessa, M. Caffa, I. Escapa, M. Gandolfo, K. Johnson, P. Puerta, L. Reiner, E. Ruigómez, S. Wing, and many others for field, laboratory, and collections help in Argentina; F. Marsh and J. Wingerath for collections assistance at USNM; and T. Bralower, D. Hughes, and M. Patzkowsky for discussions. The study was funded by grants to M.P.D. from a CIC/Smithsonian Fellowship, the Evolving Earth Foundation, the Geological Society of America, Sigma Xi, the Paleontological Society, and the P.D. Krynine Memorial Fund of the Pennsylvania State University Department of Geosciences; and to P.W., A.I, and N.R.C. from NSF awards DEB-0345750, DEB-0919071, DEB-1556666, and EAR-1925755. This work partially fulfilled requirements for a PhD degree in Geosciences from Pennsylvania State University by MPD.

References

Adroit B, Zhuang X, Wappler T, Terral J-F, Wang B (2020) A case of long-term herbivory: Specialized feeding trace on *Parrotia* (Hamamelidaceae) plant species. Royal Society Open Science 7(10): e201449. https://doi.org/10.1098/rsos.201449

Aime M (2006) Toward resolving family-level relationships in rust fungi (Uredinales). Mycoscience 47(3): 112–122. https://doi.org/10.1007/S10267-006-0281-0

Aime MC, McTaggart AR (2021) A higher-rank classification for rust fungi, with notes on genera. Fungal Systematics and Evolution 7(1): 21–47. https://doi.org/10.3114/fuse.2021.07.02

Aime MC, Bell CD, Wilson AW (2018) Deconstructing the evolutionary complexity between rust fungi (Pucciniales) and their plant hosts. Studies in Mycology 89: 143–152. https://doi.org/10.1016/j.simyco.2018.02.002

Andruchow-Colombo A, Escapa IH, Cúneo NR, Gandolfo MA (2018) *Araucaria lefipanensis* (Araucariaceae), a new species with dimorphic leaves from the Late Cretaceous of Patagonia, Argentina. American Journal of Botany 105(6): 1067–1087. https://doi.org/10.1002/ajb2.1113

Andruchow-Colombo A, Escapa IH, Carpenter RJ, Hill RS, Iglesias A, Abarzua AM, Wilf P (2019) Oldest record of the scale-leaved clade of Podocarpaceae, early Paleocene of Patagonia, Argentina. Alcheringa 43(1): 127–145. https://doi.org/10.1080/03115518.2018.1517222

Andruchow-Colombo A, Gandolfo MA, Escapa IH, Cúneo NR (2022) New genus of Cupressaceae from the Upper Cretaceous of Patagonia (Argentina) fills a gap in the evolution of the ovuliferous complex in the family. Journal of Systematics and Evolution 60(6): 1417–1439. https://doi.org/10.1111/jse.12842

Arbicheva AI, Pautov AA (2018) Leaf periderm supports longevity and functionality of crown leaves in *Agathis* species (Araucariaceae). [Revista Brasileira de Botânica.] Brazilian Journal of Botany 41(1): 155–165. https://doi.org/10.1007/s40415-017-0429-5

Barreda VD, Cúneo NR, Wilf P, Currano ED, Scasso RA, Brinkhuis H (2012) Cretaceous/Paleogene floral turnover in Patagonia: Drop in diversity, low extinction, and a *Classopollis* spike. PLoS ONE 7(12): e52455. https://doi.org/10.1371/journal.pone.0052455

Barreda VD, Zamaloa M del C, Gandolfo MA, Jaramillo C, Wilf P (2020) Early Eocene spore and pollen assemblages from the Laguna del Hunco fossil lake beds, Patagonia, Argentina. International Journal of Plant Sciences 181(6): 594–615. https://doi.org/10.1086/708386

Ben-Dov Y (1994) A Systematic Catalogue of the Mealybugs of the World (Insecta: Homoptera: Coccoidea: Pseudococcidae and Putoidae) with Data on Geographical Distribution, Host Plants, Biology and Economic Importance. Intercept Limited, Andover, 686 pp.

Brodribb TJ, Holbrook NM (2005) Water stress deforms tracheids peripheral to the leaf vein of a tropical conifer. Plant Physiology 137(3): 1139–1146. https://doi.org/10.1104/pp.104.058156

Brun LO, Chazeau J (1986) Catalogue des ravageurs d'intérêt agricole de Nouvelle-Calédonie (2^{e} éd.). ORSTOM, Centre de Nouméa, 130 pp.

Cantrill DJ (1992) Araucarian foliage from the Lower Cretaceous of southern Victoria, Australia. International Journal of Plant Sciences 153(4): 622–645. https://doi.org/10.1086/297084

Carvalho MR, Wilf P, Barrios H, Windsor DM, Currano ED, Labandeira CC, Jaramillo CA (2014) Insect leaf-chewing damage tracks herbivore richness in modern and ancient forests. PLoS ONE 9(5): e94950. https://doi.org/10.1371/journal.pone.0094950

Clyde WC, Wilf P, Iglesias A, Slingerland RL, Barnum T, Bijl PK, Bralower TJ, Brinkhuis H, Comer EE, Huber BT, Ibañez-Mejia M, Jicha BR, Krause JM, Schueth JD, Singer BS, Raigemborn MS, Schmitz MD, Sluijs A, Zamaloa MC (2014) New age constraints for the Salamanca Formation and lower Río Chico Group in the western San Jorge Basin, Patagonia, Argentina: Implications for Cretaceous-Paleogene extinction recovery and land mammal age correlations. Geological Society of America Bulletin 126(3–4): 289–306. https://doi.org/10.1130/B30915.1

Cohic F (1958) Contribution à l'étude des cochenilles d'intérêt économique de Nouvelle-Calédonie et Dépendances. Commission du Pacifique Sud, Nouméa. Document Technique 116: 1–35. https://doi.org/10.3406/bsef.1958.20393

Comer EE, Slingerland RL, Krause JM, Iglesias A, Clyde WC, Raigemborn MS, Wilf P (2015) Sedimentary facies and depositional environments of diverse early Paleocene floras, north-central San Jose Basin, Patagonia, Argentina. Palaios 30(7): 553–573. https://doi.org/10.2110/palo.2014.064

Cookson IC, Duigan SL (1951) Tertiary Araucariaceae from south-eastern Australia, with notes on living species. Australian Journal of Biological Sciences 4(4): 415–449. https://doi.org/10.1071/BI9510415

Cox JM (1987) Pseudococcidae (Insecta: Hemiptera). Fauna of New Zealand 11: 1–232.

Crisp MD, Arroyo MTK, Cook LG, Gandolfo MA, Jordan GJ, McGlone MS, Weston PH, Westoby M, Wilf P, Linder HP (2009) Phylogenetic biome conservatism on a global scale. Nature 458(7239): 754–756. https://doi.org/10.1038/nature07764

Cunéo R, Andruchow-Colombo A, De Benedetti F, Gandolfo MA (2021) Megafloras de las Formaciones La Colonia y Lefipán, Cretácico Superior de Chubut. Relatorio XXI Congreso Geológico Argentino. Puerto Madryn, Argentina, 261–272.

Dickson RC (1951) Construction of the scale covering of *Aonidiella aurantii* (Mask.). Annals of the Entomological Society of America 44(4): 596–602. https://doi.org/10.1093/aesa/44.4.596

Dilcher DL (1965) Epiphyllous Fungi from Eocene Deposits in Western Tennessee, USA. Palaeontographica. Abteilung B, Paläophytologie, 54 pp.

Disselkamp C (1954) The scale formation of the San Jose scale (*Quadraspidiotus perniciosus* Comst.). Höfchen-Briefe Bayer Pflanzenschutz-Nachrichten 7: 105–151.

Donovan MP, Wilf P, Labandeira CC, Johnson KR, Peppe DJ (2014) Novel insect leaf-mining after the end-Cretaceous extinction and the demise of Cretaceous leaf miners, Great Plains, USA. PLoS ONE 9(7): e103542. https://doi.org/10.1371/journal.pone.0103542

Donovan MP, Iglesias A, Wilf P, Labandeira CC, Cúneo NR (2017) Rapid recovery of Patagonian plant–insect associations after the end-Cretaceous extinction. Nature Ecology & Evolution 1: e0012. https://doi.org/10.1038/s41559-016-0012

Donovan MP, Iglesias A, Wilf P, Labandeira CC, Cúneo NR (2018) Diverse plant-insect associations from the latest Cretaceous and early Paleocene of Patagonia, Argentina. Ameghiniana 55(3): 303–338. https://doi.org/10.5710/AMGH.15.02.2018.3181

Donovan MP, Wilf P, Iglesias A, Cúneo NR, Labandeira CC (2020) Persistent biotic interactions of a Gondwanan conifer from Cretaceous Patagonia to modern Malesia. Communications Biology 3(1): e708. https://doi.org/10.1038/s42003-020-01428-9

Dragota S, Riederer M (2008) Comparative study on epicuticular leaf waxes of *Araucaria araucana*, *Agathis robusta* and *Wollemia nobilis* (Araucariaceae). Australian Journal of Botany 56(8): 644–650. https://doi.org/10.1071/BT08047

Ecroyd C (1982) Biological flora of New Zealand 8. *Agathis australis* (D. Don) Lindl. (Araucariaceae) Kauri. New Zealand Journal of Botany 20(1): 17–36. https://doi.org/10.1080/0028825X.1982.10426402

Escapa IH, Iglesias A, Wilf P, Catalano SA, Caraballo-Ortiz MA, Cúneo NR (2018) *Agathis* trees of Patagonia's Cretaceous-Paleogene death landscapes and their evolutionary significance. American Journal of Botany 105(8): 1345–1368. https://doi.org/10.1002/ajb2.1127

Farjon A (2010) A Handbook of the World's Conifers. Brill, Leiden, 1111 pp. https://doi.org/10.1163/9789047430629

Foldi I (1982) Étude structurale et expérimentale de la formation du bouclier chez les Cochenilles Diaspines (Hom. Coccoidea Diaspididae). Annales de la Société Entomologique de France 18: 317–330.

Foldi I (1983) Ultrastructure comparee des glandes tegumentaires des cochenilles diaspines (Homoptera: Diaspididae). International Journal of Insect Morphology & Embryology 12(5–6): 339–354. https://doi.org/10.1016/0020-7322(83)90028-4

Foldi I (1990a) Moulting and scale-cover formation. Armored Scale Insects: Their Biology. Natural Enemies and Control 4: 257–265.

Foldi I (1990b) The scale cover. Armored Scale Insects: Their Biology. Natural Enemies and Control 4: 43–57.

Gadek P, Quinn C, Ashford A (1984) Localization of the biflavonoid fraction in plant leaves, with special reference to *Agathis robusta* (C. Moore Ex F. Muell.) F.m. Bail. Australian Journal of Botany 32(1): 15–31. https://doi.org/10.1071/BT9840015

Giliomee JH (1990) The adult male. Armored Scale Insects: Their Biology. Natural Enemies and Control 4: 21–28.

Gradstein FM, Ogg JG, Schmitz M, Ogg G (2012) The Geologic Time Scale 2012. Elsevier, Oxford, 1176 pp. https://doi.org/10.1127/0078-0421/2012/0020

Gullan PJ, Miller DR, Cook LG (2005) Gall-inducing scale insects (Hemiptera: Sternorrhyncha: Coccoidea). In: Raman A, Schaefer CW, Withers TM (Eds) Biology, Ecology, and Evolution of Gall-Inducing Arthropods. Science Publishers, Inc., Enfield, 159–229.

Harris AC, Bannister JM, Lee DE (2007) Fossil scale insects (Hemiptera, Coccoidea, Diaspididae) in life position on an angiosperm leaf from an early Miocene lake deposit, Otago, New Zealand. Journal of the Royal Society of New Zealand 37(1): 1–13. https://doi.org/10.1080/03014220709510531

Heather NW, Schaumberg JB (1966) Plantation problems of kauri pine in South East Queensland. Australian Forestry 30(1): 12–19. https://doi.org/10.1080/00049158.1966.10675392

Henderson RC, Martin NA (2006) Review of the gall-inducing scale insects of New Zealand (Hemiptera: Coccoidea), with a guide to field identification. New Zealand Entomologist 29(1): 59–75. https://doi.org/10.1080/00779962.2006.9722140

Hermsen EJ, Jud NA, De Benedetti F, Gandolfo MA (2019) *Azolla* sporophytes and spores from the Late Cretaceous and Paleocene of Patagonia, Argentina. International Journal of Plant Sciences 180(7): 737–754. https://doi.org/10.1086/704377

Hill RS, Bigwood AJ (1987) Tertiary gymnosperms from Tasmania: Araucariaceae. Alcheringa 11(4): 325–335. https://doi.org/10.1080/03115518708619142

Hill RS, Merrifield HE (1993) An Early Tertiary macroflora from West Dale, southwestern Australia. Alcheringa 17(4): 285–326. https://doi.org/10.1080/03115519308619596

Hill RS, Lewis T, Carpenter RJ, Whang SS (2008) *Agathis* (Araucariaceae) macrofossils from Cainozoic sediments in south-eastern Australia. Australian Systematic Botany 21(3): 162–177. https://doi.org/10.1071/SB08006

Holmes W, Andereson H (2019) The middle Miocene Flora of the Chalk Mountain Formation, Warrumbungle Volcano Complex, NSW, Australia. Proceedings of the Linnean Society of New South Wales 141: S19–S32.

Houard C (1914) Les collections cécidologiques du laboratoire d'entomologie du Muséum d'Histoire Naturelle de Paris: Galles de Nouvelle-Calédonie. Marcellia 14: 143–182.

Houard C (1922) Les Zoocécidies des Plantes d'Afrique, d'Asie et d'Océanie 1: 1–498. https://doi.org/10.5962/bhl.title.50815

Iglesias A, Wilf P, Johnson KR, Zamuner AB, Cúneo NR, Matheos SD, Singer BS (2007) A Paleocene lowland macroflora from Patagonia reveals significantly greater richness than North American analogs. Geology 35(10): 947–950. https://doi.org/10.1130/G23889A.1

Iglesias A, Wilf P, Stiles E, Wilf R (2021) Patagonia's diverse but homogeneous early paleocene forests: Angiosperm leaves from the Danian Salamanca and Peñas Coloradas formations, San Jorge Basin, Chubut, Argentina. Palaeontologia Electronica 24: a02. ttps://doi.org/10.26879/1124

Jankiewicz LS, Dyki B, Machlanska A, Dubert F (2017) Oak leaf galls: *Neuroterus numismalis* and *Cynips quercusfolii*, their structure and ultrastructure. Acta Societatis Botanicorum Poloniae 86(2): e86. https://doi.org/10.5586/asbp.3537

Jud NA, Gandolfo MA (2021) Fossil evidence from South America for the diversification of Cunoniaceae by the earliest Palaeocene. Annals of Botany 127(3): 305–315. https://doi.org/10.1093/aob/mcaa154

Jud NA, Gandolfo MA, Iglesias A, Wilf P (2018a) Fossil flowers from the early Paleocene of Patagonia, Argentina with affinity to Schizomerieae (Cunoniaceae). Annals of Botany 121(3): 431–442. https://doi.org/10.1093/aob/mcx173

Jud NA, Iglesias A, Wilf P, Gandolfo MA (2018b) Fossil moonseeds from the Paleogene of West Gondwana (Patagonia, Argentina). American Journal of Botany 105(5): 927–942. https://doi.org/10.1002/ajb2.1092

Kausik SB (1976) Contribution to foliar anatomy of *Agathis dammara*, with a discussion on the transfusion tissue and stomatal structure. Phytomorphology 26: 263–273.

Kiessling W, Aragón E, Scasso R, Aberhan M, Kriwet J, Medina F, Fracchia D (2005) Massive corals in Paleocene siliciclastic sediments of Chubut (Argentina). Facies 51(1–4): 233–241. https://doi.org/10.1007/s10347-005-0023-3

Kooyman RM, Wilf P, Barreda VD, Carpenter RJ, Jordan GJ, Sniderman JMK, Allen A, Brodribb TJ, Crayn D, Feild TS, Laffan SW, Lusk CH, Rossetto M, Weston PH (2014)

Paleo-Antarctic rainforest into the modern Old World tropics: The rich past and threatened future of the "southern wet forest survivors.". American Journal of Botany 101(12): 2121–2135. https://doi.org/10.3732/ajb.1400340

Kooyman RM, Ivory SJ, Benfield AJ, Wilf P (2022) Gondwanan survivor lineages and the high-risk biogeography of Anthropocene Southeast Asia. Journal of Systematics and Evolution 60(4): 715–727. https://doi.org/10.1111/jse.12853

Koteja J (1990) Paleontology. Armored Scale Insects: Their Biology. Natural Enemies and Control 4: 149–163.

Koteja J (2000a) Advances in the study of fossil coccids. Polskie Pismo Entomologiczne 2: 187–218. [Hemiptera: Coccinea]

Koteja J (2000b) Scale insects (Homoptera, Coccinea) from Upper Cretaceous New Jersey amber. Studies on fossils in amber, with particular reference to the Cretaceous of New Jersey: 147–229.

Koteja J (2001) Essays on coccids (Hemiptera: Coccinea). Paleontology without fossils. Prace Muzeum Ziemi: 1–46.

Koteja J, Ben-Dov Y (2003) Notes on the fossil armoured scale insect *Aspidiotus crenulatus* (Pampaloni) (Hem., Coccoidea, Diaspididae). Bulletin de la Société Entomologique de France 108(2): 165–166. https://doi.org/10.3406/bsef.2003.16947

Labandeira CC (2002) Paleobiology of middle Eocene plant-insect associations from the Pacific Northwest. Rocky Mountain Geology 37(1): 31–59. https://doi.org/10.2113/gsrocky.37.1.31

Labandeira CC, Wappler T (2023) Arthropod and pathogen damage on fossil and modern plants: Exploring the origins and evolution of herbivory on land. Annual Review of Entomology 68(1): 341–361. https://doi.org/10.1146/annurev-ento-120120-102849

Labandeira CC, Dilcher DL, Davis DR, Wagner DL (1994) Ninety-seven million years of angiosperm-insect association: Paleobiological insights into the meaning of coevolution. Proceedings of the National Academy of Sciences of the United States of America 91(25): 12278–12282. https://doi.org/10.1073/pnas.91.25.12278

Labandeira CC, Johnson KR, Wilf P (2002a) Impact of the terminal Cretaceous event on plant–insect associations. Proceedings of the National Academy of Sciences of the United States of America 99(4): 2061–2066. https://doi.org/10.1073/pnas.042492999

Labandeira CC, Johnson KR, Lang P (2002b) Preliminary assessment of insect herbivory across the Cretaceous-Tertiary boundary: Major extinction and minimum rebound. Geological Society of America. Special Paper 361: 297–327. https://doi.org/10.1130/0-8137-2361-2.297

Labandeira CC, Wilf P, Johnson KR, Marsh F (2007) Guide to Insect (and Other) Damage Types on Compressed Plant Fossils. Version 3.0. Smithsonian Institution, Washington, 25 pp. http://paleobiology.si.edu/insects/index.html

Langenheim JH (1990) Plant Resins. American Scientist 78: 16–24. https://doi.org/10.1007/BF00988086

Langenheim JH (1996) Biology of amber-producing trees: focus on case studies of *Hymenaea* and *Agathis*. In: Amber, Resinite, and Fossil Resins. ACS Symposium Series. American Chemical Society, 31 pp. https://doi.org/10.1021/bk-1995-0617.ch001

Leckey EH, Smith DM (2015) Host fidelity over geologic time: Restricted use of oaks by oak gallwasps. Journal of Paleontology 89(2): 236–244. https://doi.org/10.1017/jpa.2014.19

Leppik EE (1965) Some viewpoints on the phylogeny of rust fungi. V. Evolution of biological specialization. Mycologia 57(1): 6–22. https://doi.org/10.1080/00275514.1965.12018189

Losos JB, Leal M, Glor RE, de Queiroz K, Hertz PE, Rodriguez Schettino L, Chamizo Lara A, Jackman TR, Larson A (2003) Niche lability in the evolution of a Caribbean lizard community. Nature 424(6948): 542–545. https://doi.org/10.1038/nature01814

Matsuda M (1927) Studies on the rotatory movements necessary for the formation of the scale in *Chrysomphalus aonidum* L. Transactions of the Natural History Society of Formosa 17: 391–417.

McKenzie EHC, Buchanan PK, Johnston PR (2002) Checklist of fungi on kauri (*Agathis australis*) in New Zealand. New Zealand Journal of Botany 40(2): 269–296. https://doi.org/10.1080/0028825X.2002.9512788

McLoughlin S, Hill RS (1996) The succession of Western Australian Phanerozoic terrestrial floras. In: Hopper SD, Chappill JA, Harvey MS, George AS (Eds) Gondwanan Heritage: Past, Present and Future of the Western Australian Biota. Surry Beatty, Sydney, 61–80.

McLoughlin S, McNamara K, George AS (2001) Ancient Floras of Western Australia. Western Australian Museum, 42 pp.

McTaggart AR, Shivas RG, van der Nest MA, Roux J, Wingfield BD, Wingfield MJ (2016) Host jumps shaped the diversity of extant rust fungi (Pucciniales). The New Phytologist 209(3): 1149–1158. https://doi.org/10.1111/nph.13686

Merkhofer L, Wilf P, Haas MT, Kooyman RM, Sack L, Scoffoni C, Cúneo NR (2015) Resolving Australian analogs for an Eocene Patagonian paleorainforest using leaf size and floristics. American Journal of Botany 102(7): 1160–1173. https://doi.org/10.3732/ajb.1500159

Metcalf C, Hockenyos GL (1930) The nature and formation of scale insect shells. Transactions of the Illinois State Academy of Science. Illinois State Academy of Science 22: 166–184.

Mille C, Henderson RC, Cazères S, Jourdan H (2016) Checklist of the scale insects (Hemiptera: Sternorrhyncha: Coccomorpha) of New Caledonia. Zoosystema 38(2): 129–176. https://doi.org/10.5252/z2016n2a1

Miller DR, Davidson JA (2005) Armored scale insect pests of trees and shrubs (Hemiptera: Diaspididae). Cornell University Press, Ithaca, 442 pp.

Mohammadian MA, Hill RS, Watling JR (2009) Stomatal plugs and their impact on fungal invasion in *Agathis robusta*. Australian Journal of Botany 57(5): 389–395. https://doi.org/10.1071/BT08175

Morison GD (1941) *Oxythrips agathidis* sp. n. (Thysanoptera, Thripidae) from Queensland. Proceedings of the Royal Entomological Society of London, Series B, Taxonomy 10(10): 203–207. https://doi.org/10.1111/j.1365-3113.1941.tb00679.x

Nuttall MJ (1983) *Pseudocoremia fenerata* (Felder) (Lepidoptera: Geometridae): a native looper. Forest and Timber Insects of New Zealand 56: 1–4.

Opler PA (1973) Fossil lepidopterous leaf mines demonstrate the age of some insect-plant relationships. Science 179(4080): 1321–1323. https://doi.org/10.1126/science.179.4080.1321

Pampaloni L (1902) Resti organici nel disolide di Melilli in Sicilia. Palaeontographia Italica 8: 121–130.

Peterson RS (1968) Rust fungi on Araucariaceae. Mycopathologia 34(1): 17–26. https://doi.org/10.1007/BF02050840

Pirozynski K (1976) Fossil fungi. Annual Review of Phytopathology 14(1): 237–246. https://doi.org/10.1146/annurev.py.14.090176.001321

Plant-SyNZ database (2017) Plant-SyNZ database. http://plant-synz.landcareresearch.co.nz/

Pole M (2008) The record of Araucariaceae macrofossils in New Zealand. Alcheringa 32(4): 405–426. https://doi.org/10.1080/03115510802417935

Pole M, Vajda V (2009) A new terrestrial Cretaceous-Paleogene site in New Zealand–Turnover in macroflora confirmed by palynology. Cretaceous Research 30(4): 917–938. https://doi.org/10.1016/j.cretres.2009.02.007

Pole MS, Hill RS, Green N, Macphail MK (1993) The Oligocene Berwick Quarry Flora – Rainforest in a drying environment. Australian Systematic Botany 6(5): 399–427. https://doi.org/10.1071/SB9930399

Porcelli F, Pellizzari G, Matile-Ferrero D, Convertini S (2012) The unusual cover of the armoured scale *Cryptaspidiotus barbusano* (Lindinger) (Hemiptera: Diaspididae: Aspidiotinae) with comments on the scale covers of other Diaspididae. Annales de la Société entomologique de France (N.S.) 48: 313–321. https://doi.org/10.1080/00379271.2012.10697781

Punithalingam E, Jones D (1971) *Aecidium* species on *Agathis*. Transactions of the British Mycological Society 57(2): 325–331. https://doi.org/10.1016/S0007-1536(71)80014-1

Pyron RA, Costa GC, Patten MA, Burbrink FT (2015) Phylogenetic niche conservatism and the evolutionary basis of ecological speciation. Biological Reviews of the Cambridge Philosophical Society 90(4): 1248–1262. https://doi.org/10.1111/brv.12154

Renault B (1893) Sur quelques nouveaux parasites des Lépidodendrons. Société d'Histoire Naturelle d'Autun, Procès-Verbaux des Séances: 168–178.

Root RB (1973) Organization of a plant-arthropod association in simple and diverse habitats: The fauna of collards (*Brassica oleracea*). Ecological Monographs 43(1): 95–124. https://doi.org/10.2307/1942161

Rossetto-Harris G, Stiles E, Wilf P, Donovan MP, Zou X (2022) Rapid character scoring and tabulation of large leaf-image libraries using Adobe Bridge. Applications in Plant Sciences 10(6): e11500. https://doi.org/10.1002/aps3.11500

Savile D (1976) Evolution of the rust fungi (Uredinales) as reflected by their ecological problems. Evolutionary biology. Springer, 137–207. https://doi.org/10.1007/978-1-4615-6950-3_4

Scasso RA, Aberhan M, Ruiz L, Weidemeyer S, Medina FA, Kiessling W (2012) Integrated bio- and lithofacies analysis of coarse-grained, tide-dominated deltaic environments across the Cretaceous/Paleogene boundary in Patagonia, Argentina. Cretaceous Research 36: 37–57. https://doi.org/10.1016/j.cretres.2012.02.002

Silvertown J, McConway K, Gowing D, Dodd M, Fay MF, Joseph JA, Dolphin K (2006) Absence of phylogenetic signal in the niche structure of meadow plant communities. Proceedings of the Royal Society of London, Series B, Biological Sciences 273: 39–44. https://doi.org/10.1098/rspb.2005.3288

Stiles E, Wilf P, Iglesias A, Gandolfo MA, Cúneo NR (2020) Cretaceous–Paleogene plant extinction and recovery in Patagonia. Paleobiology 46(4): 445–469. https://doi.org/10.1017/pab.2020.45

Stoetzel M (1976) Scale-cover formation in the Diaspididae (Homoptera: Coccoidea). Proceedings of the Entomological Society of Washington 78: 323–322.

Su T, Adams JM, Wappler T, Huang Y-J, Jacques FMB, Liu Y-S, Zhou Z-K (2015) Resilience of plant-insect interactions in an oak lineage through Quaternary climate change. Paleobiology 41(1): 174–186. https://doi.org/10.1017/pab.2014.11

Takagi S (1990) The adult female. Armored Scale Insects: Their Biology. Natural Enemies and Control 4: 5–20.

Takagi S, Tippins HH (1972) Two new species of the Diaspididae occurring on Spanish moss in North America (Homoptera: Coccoidea). Kontyû 40: 180–186.

Tiffney BH, Barghoorn ES (1974) The fossil record of the fungi. Occasional Papers of the Farlow Herbarium of Cryptogamic Botany: 1–42. https://doi.org/10.5962/p.305837

Tosolini A-MP, Pole M (2010) Insect and clitellate annelid traces in mesofossil assemblages from the Cretaceous of Australasia. Alcheringa 34(3): 397–419. https://doi.org/10.1080/03115518.2010.494914

Vea IM, Grimaldi DA (2015) Diverse new scale insects (Hemiptera: Coccoidea) in amber from the Cretaceous and Eocene with a phylogenetic framework for fossil Coccoidea. American Museum Novitates 3823(3823): 1–15. https://doi.org/10.1206/3823.1

Vellekoop J, Holwerda F, Prámparo MB, Willmott V, Schouten S, Cúneo NR, Scasso RA, Brinkhuis H (2017) Climate and sea-level changes across a shallow marine Cretaceous–Palaeogene boundary succession in Patagonia, Argentina. Palaeontology 60(4): 519–534. https://doi.org/10.1111/pala.12297

Wappler T, Ben-Dov Y (2008) Preservation of armoured scale insects on angiosperm leaves from the Eocene of Germany. Acta Palaeontologica Polonica 53(4): 627–634. https://doi.org/10.4202/app.2008.0407

Wilf P (2012) Rainforest conifers of Eocene Patagonia: Attached cones and foliage of the extant Southeast Asian and Australasian genus *Dacrycarpus* (Podocarpaceae). American Journal of Botany 99(3): 562–584. https://doi.org/10.3732/ajb.1100367

Wilf P, Escapa IH (2015) Green Web or megabiased clock? Plant fossils from Gondwanan Patagonia speak on evolutionary radiations. The New Phytologist 207(2): 283–290. https://doi.org/10.1111/nph.13114

Wilf P, Labandeira CC, Kress WJ, Staines CL, Windsor DM, Allen AL, Johnson KR (2000) Timing the radiations of leaf beetles: Hispines on gingers from latest Cretaceous to recent. Science 289(5477): 291–294. https://doi.org/10.1126/science.289.5477.291

Wilf P, Cúneo NR, Johnson KR, Hicks JF, Wing SL, Obradovich JD (2003) High plant diversity in Eocene South America: Evidence from Patagonia. Science 300(5616): 122–125. https://doi.org/10.1126/science.1080475

Wilf P, Labandeira CC, Johnson KR, Cúneo NR (2005a) Richness of plant-insect associations in Eocene Patagonia: A legacy for South American biodiversity. Proceedings of the National Academy of Sciences of the United States of America 102(25): 8944–8948. https://doi.org/10.1073/pnas.0500516102

Wilf P, Johnson KR, Cúneo NR, Smith ME, Singer BS, Gandolfo MA (2005b) Eocene plant diversity at Laguna del Hunco and Río Pichileufú, Patagonia, Argentina. American Naturalist 165(6): 634–650. https://doi.org/10.1086/430055

Wilf P, Labandeira CC, Johnson KR, Ellis B (2006) Decoupled plant and insect diversity after the end-Cretaceous extinction. Science 313(5790): 1112–1115. https://doi.org/10.1126/science.1129569

Wilf P, Cúneo NR, Escapa IH, Pol D, Woodburne MO (2013) Splendid and seldom isolated: The paleobiogeography of Patagonia. Annual Review of Earth and Planetary Sciences 41(1): 561–603. https://doi.org/10.1146/annurev-earth-050212-124217

Wilf P, Escapa IH, Cúneo NR, Kooyman RM, Johnson KR, Iglesias A (2014) First South American *Agathis* (Araucariaceae), Eocene of Patagonia. American Journal of Botany 101(1): 156–179. https://doi.org/10.3732/ajb.1300327

Wilf P, Donovan MP, Cúneo NR, Gandolfo MA (2017) The fossil flip-leaves (*Retrophyllum*, Podocarpaceae) of southern South America. American Journal of Botany 104(9): 1344–1369. https://doi.org/10.3732/ajb.1700158

Williams DJ (1985) Australian mealybugs. British Museum (Natural History), London, UK.

Williams DJ, Watson GW (1990) The Scale Insects of the Tropical South Pacific Region, Part 3: The Soft Scales (Coccidae) and Other Families. CAB International Institute of Entomology, Wallingford, 268 pp.

Wingfield BD, Ericson L, Szaro T, Burdor JJ (2004) Phylogenetic patterns in the Uredinales. Australasian Plant Pathology 33(3): 327–335. https://doi.org/10.1071/AP04020

Winkler IS, Labandeira CC, Wappler T, Wilf P (2010) Distinguishing Agromyzidae (Diptera) leaf mines in the fossil record: New taxa from the Paleogene of North America and Germany and their evolutionary implications. Journal of Paleontology 84(5): 935–954. https://doi.org/10.1666/09-163.1

Wise KAJ (1962) *Parectopa leucocyma* (Meyrick) (Lepidoptera: Gracillariidae) rediscovered as a leaf-miner of kauri (*Agathis australis* Salisb.). Transactions of the Royal Society of New Zealand 1: 373–375.

Supplementary material 1

Descriptions of DT421 (new damage type), DT86, and DT116

Authors: Michael P. Donovan, Peter Wilf, Ari Iglesias, N. Rubén Cúneo, Conrad C. Labandeira

Data type: word file

Explanation note: Descriptions of blotch mines (new damage type DT421), enigmatic structures, possibly armored scale insect (Diaspididae) covers (DT86), and columnar galls (DT116).

Link: https://doi.org/10.3897/phytokeys.226.99316.suppl1

PhytoKeys 226: 159–166 (2023)
doi: 10.3897/phytokeys.226.103309
https://phytokeys.pensoft.net

SHORT COMMUNICATION

A peer-reviewed open-access journal
PhytoKeys
Launched to accelerate biodiversity research

Typification of the name *Ranunculus rionii* (Ranunculaceae)

Zdeněk Kaplan[1,2], Sébastien Bétrisey[3], Vincent Sonnenwyl[3], Jacqueline Détraz-Méroz[4], Gregor Kozlowski[3,5]

1 *Czech Academy of Sciences, Institute of Botany, Zámek 1, 25243 Průhonice, Czech Republic* **2** *Department of Botany, Faculty of Science, Charles University, Benátská 2, 12801 Prague, Czech Republic* **3** *Natural History Museum Fribourg (NHMF), Chemin du Musée 6, 1700 Fribourg, Switzerland* **4** *Musée de la nature du Valais, Rue des Châteaux 14, 1950 Sion, Switzerland* **5** *Department of Biology and Botanical Garden, University of Fribourg, Chemin du Musée 10, 1700 Fribourg, Switzerland*

Corresponding author: Zdeněk Kaplan (kaplan@ibot.cas.cz)

Academic editor: Marco Pellegrini | Received 10 March 2023 | Accepted 1 May 2023 | Published 29 May 2023

Citation: Kaplan Z, Bétrisey S, Sonnenwyl V, Détraz-Méroz J, Kozlowski G (2023) Typification of the name *Ranunculus rionii* (Ranunculaceae). PhytoKeys 226: 159–166. https://doi.org/10.3897/phytokeys.226.103309

Abstract

Available information on the typification of the name *Ranunculus rionii* in the literature is scarce and misleading. Previously claimed type collections indicate Lagger as the collector, but the protologue discusses only the specimens collected by Rion. Original material for the name is identified, the locality of the type collection is specified, Lagger's way of writing herbarium labels for his type specimens is described, the history of the discovery of *R. rionii* is reviewed, and the name is lectotypified.

Keywords

Franz Joseph Lagger, history of botany, lectotype, nomenclature, Ranunculales

Introduction

Ranunculus sect. *Batrachium* DC. is a monophyletic group within *Ranunculus* (Hörandl and Emadzade 2012) adapted to aquatic environments and characterized by transverse ridges on the pericarp, dull white flowers and a pronounced heterophylly in some species (Cook 1963, 1966). Nonetheless, this morphological delimitation is rather weak, and these characters are not unique to this group (Hörandl et al. 2005). The section currently includes 30 recognized species widely distributed mainly in the Northern Hemisphere,

with the highest diversity in Europe (Cook 1966; Wiegleb et al. 2017), and additional cryptic taxa (Prančl et al. 2018; Koutecký et al. 2022). *Ranunculus* sect. *Batrachium* is taxonomically difficult mainly due to its species' reduced morphology, extensive phenotypic plasticity, and frequent hybridization and polyploidization (Preston and Croft 1997; Wiegleb et al. 2017; Prančl et al. 2018; Koutecký et al. 2022). The diversity of this group exhibits a complex pattern, comprising well-defined diploid species, autopolyploids, allopolyploids, cryptic species, primary hybrids and introgressants (Koutecký et al. 2022).

Although two global revisions have been published since the 1960s (Cook 1966; Wiegleb et al. 2017) and several studies dealt with nomenclatural issues (e.g., Jonsell 1996; Webster 1988; Bobrov et al. 2015), full and precise typifications are available for only a part of *R.* sect. *Batrachium* names. This uncertainty in the application of names causes potential problems of nomenclatural instability. Indeed, two names have been proposed for rejection recently to avoid the replacement of well-established names by their earlier synonyms (Bartolucci et al. 2022; Kaplan et al. 2023).

The aim of this article is to clarify the history of the discovery of *R. rionii* Lagger, to describe the process of its scientific description, to correctly identify the original material and to perform the typification of this name.

Discovery, description and typification of *R. rionii*

Ranunculus rionii is a diploid, homophyllous species distributed in Europe (mainly in its central and eastern parts), the Middle East and Tibet (Cook 1966; Wiegleb et al. 2017; Prančl et al. 2018). The species was described by Lagger (1848) based on the specimens collected and sent to him by Rion. The protologue indicates that Rion discovered what he believed was a new species in 1845. Lagger asked Rion to collect more specimens and send them to him for examination. Rion collected numerous specimens that were in flower and fruit in 1847. Lagger examined them and agreed that this was an undescribed species. However, in order not to publish anything prematurely and not to unnecessarily increase the number of species, Lagger consulted Godron, an author of the revision of the French *R.* sect. *Batrachium* (Godron 1840), to whom he sent his view and a specimen through the help of Buchinger. Godron agreed this was a new species related to *R. paucistamineus* Tausch and *R. drouetii* F.W.Schultz ex Godr. (both these names are now considered synonyms of *R. trichophyllus* Chaix). Encouraged by this unequivocal and definite judgment by a respected expert, Lagger decided to describe the new species. The type locality was indicated as "*In stagnis quibusdam circa Sedunum* (*Sitten*)". Sedunum is a Latin name, while Sitten is a German name for the Swiss town of Sion, canton of Valais. The note "*in nullius alterius Batrachii consortio*" indicated that *R. rionii* was the only species of *R.* sect. *Batrachium* found at the site.

Chanoine Rion died in 1856. F. O. Wolf and R. Ritz published his botanical results posthumously in the book Guide du botaniste en Valais (Rion et al. 1872). The account titled Plantae vasculares vallesiae includes *R. rionii* with the occurrence indicated as "Fossés et étangs de Chateau-Neuf et Maladeire près Sion, juillet-septembre, R." ("R." stands for Rion).

Three decades later, the story of the discovery of *R. rionii* was reviewed by Wolf (1879), who translated the original German protologue to French but also provided other important information. In the museum of Sion, he discovered an original text written by Rion, which was titled "*Ranunculus Rionii* Lagger vel *Ranunculus Sedunensis* mihi". Besides a detailed morphological analysis in French and Latin, Rion also specified the type locality as "Etang de la Maladeire près Sion, où il ne se trouve aucune autre forme.". Wolf added a comment that by his time, the pond of the Maladeire was already dried up, and thus the type locality of *R. rionii* was destroyed. The position of the pond was at 46°13'28"N, 7°19'15"E (WGS 84), in the western part of the present-day town of Sion. The provisional Rion's designation "*R. sedunensis*" was published in this paper merely as a synonym, was not accepted by Wolf and is therefore invalid according to the Code (Art. 36.1; Turland et al. 2018).

Available information on the typification of the name *R. rionii* in the literature is scarce. Cook (1966), in his monograph, cited the specimen "In stagnis quibusdam circa Sedunum (Sitten) Lagger." from K as the "isotype". This was not intended and cannot be considered as a lectotypification because Cook only indicated where the alleged duplicate of the type seen by him is preserved. Therefore, the requirements of the Code (Art. 7.11; Turland et al. 2018) were not met. Consequently, the provisions of Art. 9.10 (Turland et al. 2018) on correcting a misused term does not apply here. Wiegleb et al. (2017) cited another duplicate from this gathering as a "type" from BM. This typification was also not effective because it did not comply with Art. 7.11 (Turland et al. 2018), specifically with the requirement that on or after 1 January 2001, the typification statement must include the phrase "designated here" or an equivalent, and with Art. 9.23 (Turland et al. 2018) further requiring the use of the term "lectotypus", its abbreviation, or its equivalent in a modern language.

Even the information on the author of the plant name, Franz Joseph Lagger, is rare. The otherwise exhaustive monograph Taxonomic Literature (Stafleu and Cowan 1979) does not include this botanist, and the databases of Harvard University Herbaria & Libraries (https://kiki.huh.harvard.edu/databases) do not provide information on the whereabouts of his types and personal herbarium as well.

Searching in herbaria yielded numerous authentic specimens that relate to *R. rionii*. The Rion personal herbarium was donated to SION in 1860 (Burnat and Fleury 1912; Praz 2013). SION preserves a gathering of *R. rionii* consisting of five sheets collected by Rion in "Etang inférieur de Maladeire. Août. 1845" and identified by him as "*R. sedunensis* mihi". Although this is clearly the first specimen in the story of the discovery of *R. rionii*, there is no indication that this particular specimen was seen by Lagger. The provisional designation "*R. sedunensis*" given on the label is not mentioned in the protologue of *R. rionii*, while the name *R. rionii* is not given on the herbarium label. That is why this collection cannot be unequivocally considered as original material in the sense of the Code (Art. 9.4; Turland et al. 2018), as it is unclear if it was available to Lagger prior to, or at the time of, preparation of the description validating the name *R. rionii*.

Specimens labelled "*Ranunculus Rionii* Lagger! Vallesia pr. Sitten in fossis. Jul.-Sept. Lagger.", "*Ranunculus Rionii* Lagg. Prope Sedunum in Vallesia. Dr. Lagger." or "*Ranunculus Rionii* mihi. Près de Sion, Valais. Dr. Lagger.", some of them including the

year 1848, have been discovered in B, BM, GAP, JE, K, LAU, LY, LYJB, NCY, NHMF, P, PRC, S, W, WU, and ZT. Undoubtedly, duplicates of these specimens were also distributed to other herbaria around the world. The existence of these numerous collections is rather surprising because the protologue does not indicate that Lagger himself would have visited the type locality and collected any specimens. On the contrary, the protologue clearly states that Rion collected the rich gathering provided to Lagger. These collections are obviously authentic, but are they part of the original material?

Physicist and botanist Franz Joseph Lagger's personal herbarium is currently incorporated in NHMF (Kozlowski 2001). It comprises around 18,000 specimens from all over the world. The entire Lagger herbarium is now being reviewed and digitized (Swisscollnet 2023). The examination of his collections and comparative analysis of the label records show that from the present-day point of view, Lagger was not very careful in providing precise information on the collector and collection date when writing herbarium labels. He usually wrote the year of publication of the name that he published on the type specimens instead of the actual collection date (even in his own collections, only about 10% of specimens are dated) and usually also omitted the name of the actual collector of the specimens received from other botanists. These findings correspond well with the label data in the abundant Lagger's collection of *R. rionii*, individual specimens of which are now found in various herbaria. Although only the name "Lagger", and sometimes the year "1848", is given on the labels, this may well be the gathering cited in the protologue that was actually collected by Rion in 1847 and sent to Lagger on his request. In this case, all specimens from this collection would be syntypes of *R. rionii*.

The most important clue to the identification of the type and the elucidation of the story was the discovery of an authentic specimen in NCY (Fig. 1). This was collected at the type locality of *R. rionii*, the herbarium label bears the name *R. rionii* and the name of Lagger (as the other collections discussed above), but most importantly, it tracks the transfer of this specimen from Lagger through Buchinger to Godron, as the label shows a note "communicavit Buchinger" and the specimen is accompanied by the original letter from Buchinger to Godron, dated 26 September 1847 (Fig. 2). The letter contains Lagger's request on the opinion on the enclosed specimen of his *R. rionii*. In addition, it includes the description and type citation (see below), exactly in the form that later appeared in the protologue. The fact that Lagger asked Buchinger to facilitate the examination of the specimen of *R. rionii* by Godron is explicitly described in the protologue as well. This specimen is, therefore, an unequivocal original material and the best candidate for the typification of *R. rionii*. The other parts of the collection with herbarium labels written by Lagger, distributed by him to various botanists and institutions, are considered as its duplicates.

The nomenclature of *R. rionii* is summarized below:

Ranunculus rionii Lagger in Flora 31: 49. 1848. **Lectotype** (designated here): Switzerland, [herbarium label:] "Ranunculus Rionii Lagger / Sion en Valais / Lagger. / communicavit Buchinger", [enclosed letter:] "… In stagnis quibusdam circa Sedunum (Sitten) in nullius alterius Batrachii consortio, floret sub finem Augusti et initium

Figure 1. The lectotype of *Ranunculus rionii* Lagger (NCY barcode NCY023996).

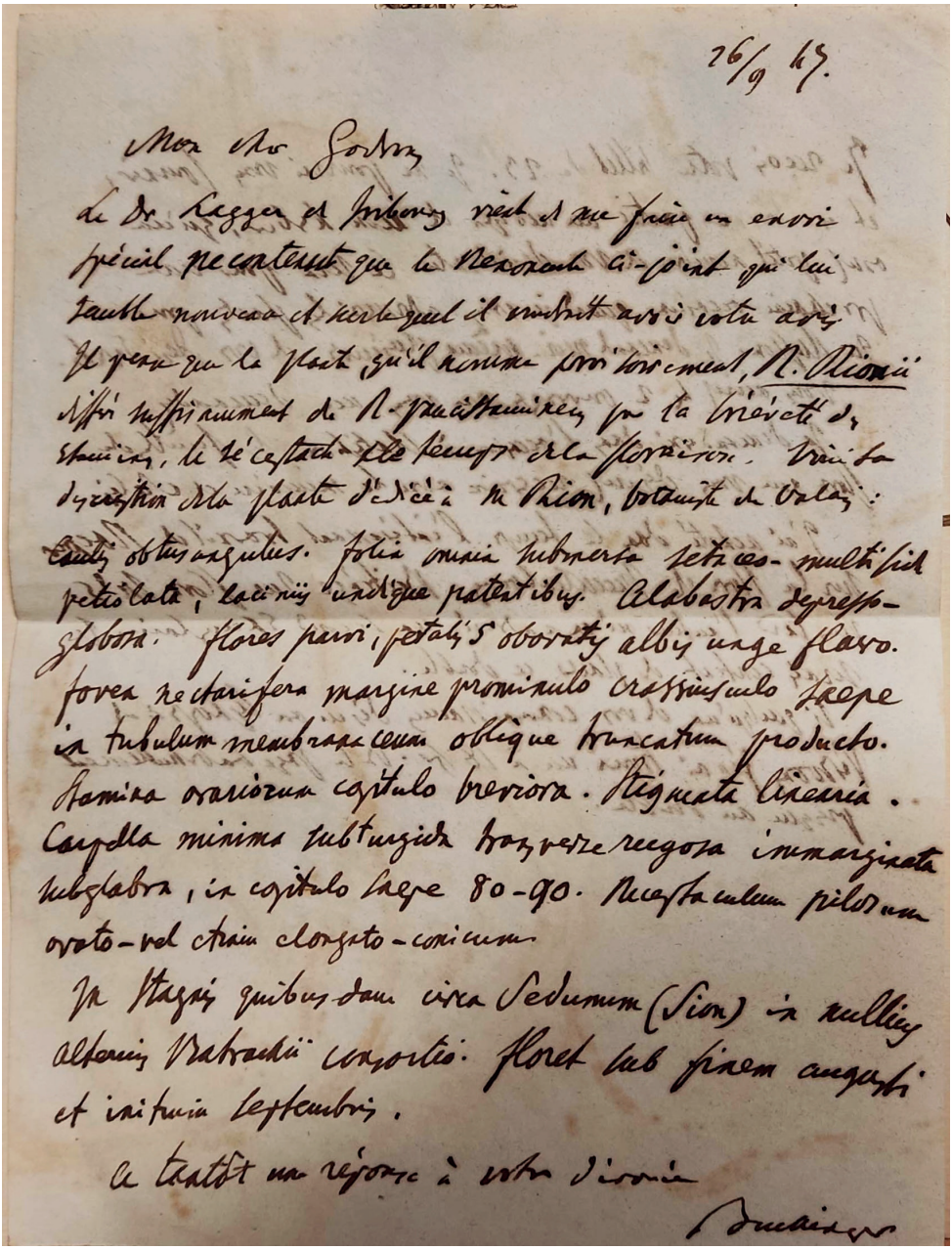

Figure 2. A letter from Buchinger to Godron on Rion's discovery of a new species and with Lagger's request on the opinion of his herbarium specimen provisionally designated as *Ranunculus rionii*.

Septembris.", [leg. *C. Rion s.n.*] (NCY barcode NCY023996!, Fig. 1; isolectotypes [with variations in label data]: B barcode B101112935!, BM barcode BM000613872!, GAP barcode GAP069572!, JE barcode JE00021497!, K barcodes K000675432!, K000675434!, K000675435!, K000675436!, LAU n.v., LY barcodes LY0052072!,

LY0675158!, LYJB barcode LYJB045434!, NHMF barcode GBIFCH05028535!, P barcodes P02558430!, P02389952!, PRC s. no.!, S no. S08-154, W n.v., WU no. 039949!, 039950!, ZT barcode ZT-00176078!).

– *Ranunculus sedunensis* Rion ex F.O.Wolf, Bull. Murith. Soc. Valais. Sci. Nat. 7–8: 38. 1879, nom. inval. [Turland et al. 2018, Art. 36.1]. Authentic specimen: Switzerland, [label 1:] "R. sedunensis mihi / … / Etang inférieur de Maladeire. août. 1845.", [label 2:] "Herbarium Rion" (SION barcode SION000399!).

Acknowledgements

We are grateful to the curators of the visited herbaria for assisting us or sending photographs of specimens. Carine Denjean from Jardins botaniques du Grand Nancy et de l'Université de Lorraine (NCY) provided valuable information and an image of the type specimen preserved in NCY. Renata Borosova and an anonymous reviewer carefully read the manuscript and suggested valuable improvements. ZK was supported by grant no. 22-10464S from the Czech Science Foundation and by long-term research development project no. RVO 67985939 of the Czech Academy of Sciences.

References

Bartolucci F, Lastrucci L, Kaplan Z, Galasso G (2022) (2924) Proposal to conserve the name *Ranunculus trichophyllus* against *R. peucedanifolius* (Ranunculaceae). Taxon 71(5): 1122–1123. https://doi.org/10.1002/tax.12814

Bobrov AA, Zalewska-Gałosz J, Jopek M, Movergoz EA (2015) *Ranunculus schmalhausenii* (section *Batrachium*, Ranunculaceae), a neglected water crowfoot endemic to Fennoscandia – a case of rapid hybrid speciation in postglacial environment of North Europe. Phytotaxa 233(2): 101–138. https://doi.org/10.11646/phytotaxa.233.2.1

Burnat E, Fleury P (1912) Le Chanoine Alphonse Rion, 1809–1856. Bulletin de la Murithienne: Société Valaisanne des Sciences Naturelles 37(1911–1912): 127–130.

Cook CDK (1963) Studies in *Ranunculus* subgenus *Batrachium* (DC.) A. Gray. II. General morphological considerations in the taxonomy of the subgenus. Watsonia 5: 294–303.

Cook CDK (1966) A monographic study of *Ranunculus* subgenus *Batrachium* (DC.) A. Gray. Mitteilungen der Botanischen Staatssammlung München 6: 47–237.

Godron G (1840) Essai sur les renoncules à fruits ridés transversalement. Mémoires de la Société Royale des Sciences, et Belles-Lettres de Nancy 1839: 8–41.

Hörandl E, Emadzade K (2012) Evolutionary classification: A case study on the diverse plant genus *Ranunculus* L. (Ranunculaceae). Perspectives in Plant Ecology, Evolution and Systematics 14(4): 310–324. https://doi.org/10.1016/j.ppees.2012.04.001

Hörandl E, Paun O, Johansson JT, Lehnebach C, Armstrong T, Chen L, Lockhart P (2005) Phylogenetic relationships and evolutionary traits in *Ranunculus* s.l. (Ranunculaceae) inferred from ITS sequence analysis. Molecular Phylogenetics and Evolution 36(2): 305–327. https://doi.org/10.1016/j.ympev.2005.02.009

Jonsell B (1996) Lectotypifications and new combinations for Flora Nordica (Vol. 1) (Lycopodiaceae–Papaveraceae). Nordic Journal of Botany 16(1): 3–8. https://doi.org/10.1111/j.1756-1051.1996.tb00210.x

Kaplan Z, Prančl J, Koutecký P (2023) (2962) Proposal to conserve the name *Ranunculus rionii* against *R. bauhini* (Ranunculaceae). Taxon 72. [in press]

Koutecký P, Prančl J, Košnar J, Koutecká E, Hanzlíčková J, Lučanová M, Nejedlá M, Kaplan Z (2022) Waking up from a taxonomist's nightmare: Emerging structure of *Ranunculus* section *Batrachium* (Ranunculaceae) in central Europe based on molecular data and genome sizes. Botanical Journal of the Linnean Society 198(4): 417–437. https://doi.org/10.1093/botlinnean/boab063

Kozlowski G (2001) Bedeutung der Herbarien des Naturhistorischen Museums Freiburg (Schweiz) für die Erforschung und Erhaltung der Freiburger Flora. Bulletin de la Société Fribourgeoise des Sciences Naturelles 90: 49–59.

Lagger F (1848) *Ranunculus Rionii*, ein neuer Wasserranunkel der Schweiz. Flora 31: 49–50.

Prančl J, Koutecký P, Trávníček P, Jarolímová V, Lučanová M, Koutecká E, Kaplan Z (2018) Cytotype variation, cryptic diversity and hybridization in *Ranunculus* sect. *Batrachium* revealed by flow cytometry and chromosome numbers. Preslia 90(3): 195–223. https://doi.org/10.23855/preslia.2018.195

Praz J-C (2013) Histoire de l'herbier valaisan. Manuscript. Herbarium, Musée de la nature du Valais, Sion.

Preston CD, Croft JM (1997) Aquatic Plants in Britain and Ireland. Harley Books, Colchester, 365 pp.

Rion Ch, Ritz R, Wolf FO (1872) Guide du botaniste en Valais. A. Galerini, Sion, 252 pp.

Stafleu FA, Cowan RS (1979) Taxonomic Literature. A Selective Guide to Botanical Publications and Collections with Dates, Commentaries and Types (ed. 2, Vol. 2). Bohn, Scheltema & Holkema, Utrecht, and W. Junk, The Hague, 991 pp.

Swisscollnet (2023) Swiss natural history collections network (SwissCollNet). https://swisscollnet.scnat.ch/en/running_projects/project_summaries [Accessed 10.02.2023]

Turland NJ, Wiersema JH, Barrie FR, Greuter W, Hawksworth DL, Herendeen PS, Knapp S, Kusber W-H, Li D-Z, Marhold K, May TW, McNeill J, Monro AM, Prado J, Price MJ, Smith GF [Eds] (2018) International Code of Nomenclature for Algae, Fungi and Plants (Shenzhen Code) Adopted by the Nineteenth International Botanical Congress Shenzhen, China, July 2017. Regnum Vegetabile 159. Koeltz Botanical Books, Glashütten. https://doi.org/10.12705/Code.2018

Webster SD (1988) *Ranunculus penicillatus* (Dumort.) Bab. in Great Britain and Ireland. Watsonia 17: 1–22.

Wiegleb G, Bobrov AA, Zalewska-Gałosz J (2017) A taxonomic account of *Ranunculus* section *Batrachium* (Ranunculaceae). Phytotaxa 319(1): 1–55. https://doi.org/10.11646/phytotaxa.319.1.1

Wolf FO (1879) Note sur le *Ranunculus Rionii*, Lagger. Bulletin de la Murithienne: Société Valaisanne des Sciences Naturelles 7–8: 36–39.